

**Modulation of Innate Immune signaling by the  
small T antigen of Merkel cell polyomavirus – the  
causative agent of Merkel cell skin cancer**

Hussein Katai Abdul-Sada

Submitted in accordance with the requirements for the  
degree of  
Doctor of Philosophy

The University of Leeds  
School of Molecular and Cellular Biology

March 2016

The candidate confirms that the work submitted is his own, except where work which has formed part of jointly authored publications has been included. The contribution of the candidate and the other authors to this work has been explicitly indicated below. The candidate confirms that appropriate credit has been given within the thesis where reference has been made to the work of others.

This copy has been supplied on the understanding that it is copyright material and that no quotation from the thesis may be published without proper acknowledgement

© 2016 The University of Leeds, Hussein K Abdul-Sada

The right of Hussein K Abdul-Sada to be identified as Author of this work has been asserted by his in accordance with the Copyright, Designs and Patents Act 1988.

jointly-authored publications

- 1- Chapter 3 and 4, mapping of MCPyV sT binding with NEMO and the phosphatases

**(Merkel cell polyomavirus small T antigen targets the NEMO adaptor protein to disrupt inflammatory signalling**, Griffiths, D. A., Abdul-Sada, H., Knight, L. M., Jackson, B. R., Richards, K., Prescott, E. L., Peach, A. H. S., Blair, G. E., Macdonald, A. & Whitehouse, A., 2013, Journal of virology, 87, 13853-13867. **Including:** Figure 7 A, B i, ii, C i, ii., Figure 8C, Figure 9 A, B, C, Figure 10 A, B, C, D

- 2- Chapter 4 binding of MCPyV sT with PP4C and sT mutants.

**(Merkel cell polyomavirus small T antigen mediates microtubule destabilization to promote cell motility and migration)**. Knight, L. M., Stakaityte, G., Jennifer, J. W., Abdul-Sada, H., Griffiths, D. A., Howell, G. J., Wheat, R., Blair, G. E., Steven, N. M. & Macdonald, A., 2015, Journal of virology, 89, 35-47. **Including:** Figure 4 C and D, mutant  $\Delta 95-111$  (Merkel Cell Polyomavirus Small T Antigen Mediates Microtubule Destabilization To Promote Cell Motility and Migration).

- 3- Review , **(Merkel Cell Polyomavirus: Molecular Insights into the Most Recently Discovered Human Tumour Virus)**, Stakaitytė G., Wood J., Knight L., Abdul-Sada H., Adzahar N., Nwogu N., Macdonald A., and Whitehouse A. Cancers (Basel). 2014 Sep; 6(3): 1267–1297. **Including:** Merkel Cell Carcinoma, Merkel Cell Polyomavirus and Figure 3.

سيدي يا موسى ابن جعفر يا ابن الصادق المصدق وأبا السلطان علي ابن موسى  
الرضا انيس النفوس وشمس الشموس، أهدي جهدي المتواضع هذا لجنابك  
راجيا ان يكون في سبيل الله تعالى .

## Acknowledgement.

I would like to express my sincere gratitude to my supervisor Dr. Andrew Macdonald for providing me with unfailing support through his meticulous suggestions and continuous guidance that made this journey possible. I would also like to thank my co-supervisor Prof. Adrian Whitehouse for his support and encouragement. I extend my thanks to all members of the Macdonald lab who worked with me, without their help and counsel, the completion of my project would have been immeasurably more difficult. Thank you to Dr. Christopher Wasson for his astute criticism and for spending extra time helping me during the practical phase. Thank you for Dr. Emma Prescott for giving hints and ideas to support my work. I would also like to thank Dr. Marietta Müller for her advice and moral support. Thank you to Ethan Morgan, Margrita Panou, Ainaa Adilah, Susan Matthews and Rajni Bhardwaj for all their assistance and for regulating the lab. Thank you to all members of Whitehouse lab who helped in publishing parts of this work. My sincere thanks also go to external collaborators who have provided critical reagents for this project.

لابد للانسان من شكر ربه اولاً. فشكراً لله على عطائه الدائم لي ، واتمنى ان يكون عملي خالصاً لوجهه الكريم. ولتأدية حق الخالق لابد من شكر المخلوقين. شكراً لعائلتي، لامي التي سمحت لي بالاعتراب عنها لاكمال دراستي، شكراً لزوجتي على دعمها المتواصل لي بكل حنان ووفاء ولاولادي الذين تحملوا تغير مزاجي المستمر بسبب ضغوط الدراسة. شكراً لآخي أحمد واخواني وجميع عائلتي كونهم كانوا يتابعون تقدمي ويسندوني باستمرار وشكراً لعزيزي صلاح لمساندتي واتمنى ان ارد لكم الجميل جميعاً.

ولا يفوتني ان أشكر مؤسسة الشهداء- العراق لتحملها تكاليف دراستي وللملحقة العراقية في أنكلترا لترتيب جميع الامور القانونية الخاصة بدراستي. كما أشكر جميع زملائي في جامعة البصرة – كلية الصيدلة لدعمهم المتواصل منذ البداية.

**Abstract.**

Merkel cell Polyomavirus (MCPyV) is implicated in the pathogenesis of Merkel cell carcinoma (MCC), a rare and highly aggressive neuroendocrine skin cancer, through expression of two oncoproteins, small T antigen (sT) and large T antigen (LT). MCPyV sT expression is essential for cell transformation, however, the mechanisms by which sT may contribute towards MCC are poorly understood. Studies from our group identified that sT is an antagonist of NF- $\kappa$ B signalling (Griffiths et al., 2013). This thesis focuses on dissecting the molecular basis of inhibition.

Co-immunoprecipitation and co-immunofluorescence studies demonstrate an interaction between sT and the critical adaptor protein NF- $\kappa$ B essential modulator (IKK $\gamma$ , NEMO) that is necessary for inhibiting NF- $\kappa$ B activation. A comprehensive mapping exercise identified the regions in each protein necessary for mediating this interaction. Mechanistically, we reveal that NEMO does not interact with sT directly, rather it forms part of a larger protein complex. Using proteomic data, we establish interactions between sT and novel protein phosphatase proteins including PP4C. In comprehensive studies, we show that a complex of PP4C and the PP4 targeting sub-unit PP4R1 are necessary for bridging sT to NEMO in vitro. In cells, depletion of PP4R1 prevents formation of the sT-NEMO complex and point mutations in sT that prevent binding to these host proteins reduce the ability of sT to impair NF- $\kappa$ B driven transcription. Finally, we demonstrate that interactions with PP4R1 and NEMO are not shared with sT proteins from other polyomaviruses tested, implicating potential unique functions for MCPyV sT amongst the *Polyomaviridae*.

This study provides convincing evidence for the molecular mechanisms that MCPyV sT utilises to evade the innate immune system and may help to explain the chronic nature of this virus.

## Table of contents

<b>Acknowledgement .....</b>	<b>III</b>
<b>Abstract .....</b>	<b>IV</b>
<b>List of tables .....</b>	<b>IX</b>
<b>List of Figures .....</b>	<b>X</b>
<b>Abbreviations.....</b>	<b>XII</b>
<b>CHAPTER 1. INTRODUCTION .....</b>	<b>1</b>
<b>1.1 MERKEL RANVIER CELLS.....</b>	<b>1</b>
<b>1.2 MERKEL CELL CARCINOMA .....</b>	<b>2</b>
1.2.1 Epidemiology of MCC .....	4
1.2.2 MCC and UV Light Exposure .....	6
<b>1.3 HUMAN POLYOMAVIRUSES .....</b>	<b>9</b>
1.3.1 Discovery of human polyomaviruses.....	<b>Error! Bookmark not defined.</b>
1.3.2 Classification of human polyomaviruses ...	<b>Error! Bookmark not defined.</b>
1.3.3 Virus Genome.....	<b>Error! Bookmark not defined.</b>
<b>1.4 MERKEL CELL POLYOMAVIRUS (MCPyV).....</b>	<b>14</b>
1.4.1 The Isolation of the Merkel Cell Polyomavirus.....	14
1.4.2 The Life Cycle of MCPyV and tissue tropism. ....	15
1.4.3 MCPyV Binding, Entry and Replication .....	16
1.4.4 Transmission of the Virus.....	18
1.4.5 Virus epidemiology.....	20
1.4.6 The Genome Structure of MCPyV.....	21
1.4.6.1 The Early Region .....	23
1.4.6.1.1 Large T Antigen.....	23
1.4.6.1.2 The 57kT protein.....	28
1.4.6.1.3 ALTO protein.....	28
1.4.6.1.4 Small T Antigen (sT).....	30
1.4.6.1.5 MicroRNA.....	31
1.4.6.2 Structural Proteins encoded by the Late Region .....	32
<b>1.5 MCPyV ST INVOLVEMENT IN VIRAL REPLICATION AND CELL TRANSFORMATION</b>	<b>33</b>
<b>1.6 MCPyV AVOIDANCE OF THE IMMUNE SYSTEM .....</b>	<b>36</b>
<b>1.7 MODIFICATION OF THE NF-<math>\kappa</math>B PATHWAY BY MCPyV ST.....</b>	<b>38</b>
1.7.1 Composition of NF- $\kappa$ B.....	38
1.7.1.1 NF- $\kappa$ B dimers.....	38
1.7.1.2 I $\kappa$ B composition.....	39
1.7.1.3 IKK Complex Structure.....	42
1.7.1.3.1 IKK Kinases .....	42
1.7.1.3.2 NF- $\kappa$ B essential modulator (NEMO, IKKy).....	43
1.7.2 The Canonical NF- $\kappa$ B Pathway .....	47
<b>1.8 ROLE OF PROTEIN PHOSPHATASES IN CELL SIGNALING .....</b>	<b>51</b>
1.8.1 Protein Phosphatase 2.....	51

1.8.1.1 PP2A Function in Cellular Processes .....	53
8.1.2 The Correlation between MCPyV sT and PP2A .....	54
1.8.2 Protein Phosphatase 4.....	56
<b>1.9 NF-<math>\kappa</math>B AS A TARGET FOR VIRUS IMMUNE EVASION .....</b>	<b>58</b>
<b>1.10 AIM OF STUDY.....</b>	<b>62</b>
<b>CHAPTER 2 MATERIAL AND METHODS.....</b>	<b>63</b>
<b>2.1 COMPETENT BACTERIAL STRAIN AND STORAGE .....</b>	<b>63</b>
<b>2.2 CLONING VECTORS.....</b>	<b>64</b>
<b>2.3 DNA MANIPULATION AND PLASMID CONSTRUCTION.....</b>	<b>65</b>
2.3.1 Primers.....	65
2.3.2 Polymerase Chain Reaction (PCR).....	67
2.3.3 Purification of PCR products .....	67
2.3.4 Colony PCR screening.....	67
2.3.5 Internal deletion polymerase chain reaction.....	68
2.3.6 Site directed mutagenesis.....	68
<b>2.4 DNA PREPARATION .....</b>	<b>68</b>
2.4.1 Restriction enzyme digestion .....	68
2.4.2 Agarose gel electrophoresis.....	69
2.4.3 DNA sequences.....	69
2.4.4 Ligation of DNA fragments .....	69
2.4.5 Transformation of competent bacteria.....	70
<b>2.5 PURIFICATION OF DNA.....</b>	<b>70</b>
2.5.1 Small scale DNA purification (minipreps) .....	70
2.5.2 Large scale DNA purification (maxipreps) .....	71
<b>2.6 MAMMALIAN CELL PREPARATION.....</b>	<b>71</b>
2.6.1 Cell culture:.....	71
2.6.2 Thawing and preparing of cells .....	72
2.6.3 Counting cells and seeding out .....	72
2.6.4 Passage of cells:.....	72
2.6.5 Transfection of cell lines .....	72
2.6.6 Harvesting cells .....	73
<b>2.7 PROTEIN PREPARATION.....</b>	<b>73</b>
2.7.1 Protein concentration estimation.....	73
2.7.2 SDS polyacrylamide gel electrophoresis (SDS-PAGE) .....	74
2.7.3 Western blotting.....	74
2.7.4 Re-probing the membrane.....	77
2.7.5 Densitometry analysis of Western blots .....	78
<b>2.8 PROTEIN INTERACTIONS.....</b>	<b>78</b>
2.8.1 Co-Immunoprecipitation (Co-IP).....	78
2.8.1.1 GFP Trap precipitation .....	78
2.8.1.2 FLAG Agarose precipitation .....	79
2.8.2 Co-immunofluorescence (Co-IF).....	79
2.8.2.1 Cell fixation .....	79
2.8.2.2 Staining cells with specific antibodies.....	79
2.8.2.3 Imaging and confocal microscopy.....	80
<b>2.9 LUCIFERASE REPORTER ASSAYS.....</b>	<b>80</b>
<b>2.10 SUBCELLULAR FRACTIONATION .....</b>	<b>81</b>

2.10.1 Cytoplasm and nucleus isolation.....	81
2.10.2 Membrane fractionation. ....	81
<b>2.11 PROTEIN EXPRESSION IN A CELL FREE SYSTEM. ....</b>	<b>82</b>
2.11.1 Protein expression in bacterial cells.....	82
2.11.2 GST pulldown assays. ....	83
<b>2.12 EVALUATION OF siRNA-MEDIATED GENE SILENCING. ....</b>	<b>83</b>
<b>CHAPTER 3. MCPyV sT INHIBITS THE NF-<math>\kappa</math>B PATHWAY BY TARGETING NEMO.....</b>	<b>85</b>
<b>3.1 INTRODUCTION.....</b>	<b>85</b>
<b>3.2 RESULTS.....</b>	<b>87</b>
3.2.1 Subcellular fractionation of sT in MCC13. ....	87
3.2.1.1 MCPyV sT is a soluble protein localised in the cytoplasm. ....	87
3.2.1.2 Localization of MCPyV sT in the cytoplasm of MCC13. ....	88
3.2.2 MCPyV sT blocks NF- $\kappa$ B signalling pathway.....	88
3.2.3 Screening for potential host binding proteins of MCPyV sT involved in NF- $\kappa$ B activation. ....	92
3.2.3.1 MCPyV sT interacts with the NEMO.....	92
3.2.3.2 Colocalization of MCPyV sT with endogenous NEMO in MCC13.....	93
3.2.4 Generating mutations in MCPyV sT to map the interaction with NEMO. ....	96
3.2.4.1 Residues 95-128 within MCPyV sT are required for the interaction with NEMO. ....	96
3.2.4.2 NEMO binds to amino acids within 95-111 of sT. ....	99
3.2.4.3 MCPyV sT residues 101-103 are required for the interaction with NEMO. ....	99
3.2.5 Impact of point mutations on the ability of MCPyV sT to inhibit the NF- $\kappa$ B pathway. ....	100
3.2.6 Identifying the regions within NEMO necessary for the interaction with MCPyV sT. ....	105
3.2.6.1 Generation and analysis of NEMO truncation mutants. ....	105
3.2.6.2 MCPyV-sT interacts with the NEMO ubiquitin-binding domain. ....	107
3.2.6.3 Disease associated mutations within the ubiquitin-binding domain of NEMO prevent the interaction with MCPyV sT. ....	107
<b>3.3 DISCUSSION: .....</b>	<b>110</b>
3.3.1 MCPyV sT is a soluble, cytoplasmic protein in MCC13 cells. ....	110
3.3.2 MCPyV sT inhibits NF- $\kappa$ B activation.....	110
3.3.3 Interaction of MCPyV sT with NEMO. ....	111
3.3.4 Residues 101-103 in MCPyV sT are required for targeting NEMO.....	113
3.3.5 The role of the point mutants of sT in NF- $\kappa$ B pathway.....	114
3.3.6 The NEMO ubiquitin-binding domain is needed for the interaction with sT in cells. ....	114
<b>CHAPTER 4. MCPyV sT INTERACTS WITH A NUMBER OF PROTEIN PHOSPHATASE SUBUNITS IN CELLS.....</b>	<b>116</b>
<b>4.1 INTRODUCTION.....</b>	<b>116</b>
<b>4.2 RESULTS.....</b>	<b>118</b>
4.2.1 MCPyV sT targets protein phosphatases 4 C subunit. ....	118
4.2.2 Colocalization of MCPyV sT with endogenous PP4C in MCC13 cells. .	119

4.2.3 Residues 95-128 within MCPyV sT are required for the interaction with PP4C.....	121
4.2.4 PP4C binds to residues 95-111 within sT.....	122
4.2.5 MCPyV sT residues 100-103 are required for the interaction with PP4C. .....	125
4.2.6 Two amino acids (102-103) in MCPyV sT are required for the interaction with PP4C.....	125
4.2.7 MCPyV sT targets other protein phosphatases in cells. ....	128
4.2.8 Co-immunoprecipitation of sT with the A $\alpha$ , A $\beta$ and catalytic (C) sub-units of PP2A. ....	128
3.2.9 Mapping the regions of sT necessary for interacting with PP2A A $\alpha$ and PP2A A $\beta$ . ....	128
3.2.9.1 Mutation of amino acid 103 in MCPyV sT decreases the interaction with PP2A A $\beta$ . ....	129
<b>4.3 DISCUSSION.....</b>	<b>133</b>
4.3.1 MCPyV sT targets PP4C.....	133
4.3.2 MCPyV sT interacts with the two isoforms of PP2A. ....	134
<b>CHAPTER 5. CHARACTERISATION OF THE PROTEIN COMPLEXES ASSOCIATED WITH MCPYV ST .....</b>	<b>136</b>
<b>5.1 INTRODUCTION.....</b>	<b>136</b>
<b>5.2 RESULT .....</b>	<b>137</b>
5.2.1 Identification of protein-protein interactions <i>in vitro</i> .....	137
5.2.2 Validating the expression of bacterial GST-sT. ....	137
5.2.3 IVT production of sT binding partners. ....	137
5.2.4 MCPyV-sT does not bind NEMO directly. ....	140
5.2.5 MCPyV-sT binds to PP4C directly.....	140
5.2.6 PP4R1 is a PP4C binding protein and novel target of MCPyV sT. ....	143
5.2.6.1 PP4R1 interacts with NEMO in cells.....	143
5.2.6.2 Co-immunoprecipitation assay confirmed the interaction of PP4R1 with PP4C. ....	143
5.2.6.3 MCPyV-sT targets PP4R1.....	146
5.2.6.4 Mapping the region in sT required for the interaction with PP4R1 .....	146
5.2.6.5 Amino acids 101-103 in sT are required for the interaction with PP4R1 .....	146
5.2.7. MCPyV-sT recruits PP4R1 to interact with NEMO. ....	150
5.2.8 Direct interaction of PP2A A $\alpha$ or PP2A A $\beta$ with MCPyV sT. ....	150
5.2.9 MCPyV sT residues 102 and 103 necessary for the direct interaction with host proteins. ....	152
<b>5.3 DISCUSSION.....</b>	<b>155</b>
5.3.1 MCPyV sT does not interact with NEMO directly. ....	155
5.3.2 A novel interaction between MCPyV sT and PP4R1. ....	156
5.3.3 MCPyV sT forms a complex consisting of PP4R1-PP4C-NEMO.....	156
5.3.4 Direct interaction between MCPyV sT and PP2A isoforms.....	157
5.3.6 Amino acids R102 and F103 in sT mediate the direct interactions with phosphatase sub-units <i>in vitro</i> . ....	158

<b>CHAPTER 6. CONTRIBUTION OF PP4C-PP4R1 TO THE INHIBITION OF NF-<math>\kappa</math>B ACTIVATION IN MCPyV ST EXPRESSING CELLS .....</b>	<b>159</b>
<b>6.1 INTRODUCTION.....</b>	<b>159</b>
<b>6.2 RESULTS .....</b>	<b>160</b>
6.2.1 Validation of the efficiency of siRNA targeting PP4C.....	160
6.2.2 Validation of siRNA PP4R1 efficacy .....	160
6.2.3 Co-immunoprecipitation of MCPyV sT with cellular proteins during PP4C silencing. ....	163
6.2.4 Co-immunoprecipitation of MCPyV sT with cellular proteins during silencing of PP4 R1. ....	163
6.2.5 Specificity of host binding partners amongst PyV sT proteins. ....	164
<b>6.3. DISCUSSION.....</b>	<b>169</b>
6.3.1 PP4R1 is essential for the interaction with NEMO in cells. ....	169
6.3.2 MCPyV sT binds to a unique range of host proteins associated with immune evasion. ....	170
<b>CHAPTER 7. SUMMARY AND CONCLUSION .....</b>	<b>172</b>
<b>BIBLIOGRAPHY .....</b>	<b>179</b>

## List of tables

Table 2.1 Information about type of competent bacteria.....	61
Table 2.2 Information about cloning vectors.....	62
Table 2.3 Primers and their sequences .....	63
Table 2.4 Information of primary antibodies used in this study.....	74
Table 2.5 Information of secondary antibodies used in this study.....	76
Table 2.6 Sequences of siRNA of PP4C and PP4R1 .....	82

## List of illustrative Material

Figure 1.1 Merkel cell in skin cross section .....	8
Figure 1.2 Schematic for attachment of MCPyV with cell membrane .....	18
Figure 1.3 MCPyV genome organisation .....	24
Figure 1.4 Schematic of early region protein of MCPyV .....	26
Figure 1.5 MCPyV LT binding domains .....	28
Figure 1.6 MCPyV sT binding domains .....	31
Figure 1.7 NF- $\kappa$ B family sub-units domains .....	40
Figure 1.8 IKK catalytic sub-units binding domains .....	42
Figure 1.9 NEMO binding domains .....	46
Figure 1.10 Activation NF- $\kappa$ B canonical pathway.....	48
Figure 1.11 NF- $\kappa$ B canonical pathway and target sites of some viruses .....	59
Figure 3.1 Subcellular fractionation of MCPyV sT .....	87
Figure 3.2 Cellular localization of GFP-MCPyV sT .....	88
Figure 3.3 MCPyV sT mediate NF- $\kappa$ B inhibition .....	89
Figure 3.4 Interaction of MCPyV sT with NEMO .....	92
Figure 3.5 Colocalization of MCPyV sT with NEMO in MCC13 cells.....	93
Figure 3.6 Generation of different MCPyV sT C-terminal truncations.....	95
Figure 3.7 Co-IP the interaction of MCPyV sT truncation with NEMO.....	96
Figure 3.8 Co-IP of two deletion of MCPyV sT with NEMO.....	99
Figure 3.9 Co-IP of alanine mutants of MCPyV with NEMO .....	100

Figure 3.10 Co-IP of point mutants MCPyV sT with NEMO .....101

Figure 3.11 Luciferase assay show the role two point mutants MCPyV sT in NF- $\kappa$ B activation .....102

Figure 3.12 Co-IP od NEMO truncation with MCPyV sT.....104

Figure 3.13 Co-IP of small truncation of NEMO with MCPyV sT.....106

Figure 3.14 Point mutant of NEMO binds MCPyV sT .....107

Figure 4.1 Co-IP of MCPyV sT with PP4C .....117

Figure 4.2 Co-IF of MCPyV sT with PP4C .....118

Figure 4.3 Mapping MCPyV sT binding site with PP4C .....120

Figure 4.4 Co-IP of MCPyV sT deletion mutants with PP4C .....121

Figure 4.5 Co-IP of Alanine mutant MCPyV sT with PP4C .....123

Figure 4.6 Two point mutant of MCPyV sT bind PP4C.....124

Figure 4.7 Co-IP of MCPyV sT with PP2A sub-units .....127

Figure 4.8 Co-IP of mutant deletion of MCPyV sT with PP2A .....128

Figure 4.9 Co-IP Point mutant MCPyV sT with PP2A A $\beta$  .....129

Figure 5.1 Protocols of direct binding assay .....135

Figure 5.2 expression proteins of direct binding assay .....136

Figure 5.3 MCPyV sT did not bind NEMO directly.....138

Figure 5.4 MCPyV sT bind PP4C directly .....	139
Figure 5.5 Binding of PP4R1 with NEMO .....	141
Figure 5.6 Binding of PP4R1 with PP4C .....	142
Figure 5.7 Interaction of MCPyV sT with PP4R1 .....	144
Figure 5.8 Mapping interaction of MCPyV sT with PP4R1 .....	145
Figure 5.9 Interaction of point mutant of MCPyV sT with PP4R1 .....	146
Figure 5.10 Interaction of MCPyV sT with PP4C-PP4R1 and NEMO .....	148
Figure 5.11 Direct interaction of MCPyV sT with PP2A .....	150
Figure 5.12 Direct interaction of point mutants with host proteins .....	151
Figure 6.1 Silencing of PP4C by specific siRNA of PP4C .....	158
Figure 6.2 Silencing of PP4C by specific siRNA of PP4C .....	159
Figure 6.3 Co-IP of MCPyV sT with host protein during silencing of PP4C.....	162
Figure 6.4 Co-IP of MCPyV sT with host protein during silencing of PP4R1.....	163
Figure 6.5 Co-IP of other Polyomaviruses sTs with host proteins .....	164

## Abbreviations

$\alpha$ -	anti-
$^{\circ}\text{C}$	degrees Celsius
$\mu$	micro
3'	three prime
5'	five prime
$\beta$	Beta
$\gamma$	Gamma
$\varepsilon$	Epsilon
$\Delta$	Deletion mutant
A	Alanine
ABIN	A20 binding inhibitor of NF- $\kappa$ B
ADR-RES	ADR-RES cell line
AIDS	acquired immune deficiency syndrome
ALTO	Alternate frame of the Large T Open reading frame
APS	ammonium persulphate
APUD	Amine Precursor Uptake and Decarboxylation
ATP	adenosine triphosphate
BCA	bicinchoninic acid
BLAST	basic local alignment search tool
BKPyV	BK polyomavirus
BIRC5	apoptosis repeat-containing 5
BL21	Competent <i>E. coli</i>
Bps	base pairs
BSA	bovine serum albumin
BTL-Tn 5B1–4	High Five, Tn5
CC	coiled-coil
CDK	cyclin-dependent kinase
cDNA	complementary deoxyribonucleic acid
CMV	cytomegalovirus
Co-IP	co-immuno-precipitation
CR1	conserved region 1

Cre	Cyclization recombination enzymes
C-terminus	carboxyl-terminus
D	Aspartic Acid
DAPI	4',6-diamidino-2-phenylindole
ddH <sub>2</sub> O	double-distilled water
DMEM	Dulbecco's modified Eagle's medium
DnaJ	heat shock induced protein
dNTP	deoxynucleotide triphosphates
dpi	dots per inch
DTT	dithiothreitol
DTS	digital transcriptome subtraction
E	Glutamic Acid
E4orf4	E4 open reading frame 4
e.g.	exempli gratia
EBV	Epstein-Barr virus
ECL	chemiluminescent solution
EDTA	ethylenediaminetetraacetic acid
EE	Glu-Glu-(EEEEYMPME)
eIF4E	Eukaryotic initiation factor 4E
ELISA	enzyme linked immunosorbent assay
ER	endoplasmic reticulum
F	Phenylalanine
FBS	Fetal Bovine Serum
FLAG	octapeptide DYKDDDDK
Fwd	Forward
G	Glycine
GAGs	glycosam-inoglycans
GAPDH	glyceraldehyde 3-phosphate dehydrogenase
GFP	green fluorescent protein
GST	Glutathione-S-Transferase
GTP	guanosine tri-phosphate
Gluc	Gaussia luciferase
GT1b	Ganglioside
h	hour(s)
H1	histone 1
HA	haemagglutinin
HCMV	human cytomegalovirus
HCV	Hepatitis C Virus
HDAC3	histone deacetylase 3
HEK293	Human embryonic kidney 293
HEK293T	Human embryonic kidney 293 T antigen cells
HEAT	Huntington/elongation/A sub-unit/TOR
HIV	human immunodeficiency virus
HLX	helix
HLH	helix-loop-helix
HPK1	haematopoietic progenitor kinase1
HPV	human papillomavirus
HPyV	human polyomavirus
Hsc 70	heat-shock protein cognate 70
HTLV-1	T-cell leukaemia virus type 1

IAP	Inhibitors of apoptosis proteins
IFN	interferon
IgG	immunoglobulin G
IκB	inhibitors nuclear factor of kappa light polypeptide gene enhancer in B-cells
IKK	inhibitor of nuclear factor kappa-B kinase
IL	Interleukin
IP	immuno-precipitation
IPTG	isopropyl-1-thio-D-galactosid β
IRS	insulin receptor substrate
JCPyV	JC polyomavirus
K	Cytokeratin
KOD	Kodakara
KSHV	Kaposi's sarcoma-associated herpes virus
kDa	kilo Dalton
KIPyV	Karolinska Institute polyoma Virus
KLD	Kinase-Ligase-DpnI
kT	Kilo Dalton T antigen
l	Litre
L	Lysine
LB	Luria-Bertani
LDS	lithium dodecyl sulphate
LMP1	latent membrane protein 1
LSD	LT-stabilisation domain
LT	Large Tumour antigen
LTR	long terminal repeat
LZ	leucine zipper
M	molar concentration
m	milli
M1-Ub	linear ubiquitin
MALME-3M	MALME-3M melanoma cell line
MAP	mitogen-activated protein
MaTi	MaTi cell line
MC159	<i>Molluscum contagiosum</i> 159
MCC	Merkel cell carcinoma
MCPyV	Merkel cell polyomavirus
mg	milligram(s)
MHC	major histocompatibility complex
min	minute(s)
MKL-1	MKL-1 cell line
ml	millilitre(s)
mM	millimolar
mRNA	messenger ribonucleic acid
miR	micro RNA
miRNA	micro RNA
mTOR	mammalian target of rapamycin
MXPyV	Mexican polyomavirus
MWPyV	Malawi polyomavirus
N	Asparagine
NCI-60	NCI-60 Human Tumor Cell Lines

NCCR	Non-Coding Regulatory Region
NDEL1	nuclear distribution element-like 1
NEMO	NF- $\kappa$ B essential modulator
NEB	New England BioLabs
Neu5Ac-a2, 3-Gal	N-acetylneuraminic acid galactose
NF- $\kappa$ B	nuclear factor of kappa light polypeptide gene enhancer in B-cells
ng	nanogramme
NLS	nuclear localisation signal
nm	Nanometre
NMR	Nuclear Magnetic Resonance
NOA	NEMO Optineurin ABIN
N-terminus	amino-terminus
o/n	overnight
OD600	optical density measured at 600 nm
OBD	origin-binding domain
Op18	Oncoprotein 18
ORF	open reading frame
Ori	origin of replication
p53	protein 53 kDa
PBS	phosphate buffered saline
PCR	polymerase chain reaction
PEA-15	astrocytic phosphoprotein
pH	$-\log_{10}$ concentration of hydrogen ions
PI3K	phosphatidylinositol 3-kinase
PLCG1	Phospholipase C gamma 1
PML	progressive multifocal leukoencephalopathy
Pol	protein polymerase
PP2A	protein phosphatase 2A
PP2C	protein phosphatase 2C
PP4C	protein phosphatase 4C
PP4R	protein phosphatase 4 regulatory subunit
PPM	protein phosphatases dependent on $Mg^{+2}$ or $Mn^{+2}$
PPP	phosphoprotein phosphatases
PPP2	phosphoprotein phosphatase gene 2
pRb	retinoblastoma-associated protein
pRLTK	Renilla luciferase thymidine kinase
PTP	protein tyrosine phosphatases
PVAN	polyomavirus-associated nephropathy
PyV	murine polyomavirus
Q	Glutamine
qPCR	quantitative real-time polymerase chain reaction
R	Arginine
Ref	reference
RHD	Rel homology domain
REP	Rab escort protein
RIP1	receptor-interacting protein 1
RNA	ribonucleic acid
RDA	representation difference analysis
RSV	respiratory syncytial virus

SAPK	stress-activated protein kinase
SCF	SKP1, CUL1 and F-box protein
SDS	sodium dodecyl sulphate
SDS-PAGE	sodium dodecyl sulphate polyacrylamide gel electrophoresis
sec	second(s)
SF	soluble fraction
SFKs	The Src family tyrosine kinases
SILAC	stable isotope labelling by/with amino acids in cell culture
si	small interfering
sT	small Tumour antigen
STLPyV	Saint Louis polyomavirus
SV40	simian vacuolating virus 40
T	T antigen
TAD	transcription activation domain
TATA	core DNA sequence 5'-TATAAA-3'
TBS	Tris buffered saline
TBST	Tris buffered saline containing Tween-20
TEMED	tetramethylethylenediamine
TfR	transferrin receptor
TLR9	Toll-like receptor 9
TM	trans-membrane
TNF	Tumour Necrosis Factor
TNT	Transcription/Translation
TRADD	TNF receptor 1-associated death domain
TRAF	TNF receptor-associated factor
TSPyV	Trichodysplasia spinulosa-associated polyomavirus
Ub	ubiquitin
UBAN	ubiquitin-binding in ABIN and NEMO
ULD	ubiquitin-like domain
UK	United Kingdom
UISO	UISO cell line
UV	ultraviolet
V	volts
Vam6p	vesicle-associated membrane protein
vFLIP	FLICE inhibitory protein
VLP	virus-like particle
VP	viral protein
Vpr	Viral Protein R
W	Tryptophan
w/v	weight per volume
WaGa	WaGa cell line
WHIMS	Hypogammaglobulinemia, wart and Myelokathexis Syndrome
WT	wildtype
WUPyV	Washington University Polyomavirus
x g	times gravitational force
XL1 Blue	competent <i>E. coli</i>
XR-EDA-ID	anhidrotic ectodermal dysplasia with immunodeficiency

Y  
ZF

Tyrosine  
zinc finger

# Chapter 1. Introduction

## 1.1 Merkel Ranvier cells

Merkel Ranvier cells, also known as Merkel cells, are receptor cells first identified by Fredrich Sigmund Merkel, a German anatomist and pathologist, in 1875 (Merkel, 1875). Although first identified by Merkel in the skin of birds and mammals, Merkel cells have since been found to be common to all vertebrates (Fox et al., 1980, Tweedle, 1978, Saxod, 1978). In mammals, Merkel cells are commonly found in the Stratum basale, in particular, the epidermal invaginations of the palmar (Halata et al., 2003) and plantar surfaces (Johnson et al., 2000). They are also found co-localised with Langerhans cells in the bulge of hair follicles (Taira et al., 2002), as well as mucous membranes, such as the oral mucosa (Righi et al., 2006), although in varying density and distribution. Merkel cells are commonly located at the end of sensory nerves and in such cases these are termed Merkel nerve endings (Figure 1.1). Merkel cells are oval in shape and transparent, making them difficult to examine by light microscopy, due to their absence of tonofilament in the cell cytoplasm. Although this makes them easy to differentiate from keratinocytes, they can be difficult to distinguish from Langerhans cells, Melanocytes and Lymphocytes (Merot et al., 1987).

In addition to the common cell organelles such as mitochondria, free ribosomes, lysosomes, microfilaments, vacuoles and lobulated nucleus, the cytoplasm of Merkel cells also contains membrane bound melanosomes; melanin granules; dense core neurosecretory granules; cytokeratin (K); and desmosomal proteins (Saurat et al., 1984, Moll et al., 1984).

Despite being first identified over 100 years ago, the developmental origin of Merkel cells is still unclear and a subject of debate. Some consider the presence of Merkel cells in the dermis of foetal and newborn mammalian skin an indication that Merkel cells originate from the neural crest, whilst others

believe the source of Merkel cells to be ectoderm at stem cells (Halata et al., 2003, Halata et al., 1999, Lane and Whitear, 1977).

Similarly, a consensus is lacking as to the function of Merkel cells. The accumulation of neuropeptides observed at the nerve fibre junction in these cells may indicate these cells play a role in the expression of voltage gated ion channels (essential for synaptic transmission) (Piskorowski et al., 2008). Others believe, based on histochemical composition, that Merkel cells belong to a group of cells that secrete low molecular weight polypeptide hormones called the Amine Precursor Uptake and Decarboxylation (APUD) and have a neuroendocrine function (Pearse, 1980, Pearse, 1986). In addition, Merkel cells can be found in hair follicles, attached to Langerhan cells and it may be they have a distinct function in this location (Taira et al., 2002).

It is important to note that Merkel cells found independently of neurones in the skin and mucosa are believed to have a neuroendocrine, as opposed sensory receptor, role. It is these cells that are believed to be the origin of the unusual but highly malignant skin cancer Merkel cell carcinoma (Gould et al., 1985).

## **1.2 Merkel cell carcinoma**

Merkel cell carcinoma (MCC) is a primary cutaneous neuroendocrine carcinoma first identified by Toker in 1972, who conceived the term trabecular carcinoma, on account of the solid trabeculae (solid projections within the skin) present on the tumours of the patients he diagnosed with the disease. MCCs usually appear as solid bumps purplish-reddish in colour and usually painless, on the surface of the skin. They are highly metastatic and sometimes form ulcers (Toker, 1972).

The tumours are present on various parts of the patient's bodies such as; leg, lip, forearm, buttock and face, and are painless, bluish-red or flesh toned in colour (Toker, 1972). In the 1980's the cancer was renamed Merkel cell

carcinoma as techniques including immunohistochemistry and electron microscopy were utilised and revealed the role of Merkel cells in these tumours (Wolf-Peeters et al., 1980).

Immunohistochemistry techniques revealed the presence of neuropeptides synaptophysin, chromogranin and others as well as the detection of cytokeratins 8, 18, 19, 20 and their prenuclear distribution (Pilloni et al., 2009, Jensen et al., 2000, Leech et al., 2001). Tang and Toker also used electron microscopy to study MCC tumour and found they contained dense-core neuroendocrine granules, were subject to plasma cell infiltration (as indicated by the presence of peripheral lymphocytes) and contained peritumoural connective tissue (Tang and Toker, 1978).

Later, immunohistochemical assays were employed in the diagnosis of MCC with the presence of cytokeratins, thyroid transcription factor, leukocyte common antigen, chromogranin and synaptophysin considered indicative of MCC (Sidiropoulos et al., 2011).

A detailed morphology of MCC tumour cells is available due to advances in electron microscopy. Focal trabecular pattern are common in the vast majority of MCCs. The cells are enlarged with spike like appendages protruding from the membrane thought to be involved in cell-to-cell connection. The cytoplasm contains hemidesmosomes with rosette like attachments, densesomes, fine cytofilaments and dense granules (Figure 1.1) (Kontochristopoulos et al., 2000).

Genetic screening has found genetic abnormalities in most MCC cases with abnormalities commonly found on chromosomes 1, 6, 11 and 16. These abnormalities may play a role in the aetiology of the cancer although the cause of MCC may be complex and several hypotheses have been put forward (Van Gele et al., 1998, Frigerio et al., 1983).

Ultra violet radiation exposure is considered a risk factor in the development of MCC as tumours develop more prevalently in areas of the body exposed to the sun (50% head and neck area, 40% extremities, <10% trunk and

genitals) (Agelli and Clegg, 2003, Tennvall et al., 1989, Chen, 1994, Goepfert et al., 1984, Gillenwater et al., 2001, Brissett et al., 2002).

A significant finding in the aetiology of this cancer came with the identification of Merkel Cell Polyomavirus (MCPyV). MCPyV is a small, non-enveloped, double stranded DNA virus, which has been found to be present in the majority of MCC tumours (Feng et al., 2008). Whilst both infected and non-infected tumours have high mitotic activity, immunohistochemical techniques have identified morphological differences in the MCPyV associated and non MCPyV associated MCC tumour cells, with MCPyV infected tumours having round nuclei and a scant cytoplasm and non MCPyV infected tumours having an irregular shaped nuclei and abundant cytoplasm (Kuwamoto et al., 2011).

A further breakthrough came when Tolstov and colleagues developed an enzyme linked immunosorbent assay (ELISA) for the detection of MCPyV VP1 and VP2 proteins in blood samples, allowing for rapid diagnosis of MCPyV infection. The success of this ELISA was largely due to the low cross reactivity of the anti-VP1 antibody to other similar viruses, avoiding false positive results (Tolstov et al., 2009).

Further research has shown that MCPyV is highly oncogenic and metastatic. Aided by its ability to travel through the lymphatic drainage of the body, MCPyV can cause MCC to develop at other organ sites. These sites include; lymph node, pancreas, breast, duodenum and colon epithelium, and lip and palatine tonsil (Mehran et al., 2002, Bachmann et al., 2005, Cusick and Refsum, 2004, Senda et al., 1999, Nagy et al., 2005, Howard et al., 2006).

### **1.2.1 Epidemiology of MCC**

Epidemiological studies have indicated that more than 74% of MCC cases occur in people over 65 and most of them in whites of both men and women but men have a significantly higher incidence (Agelli and Clegg, 2003). Worryingly the incidence has increased and the prognosis is poor with 4.4

cases per million in 15 years rising to 2.2 per million in one year. More than 50% of infected patients die within one year of diagnosis, in line with mortality rates for other skin cancers (Hodgson, 2005, Agelli and Clegg, 2003, Bichakjian et al., 2007). MCC can manifest as a secondary complication in other conditions such as chronic lymphocytic leukaemia, malignancies of the biliary tract, multiple myeloma and other malignancies (Craig et al., 2009, Howard et al., 2006, Kressin and Kim, 2012).

MCC is most likely to infect people with a lighter skin tone as well as people who have undergone organ transplant or who have human immunodeficiency virus (HIV) or acquired immune deficiency syndrome (AIDS) infection, the auto-immune diseases or/and lymphoproliferative disorder like chronic lymphocytic leukaemia (Lanoy et al., 2010, Engels et al., 2002, Dworkin et al., 2009, Tadmor et al., 2011). In the US, the annual number of individuals receiving an MCC diagnosis is 950-2300. Due to factors such as population ageing, the increasing prevalence of adverse effects of sun exposure, and the growing number of immunocompromised cases, this figure is on the rise (Albores-Saavedra et al., 2010, Iyer et al., 2014). Usually found on the sun-exposed skin of white individuals of over fifty years of age, MCC is a rare malignancy of the skin that displays age-dependent incidence rates of 0.18-0.41 for every 100000 white individuals (Eng et al., 2007, Miller and Rabkin, 1999).

Research revealed that, of 3870 MCC cases, female and male individuals accounted for 1490 (38.5%) and 2380 (61.5%) cases, respectively. Individuals' age was in the range 60-85 years and 94.9% of them were Caucasian. By contrast, individuals of African origin were not usually affected. The salivary glands, nasal cavity, lip, lymph nodes, vulva, vagina and oesophagus, cervical squamous cell carcinomas and adenocarcinomas were the main sites of MCC (Albores-Saavedra et al., 2010).

Furthermore, it was observed that, compared to men, women were more likely to survive over a ten-year period (Albores-Saavedra et al., 2010). In a different study, 6700 individuals suffered from local, nodal and distant metastatic diseases in a proportion of 66%, 27% and 7%, respectively, with

a five-year survival rate of 64%, 39% and 18%, respectively (Lemos et al., 2010). Additionally, severely immunosuppressed individuals, such as those who received organ transplant or had lymphoma or HIV infection, displayed a higher incidence rate of MCC (Lanoy et al., 2010).

Immunosuppression has been associated with a range of cancers with an infection-based aetiology, including Kaposi's sarcoma-associated herpes virus (KSHV), lymphomas, cervical, oropharyngeal, and penile cancers in individuals with HIV, and non-melanoma skin cancers, lymphomas, and cancers of the oral cavity, vulva, and vagina in individuals who had undergone organ transplant. The prevalence of MCC in immunocompromised people served to reinforce the notion regarding the infectious aetiology of MCC (Engels et al., 2008, Palella Jr et al., 1998).

### **1.2.2 MCC and UV Light Exposure**

Sun-exposed skin surfaces are conducive to tumour development, meaning that a major risk factor for MCC is exposure to ultraviolet (UV) light. The correlation between MCC and UV exposure has been supported by epidemiological findings, but there is currently insufficient proof for how UV causes the condition to develop (Schwarz and Schwarz, 2011).

Inhibition of immune surveillance is one mechanism through which UV light has been proposed to trigger MCC pathogenesis (Feng et al., 2008, Schwarz and Schwarz, 2011, Schneider et al., 2013). As previously mentioned, individuals older than fifty years of age are most susceptible to MCC, **this might be as a result of their tendency to exposure to the sun (Syrigos et al., 2005).**

Furthermore, by comparison to primary malignant melanomas on body surfaces that are not exposed to the sun, those on sun-exposed surfaces often **induces reactivation of herpes simplex virus** (Lundberg et al., 2006, Sadowska et al., 2003) Viral pathogenesis may be better understood based on the correlation between MCPyV and UV exposure. For example, it was reported that UV exposure triggered the *in vitro* activation of the MCPyV

Non-Coding Regulatory Region (NCRR), while sT transcript levels rose in a dose-dependent manner upon skin exposure to solar simulated radiation (Mogha et al., 2010).

Furthermore, normal repair mechanisms in UV-exposed cells are likely to be affected by viral presence, because UV radiation exposure was noted to suppress cell cycle and hinder complete DNA damage repair, which was associated with LT, in an MCC cell line infected with MCPyV (Demetriou et al., 2012, Purdie et al., 1999). By contrast, *in vivo* irradiation of skin exposed to UV led to an increase in sT, implying a UV-based regulation of the activity of the MCPyV early promoter (Mogha et al., 2010)

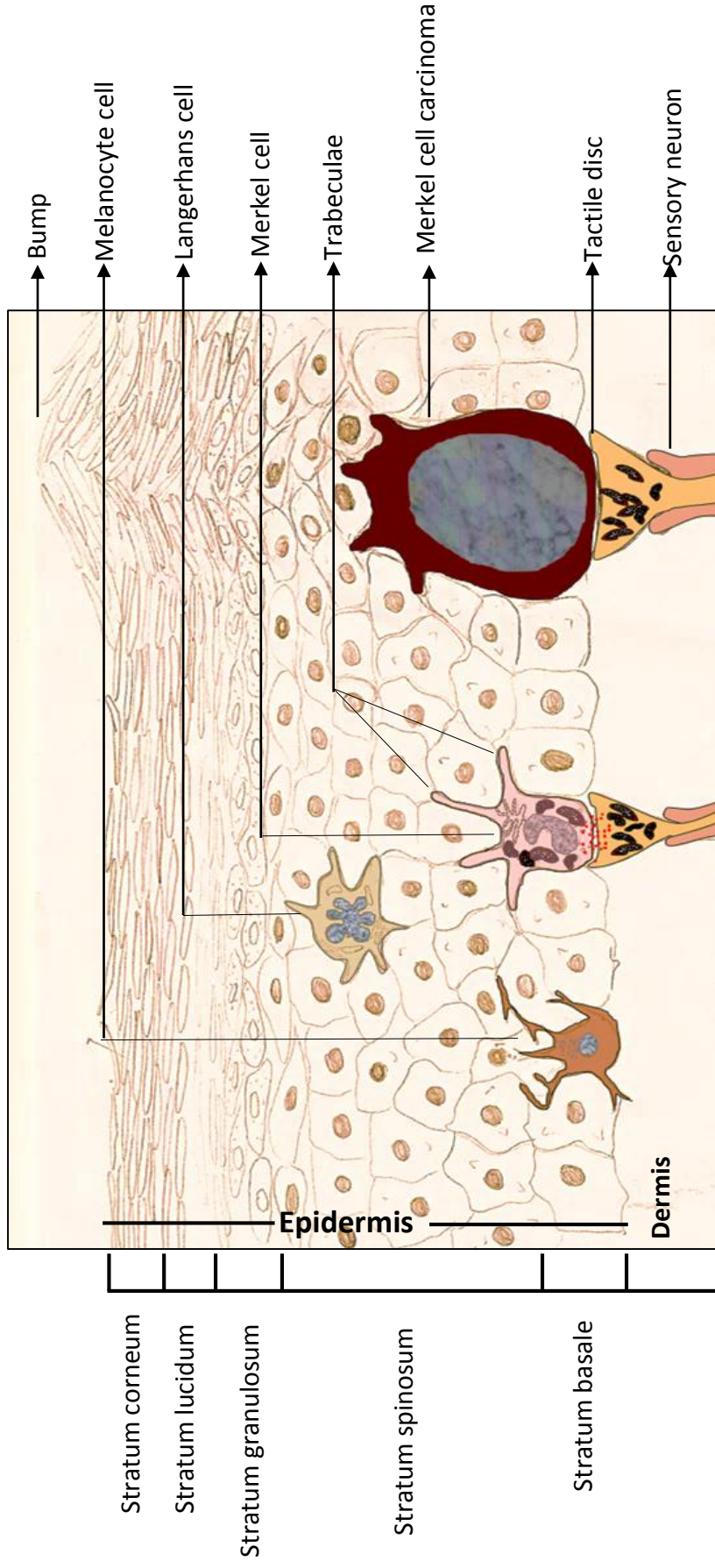


Figure 1.1 Skin cross section illustrating different type of cells in both epidermis and dermis. Six stratum in the epidermis is starting from up to down, Stratum corneum which showed bump in the right side, Stratum lucidum; stratum granulosum; stratum spinosum in which Langerhans cells lie; stratum basale contains Merkel cell and Melanocyte cell. Dermis layer showed sensory neuron and tactile disc. Difference between normal Merkel cell and Merkel Cell carcinoma which are bigger with abnormal nucleus.

### 1.3 Human Polyomaviruses

The first polyomavirus discovered was a mouse species identified in 1952 by Kilham (Kilham and Murphy, 1953) and quickly verified by an independent identification of the virus by Gross in 1953, who isolated the virus from a murine salivary gland cancer sample (Gross, 1953). The oncogenic role of this virus was confirmed four years later by Stewart who experimentally infected mice with the virus resulting in the development of multiple tumours within the host animals (Stewart et al., 1958).

Hence the virus name derived from the Greek word poly for many and oma for tumours. An in vitro cell culture system helped to further identify polyomavirus species and led to the identification of the first primate polyomavirus, named simian Vacuolating virus 40 (SV40), although this was discovered serendipitously in a polio virus vaccine study using rhesus monkey kidney cells (Sweet and Hilleman, 1960, Eddy et al., 1962). Subsequently, human tumours were screened for the presence of SV40 and traces of the virus were identified in a limited number of cancers such as pleural mesothelioma and osteosarcoma. However, evidence of SV40 as a causative agent in these tumours or even as a human pathogen remains lacking, as indicated (Poulin and DeCaprio, 2006).

Since 2007, with the help by new molecular techniques, particularly unbiased deep sequencing, rolling circle amplification (RCA), generic polymerase chain reaction (PCR), pyrosequencing, multiple displacement amplification (MDA), and complementary DNA library screening, the number of known human members of the Polyomaviridae family has grown by the discovery of 13 species isolated from humans and use of such advanced molecular analysis of viral genomes is likely to yield additional novel human polyomavirus (Table 1.1).

Table 1.1 list of Human polyomaviruses and their references.

<b>Human Polyomavirus</b>	<b>Clinical aspects</b>	<b>Sample</b>	<b>Identification method</b>	<b>References</b>
BKPyV	polyomavirus-associated nephropathy (PVAN)	urine sample of a Sudanese kidney transplant recipient	-Electron microscopy -Serologic testing	(Gardner et al., 1971)
JCPyV	Progressive multifocal leukoencephalopathy	extracts isolated from brain which obtained at necropsy	-Electron-microscopy -Serologic testing	(Padgett et al., 1971)
Karolinska Institute polyomavirus (KIPyV)	respiratory tract infection	paediatric nasopharyngeal aspirates	unbiased deep sequencing	(Allander et al., 2007)
Washington University Polyomavirus (WUPyV)	respiratory tract infection	paediatric nasopharyngeal aspirates	high throughput sequencing strategy	(Gaynor et al., 2007)
Merkel cell polyomavirus MCPyV	MCC tumour mRNA samples	Most MCC	digital subtraction	(Feng et al., 2008)
Human polyomavirus 6 (HPyV 6)	skin swab specimens	Normal skin flora and has not been associated with a specific clinical aspect	Rolling circle amplification (RCA)	(Schowalter et al., 2010)
Human polyomavirus 7 (HPyV 7)	skin swab specimens	Normal skin flora and has not been associated with a specific clinical aspect	Rolling circle amplification	(Schowalter et al., 2010)
Human polyomavirus 8 (HPyV8)	trichodysplasia spinulosa skin lesions	Trichodysplasia spinulosa-associated PyV (TSPyV) disease.	Rolling-circle amplification	(van der Meijden et al., 2010)
human polyomavirus	serum of a kidney	there is a suspicion of its	high-throughput nucleotide	(Sauvage et al.,

9 (HPyV9)	transplant patient	correlated with renal infection	sequencing	2011)
human polyomavirus 10 (HPyV10)	condyloma sample from a patient with Hypogammaglobulinemia, wart and Myelokathexis Syndrome (WHIMS)	there is a suspicion of its correlated with Hypogammaglobulinemia, wart and Myelokathexis Syndrome (WHIMS)	Rolling circle amplification	(Buck et al., 2012).
Mexican polyomavirus (MXPvV)	stool samples	Is not yet been associated with disease	Unbiased deep sequencing	(Yu et al., 2012).
Malawai polyomavirus (MWPvV)	stool sample	Is not yet been associated with disease	Real-Time PCR & Pyrosequencing Strategy	(Siebrasse et al., 2012).
Saint Louis polyomavirus (STLPvV)	stool sample	Is not yet been associated with disease	Multiple displacement amplification (MDA)	(Lim et al., 2013)
human polyomavirus 12 (HPyV12)	liver, colon and rectum biopsies and feces	Is not yet been associated with disease	-Generic PCR -Real-time PCR -Conventional nested PCR	(Korup et al., 2013).
New Jersey polyomavirus (HPyV13-NJPvV-2013)	muscle biopsy of pancreatic transplant patient	may contributed to muscle and ocular damage	Electron microscopy and high-throughput nucleotide sequencing	(Mishra et al., 2014).





## 1.4 Merkel Cell Polyomavirus (MCPyV)

### 1.4.1 The Isolation of the Merkel Cell Polyomavirus

The Chang-Moore research group at the University of Pittsburgh revolutionised the principles of representation difference analysis (RDA) (Lisitsyn and Wigler, 1993). This assisted with their earlier finding of KSHV (Chang et al., 1994). By combining RDA with the available sequences of the complete human genome a new method, digital transcriptome subtraction (DTS), was devised. In 2008, the group used this new method to discover a viral agent in MCC called Merkel Cell Polyomavirus (MCPyV) (Feng et al., 2008). DTS combines high-throughput cDNA sequencing with *in silico* methods to exclude human sequences from tissue samples. cDNA libraries are created from each normal and diseased tissue sample by subjecting the sample to sequencing and then matching the results against human sequence databases (Feng et al., 2007). By scrutinising hundreds of thousands of cDNA sequences from four MCC tumours, the Chang-Moore research group identified a cDNA sequence that bore significant similarity to the large T antigens of lymphotropic polyomavirus that is known to initiate cancer in animal **model system** (Feng et al., 2008).

Using PCR walking method and primers derived from the DTS viral transcript, the complete closed circular genome of MCPyV 350 (5387 base pairs (bp)) and MCPyV 339 (5201 bp) were sequenced. In samples collect from **ten** MCC patients, MCPyV DNA was detectable by Southern blot **and** polymerase chain reaction products of 8 samples, leaving a small subgroup of MCC tumours in which the virus was absent (Feng et al., 2008).

Such findings were corroborated by subsequent studies, with MCPyV sequences isolated from the majority of MCC patients (80-97%) (Becker et al., 2009, Rodig et al., 2012, Bhatia et al., 2010). An important observation made by different studies is that most patients acquire the MCPyV infection by adulthood, as is the case with other human polyomaviruses (Nicol et al., 2013, Carter et al., 2009).

#### 1.4.2 The Life Cycle of MCPyV and tissue tropism.

Due to the discovery of MCPyV within a malignancy instead of its natural host cell, its cellular tropism is yet to be determined. Nonetheless, the host cell is likely to derive from an epidermal source, as indicated by the origin of the Merkel cell carcinoma and the observation regarding the skin shedding of MCPyV at regular intervals (Schowalter et al., 2010).

Whilst tissue tropism and the natural reservoir of MCPyV infection remain unknown, there has been a concerted effort to find an appropriate cell culture system for MCPyV to determine the oncogenic activity of the virus. Aiming to study MCPyV tissue tropism, Buck and colleagues used MCPyV-based vectors encapsidating a secreted Gaussia luciferase (Gluc) reporter plasmid (Pastrana et al., 2009). They expanded their study by using in addition to MCC tumour originating cell lines (WaGa, MaTi, UISO, and MKL-1), the NCI-60 panel of human cancer cell lines. The sixty different cell lines that **comprise** the NCI-60 panel are derived from brain, breast, colon, kidney, lung, ovary, and prostate tumours, as well as leukaemia and melanoma cell lines. In contrast to ovarian cancer cell line (NCI/ADR-RES), which produced the greatest MCPyV titre, leukaemia and colon cancer cell lines have been shown to be resistant to MCPyV transduction. The titre of the NCI/ADR-RES cell line was more than twice that of the MALME-3M melanoma cell line, which was the second most transducible cell line. The data reveals that MCPyV is able to transduce a wide range of solid tumours, but this finding is not duplicated in cultured cell lines, where MCPyV replication is weak (Schowalter et al., 2012). Spurgeon and colleagues tried to study the oncogenic activity of MCPyV LT by developing a tissue-specific mouse model. Expression of MCPyV LT and sT antigens in epidermal stratified squamous epithelial cells of mice and Merkel cells was induced by the expression of Human keratin 14-mediated Cre recombinase (Cyclization recombination enzymes). In response to expressing MCPyV T antigens, the mice developed different skin disorders including hyperkeratosis, hyperplasia, and thickened patches of skin called acanthosis. Further

abnormalities were observed in the eyes, footpads, and whisker pads. Almost 50% of the mice developed skin papillomas (Spurgeon et al., 2015).

Recently, Li and colleagues tried to develop a new cell culture systems to help in MCPyV genome replication and production of infectious particles. They used BTL-Tn 5B1–4 (also known as High Five, Tn5) cell line derived from the *Trichoplusia ni* moth and it appeared to be an effective generator of MCPyV-like particles. Yet the yield of viral particles created by the replication systems have not been employed for structural analysis, probably because of the low volume of virions generated (Li et al., 2015a) .

### 1.4.3 MCPyV Binding, Entry and Replication

For binding and entering cells, viruses utilise on interactions with particular receptor molecules on the host cells. Hence, a viral entry pathway is made up of a series of coordinated attachments between viral proteins and cellular receptors such as proteins or other biomolecules (Neu et al., 2012). MCPyV entry is initiated by the major capsid protein VP1, which attaches to cellular receptors to promote internalization and transport of the viral genome into the nucleus for replication. Unlike other polyomaviruses, including MPyV, SV40, BKPyV and JCPyV, which undertake cell binding and internalisation solely with carbohydrates containing sialic acid, MCPyV VP1 detects the disaccharide N-acetylneuraminic acid galactose motif (Neu5Ac-a2, 3-Gal) (Figure 1.2), through a shallow binding site on its apical surface (Neu et al., 2012, Tsai et al., 2003, Neu et al., 2013, Maginnis et al., 2014).

The crystal structure of VP1 identified that five VP1 monomers arranged around a central five-fold axis to form a symmetric ring shape of homopentamer. Each of VP1 monomer is consist of two  $\beta$ -sheets which form a  $\beta$ -sandwich with jelly-roll topology. This unique structure looks to be important for virus to interact with cell surfaces (Neu et al., 2012).

The singular character of MCPyV among members of the Polyomaviridae family is further reinforced by the fact that VP1 mutations do not prevent

MCPyV pseudovirions from binding to cells (Neu et al., 2012, Schowalter and Buck, 2013).

VP1 mediates MCPyV entry by binding initially to sulphated carbohydrates called glycosaminoglycans (GAGs) (e.g. heparin sulphate and chondroitin sulphate). Post-attachment of VP1 with Sialic acid is crucial for a post-attachment step of MCPyV infection (Neu et al., 2012, Sapp and Day, 2009).

Following the interaction between VP1 and GT1b, the virus is transferred in a retrograde way to the endoplasmic reticulum (ER) lumen and the caveolin-free membrane structures. Endocytosis mediated by caveolae leads to internalisation of MCPyV, which is then transferred through the cytoplasm of the host cell to the ER. At the ER, MCPyV is uncoated during infection, while endosomal and lysosomal trafficking enable viral genomes to migrate from the cell membrane to the nucleus, where they are imported by the nuclear import mechanism of the host (Schowalter and Buck, 2013).

Right after uncoating and transfer of the episomal viral genome to the nucleus, the transcription of the early region is **initiated at the early promoter**. This process relies on T antigens and therefore their transcription occurs immediately after enters the cell nucleus. Under the action of these genes, the cells enter the S-phase, the cellular environment being modified to enable viral replication (Puntener and Greber, 2009). When T antigen expression reaches adequate levels, the MCPyV genome-encoded miRNA is likely to suppress further early gene transcription in order to "**prioritise**" viral replication and transcription of late region capsid **gene** (Theiss et al., 2015). MCPyV is similar to other polyomaviruses in its necessity for T antigens to start genome replication. The oligomerisation of LT gives rise to hexameric molecules, two of which attach to the replication origin in a head-to-head orientation. Subsequently, viral DNA is unwound by the LT helicase and replication **proceeds** in a bidirectional way (i.e. hexamer movement in opposite directions) (Wessel and Schweizer, 1992, Kwun et al., 2009).

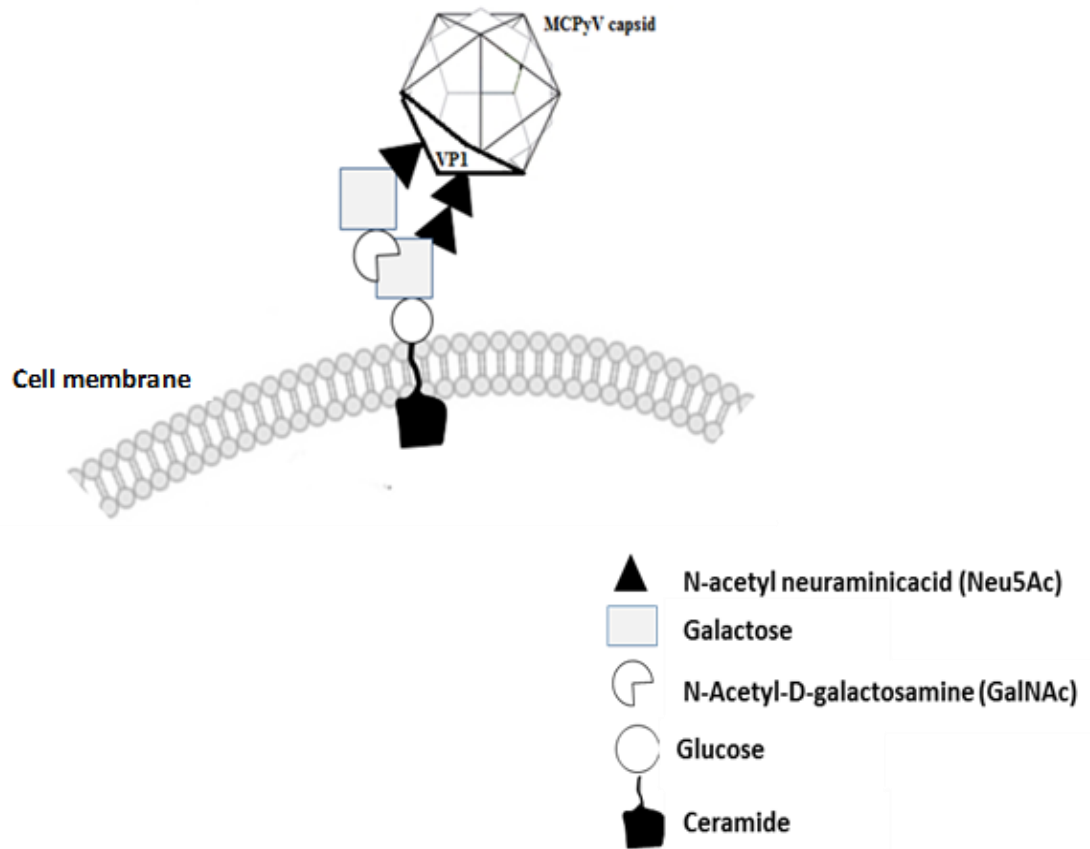


Figure 1.2: Schematic illustrates attachment of MCPyV to the plasma membrane. VP1 binds GTb1 which contains Neu5Ac, Galactose, Glucose and N-acetyl-D-galactosamine and all these may allow the virus to enter the cell through ceramide which diffuses within the cell membrane.

#### 1.4.4 Transmission of the Virus

MCPyV is part of the normal skin flora and therefore it can be found on all skin surfaces, similar to HPyV6 and HPyV7. It is believed that MCPyV causes a persistent skin infection, since the DNA sequence was observed to be the same on different skin surfaces of the same patient (Wieland et al., 2009, Schowalter et al., 2010, Duncavage and Pfeifer, 2011).

As highlighted by many studies, the prevalence of the infection among adults suggests that individuals become infected with MCPyV at a young age and this primary infection lacks symptoms (Martel-Jantin et al., 2013, Tolstov et al., 2009). However, no in-depth study has so far been conducted

on how the primary MCPyV infection is disseminated and transmitted or on the occurrence of a latent phase (Foulongne et al., 2010).

It has been reported that a proportion of 60-70% of individuals acquired primary MCPyV infections when they were younger than six years of age (Martel-Jantin et al., 2013). Although, it is unlikely that the virus is transmitted from mother to child because foetal autopsy samples were not found to contain MCPyV, perinatal transmission during birth might still occur. Nevertheless, the most probable mode of transmission of MCPyV is via saliva and/or skin contact, especially among young siblings and between mother and child, as indicated by correlations in MCPyV infection and serological status (Sadeghi et al., 2010).

Nasopharyngeal aspirates from children and adults were found to contain MCPyV DNA in a proportion of 0.6-1.3% and 2.1-8.5%, respectively (Carter et al., 2009, Bialasiewicz et al., 2009, Gaynor et al., 2007). Meanwhile, tonsils, lung tissues, and bronchoalveolar and bronchoaspirates displayed MCPyV in proportions of 3.5%, 6.7% and 17.2%, respectively. Therefore, an aerodigestive transmission mode is implied by the occurrence of MCPyV in both upper and lower respiratory tract (Saláková et al., 2015, Babakir-Mina et al., 2010).

On the other hand, cerebrospinal fluid, peripheral blood mononuclear cells, plasma/blood, brain or prostate tissue samples, or frozen autopsy samples from immunocompetent as well as immunosuppressed individuals did not exhibit MCPyV (Kassem et al., 2008, Gustafsson et al., 2013, Laude et al., 2010, Sadeghi et al., 2010). However, urine and serum samples were reported to contain MCPyV DNA sequences in a proportion of 15-25% and 0.1-12%, respectively (Husseiny et al., 2010, Bofill-Mas et al., 2010). MCPyV may also be transmitted via blood as its **presence in serum** was detected by some studies. However, given that the majority of adults possess MCPyV antibodies, this transmission mode is unlikely to have subsequent involvement (Carter et al., 2009). **Furthermore, contamination of urethral openings during urine sample collection may explain the low MCPyV copy number in urine** (Husseiny et al., 2010). Everything coming

into contact with people may display viral DNA presence, as 85% of environmental surfaces that were examined, including urban waste and river water, were found to contain MCPyV (Calgua et al., 2013, Bofill-Mas et al., 2010). The fact that the encapsulated DNA originated from possibly infectious viruses was suggested by the detection of viral MCPyV DNA in environmental surface samples following DNase treatment conducted prior to nucleic acid extraction (Foulongne et al., 2011). Another study corroborated this finding, therefore implying that individuals may also acquire MCPyV infection from environmental sources (Schowalter et al., 2010).

#### **1.4.5 Virus epidemiology**

A number of independent researchers have produced compelling evidence that MCC tumours sampled from various countries contained the MCPyV genome. Corroborating the initial findings of Feng and colleagues, the majority of studies detected MCPyV in a proportion of 80% of MCC tumours (Feng et al., 2008, Garneski et al., 2009, Ridd et al., 2009, Paulson et al., 2009, Loyo et al., 2010, Martel-Jantin et al., 2014). Healthy human skin is highly susceptible to MCPyV infection, which can occur throughout the surface of the body (Schowalter et al., 2010, Foulongne et al., 2010). In spite of this, MCPyV viral loads are over 60 times higher in MCC tumours than in other skin sites. The geographical location of the research population, the conditions under which tissue samples are stored, PCR type and primer set are the major factors that determine the extent to which MCPyV DNA can be detected in tissue samples. In the populations that have been investigated, measurements based on ELISA or Luminex assays designed to identify MCPyV-specific IgG antibodies revealed a consistently high MCPyV seroprevalence, in the range of 46-88% (Touzé et al., 2010).

The results of a MCPyV epidemiological research conducted on a healthy population from China indicated that females exhibited lower seropositivity than males (57.7% vs 64.5%); nonetheless, seropositivity increased with age in both males and females. By contrast, sexual behaviour and MCPyV

seropositivity were not found to be correlated (Zhang et al., 2014). The relation between age and seropositivity was highlighted by Viscidi and colleagues as well, observing that children younger than 10 years old had a 45% seroprevalence, which rose to 60% in the following ten years and reached the highest percentage at 60-69 years of age (81%) (Viscidi et al., 2011).

MCPyV seroprevalence was confirmed in around one-fourth of tested children. Investigating children 1-5 years old, Kean and colleagues obtained a seroprevalence of 20.5%, while children 2-5 years old were found to hold seroprevalence in a proportion of 43% (Kean et al., 2009).

In a more recent study on 1-12 year-old children from Sweden, Faust and colleagues documented a seroprevalence of 32%. Moreover, among children younger than 3 years old who were found to be MCPyV-seronegative, 33% seroconverted when subjected to new testing 5-8 years after initial testing. Meanwhile, 9% and 35% seroprevalence was detected in children 1-4 years old and 4-13 years old, respectively (Faust and Dillner, 2014, Chen et al., 2011).

#### **1.4.6 The Genome Structure of MCPyV**

MCPyV does not differ significantly from other polyomaviruses in terms of genetic composition (Feng et al., 2008). A circular DNA genome with double strands and 5387 base-pairs is displayed by the prototype virus MCV350 (Figure 1.3). Since MCPyV is a polyomavirus, its genome presents bidirectional early and late coding regions between which is the non-coding regulatory region (NCRR) containing the **regulator of viral replication**. Although they are similarly long, early and late transcripts are encoded on parallel strands of the viral genome (Feng et al., 2008, Shuda et al., 2008). The MCPyV genome shows the greatest similarity with the African Green Monkey lymphotropic polyomavirus (Dalianis et al., 2009).

A temporally-modulated cascade of gene expression is enabled by the separation of the early and late transcriptional units and is associated with the beginning of viral DNA replication, which is similar to that of other DNA viruses (Feng et al., 2011). Infection is immediately followed by expression of the early genes related to the T antigen locus, which take part in viral genome replication. DNA replication is followed by the transcriptional activation of the late region for expression of the gene products constituting the structural elements of the viral capsid and participating in the production of progeny virion in the late infection phase (Cole, 2001). However, although it shares these features with other polyomaviruses, the MCPyV viral genome also presents a number of singular features. For instance, Merkel cell polyomavirus is more similar to murine polyomaviruses than to other human polyomaviruses with regard to the gene products of early (large and small T antigens) as well as late regions (VP1 and VP2) (Feng et al., 2008).

As in the case of other polyomaviruses, a 71-base pair minimum replication origin is incorporated within the NCRR of MCPyV, possessing an AT-rich tract which participates in DNA melting, a region comprising 8 G(A/G)GGC pentanucleotide sequences that are responsible for attaching the origin-binding domain (OBD) in the LT core in order to regulate the aggregation of LT proteins on the DNA. However, unlike other polyomaviruses, a greater number of pentanucleotide sequences are present within the MCPyV origin, they are more closely associated and four of them play a crucial role in virus replication (Feng et al., 2008, Johnson, 2010).

Recent studies detected the association between the OBD of MCPyV LT and a segment of the MCPyV replication origin, which confirmed that LT proteins attached to the replication origin are the sites of OBD-OBD intermolecular interactions. Moreover, the singular combination of pentanucleotide sequences necessary for successful MCPyV replication was described and validated by the crystal structure (Kwun et al., 2009). However, due to the greater spatial division between OBD-binding pentanucleotide sequences, the SV40 origin does not exhibit these intermolecular interactions (VanLoock et al., 2002, Wessel et al., 1992).

However the NCRR also contains bidirectional transcriptional promoters and regulatory elements for early and late viral gene expression. (Harrison et al., 2011, Shuda et al., 2008). Four of these pentanucleotide sequences sites are absolutely required for virus replication (Kwun et al., 2009).

#### **1.4.6.1 The Early Region**

The early coding region of the MCPyV genome produces four proteins translated from transcripts that result from differential splicing. Known as tumour antigens or T antigens, these proteins led to the labelling of the early region as the “T antigen locus”, comprising Large and Small T antigens (LT and sT), 57kT (Feng et al., 2008, Shuda et al., 2008), as well as alternative Large T open reading frame (ALTO) that was most recently identified (Carter et al., 2013). The first three have the same N-terminal 78 amino acids but terminate at different C-terminal residues. The 57kT and LT are identical except for a deletion in the C terminal region of the protein (Figure 1.4). In addition, The ALTO results from a +1 frameshift relative to the second exon of LT. The function of 57kT and ALTO in MCPyV genome replication is currently unclear (Carter et al., 2013).

##### **1.4.6.1.1 Large T Antigen**

The MCPyV LT antigen is composed of two exons that are responsible for encoding 816 amino acids. It shares many functionally important roles with LTs of other polyomaviruses, for example regions implicated in viral replication. MCPyV LT shares about 30% amino acid identity with other human polyomaviruses. They share the same LXXLL sequence, known as conserved region 1 (CR1) and LXCXE sequence, called the retinoblastoma protein (pRB) binding motif (except for HPyV12, which lacks a recognisable pRB binding domain) (Korup et al., 2013). **Similar effect of LXCXE domain of DNA tumour viruses, including E7 from human papillomavirus (HPV) and**

E1A from adenovirus showed to be required for inhibiting retinoblastoma tumour suppressor and antagonizing with DNA sensing (Lau et al, 2015).

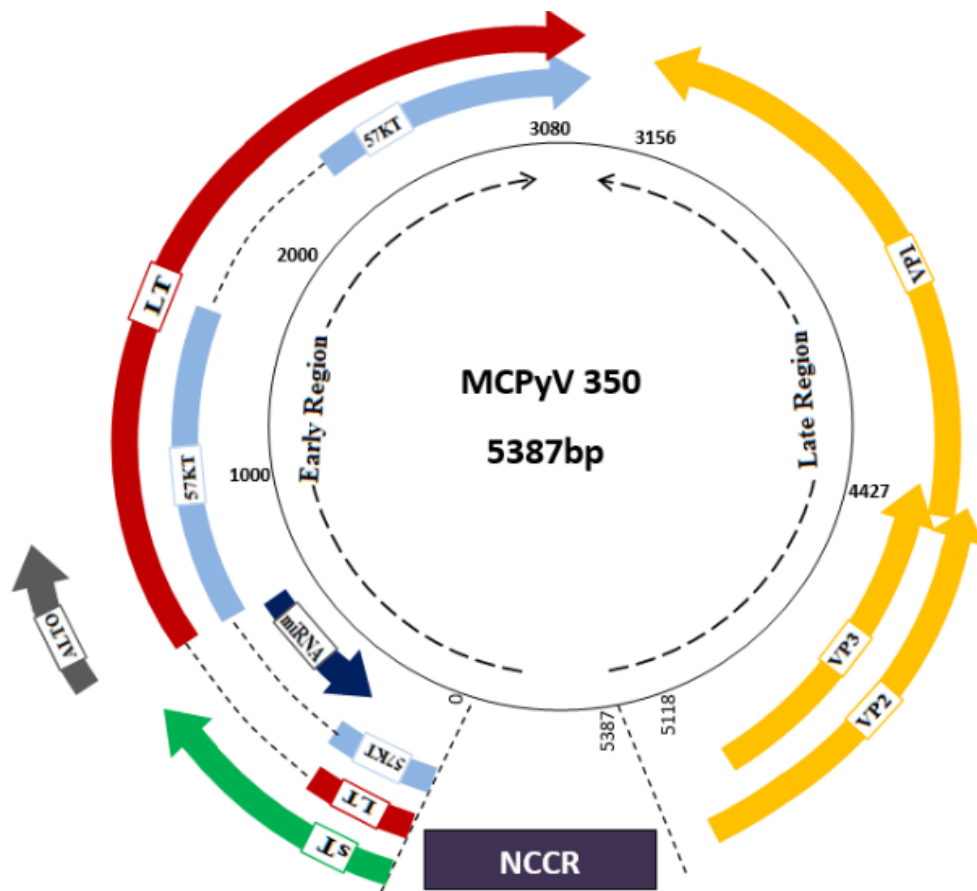


Figure 1.3 Genome organisation of MCPyV. MCPyV strain 350 composed 5387bp and organised into three regions: early region, late region and non-coding control region (NCCR). Proteins illustrated as coloured arrows. Early region contains Large T antigen (LT, Red); Small T (sT, Green); 57KT protein (Light Blue), ALTO (Gray) and miRNA (Dark Blue). The structural proteins VP1, VP2 and VP3 are shown in yellow colour.

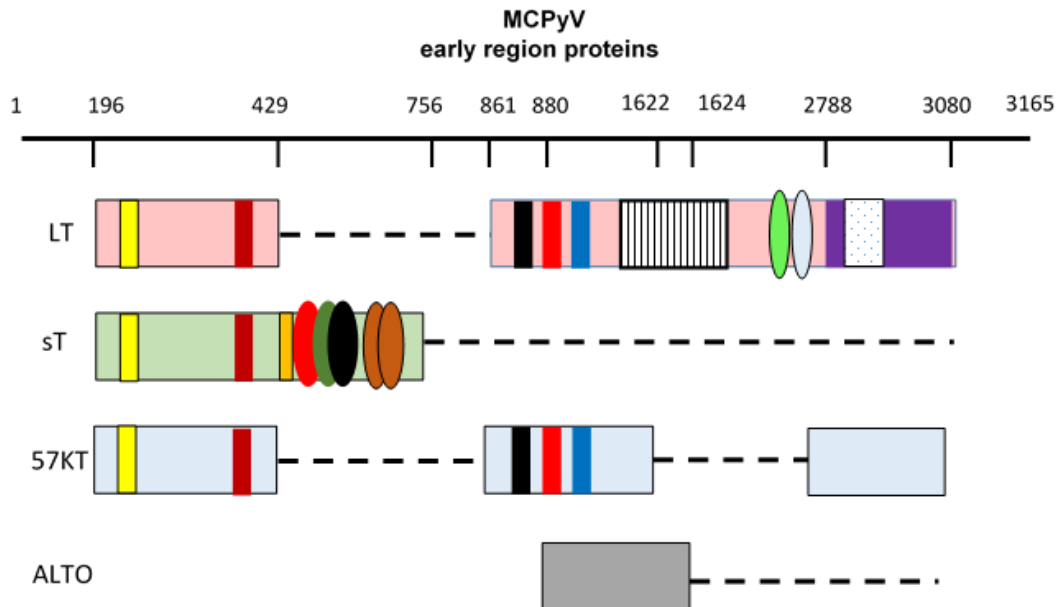
In addition, the conserved DNA binding domain and helicase domain constitute the components of the C-terminus. The majority of the domains that participate in viral DNA replication, such as OBD, ATPase domain, and helicase domains, are found in the carboxyterminal half of LT, which is also where tumour-specific mutations occur (Figure 1.5) (Shuda et al., 2008, Nakamura et al., 2010). After MCPyV LT translation, it recognizes and interacts with GAGGC pentanucleotide repeats within the viral origin.

In turn, this interaction is responsible for triggering core origin melting and unwinding, after which host replication factors like polymerase  $\alpha$  primase bind and are required for initiation of viral and replication (Kwun et al., 2009). The full-length LT sequence can integrate into the host cell genome and initiate its DNA replication. However, integration of this full length LT may lead to replication fork collision and cause DNA breakage leading to cell death (Tsang et al., 2014).

Moreover, it was observed that MCPyV DNA integration in the MCC genome exhibited mutation in the C terminus of LT, resulting in truncated LT expression. In addition, transcription is also modulated by LT, which is of significance during infection, as it inhibits early transcription and at the same time it promotes late viral gene expression. The capacity of LT to activate viral origin DNA replication was significantly affected by LT phosphorylation at amino acids T297 and T299 (Diaz et al., 2014).

The interaction between LT and the RB family (pRB, p107 and p130) led to the discovery that LT is involved in cell transformation. Underpinning the LT-pRB interaction, pRB negatively modulates cell transformation by preferentially interacting with the E2F transcription factor. The expression of genes involved in cell progression is controlled by E2F in an inactive state when attached to pRB (Borchert et al., 2014). The E2F-pRB interplay is interrupted by particular cyclin-dependent kinases that phosphorylate pRB, leading to the regulation of the expression of genes necessary for cell cycle progression. Studies on the correlation between the MCPyV DNA level and pRB expression level in MCC provided evidence that, in MCC, the level of MCPyV DNA and the level of pRB were directly proportional (Bhatia et al., 2010).

A chaperone DnaJ domain (HPDKGG), which recognize heat shock protein 40, (Hsp40) is another key domain in the LT C-terminal whose interaction with the heat-shock protein cognate 70 (Hsc 70) is considered to be essential for viral replication (Whalen et al., 2005). This **interaction** is also responsible for interrupting the interaction between pRB and E2F, leading to E2F release (Kwun et al., 2009).



	conserve region 1 (CR1)		Zinc finger
	A chaperone (DnaJ)		Leucine Zipper
	MCPyV-unique region (MUR)		NEMO domain
	hVam6p		PP4C domain
	Retinoblastoma Protein (pRB)		PP2A A $\beta$
	LT Stabilization Domain (LSD)		PP2A A $\alpha$
	Origin Binding Domain(OBD)		ATPase-Helicase

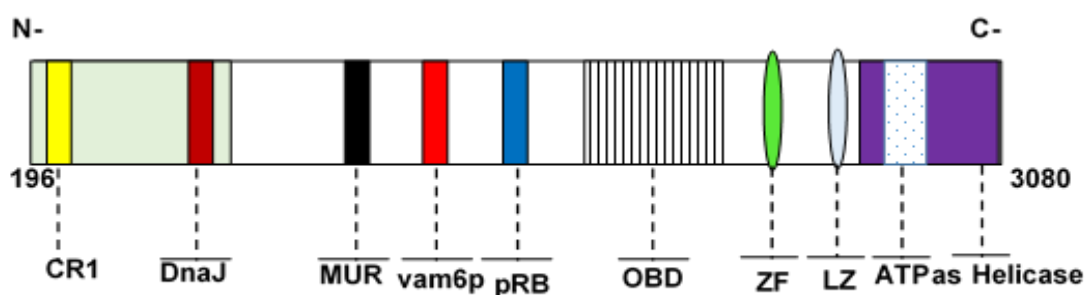
Figure 1.4 Schematic illustration early region proteins of MCPyV. LT, sT, 57KT and ALTO protein. LT, sT and 57KT have conserve of N-terminal domains, each has conserved region 1 (CR1) and DnaJ domains. At the C-terminus of LT and 57KT there are conserve of vam6p, pRB and MUR domains. The sT contains unique domains near to the C-terminus, a domain of 5 amino acids (91-95) called the LSD required for stability of LT, different domains for interaction with NEMO, PP4C, PP2A A $\beta$  lie between residues (95-111) and two motifs for binding PP2A A $\alpha$  (R7 and L142). LT has conserved unique C-terminal regions, OBD, zinc fingers and leucine zipper, ATPase-Helicase.

Unlike the case of SV40 LT, MCPyV LT has not been confirmed to bind the tumour suppressor protein p53 directly, but MCPyV-positive MCC cells were observed to contain a low level of p53. Furthermore, compared to full-length LT, truncated LT derived from an MCC tumour was not reported to have any impact on p53 expression, due to the fact that no p53 binding domain is possessed by the tumour-related T antigen deletion mutations occurring in the LTs of MCC-related MCPyV genome (Shuda et al., 2008, Borchert et al., 2014).

Clearly, SV40 and MCPyV LTs must have different mechanisms to modulate p53. In SV40, LT induces DNA damage stimulated kinases that phosphorylate and activate p53, whereas MCPyV LT stimulates the kinases to activate p53 leading to an induction cell of cycle arrest and inhibition cell of proliferation (Li et al., 2007b).

Belonging to the group of apoptosis inhibitors (IAP), Survivin or baculoviral inhibitor of apoptosis repeat-containing 5 (BIRC5) is an oncoprotein recruited by MCPyV LT to prevent infected cells from dying. The findings indicated that, in contrast to MCC without MCPyV association, MCC associated with MCPyV exhibited a sevenfold increase in Survivin expression. The Survivin expression level declined as a result of LT knockdown, and this provided evidence not only for the relationship between LT and Survivin but also for the key role played by Survivin in cell survival (Arora et al., 2012).

Another feature that distinguishes MCPyV LT from other polyomaviruses is that it includes a 200 amino acid region known as MCPyV-Unique Region (MUR). The significance of this region arises from its interaction with the vesicle-associated membrane protein (Vam6p), which, after it is expressed in transfected cells, exhibits a cytosolic distribution and induced perinuclear lysosome clustering. Furthermore, Vam6p is relocated to the nucleus as a result of being co-expressed with MCPyV LT during interaction with LT and lysosome clustering suppression (Figure 1.5) (Liu et al., 2011).



#### 1.4.6.1.2 The 57kT protein.

The 57 kDa protein (57kT) is encoded by the MCPyV early region. Its initial

Figure 1.5 Schematic illustration binding domains of MCPyV LT which contains 2884 pb. In N-terminal there are conservative region 1 (CR1, Yellow) and DnaJ (Black Red), in early C-terminal there is MCPyV-unique region (MUR, Black) and in C-terminal there are vesicle-associated membrane protein (Vam6p, Red), Protein Retinoblastoma (PRB, Blue), Origin Binding Domain(OBD, strips) and in the end of C-terminal there are Znic finger domain (ZF, Green), Leucine Zipper (LZ, light blue), ATPase domain (dotes) and at the extreme is Helicase domain (Purple)

expression follows co-transfection with LT and is succeeded by expression of other viral proteins. The protein comprises 432 amino acids divided into three exons. Aside from the CR1 and DnaJ domains, the same 78 amino acids at the N-terminus are contained by the first exon of LT as well as sT (Feng et al., 2008). Similarly, the LT binding domains in the second exon are the same as those of pRB, nuclear localisation signal (NLS) and OBD, whilst also possessing the same 200 amino acids of MUR in LT. The third exon has the same 100 amino acids as the C-terminus of LT. However, the role played by 57kT in the life cycle of MCPyV remains unknown. Furthermore, viral replication has not been observed to be affected by the interaction of 57kT with LT or sT (Feng et al., 2008, Shuda et al., 2008). Interestingly, SV40 was noted to generate an analogous protein, termed the 17kT antigen (135aa), which was reported to have some effect on the phenotype of rat fibroblast cells (Zerrahn et al., 1993).

#### 1.4.6.1.3 ALTO protein.

The discovery in the early region of the alternative large T open reading frame (ALTO) as the outcome of overprinting of the LT second exon was made during studies of the replication of the MCPyV genome. Just like LT,

the C-terminus of ALTO contains the residues 880-1624. Further research has demonstrated that only MCPyV and three hominoid polyomaviruses (ChimpPyV1, ChimpPyV2, and GorillaPyV1) encode this protein. Furthermore, ALTO shares similarities with the Middle T antigen (MT) of murine polyomavirus (MPyV), as they are both the result of LT overprinting, whilst also displaying a correlation with the transforming protein of MPyV MT via a conserved hydrophobic C-terminus (Carter et al., 2013).

It thus describes a previously unknown group of mammalian polyomaviruses, encompassing PyVs from mouse, hamster, raccoon, bat gorilla, chimp and human, and spanning the same C-terminal region of both MCPyV and MPyV (Fluck and Schaffhausen, 2009). However, in comparison to MT, the transforming activity of ALTO on MCPyV genome replication has not been established so far. Empirical studies have pointed to the fact that viral DNA replication is not influenced by whether or not ALTO is present (Carter et al., 2013).

In unpublished data, Carter and colleague shed new light on ALTO. In particular, they highlighted two regions with homologous sequences between MCPyV and MPyV, namely, the C-terminal hydrophobic domain involved in MPyV subcellular localisation and transformation activity, and a region circumscribing a tyrosine subjected to MT phosphorylation (Y322) and in charge of activating Phospholipase C gamma 1 (PLCG1). Activation of PLCG1, which required is to activate a family of non-receptor tyrosine kinases called (SFKs), was associated with overexpression of ALTO as a result of ALTO Y114 phosphorylation. Moreover, MT interacted with members of SFKs like (Src, Fyn and Yes). Phosphorylation of Y114 in ALTO was enhanced when ALTO and SFKs were co-expressed. Since SFKs exhibit a number of identical biological features, they may help to improve understanding of how ALTO is involved in MCPyV replication (Carter et al. personal communication).

#### 1.4.6.1.4 Small T Antigen (sT)

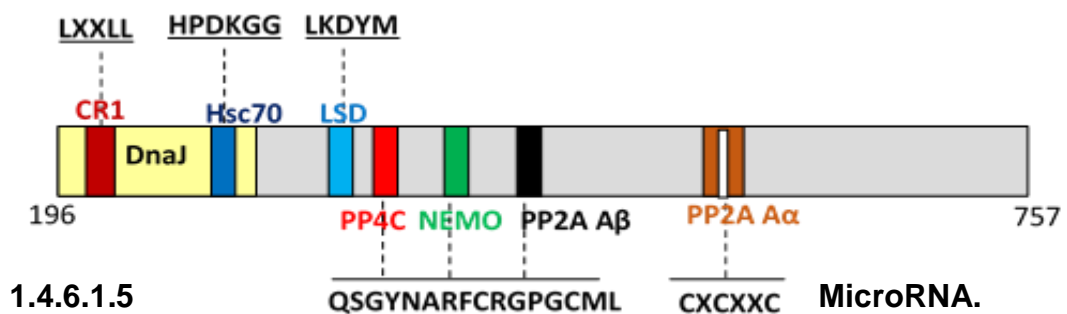
MCPyV sT contains 186 amino acids. In the N-terminus, it shares 78 amino acids with LT and 57KT. It has the same conserved region 1 (CR1, LXXLL) and heat shock protein binding DnaJ motifs (HPDKGG). In contrast to LT, the role of CR1 and DnaJ domains in sT is not clear. However, the C-terminus of sT (80-186) is not conserved in LT or 57KT. This unique region contains essential binding domains for interactions with a number of cellular proteins (Figure 1.6) (Feng et al., 2008, Shuda et al., 2008).

Mutagenesis screening studies have emphasized MCPyV sT, like other polyomaviruses, possesses a capability to target protein phosphatase 2A (PP2A) **which will be discussed in detail in section 1.8.1** (Pallas et al., 1990, Kumar and Rangarajan, 2009, Bollag et al., 2010, Berrios et al., 2014). With the fact that the role of sT of these viruses is different, SV40 and JCPyV use their sT to bind PP2A to influence cell transformation and cell cycle progression whereas targeting of MCPyV sT to PP2A is not critical for transformation properties. Mapping studies showed that the interaction between MCPyV sT and the structural sub-unit A isoform  $\alpha$  of PP2A was dependent upon residues R7 and L142 in sT. Substitutions in R7 and L142 disrupted the sT/PP2A binding interaction but retained their ability to transform rodent fibroblasts (Shuda et al., 2011, Rodriguez-Viciana et al., 2006). In contrast, the sT-PP2A complex is essential for SV40 infection (Guernon et al., 2011, Hahn et al., 2002).

With roles in LT stabilisation and viral replication, the LT-stabilisation domain (LSD) is an additional sT binding site that was recently delineated within residues 91-95. This is an important region for targeting the complex of Skp1, Cul1, and F box protein ubiquitin ligase protein complex, SCF<sup>Fbw7</sup>, which is known as the Cellular Ubiquitin Ligase (Kwun et al., 2013). The function of SCF<sup>Fbw7</sup> is to suppress MCC viral replication by targeting LT and breaking it down by the proteasome. In turn, SCF<sup>Fbw7</sup> is targeted by sT with the purpose of hindering proteasomal degradation of LT, hence activating cell transformation. This clearly illustrates how MCPyV sT and LT cooperate to benefit the development of MCC. What is more, research on rodents

revealed that the recently delineated LSD domain of MCPyV sT might alone be involved in cell transformation, in addition to LT stabilisation and viral replication. Meanwhile, LSD domain mutations make sT unable to trigger transformation. However, unlike other polyomaviruses, this capability of sT has no connection to PP2A, as demonstrated by the fact that sT continues to bind PP2A after mutations impair its ability to trigger transformation (Kwun et al., 2013).

Another interaction partner for MCPyV sT was identified by Griffith and colleagues which observed the existence of a key sT binding domain in the proximity of its C-terminus in residues 96-111, which was associated with NEMO and two protein phosphatases, namely, protein phosphatase 4 (PP4C) and a sub-unit of  $\beta$  isoform of protein phosphatase 2A (PP2A A $\beta$ ). The immune response of the host is disrupted by the interplay between sT and these cellular proteins. The cause of this disruption is the fact that the interaction of MCPyV sT with NEMO interferes with the immune signalling pathway of Nuclear Factor kappa-light-chain-enhancer of activated B cells (NF- $\kappa$ B) (Griffiths et al., 2013). It is worth noting that the upregulation of NF- $\kappa$ B activation by SV40 sT is dependent on PP2A (Moreno et al., 2004).



It is Figure 1.6 Schematic illustration multiply spliced of MCPyV sT domains. CR1 form sequences (LXXLL) domains in C-terminus (Dark red), DnaJ-Hsc70 (HPDKGG) (Yellow), and LSD (light blue) refers to LT stabilization domain (LKDYM). Domains of three cellular proteins PP4C, NEMO PP2A A $\beta$  and PP2A A $\alpha$  located within residues 95-111 and coloured as red, green black respectively. Two binding sites of PP2A A $\alpha$  (R7 and L142) (Brown).

hypothesised that genes involved in fostering immune evasion and regulation

of viral DNA replication are targeted by a virus-encoded microRNA (miRNA). A 22-nucleotide viral miRNA expressed by the MCPyV genome to form two mature miRNA (MCPyV-miR-M1-5p) and (MCPyV-miR-M1-3p) (Seo et al., 2009). Evidence confirms that the miRNA-M1 of MCPyV possesses an ability to decrease the expression level of viral genes which are essential for viral DNA replication (Theiss et al., 2015). The complete reverse complement of miRNA to MCPyV LT sequence near the LXCXE motif **suggests that this early protein is targeted by miRNA which induces LT gene silencing by binding the target site of mRNA and subsequently preventing LT production either by suppressing protein synthesis or by initiating mRNA degradation** (Seo et al., 2009).

The role of miRNA on DNA replication of SV40, murine PyV, and BKPyV and their LT expression level was illustrated by knock down of their miRNAs which showed that the lack of miRNA increased the level of LT and DNA replication in these viruses (Zhang et al., 2014, Sullivan et al., 2005, Broekema et al., 2013). Additionally, various cellular targets with roles in transformation may also be affected by the miRNA (Houben et al., 2010, Seo et al., 2009, Scaria and Jadhav, 2007). The findings of one study revealed that around half of MCPyV-positive MCC tumours had conserved miRNA expression, the level of which was dependent on the viral genome copy number (Lee et al., 2011). Further research is needed to elucidate the function of MCPyV miRNA in MCC tumours. A close correlation between miRNA overexpression and MCC metastases, as opposed to normal MCC, was reported and may provide an indication regarding miRNA function (Xie et al., 2014).

#### **1.4.6.2 Structural Proteins encoded by the Late Region**

The late region of viral DNA expresses the structural proteins consisting of VP1, VP2, VP3 and in some polyomaviruses VP4. These proteins are required for the initial interaction between the virus and the target host cell. Like other polyomaviruses, MCPyV is non-enveloped and its capsid consists of 360 capsomers of the major capsid protein VP1. VP1 is arranged in 72 pentamers in the outer side of the capsid and each of the 72 pentamers is

linked with one copy of either VP2 or VP3. This structure provides the icosahedral form of the virus capsid (Campanero-Rhodes et al., 2007, Low et al., 2006, Erickson et al., 2009, Schowalter and Buck, 2013). By contrast to other polyomaviruses, the third capsid gene, VP3, cannot be detected in MCPyV-infected cells. This is consistent with the fact that MCPyV was less affected by VP3 knockdown than by VP2 knockdown, which reduces native MCPyV infectivity by 100 times. Unlike VP1 and VP2, a functional VP3 protein is not encoded by MCPyV, as the conserved M, A and L motif underlying the amino-terminus of other polyomavirus VP3 proteins is absent in MCPyV (Schowalter and Buck, 2013).

## **1.5 MCPyV sT Involvement in Viral Replication and Cell transformation**

Despite the lack of clarity surrounding the processes through which MCPyV triggers transformation, a number of findings have indicated that MCPyV tumour antigens mediate cellular transformation and replication.

It has been suggested that MCPyV LT is the primary viral oncoprotein underpinning MCC transformation, while sT has merely a secondary role; however, sT is capable of triggering serum-free human cell proliferation, something which LT cannot do (Feng et al., 2008). By contrast to SV40 sT antigen, MCPyV sT can not only mediate transformation by LT, but also trigger it on its own (Saenz-Robles et al., 2001). This has been confirmed by the fact that MCC cell development and replication were retarded by sT knockdown (Kwun et al., 2009, Shuda et al., 2011).

Transformation of rodent fibroblasts and serum-free growth of human fibroblasts were not promoted by MCPyV LT expression, but by sT expression. This conclusion was derived from experimental work involving the cloning of codon-optimised cDNAs for MCPyV sT and LT into lentivirus vectors followed

by expression in Rat-1 fibroblast cells. Dense foci were observed to be formed solely in cells with sT expression and not by the empty vector (Shuda et al., 2011).

Stimulation of the hyperphosphorylation of Eukaryotic initiation factor 4E (eIF4E) binding protein (4E-BP1), an important protein translation regulator, is one potential mechanism through which cell transformation is regulated by sT. In eukaryotes, translation initiation is enabled at the mRNA 5' cap to which the eIF4F multi-subunit translation factor promotes ribosomal binding to mRNAs that have a 5'-methylguanosine cap (Buchkovich et al., 2008). The 4E-BP1 is an important regulator of this process. 4E-BP1 isolates eIF4E, preventing the association of ribosomal subunits with the capped mRNA. Studies have emphasised the significance to tumorigenesis of cap-dependent translation controlled by the phosphatidylinositol 3-kinase (PI3K) in the PI3K-AKT-mTOR signalling pathway (Fukuglta et al., 1994, Polivka and Janku, 2014, Musa and Schneider, 2015). Induction of cap-dependent translation may be a factor in tumour cell growth, as demonstrated by rodent cell transformation detected in response to overexpression of eIF4E (Avdulov et al., 2004, Truitt et al., 2015). Manipulating cell transformation in this manner can make the pathway attractive for viruses to exploit. For example, poliovirus cleaves eIF4F, inactivating the complex, and preventing cap-dependent translation and activates the translational repressor 4E-BP1 (Gingras et al., 1996). Adenovirus stimulates PI3K-AKT-mTOR signalling to activate phosphorylation of 4E-BP1 early on during infection (Arias et al., 2009). Similar to that, respiratory syncytial virus (RSV) by unknown mechanism able to enhance 4E-BP1 phosphorylation to activate viral replication (Pérez-Gil et al., 2015).

SV40 also showed capable to activate eIF4E through interaction of SV40 sT to PP2A and prevent dephosphorylation of protein kinase B (AKT) and as a result prevent 4E-BP1 dephosphorylation which releases eIF4E and promotes cell transformation (Yu et al., 2005, Hahn et al., 2002, Rodriguez-Viciana et al., 2006). In contrast to SV40 sT, the interaction between MCPyV sT and PP2A A $\alpha$  did not induce the activation of AKT (Shuda et al., 2011).

MCPyV sT was noted to act downstream, thus preserving 4E-BP1 hyperphosphorylation; this resulted in impaired cap-dependent translation. Shuda and colleagues found that the MCPyV sT-initiated inhibition of 4E-BP1 dephosphorylation or turnover resulted in elevated steady-state levels of hyperphosphorylated 4E-BP1 leading to dysregulated cap-dependent translation (Beretta et al., 1996). It is reasonable to conclude that the phenomenon is not a result of sT interaction with PP2A A $\alpha$ ; the sT mutants (R7A and L142A), which prevent sT binding to PP2A, demonstrated the same behaviour as wild type sT, preserving their ability to hyperphosphorylate 4E-BP1 and not influencing 4E-BP1 levels stimulated by MCPyV sT (Shuda et al., 2011).

**MCC is highly metastatic and has the potential to spread to a number of sites** including the pancreas, stomach, breast, lymph node and others, in some cases it may lead to death (Bernstein et al., 2014, Vernadakis et al., 2013). Knight and colleagues confirmed that cells expressing MCPyV sT increased their motility and migration (Knight et al., 2015). Expression levels of proteins related to microtubule assembly were increased in the presence of MCPyV sT in contrast to non-transfected cells (Knight et al., 2015). Furthermore, by using scratch and Transwell migration assays, expression of sT was shown to up-regulate cell migration. Stathmin, also named Oncoprotein 18 (Op18), is a microtubule-binding protein, which regulates polymerization of the microtubule network. Phosphorylation of stathmin leads to a release of tubulin and helps microtubule network assembly. MCPyV sT interacts with stathmin and reduces its phosphorylation (Griffith et al., 2013). The effects of the PP2A A $\alpha$ , PP2A A $\beta$  and PP4C phosphatases on stathmin phosphorylation in presence of MCPyV sT were analysed and showed that PP2A A $\alpha$  effects the stabilization of microtubules in control as well as the MCPyV sT transfected cells. In addition the mutant sT-R7A, which stops binding of PP2A A $\alpha$  (Shuda et al., 2011, Griffith et al., 2013) conserved its ability to destabilize microtubules. The other phosphatases PP4C and PP2A A $\beta$  caused stabilization in infected cells and the mutant sT-  $\Delta$ 95-111, which diminished the interaction with PP4C and PP2A A $\beta$  (Griffith et al., 2013), caused microtubule stabilization. These data suggest that MCPyV sT recruits

PP4C and/or PP2A A $\beta$  to mediate stathmin dephosphorylation and this may affect microtubule assembly and allow increased cell migration. This suggests a possible molecular mechanism for the highly metastatic phenotype associated with MCC (Knight et al., 2015). An observation on microtubule stabilization during viral infection suggested that viruses recruit their proteins to cause microtubule instability to help dissemination. For example, the core protein of Hepatitis C Virus (HCV) plays an essential role in viral entry by its interaction with microtubules and this leads to microtubule polymerization (Roohvand et al., 2009).

## 1.6 MCPyV Avoidance of the Immune System

The vital role played by the immune system is highlighted by the increasing amount of evidence pointing to the fact that the risk of MCC development is five to fifty times greater among individuals with dysfunctional T cells (Bhatia et al., 2011, Iyer et al., 2011, Afanasiev et al., 2013). Nevertheless, MCPyV-positive MCC may also occur in individuals whose immune system has not been compromised, implying that the immune system is not completely effective in targeting the virus and infected cells. As in the case of other chronic viral diseases, the immune response can be evaded by MCPyV by impairing the innate defence mechanism.

To detect viral dsDNA in epithelial and MCC cells, the immune system relies on the Toll-like receptor 9 (TLR9) which is suppressed by the MCPyV oncoproteins LT and sT (Shahzad et al., 2013). **TLR9 is one of the primary sensors that detect a wide variety of microbial components and elicits innate immune responses through activation of NF- $\kappa$ B, which regulates the expression of inflammatory cytokine genes. MCPyV LT mediates suppression of TLR9 through reduction in the mRNA levels** of the transcription factor CCAAT-enhancer-binding protein (C/EBP $\beta$ ) which interacts with the CCAAT motif that is contained in a number of gene promoters (Kawai and Akira, 2007). The involvement of sT alongside LT in TLR9 suppression is suggested by the fact that the mRNA levels of TLR9

rise slightly when sT is inhibited (Shahzad et al., 2013). Aside from MCPyV LT, BKPyV LT can also suppress TLR9, whereas the LTs of JCPyV, KIPyV and WUPyV cannot (Koralnik et al., 2001, Shahzad et al., 2013).

It is worth noting that C/EBP $\beta$  is actively involved in the regulation of IL-6, IL-8 and tumour necrosis factor alpha (TNF- $\alpha$ ) cytokine transcription (Li et al., 2007a). Furthermore, through down-regulation of cyclin-dependent kinase (CDK2 and CDK4) and E2F complex activity (Johnson, 2005), C/EBP $\beta$  also has an inhibitory effect on tumours. Hence, the immune response may be disrupted and cell proliferation promoted through C/EBP $\beta$  inhibition mediated by MCPyV LT (Shahzad et al., 2013). A comparative analysis of MCPyV-positive and MCPyV-negative tumours revealed that the former had a greater count of infiltrating CD8<sup>+</sup> T-cells (Lauttia et al., 2014).

The NF- $\kappa$ B signalling pathway has also highlighted the impact of MCPyV on the immune response. MCPyV has been shown to downregulate NF- $\kappa$ B which is involved in regulating several proinflammatory and antiviral response genes. By interacting with cellular proteins, including NEMO and cellular protein phosphatases, MCPyV sT induced down-regulation of the NF- $\kappa$ B pathway. This was identified by detection of a reduced level of p50 and RelA in the nucleus of MCC when stimulated with TNF- $\alpha$  in the presence of MCPyV sT. In addition, the phosphorylated form of IKK $\alpha$  and IKK $\beta$  was decreased following transfection of MCPyV sT (Griffiths et al., 2013). The importance of MCPyV sT in targetting NF- $\kappa$ B is still unclear. Some strategies of other viruses may explain the benefits to the virus in targetting the NF- $\kappa$ B pathway. Some viruses activate NF- $\kappa$ B to block apoptosis like HIV, whereas other viruses such as adenovirus inhibit the pathway to enhance viral replication (Zhang et al., 2012, Heimberg et al., 2001).

## 1.7 Modification of the NF- $\kappa$ B pathway by MCPyV sT.

### 1.7.1 Composition of NF- $\kappa$ B.

A range of biological processes, including inflammatory reaction, proliferation, cell apoptosis, embryonic and tissue development, as well as tumour development, are dependent on the transcription factor nuclear factor-kappa B (NF- $\kappa$ B) (Ghosh et al., 1995). However, of all of these processes, the role of NF- $\kappa$ B in regulating the innate immune response is best understood. It was over twenty years ago that this transcription factor was discovered in the laboratory of David Baltimore and was observed to have inducible activity with selective attachment to particular DNA motifs of around 10 bp called  $\kappa$ B sites, whilst at the same time it was capable of regulating target gene transcription (Gilmore and Temin, 1986, Baeuerle and Baltimore, 1988).

#### 1.7.1.1 NF- $\kappa$ B dimers

The NF- $\kappa$ B family is comprised of five polypeptide sub-units, which are classified in two sub-families (NF- $\kappa$ B and Rel). NF- $\kappa$ B can be composed of NF- $\kappa$ B1 (p105/p50) and NF- $\kappa$ B2 (p100/p52), encoded by *NFKB1* and *NFKB2* genes respectively. The Rel subfamily contains RelA (also known as p65), RelB and c-Rel are encoded by *RELA*, *RELB* and *REL* respectively (Ghosh et al., 1998).

By interacting with one another, these factors create homo- and heterodimeric complexes with distinct transcriptional activity. Up to fifteen distinct dimers can be produced by the members of the NF- $\kappa$ B protein family by associating in different ways. Nonetheless, no validation has been extended so far regarding the physiological existence and relevance for every potential dimeric complex (Ryseck et al., 1992). Among all the Rel dimers, the one present in nearly every type of cell is the p50/p65 heterodimer. Characterisations have also been made of the dimeric complexes p65/p65, p65/c-Rel, p65/p52, c-Rel/c-Rel, p52/c-Rel, p50/c-Rel,

p50/p50, RelB/p50, and RelB/p52, of which some occur solely in certain cell subsets (Dobrzanski et al., 1994) .

Furthermore, they have the same conserved amino-terminal Rel homology domain (RHD) of 300 amino acids (Müller et al., 1995). A number of processes require RHD sequences, including dimerization, DNA binding, interaction with nuclear factor of kappa light polypeptide gene enhancer in B-cells inhibitors (I $\kappa$ Bs), and nuclear translocation (Figure 1.7).

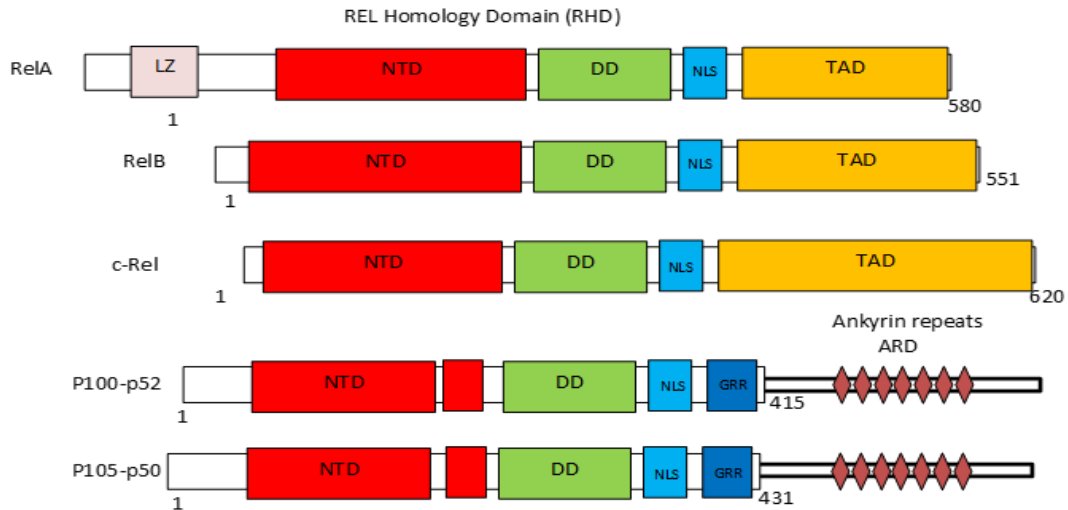
Specific DNA attachment to the NF- $\kappa$ B consensus sequence within regulatory elements of NF- $\kappa$ B target genes (5' GGGPuNNPyPyCC-3') is mediated by the amino-terminal part of RHD, while dimerization and interaction with I $\kappa$ Bs are underpinned by the carboxy-terminal part, as observed from crystal structures of p50 homo- and p50/p65 heterodimers attached to DNA (Ghosh et al., 1995). Several copies of an approximate 33 amino acid sequence, known as ankyrin repeats, are present in every known I $\kappa$ Bs and are responsible for facilitating the interaction between I $\kappa$ Bs and NF- $\kappa$ B dimers. The nuclear translocation of NF- $\kappa$ B is avoided through the interplay between the ankyrin repeats and a RHD region of NF- $\kappa$ B proteins (Kawai and Akira, 2007, Müller et al., 1995).

#### **1.7.1.2 I $\kappa$ B composition**

The inhibitor of NF- $\kappa$ B (I $\kappa$ B) was discovered in nine protein forms composed of I $\kappa$ B $\alpha$ , I $\kappa$ B $\beta$ , I $\kappa$ B $\epsilon$ , I $\kappa$ B $\zeta$ , I $\kappa$ B $\eta$ , Bcl-3, I $\kappa$ BNS in addition to the homolog p100 and p105 proteins (Verma et al., 1995). Three of these polypeptides, I $\kappa$ B $\alpha$ , I $\kappa$ B $\beta$  and I $\kappa$ B $\epsilon$  are associated with NF- $\kappa$ B dimers and contain both RelA and c-Rel subunit or at least one of them with other subunit, this complex leads to the prevention translocation of NF- $\kappa$ B to the nucleus (Anest et al., 2004).

The three classic isoforms I $\kappa$ B $\alpha$ , I $\kappa$ B $\beta$  and I $\kappa$ B $\epsilon$ , contain between 5-8 copies of an ankyrin repeat (Basith et al., 2013, Sachdev et al., 1998). It composed

of three main regions, the N-terminal region, where ubiquitination and inducible phosphorylation happens; the Ankyrin repeat domain (ARD) which



Figure

1.7

Schematic illustrates domain of the mammalian NF- $\kappa$ B family subunits. The five subunits are RelA (1-580bp), RelB (1-551bp), c-Rel (1-620bp), p100/p25 (1-415 bp) and p105/p50 (1-431bp). All subunits have the conserved Rel homology domain (RHD) consist of two folded domains referred to as the N-terminus domain (NTD, Red) and dimerization domain (DD, Green). A nuclear localization signal (NLS, light blue) lies at the extreme C-terminus of the RHD. A transcription activation domain (TAD, Orange) is located in the C-terminus. The p100 (p52) and p105 (p50) contains a glycine-rich region (GRR, Dark Blue) in addition to RHD. The C-terminus of p52 and p50 contain unique seven repeat sequences called Ankyrin repeat domain (ARD, Brown).

responsible for NF- $\kappa$ B binding, and an acid-based C-terminus sequence which is essential for basal degradation of unbound I $\kappa$ B $\alpha$  (Whiteside and Israël, 1997). I $\kappa$ B $\alpha$  in unstimulated cells freely shuttles between the cytoplasm and nucleus. However, the predominant migration in most cells is the nuclear export of I $\kappa$ B $\alpha$ , leading to its build up in the cytoplasm (Rao et al., 2010). During stimulation by bacterial lipopolysaccharide, oxidants, phorbol esters, proinflammatory cytokines, UV light and viral infection, I $\kappa$ B $\alpha$  is induced to be phosphorylated at the N-terminus of serine residues (S 32) and (S36) by IKK $\beta$  leading to I $\kappa$ B $\alpha$  degradation which enables the free NF- $\kappa$ B dimer to translocate to the nucleus and activate  $\kappa$ B-dependent gene expression (Xu et al., 2011, Tsuchiya et al., 2010).

### 1.7.1.3 IKK Complex Structure

#### 1.7.1.3.1 IKK Kinases

The NF- $\kappa$ B cascade is centred on the IKK kinase complex, which consists of two I $\kappa$ B kinases, namely, IKK $\alpha$  and IKK $\beta$ , and a regulatory subunit, the NF- $\kappa$ B essential modulator NEMO (Mercurio et al., 1997, Yamaoka et al., 1998, Courtois et al., 2001). Activating signal and cell type determine two distinct NF- $\kappa$ B pathways, the canonical pathway, which is based on IKK $\beta$  and NEMO, and the non-canonical pathway, which is based predominantly on IKK $\alpha$  (Senftleben et al., 2001).

The discovery of the kinases phosphorylating I $\kappa$ B inhibitors was made when a cytoplasmic complex of high molecular weight that migrated around 700-900 kDa and included two interconnected catalytic subunits (IKK $\alpha$  and IKK $\beta$ ) was subjected to biochemical purification (Mercurio et al., 1997). These two subunits displayed a 52% sequence identity and were structurally similar, comprising a kinase domain (KD) at the N-terminus between residues 15 and 301 which contains the catalytic function of protein kinases and leucine zipper (LZ) whose role is to allow homo- or heterodimerization of the kinases is present in residues 455-483 and 458-486 of IKK $\alpha$  and IKK $\beta$  respectively. They also share helix-loop-helix (HLH) domains that function in modulating IKK kinase activity and lie in residues 599-638 and 603-642 of IKK $\alpha$  and IKK $\beta$  respectively. Both IKK $\alpha$  and IKK $\beta$  contain a C-terminal NEMO binding domain (NBD) (DiDonato et al., 1997). IKK $\beta$  appears to have an additional ubiquitin-like domain (ULD) following the KD, this is implicated in proteasomal degradation and is not predicted in the corresponding region of IKK $\alpha$  (Kwak et al., 2000, May et al., 2004).

A small peptide sequence at the carboxy terminus of both kinases has been established to be the interaction domain between NEMO and the kinase subunits. It is worth noting that the interaction between IKK and NEMO is suppressed by a deletion of an 11-amino-acid peptide (aa 735-745) at the carboxy terminus of IKK $\beta$ , thus serving as an efficient and specialised NF- $\kappa$ B inhibitor (Figure 1.8) (May et al., 2000).

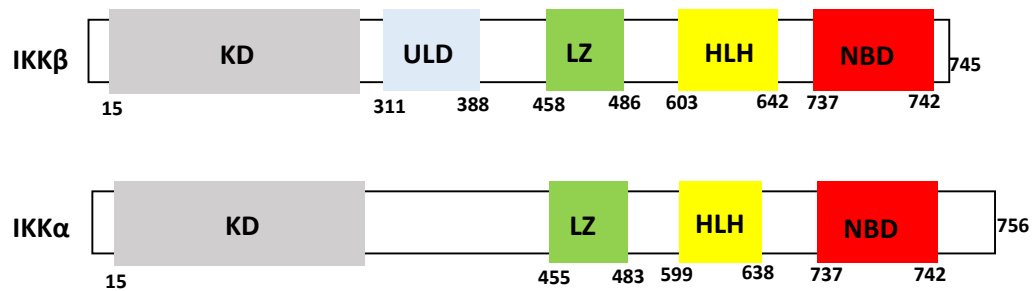


Figure 1.8 Domain organization schematic of the mammalian catalytic subunits of the IKK complex, IKK $\alpha$  (1-745bp) and IKK $\beta$  (1-756bp). Both subunits share four main domains, KD (Grey) refers to the kinase domain in N-terminus; LZ refers to leucine zipper (Green) which serves in dimerization; helix-loop-helix (HLH, Yellow) domain in C-terminal can regulate kinase activity of IKK. At the extreme C-terminus NEMO binding domains (NBD, Red) which are responsible for interaction with NEMO to form the IKK complex. IKK $\beta$  includes a unique motif required for ubiquitination called the ubiquitin-like domain (ULD, Light Blue) which sequenced between residues 311-388.

### 1.7.1.3.2 NF- $\kappa$ B essential modulator (NEMO, IKK $\gamma$ )

The NF- $\kappa$ B pathway is regulated by the NF- $\kappa$ B essential modulator NEMO, otherwise known as IKK $\gamma$ , IKKAP1, and FIP3, since signalling as a reaction to extracellular stimuli is suppressed by genetic inactivation (Makris et al., 2000). A 23 kb gene, NEMO contains ten exons and encoded a protein of 419 amino acids with a molecular mass of 48 kDa. It represents the regulatory element of the IKK complex (Majumdar and Aggarwal, 2001).

NEMO has a pivotal role in regulating the upstream receptor signalling complexes with the catalytic IKKs. The importance of NEMO was shown by Rudolph and colleagues when they generated NEMO-deficient mouse embryos. Mouse embryonic fibroblasts deficient in NEMO lacked NF- $\kappa$ B activity and the knockout mice died due to high rates of hepatic apoptosis after stimulation with TNF $\alpha$ , IL-1, LPS, and the dsRNA mimic poly IC (Bonizzi and Karin, 2004, Rudolph et al., 2000).

Structurally human NEMO protein is arranged in five domains; helix 1 (HLX1,  $\alpha$ H1), coiled-coil 1 (CC1), helix 2 (HLX2,  $\alpha$ H2) in N termin and a coiled-coil 2

(CC2), a leucine zipper (LZ) and a zinc finger (ZF) in its C terminal (Figure 1.9) (May et al., 2002).

NEMO is composed of two  $\alpha$  helical regions,  $\alpha$ H1 and  $\alpha$ H2, positioned before and after CC1. The region of interaction with IKK lies between amino acids 44-111 and is essential for IKK complex assembly, since mutations in this region of NEMO fail to form active IKK complexes (Ghosh and Karin, 2002, Marienfeld et al., 2006, Rushe et al., 2008, Cote et al., 2013).

The C-terminus of NEMO comprises several domains critical for correct functioning of the IKK complex, including a second coiled coil domain (CC2 residues 253–285), a leucine zipper (LZ 300–343), a Zinc Finger domain (ZF 394–419), and a sequence called the NEMO Optineurin ABIN (NOA/UBAN) domain, found within residues 298–330 (Tegethoff et al., 2003, Huang et al., 2002, Emmerich et al., 2013). This C-terminal region of NEMO is necessary for recognition of various types of ubiquitin molecules and essential for successful activation of the NF- $\kappa$ B pathway in response to upstream signalling events. The UBAN domain and ZF have a high preference for binding to linear ubiquitin (M1-Ub) (Emmerich et al., 2013) and lysine-63 (K63) linked ubiquitin chains (Rahighi et al., 2009, Hadian et al., 2011, Grubisha et al., 2010, Dynek et al., 2010, Kensche et al., 2012, Emmerich et al., 2013, Laplantine et al., 2009).

Grubisha and colleagues observed that the UBAN domain displays more than 100 fold higher affinity for M1-Ub versus K63-Ub (Lo et al., 2009, Grubisha et al., 2010). The CC2-LZ region possesses ubiquitin-binding domain (UBD) that is believed to be the site of trimerisation or tetramerisation and responsible for interacting with ubiquitin sites (Grubisha et al., 2010).

Several studies confirmed that the CC2-LZ domain of NEMO is responsible for oligomerisation and stabilization of NEMO. Mutant substitutions within this region obliterated NF- $\kappa$ B activation due to disruption of CC2-LZ oligomerisation (Iwai and Tokunaga, 2009, Tokunaga et al., 2009, Cordier et al., 2008, Fusco et al., 2008).

Very recently, Vincendeau and colleagues identified that the NEMO-UBAN domain is critical for IKK activation in response to TNF $\alpha$ , but not IL-1 $\beta$  stimulation. They used chemical shift perturbations and Nuclear Magnetic Resonance (NMR) techniques to determine specific amino acids in the CC2-LZ region required for NEMO to bind M1-Ub. Each of V300, A303, Q304, D311, E324 and E320 is required for the interaction with M1-Ub and mutation of these residues abolished NF- $\kappa$ B signalling (Vincendeau et al., 2016).

The inclusion of the ubiquitin binding site of NEMO within the LZ region was indicated by the surface conservation pattern. The LZ region is identical with the UBAN domain possessed by NEMO, Optineurin (OPTN), and A20 binding inhibitor of NF- $\kappa$ B (ABIN) (Wagner et al., 2008).

Table 1.2 Some proteins involved in NF- $\kappa$ B pathway and their targets and roles in the pathway.

Interestingly, all of these proteins function within the NF- $\kappa$ B pathway, although their roles are likely to be antagonistic to inhibit the pathway. For example, NRP (NEMO related protein) or Optineurin is able to form a complex with the IKK-related kinase TBK1 and the ubiquitin ligase TRAF3. By this complex, Optineurin contests with NEMO in its interaction with RIP1 and inhibits NF- $\kappa$ B signalling responses to IFN $\beta$  stimulation (Mankouri et al., 2010). Another way of blocking NF- $\kappa$ B activation comes from interaction of ABIN1 with either NEMO or the deubiquitinating enzyme A20 to deubiquitinate NEMO and inhibit formation of the IKK complex (Mauro et al., 2006). The loss of interaction between NEMO and A20 leads to prolonged accumulation of K63-ubiquitinated RIP within the TNFR1 signalling complex. Recruitment of A20 to the C-terminal domain of NEMO represents a mechanism that limits NF- $\kappa$ B activation by NEMO, and its absence results in an autoinflammatory disease (Zilberman-Rudenko et al., 2016).

It has very recently been shown that a group of males who develop autoinflammatory disease harbour mutations leading to truncation of the NEMO C-terminus which impaired its interaction with A20 (Zilberman-Rudenko et al., 2016). This protein has been shown to inhibit NF- $\kappa$ B activation as well as TNF-mediated apoptosis (Shembade et al., 2010).

Notably, NF- $\kappa$ B activation also disrupted by naturally occurring point mutations in the UBAN domain of NEMO, leading to various severe X-linked immunodeficiency diseases in humans including ectodermal dysplasia (Mancini et al., 2008). Human X-linked recessive anhidrotic ectodermal dysplasia with immunodeficiency (XR-EDA-ID) was determined to stem from a mutation in Aspartic acid residue (D311) of NEMO to Asparagine (N) or Glycine (G). The genetic disorder Incontinentia Pigmenti was discovered to develop when Glutamic acid (E315) in NEMO was mutated to G315. Mutation occurs in the ZF domain and adjacent proline-rich sequence of NEMO was associated with different inflammatory diseases like severe colitis and dermatitis (Zilberman-Rudenko et al., 2016). Hypomorphic mutations of NEMO also have been identified in up to one hundred male patients, while

NF- $\kappa$ B activation was found to be suppressed by around 43 distinct mutations (Chang et al., 2008, Filipe-Santos et al., 2006, Fusco et al., 2008).

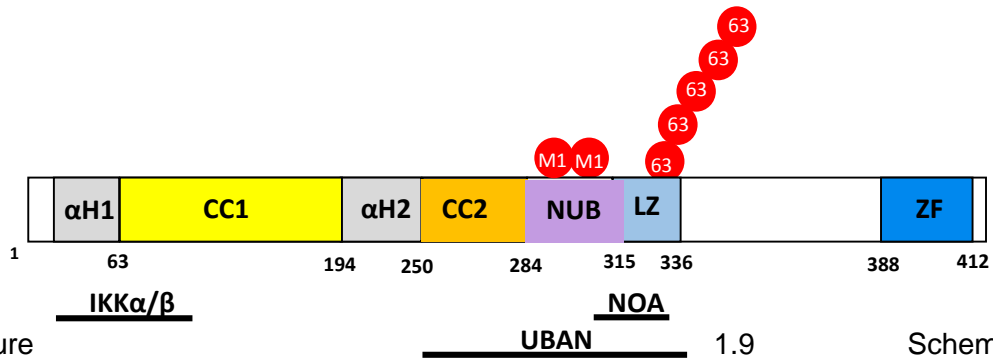


Figure 1.9 Schematic representation of different NEMO domain. At the N-terminus, there are the alpha helical region 1 ( $\alpha$ H1, Gray) and coiled-coil 1 (CC1, Yellow). Part of these two domains contain the region for binding IKK $\alpha$  and  $\beta$ . Another alpha helical region ( $\alpha$ H2, Gray) lies after CC1. The C-terminal another coiled coil called CC2 (Orange) is present and forms Ubiquitin binding in ABIN and NEMO region (UBAN) in cooperation with with the next two domains, NEMO ubiquitin binding (NUB, Purple) and Leucine Zipper (LZ, Light Blue). The UBAN domain is essential for ubiquitin linking. NEMO Optineurin ABIN (NOA) also identified within UBAN domain and in addition to its role as a binding domain for NEMO, OPTN and ABIN, it is important for binding linear ubiquitin chains (M1) and K63 polyubiquitination (Red circles). At the extreme C-terminus, there is a zinc finger (ZF, Blue) which may also help in binding with K63 ubiquitin chains.

### 1.7.2 The Canonical NF- $\kappa$ B Pathway

NF- $\kappa$ B affects most aspects of cellular physiology such as immunity, inflammation, apoptosis, cell survival, growth, and proliferation. Two signaling pathways known as the canonical (classical) and non-canonical (alternative) pathways are able to promote the activation of NF- $\kappa$ B (Gilmore, 2006, Scheidereit, 2006). This study concentrates on the role of MCPyV sT on the canonical pathway. The activity of NF- $\kappa$ B is directly controlled by the I $\kappa$ B protein in the cytoplasm of the cell through the formation of I $\kappa$ B:NF- $\kappa$ B complexes. A series of positive and negative regulatory elements are involved in regulation of the pathway starting from cell stimulation to

transcription of target genes (Whiteside and Israël 1997). A wide array of stimuli including pro-inflammatory cytokines such as antigen receptors, IL-1, TNF $\alpha$  as well as pattern recognition receptors (PRRs), leads to the onset of signaling cascades that phosphorylate the IKK complex (Bonizzi and Karin, 2004).

The stimulation regulated by TNF receptor-associated factor 6 (TRAF6) is sufficient to activate the TRAF6-regulated IKK activator, TAK. A complex of TRAF6 and TAK protein kinase initiates phosphorylation of IKK and mediates proteasomal degradation of I $\kappa$ B, enabling the active the NF- $\kappa$ B transcription factor subunits to translocate to the nucleus and induce target gene expression.

As a result of I $\kappa$ B phosphorylation by the IKK complex, I $\kappa$ B is destroyed by activation of the E3 ubiquitin ligase of beta transducin repeat containing protein (SCF <sup>$\beta$ TRCP</sup>), which mediates I $\kappa$ B degradation by the proteasome. This allows the free NF- $\kappa$ B to accumulate in the nucleus, where it binds to particular  $\kappa$ B DNA sequences. These sequences, which are located in promoter regions, are responsible for activating transcription of various genes implicated in cell adhesion, cell survival, growth regulation, and immune and inflammatory responses. It could also lead to the expression of the I $\kappa$ B $\alpha$  genes, which function as a negative feedback loop to sequester NF- $\kappa$ B subunits and terminate signaling unless a persistent activation signal is present (Ohshima and Ichikawa, 2014, Hoffmann et al., 2006, Huang et al., 2000).

Zhang and colleagues demonstrated the importance of TAK in phosphorylation of S176 and S177 in IKK $\alpha$  and IKK $\beta$  respectively, which are also necessary for formation of M1 ubiquitin chains and mediate their interaction with NEMO (Zhang et al., 2014).

Ubiquitin polypeptides are involved in a number of aspects of the NF- $\kappa$ B pathway. Ubiquitin chain formation requires three enzymes, ubiquitin activating enzyme E1, an ubiquitin conjugating enzyme E2 and an ubiquitin ligase. The complex catalyses formation of single or poly ubiquitin chains

(Lewis et al., 2015). The most known ubiquitin chains that are involved in the NF- $\kappa$ B pathway are M1-Ub which cause protein stability for NEMO and K63-Ub are required for activation of a number of enzymes in the NF- $\kappa$ B pathway and also prevent degradation by proteasomes and K48-linked ubiquitin chains (K48-Ub) which are responsible for mediating protein degradation by proteasomes (Figure 1.10) (Iwai et al., 2014, Nathan et al., 2013, Walczak et al., 2012). Another adapter protein involved in this pathway called receptor-interacting protein 1 (RIP1), a kinase protein which has one site of ubiquitination at K377 and by this it bind K63-linked ubiquitination. By linked the polyubiquitination chain with NEMO, RIP1 induces activation of IKK (Yang et al., 2011). Ea and colleagues found that ubiquitinated RIP1 is associated with NEMO during TNF- $\alpha$  stimulation and mutation RIP1-K377R which prevent RIP1 polyubiquitination leads to abolish the interaction with NEMO and as a result impair IKK activation (Ea et al., 2006).

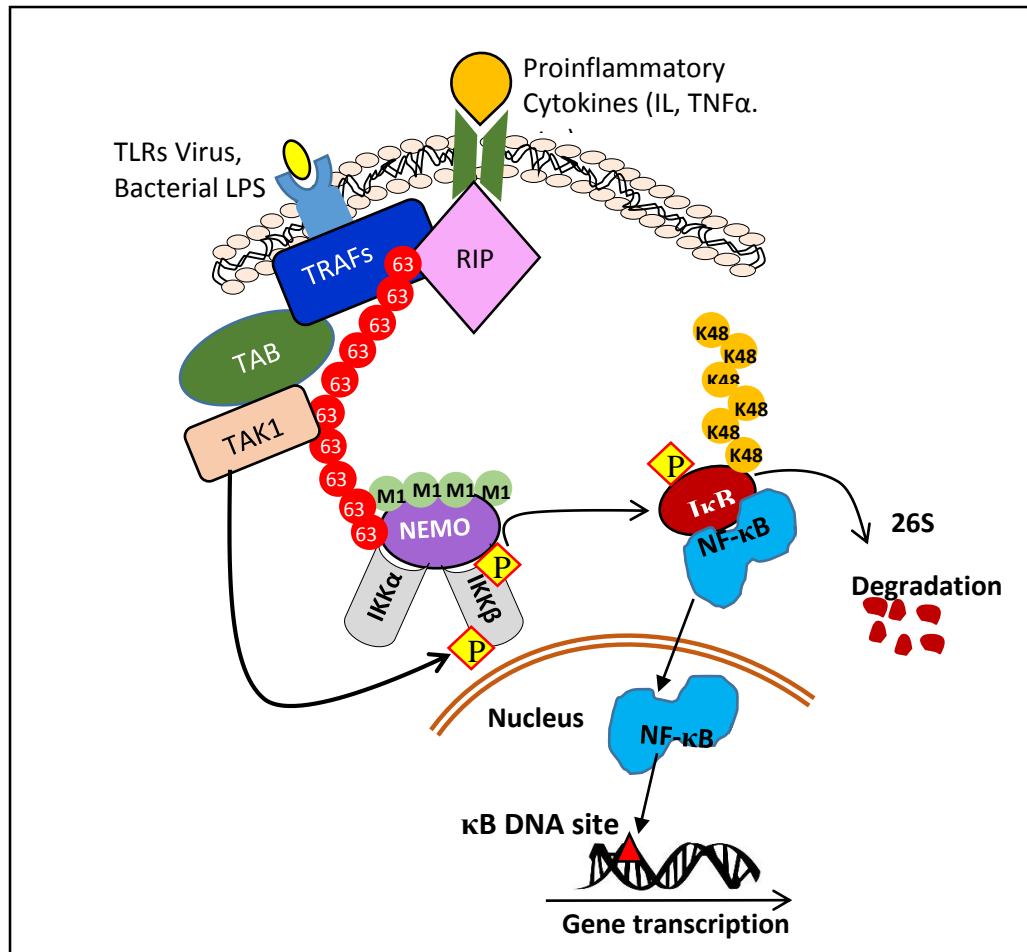


Figure 1.10 NF- $\kappa$ B pathway involves signalling by proinflammatory cytokines (Orange) or TLRs and LPS (Yellow). The pathway is activated when these stimulators associated with their cellular receptor on the cell membrane. This will activate TRAF are family proteins (Dark Blue) or RIPs (Pink) and this will allow the K63 ubiquitin link chain (circle Red) to NEMO (Purple) which also binds linear ubiquitin (M1, light Orange). TAB (Green) and TAK1 (Pink) phosphorylate IKK complex and mediate I $\kappa$ B (Black Red) phosphorylation which binds K48 ubiquitin chain (Circle Orange) and is subsequently degraded by 26S proteasome allowing NF- $\kappa$ B (Blue) to be translocated to the nucleus, binding to  $\kappa$ B DNA sites and activating gene transcription.

## **1.8 Role of Protein Phosphatases in cell signaling**

One major element of the intracellular signaling system is reversible protein serine/threonine phosphorylation. The findings of protein phosphatase studies have confirmed that cellular processes entailing protein phosphorylation depend as much on these enzymes for regulation as they do on kinases (Mumby and Walter, 1993). Protein kinases and phosphatases serve as essential checkpoint regulators and switches as they both contribute to the regulation of phosphorylation and de-phosphorylation of proteins in accordance with the physiological requirements of cells. The family of protein tyrosine phosphatases (PTP) encompasses over two thirds of the 150 members of the protein phosphatase superfamily and is responsible for the de-phosphorylation of phosphotyrosine and occasionally phosphoserine and phosphothreonine. Of the rest of the enzymes, most are associated exclusively with either phosphorylated serine or threonine residues, forming two distinct groups (Cohen, 2002, Moorhead et al., 2009), namely, phosphoprotein phosphatases (PPP) and protein phosphatases dependent on  $Mg^{2+}$  or  $Mn^{2+}$  (PPM). Protein phosphatase type 2C (PP2C) is the major representative of PPM, while PPP includes five subfamilies, among which are the PPP1 subfamily, comprising PP1, and the PP2/4/6 subfamily including PP2A, PP4 and PP6 (Cohen, 1997).

### **1.8.1 Protein Phosphatase 2**

In their basic form, protein phosphatase 2 (PP2A) holoenzymes are mainly heterotrimers characterised by the correlation between a core dimer (PP2AD), consisting of a structural A subunit (PR65) and a catalytic C subunit (PP2AC), and a third variably regulatory B sub-unit (Kremmer et al., 1997).

A number of different genes encode these sub-units and they are combined to form multiple heterotrimers (A-C-B) or heterodimers (A-C) present in various isoforms in cells (Mayer-Jaekel and Hemmings, 1994, Cohen, 1997).

PP2AC is expressed in the majority of tissues, especially in the heart and the brain. To keep it constant, the level of PP2AC protein expression (37kDa) is subjected to translational regulation (Nishikawa et al., 1994). PP2C can occur in two isoforms, namely, C $\alpha$  and C $\beta$ , which have a sequence that is 97% identical and are each made up of 309 amino acids. Furthermore, the plasma membrane is the main site of C $\alpha$  expression, while the cytoplasm and nucleus are the locations of C $\beta$  expression (Khew-Goodall and Hemmings, 1988). The PP2C amino acid sequence in humans and yeast is 86% similar, and it is also 50% and 40% similar to the sequences in PP1 and PP2B, respectively (Evans et al., 1999).

As in the case of PP2AC, two different genes, PPP2R1A and PPP2R1B, encode the PP2A scaffold sub-unit, giving rise to the isoforms A $\alpha$  and A $\beta$  which have broad expression, are identical in a proportion of 86%, and are fragmented within the cytoplasm (Price and Mumby, 2000, Hendrix et al., 1993). However, of the two, PP2A A $\alpha$  is the dominant sub-unit, representing around 90% of the PP2A and 0.1% of the overall cell protein.

The rest of the 10% of PP2A is made up by A $\beta$ , determining preferential interaction with catalytic subunit (C) and regulatory sub-units (B). The scaffold unit stands out from other sub-units in terms of structure. The Huntington/elongation/A sub-unit/TOR (HEAT) sequence consists of 15 tandem repeats with 39 amino acids each making up the PP2A A (Zhou et al., 2003).

Two  $\alpha$ -helices are presented by every repeat, linked by inter- and intra-repeat loops. The catalytic and regulatory sub-units respectively attach to 11-15 and 1-10 repeats of the HEAT sequence. The catalytic subunit is associated with a scaffold unit that creates a base by folding and also display a structure in the shape of a horseshoe. The recruitment of the regulatory

sub-unit as well as other PP2A substrates is facilitated by such flexible folding (Cho and Xu, 2007).

### 1.8.1.1 PP2A Function in Cellular Processes

Although a considerable degree of ambiguity surrounds PP2A function and substrate, it has been confirmed to be involved in the regulation of different biological processes, including DNA replication, transcription and translation, signal transduction, cell proliferation, cytoskeleton dynamics, cell motility and apoptosis, as well as cell transformation and cancer (Sablina and Hahn, 2007). In relation to this regulatory function, PP2A A $\alpha$  contributes to the regulation of a number of pathways, including phosphatidylinositol 3-kinase (PI3K) and the AKT pathway (Sablina and Hahn, 2007). Studies have reported tumour suppressor p53 de-phosphorylation by PP2A A $\alpha$  at Thr-55, as a result of which p53 and Cdk inhibitor p21 were activated while cell proliferation was suppressed (Li et al., 2007b). Additionally, PP2A A $\alpha$  also dephosphorylates the c-Myc oncogene and CDC25c, inactivating c-Myc and hindering progression of the cell cycle, respectively (Arnold and Sears, 2006, Forester et al., 2007). What is more, PP2A A $\alpha$  targets the M-type potassium channel and therefore contributes to the regulation of Glycogen synthase kinase-3 $\beta$  (Kapfhamer et al., 2010). Such research findings hint at the fact that PP2A links the PP2A AC core to the substrate proteins participating in cell development and proliferation, and it is from this that PP2A derives its tumour-inhibitory function. The observed displacement of the B sub-unit site of PP2A by certain viral oncoproteins validates this perspective. Furthermore, a number of cancers have been associated with PP2A mutations, such as lung carcinoma (E64D), breast carcinoma (E64G and  $\Delta$ 171–589), malignant melanoma (R418W), and ovarian carcinoma (R182W, R183W and R183G) (Ruediger et al., 2001, Ruediger et al., 2011). These mutations work together with LT, hTERT and H-RAS to transform healthy cells into transformed ones by inhibiting the expression of the PP2A B56 $\gamma$

regulatory B sub-unit or partly exhausting the structural A $\alpha$  sub-unit (Chen et al., 2004).

Ra1A inactivation and suppression of its transforming function result from its de-phosphorylation at Ser183 and Ser194 undertaken by complexes that contain PP2A A $\beta$ . Hence, through regulation of Ra1A function, PP2A A $\beta$  converts immortalised human cells and therefore can be considered to be a gene that inhibits tumorigenesis. This is confirmed by the fact that cells where PP2A A $\beta$  has been knocked down are not only cancerous in nature but also demonstrate activated Ra1A (Sablina and Hahn, 2007). Colon, neck and breast cancers are usually associated with A $\beta$  inactivating mutations (Wang et al., 1998). Although various human cancers, including colon (8-15%), lung (15%), breast (13%), and tumour cell lines (6%), manifest structural PP2A A $\beta$  subunit mutations (e.g. point mutations, deletions, frameshifts, and splicing abnormalities) it is still unclear what functional implications these mutations have on cell transformation. Furthermore, 16 out of 32 cancer cell lines extracted from human lung, colon, breast and cervical carcinomas also exhibited PP2A A $\beta$  subunit expression, albeit decreased (Ruediger et al., 2001, Calin et al., 2000, Zhou et al., 2003).

Research revealed that these mutations cannot bind to B and/or C subunits *in vitro*. Aside from mutations, the localisation of the PP2A A $\beta$  at 11q23 is also worth noting, as human cancers usually exhibit deletion of this chromosomal region (Baysal et al., 2001).

### **8.1.2 The Correlation between MCPyV sT and PP2A**

Cellular pathway deregulation via phosphatase targeting is the aim of many viruses and, to this end, they have devised complex strategies. For instance, PP2A is targeted by the Adenovirus and by the hepatitis C virus (HCV) to respectively trigger cell death and to deregulate the extracellular signal-regulated kinase (ERK) pathway (Kleinberger and Shenk, 1993, Georgopoulou et al., 2006), while the human papillomavirus 16 (HPV 16) encoded E7 binds both catalytic and structural units of PP2A with the

purpose of preventing AKT from being dephosphorylated (Pim et al., 2005). Furthermore, research demonstrated that PP2A interacts with SV40 and that the virus gains control of different signalling pathways, such as PI3K-AKT-mTOR, the MAPK pathway, and the stress-activated protein kinase (SAPK) pathway, through the mediation of SV40 sT (Buchkovich et al., 2008, Sontag et al., 1993).

The discrepancies between the two A isoforms are detected by small DNA tumour viruses. Both PP2A A $\alpha$  and A $\beta$  are bound by MCPyV sT and murine Py sT, whereas PP2A A $\alpha$  is bound by SV40 sT and monkey polyomavirus. In contrast, PP2A A $\beta$  binds weakly with SV40 sT (Pallas et al., 1990, Hwang et al., 2013). The two isoforms of PP2A C subunit (C $\alpha$  and C $\beta$ ) showed interaction with sT of both MCPyV and SV40 (Griffiths et al., 2013, Hwang et al., 2013, Kwun et al., 2015). Mutagenesis studies based on alanine substitution found three amino acids in MCPyV sT (R7, L142 and K134) are required for the interaction with PP2A A $\alpha$  (Kwun et al., 2015). In contrast, the residues R7, R21 and P132 was shown to be required for SV40 to bind PP2A (Cho et al., 2007).

The MCPyV sT mutants that stop binding to PP2A conserved their ability to hyperphosphorylate 4E-BP1 through their binding to Fbw7. This confirms that sT-mediated 4E-BP1 phosphorylation does not require PP2A recruitment. In addition, both SV40 and MCPyV sT block the assembly of B56 $\alpha$  subunit to A sub-unit of PP2A (Kwun et al., 2015).

Moreover, the interaction between MCPyV sT and PP2A A $\alpha$  was not required to augment cell mobility and migration. Rather, an internal deletion mutant ( $\Delta$ 95-111) which abrogates the interaction with PP2A A $\beta$  and additional phosphatases like PP4C prevented the increased migration (Knight et al., 2015).

### 1.8.2 Protein Phosphatase 4

A widespread PP2A-related protein serine/threonine phosphatase belonging to the PPP family, protein phosphatase 4 (PPP4) or protein phosphatase X has roles in different cellular processes. PP4 is also a holoenzyme as PP2A and therefore is made up of structural (A), regulatory (B) and catalytic (C) sub-units (Kloeker and Wadzinski, 1999). Determined on the basis of multiple cDNAs, mammalian PP4C has an amino acid sequence that is 65% identical to that of PP2A C $\alpha$  and PP2A C $\beta$  isoforms. It was isolated from cytoplasmic and nucleus with molecular mass between 450-600 kDa. A number of regulatory subunits, including PP4R1, PP4R2, PP4R3 $\alpha$ , PP4R3 $\beta$ , and PP4R4 were detected (Chowdhury et al., 2008, Gingras et al., 2005, Chen et al., 2008, Helps et al., 1998)

PP4C works in association with these regulatory subunits to form a complex. PP4C-PP4R1 is present primarily in the cytoplasm while PP4C-PP4R2 can be found in the centrosome, possessing a molecular mass of 105 kDa and 55 kDa, respectively. The regulatory sub-units possess a negative regulatory effect on PP4C. They prevent catalytic activity of PP4C or effect on substrate recognition (Chen et al., 2008).

It is still not completely clear what the biological role of PP4 is, but there is some evidence that it is related to centrosome/spindle pole bodies and the processes of nucleation, development and/or stabilisation of microtubules which, through the formation of the mitotic spindle, are essential to all mitotic processes as well as to a range of subcellular activities (Helps et al., 1998, Kirschner and Mitchison, 1986).

Different substrates were shown to have PP4C catalytic activity. In addition to initiating the de-phosphorylation of various proteins in a number of pathways, this catalytic activity also takes part in microtubule organisation of the cytoskeleton by dephosphorylating nuclear distribution element-like 1 (NDEL1), which controls microtubule filament, and hence regulating cyclin-dependent kinase 1 (Cdk1) in the interphase (Toyo-oka et al., 2008). Furthermore, it has been demonstrated that PP4C is involved in regulating

apoptosis, cell proliferation, and cell mutation rate. When PP4C was inhibited, apoptosis was impaired but cell proliferation was improved by dephosphorylating a number of important anti-apoptosis proteins, especially the astrocytic phosphoprotein (PEA-15) and Bcl-2-associated death promoter (Bad) (Mourtada-Maarabouni and Williams, 2008). Regarding T-cell signalling, the involvement of PP4C takes the form of control of haematopoietic progenitor kinase1 (HPK1) (Zhou et al., 2004). One study revealed that insulin signalling and TNF- $\alpha$  stimulated degradation IRS-4 were suppressed when PP4C negatively regulated at least one serine residue in the insulin receptor substrate (IRS). Moreover, transcriptional regulation and cell cycle progression were observed to be modified when PP4C was dephosphorylated in histone deacetylase 3 (HDAC3) (Zhang et al., 2005). The involvement of PP4C in a prolonged checkpoint arrest in human cells following damage to the DNA was confirmed by PP4C dephosphorylation of  $\gamma$ H2AX (Nakada et al., 2008).

The findings of recent studies indicate that PP4C may be actively involved in the progression of some cancers, such as breast and lung cancer, and pancreatic ductal adenocarcinoma, where it has shown elevated expression (Wang et al., 2008, Weng et al., 2012). PP4C overexpression causes deregulation of the PI3K/AKT-dependent signalling pathway, which has been shown to favour tumorigenesis and lung metastasis *in vivo*. Moreover, the correlation of PP4C with distant metastasis is suggested by its high expression in pancreatic ductal adenocarcinoma by contrast to non-cancerous pancreatic tissue (Li et al., 2015b, Weng et al., 2012). Another study reported that PP4C was involved in metastasis as well, interacting and dephosphorylating the microtubule-associated protein (MAP) Stathmin during MCPyV sT expression. Stathmin and acetylated tubulin phosphorylation is augmented by the sT mutant which suppresses PP4C. This suggests that PP4C participates in microtubule destabilisation triggered by MCPyV sT and cell mobility (Knight et al., 2015).

The importance of PP4C and its regulatory subunit PP4R1 in signalling pathway was explained by Tikhonova and Aifantis in T lymphocytes, they

demonstrated that NF- $\kappa$ B is negatively regulated by PP4R1 which targets the phosphatase activity of PP4C to dephosphorylate and inactivate the IKK complex (Tikhonova and Aifantis, 2012). Primary human T lymphocyte activation and proliferation were observed to stimulate PP4R1 expression, whereas PP4R1 deficiency resulted in sustained and heightened IKK activity, T cell hyperactivation, and abnormal NF- $\kappa$ B signalling in T cell lymphomas dependent on NF- $\kappa$ B. As with PP4C, regulation of histone deacetylase 3 activity and influence of centrosome microtubule development have also been attributed to PP4R1 (Tikhonova and Aifantis, 2012, Zhang et al., 2005).

## 1.9 NF- $\kappa$ B as a target for virus immune evasion

Several viruses utilise their proteins to target the NF- $\kappa$ B pathway to facilitate their replication, host cell survival, and evasion of immune responses. A range of viruses have evolved mechanisms to activate the NF- $\kappa$ B pathway to enhance their replication by preventing apoptosis, whereas other viruses inhibit the pathway to trigger apoptosis as a mechanism of virus dissemination (Figure 1.11) (Ghosh et al., 1998). A good example of this can be seen in human immunodeficiency virus type 1 (HIV-1) that has two NF- $\kappa$ B binding sites in its long terminal repeat (LTR) that bind to RHR sites in NF- $\kappa$ B dimers, stimulating the NF- $\kappa$ B pathway and as a result increase its replication activity. (Nourbakhsh et al., 2001). Furthermore, NF- $\kappa$ B is augmented due to early-encoded HIV-1 TAT proteins interacting directly with I $\kappa$ B $\alpha$  and p65 and this can prevent apoptosis of the infected cell (Fiume et al., 2011).

A further example is that of the human T-cell leukaemia virus type 1 (HTLV-1) oncoprotein, TAX. This protein promotes viral replication and NF- $\kappa$ B activation, enabling cells infected by HTLV-1 to endure, evolve, and multiply. TAX exerts its effect by binding to the regulatory NEMO sub-unit, which causes continual activation of IKK $\alpha$  and IKK $\beta$ , the breakdown of I $\kappa$ B and activation of NF- $\kappa$ B pathway (Xiao and Sun, 2000).

The Epstein-Barr virus (EBV) is associated with several human cancers and is credited as being causal for lymphoproliferative disease. The EBV oncoprotein, LMP1 which stimulates the C-terminus activating region 1, interacts with signalling proteins, such as TRAFs, TRADD, or RIP. These in turn activate the IKK complex, and consequently I $\kappa$ B $\alpha$  is phosphorylated releasing NF- $\kappa$ B (Edwards et al., 2015).

Hepatitis B virus (HBV) interrupts the canonical NF- $\kappa$ B pathways by encoding a protein polymerase (Pol), which retains NF- $\kappa$ B sub-units in the cytosol through inhibition of the IKK assembly. This is achieved by preventing NEMO from combining with CDC37/Hsp90 which is an essential stage in IKK complex assembly (Liu et al., 2014).

Other viruses succeed by preventing NF- $\kappa$ B from leaving the cytosol and entering the nucleus. The viruses express proteins that interact with the IKK complex to inhibit I $\kappa$ B destruction. Some viruses disrupt phosphorylation of the IKK complex catalytic sub-units. This method is used by EBNA1 protein of the Epstein-Barr virus to inhibit the classical NF- $\kappa$ B pathway; it indirectly reduces the phosphorylation of I $\kappa$ B $\alpha$  by stopping the IKK catalytic sub-units from being phosphorylated (Valentine et al., 2010) Hepatitis C virus (HCV) provides a further example of viral targeting of the IKK complex. To suppress NF- $\kappa$ B, HCV core protein targets and prevents IKK $\beta$  kinase action (Rocak and Linder, 2004). Viruses, such as human cytomegalovirus (CMV) and *Molluscum Contagiosum* virus (MCV) take the approach of impeding NF- $\kappa$ B activation by interacting with NEMO to interfere with the IKK complex and inhibit I $\kappa$ B destruction. To inhibit the NF- $\kappa$ B pathway, **MCV proteins** MC159 and MC160 that bear two tandem death effector domains (DEDs) correspondingly interact with NEMO and IKK $\alpha/\beta$  (Nichols and Shisler, 2006, Randall et al., 2012, Krause et al., 2014).

Inhibition of apoptosis is another technique employed by viruses, as shown by research into KSHV. The virus can also prompt activation of the NF- $\kappa$ B pathway by encoding a fragment of transactivator viral FLIP protein (vFLIP). The pathway is disrupted when the fragment binds to the CC region that

extends between residues 150 to 272, preventing NEMO regulation (Bagneris et al., 2008).

By binding to PP2A, SV40 sT antigen disrupts the enzyme's function and removing inhibitory regulation of the MAPK pathway and promoting cell growth (Sontag et al., 1993). The effect of PP2A inhibition is the activation of calcium-independent protein kinase C $\zeta$  isoform (PKC $\zeta$ ) and PI3K; in part due to NF- $\kappa$ B activation, these kinases are critical for TNF $\alpha$ -induced endothelial permeability (Leitges et al., 2001). PKC $\zeta$  prompted by TNF $\alpha$  results in the destruction of I $\kappa$ B $\alpha$  and the activation of NF- $\kappa$ B. Cells that have been transfected with SV40 sT have been shown to enhance the expression of NF- $\kappa$ B-driven genes by 14 times compared to untransfected cells (Sontag et al., 1997).

Further evidence to back the effect of MCPyV on NF- $\kappa$ B comes from the MCPyV-positive MCC cell line MKL-1 that exhibited 60% lower I $\kappa$ B levels compared to MCPyV-negative MCC13 cells. In addition, MCC cells that were virus-positive displayed reduced expression of NF- $\kappa$ B and related genes compared to virus-negative MCC. These studies deliver evidence that MCPyV has an unfavourable effect on the NF- $\kappa$ B pathway. It also indicates that MCPyV sT promotes the survival of the virus by modifying immune responses. It is uncertain whether this quality is available to the sT of other HPyV; but it is noted that residues 95–111 are not conserved, yet these are critical to the interaction between MCPyV sT, NEMO, PP2A and PP4C (Griffith et al., 2013).

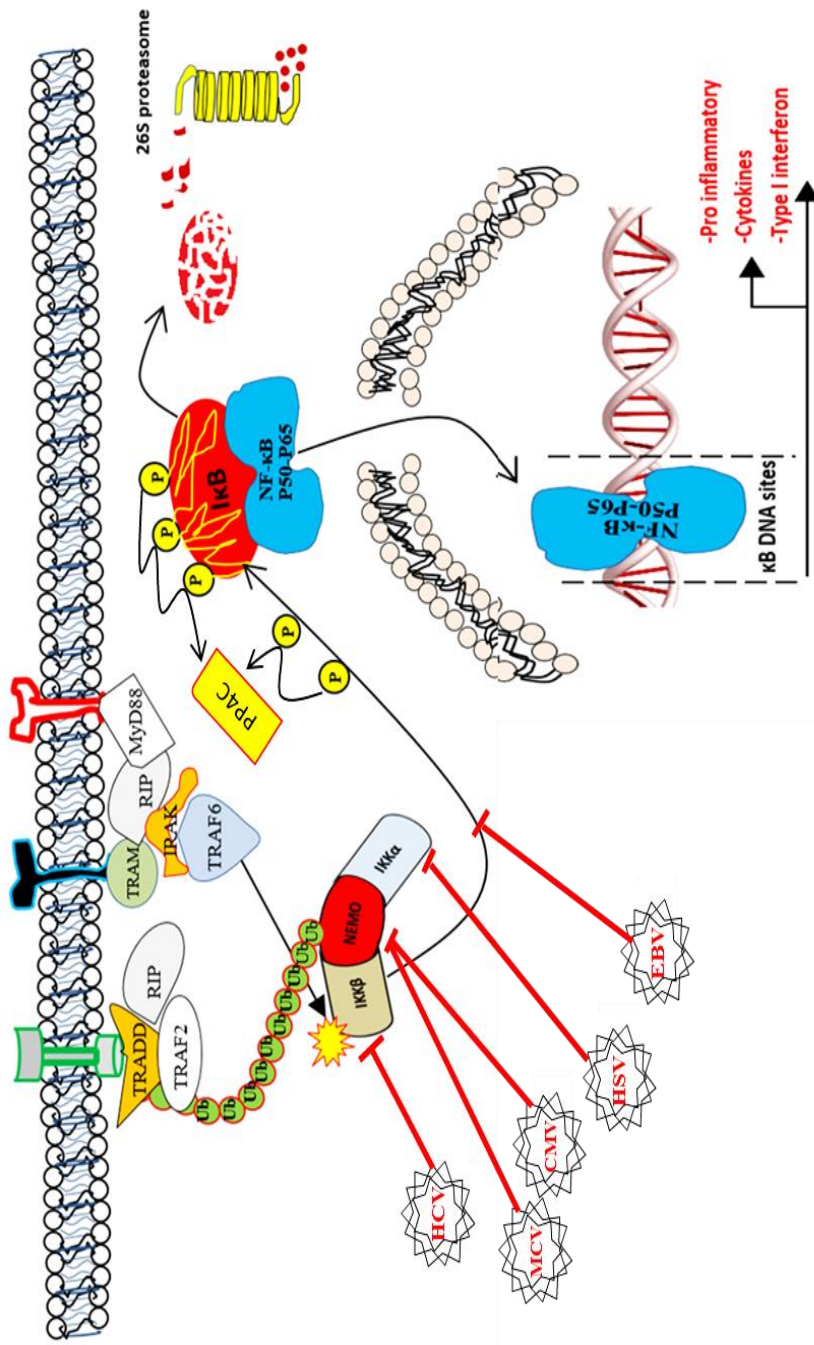


Figure 1.11: Schematic illustrates canonical NF- $\kappa$ B pathway and target sites of some viruses. Several membrane receptors including TLRs viruses and bacterial LPS, cytokines and TNF $\alpha$ . Signal initiated by kinases and adaptors TRAFs which activate IKK complex (Yellow star) and this happen by different ubiquitination chains. This complex phosphorylates I $\kappa$ B which catch NF- $\kappa$ B (p50-p65) and subsequently degraded by 26S proteasome. This releases the NF- $\kappa$ B to translocate to the nucleus and bind to  $\kappa$ B DNA site to promote genes of proinflammatory, cytokines and type1 interferon. Five examples of viruses that target IKK complex sub-units were mentioned, HCV targets IKK $\beta$ ; MCV and CMV target NEMO; HSV invades IKK $\alpha$  and EBV used as an example for viruses that stop phosphorylation activity of IKK complex.

## 1.10 Aim of study.

Whilst great strides have been made in our understanding of the oncogenic properties of MCPyV sT, we do not yet have a comprehensive knowledge of the molecular basis for its functions in cells. Moreover, we lack a detailed understanding of the host protein interaction partners required for sT mediated immune evasion. The ultimate aim of this PhD study was to characterise the molecular mechanisms by which MCPyV sT interacts with key components of the innate immune signalling pathway. **We concentrated on the role of MCPyV sT in the NF- $\kappa$ B pathway through its interaction with NEMO and phosphatase enzymes that may be involved in pathway regulation.** For this purpose the specific objectives of this study were:

- To investigate the molecular basis for the observed interaction with the NEMO adaptor protein
- To define the contribution of host protein phosphatases to the observed inhibition of NF- $\kappa$ B signalling
- To investigate if these interactions are unique to MCPyV sT or can be found in other human polyomaviruses

## Chapter 2 Material and Methods

### 2.1 Competent Bacterial strain and storage

Several *Escherichia coli* strains (New England BioLabs (NEB), USA) were used for cloning target genes (Tablet 2.1). Bacteria were cultured in Luria-Bertani (LB medium, 3% w/v tryptone soya broth, 0.5 w/v yeast extract) and incubated for 24h at 37°C with shaking. For long term storage, 1ml of 24h bacterial culture was centrifuged 5 min at 3000 g. The supernatant was removed and the bacteria were re-suspended in equal volume of LB with antibiotic and 87 % glycerol. The bacteria were stored at -80°C until used. To use the storage bacteria again, some frozen bacteria was quickly scraped by sterile loop refreshed with 5 ml LB broth and incubated at 37°C for 1h then streaked on LB agar plate with appropriate antibiotic.

*Table 2.1 Information about type of competent bacteria.*

<b><i>E. coli</i> strain</b>	<b>The experiment</b>	<b>Company</b>
DH5α	General DNA manipulation	Invitrogen
BL21 (Rosetta)	Expression of GST-sT in Bacteria	New England Biolabs (NEB)
NEB 5-alpha (C 2987)	Q5 site directed mutagenesis	New England Biolabs (NEB)
XL1 Blue	Internal deletion mutants transformation	New England Biolabs (NEB)

## 2.2 Cloning Vectors.

Circular DNA vectors were used to carry a target DNA fragment (Table 2.2). The double stranded DNA of the vector was cut by using compatible restriction endonucleases.

*Table 2.2 Information about cloning vectors.*

Vector	Description	Used for
pEGFP-C1	Eukaryotic expression vector for C-terminal Enhanced Green Fluorescent Protein (EGFP).	To clone MCPyV sT and its truncations mutants, other polyomavirus sT.
pEF4:HA	Derivative of the pEF4 eukaryotic expression vector with a 5' single HA tag	Encoding for HA-tagged human PP4R1, full-length protein (aa 1-950).
pcDNA3.1+	Mammalian expression vector with the CMV promoter	To clone FLAG-PP4C, IKK $\alpha$ , $\beta$ , FLAG-NEMO.
pGEX	pGEX vectors, GST Gene Fusion System	For producing bacterial sT protein and GST-NEMO

## 2.3 DNA manipulation and plasmid construction.

### 2.3.1 Primers.

Oligonucleotide primers were purchased in lyophilized form and dissolved in ddH<sub>2</sub>O to a final concentration of 100 pmol/μl and stored at -20°C. Oligonucleotides used in this project are listed in (Table 2.3).

*Table 2.3 Primers and their sequences*

Primer	DNA sequence (5' to 3')
MCPyV sT full length Forward	gcgc <b>gaattc</b> tatggatttagtcctaaatagg
MCPyV sT full length Reverse	gcg <b>ggatcc</b> tagaaaaggtgcagatgc
R7A MCPyV sT Forward	gcgc <b>gaattc</b> tatggatttagtcctaaatgcgaaagaaag agag
MCPyV-1-162 reverse	gcg <b>ggatcc</b> taagtaggaggaaatcc
MCPyV-1-128 reverse	gcg <b>ggatcc</b> tagcgagacaacttacagc
MCPyV-1-95 reverse	gcg <b>ggatcc</b> ttacatataatccttaaagtcc
MCPyV-1-64 reverse	gcg <b>ggatcc</b> tactggaattgctccaaaggg
MCPyV-1-32 reverse	gcg <b>ggatcc</b> taagcttcatcagaggg
Δ95-111 MCPyV-sT Forward	gcgc <b>gaattc</b> atgcttaagcaacttagagattct
Δ95-111 MCPyV-sT Reverse	gcg <b>ggatcc</b> caaagtgatataat
Δ111-128 MCPyV-sT forward	gcgc <b>gaattc</b> cctaagcaacttagagattctaagtgc
Δ111-128 MCPyV-sT forward	gcg <b>ggatcc</b> gctagattttgcagaggtcctggg
A96-99 MCPyV-sT forward	<b>gcagct</b> aatgctagattttgcagag
A96-99 MCPyV-sT reverse	<b>agctgc</b> catataatccttaaagttccatattc
A100-103MCPyV-sT forward	<b>gcagct</b> tgagagtcctgggtgc

A100-103 MCPyV-sT reverse	<b>agcagc</b> atatccactttgcatataatcctttaaagttcc
A104-107 MCPyV-sT forward	<b>gctgct</b> gggtgcatgcttaagcaac
A104-107 MCPyV-sT reverse	<b>tgcggc</b> aaatctagcattatatccactttgc
A108-111 MCPyV-sT forward	<b>gcggct</b> aagcaacttagagattctaag
A108-111 MCPyV-sT forward	<b>ggccgc</b> caggacctctgcaaatctag
N100A MCPyV-sT forward	aagtggatat <b>gctgct</b> tagattttgcagag
N100A MCPyV-sT reverse	tgcatataatcctttaaagttcc
A101R MCPyV-sT forward	tggatataat <b>cgtag</b> attttgcagaggtc
A101R MCPyV-sT reverse	ctttgcatataatcctttaaagttc
R102A MCPyV-sT forward	atataatgct <b>gc</b> attttgcagaggtc
R102A MCPyV-sT reverse	ccactttgcatataatcctttaaag
F103A MCPyV-sT forward	taatgctagag <b>gctg</b> cagaggtcc
F103A MCPyV-sT reverse	tatccactttgcatataatcc
BKPyV sT forward	gcg <b>gaattc</b> tatggataaagttctaacagg
BKPyV sT reverse	gcg <b>ggatcct</b> taaagctttagatctctgaaggg
SV40 sT forward	gcg <b>gaattc</b> tatggataaagtttaaacagagagg
SV40 sT reverse	gcg <b>ggatcct</b> tagagctttaaactctgtaggtagt
JCPyV MAD1 sT forward	gcg <b>gaattc</b> tatggacaaagtgtgaatagggagg
JCPyV MAD1 sT reverse	gcg <b>ggatcct</b> taaagctttagatccctgtaggg

### **2.3.2 Polymerase Chain Reaction (PCR)**

Based on the method developed by Mullis and colleagues (Mullis et al., 1992), PCR was performed for amplification of specific sequences. KOD DNA polymerase kit (Merck, UK) was used in a final volume of 50  $\mu$ l containing template vector DNA (100-500 ng), 1 Unit of KOD DNA polymerase, 1 x KOD DNA polymerase buffer, 200  $\mu$ M of deoxynucleotide triphosphates (dNTP), 2.5 nM  $MgCl_2$ , with 10% v/v dimethyl sulphoxide (DMSO) and 0.5  $\mu$ M of each forward and reverse primer (Table 2.3). The reaction was run in an MJ research PTC-200 Thermal Cycler (GMI). A typical program starts with a 20 sec denaturation at 95 °C in order to ensure that the majority of the DNA is denatured. Followed by denaturation (95°C, 20 sec), primers annealing temperature by (50-68°C, 20 sec) or 5 degrees below the melting temperature of the primers and fragment extension (72°C, ~1 min/kb). This was repeated for 40 cycles and followed by a final extension (72°C, 1 min) before the end of the PCR. The time spent at the different steps was dictated by size of the template.

### **2.3.3 Purification of PCR products**

Purification of PCR products was achieved using a QIAGEN Plasmid Purification Kit (Qiagen, Germany) according to the manufacturers' instructions. Purification is based on providing a silica membrane for DNA binding in a high salt buffer. Impurities were removed by washing with an additional salt buffer and DNA was subsequently eluted by 50  $\mu$ l of low-salt buffer or ddH<sub>2</sub>O.

### **2.3.4 Colony PCR screening.**

Single colonies of bacteria were picked with a sterile tip from an LB plate and used to inoculate 200  $\mu$ l of LB media and the residual bacteria on the tip was used as a template for a PCR reaction using Taq DNA polymerase and appropriate primer pairs. Positive PCR sequences were examined by agarose gel electrophoresis.

### **2.3.5 Internal deletion polymerase chain reaction.**

The QuikChange site directed mutagenesis kit (Stratagene) was used to generate internal deletion mutants, as described in the manufacturer's instructions. Primers for the desired deletion mutation were designed using software for QuikChange site directed mutagenesis applications (Table 2.3). Amplification of mutation by PCR was performed using PfuTurbo® DNA polymerase. PCR products were treated with Dpn I endonuclease to digest the parental DNA template and to select for DNA containing the desired mutation. Mutants were transformed into XL1-Blue super competent cells and their sequences were confirmed by GATC-Biotech (Germany).

### **2.3.6 Site directed mutagenesis**

Saturation alanine scanning mutagenesis was performed using the Q5 site directed mutagenesis kit (New England Biolabs) according to the manufacturer's protocol. Primer pairs were designed with 5'ends annealing back to back by using the online NEB primer design software ([www.NEBBaseChanger.neb.com](http://www.NEBBaseChanger.neb.com)). The protocol is based on exponential PCR amplification using the Q5 hot start high fidelity DNA polymerase followed by treatment with a Kinase-Ligase-DpnI (KLD) enzyme mix to circularise the PCR products and remove the template DNA. The DNA was then transformed into NEB 5-alpha C 2987 competent cells. Bacteria were subsequently cultured in 950 µl of SOC media (2% (w/v) Tryptone; 0.5% (w/v) Yeast extract; 10 mM NaCl; 2.5 sterilized at 121°C, and then sterile 10 mM MgCl<sub>2</sub> and 20 mM Glucose were added).

## **2.4 DNA preparation**

### **2.4.1 Restriction enzyme digestion**

Amplified DNAs were cloned into a suitable vector (Table 2.2), both insert DNA and vector plasmid were digested using two high fidelity endonucleases (NEB, USA). For all mutagenesis, BamHI was used at the 5' termini of the insert sequence and EcoRI at the 3' termini. Reactions were

carried out in a total volume of 30  $\mu$ l, 1  $\mu$ g of DNA was digested with 10 units of each endonuclease with 3  $\mu$ l of NEB buffer 4 and the reaction volume was increased to 30  $\mu$ l with ddH<sub>2</sub>O. Samples were incubated for 1 hour at 37°C.

#### **2.4.2 Agarose gel electrophoresis**

Agarose gel electrophoresis was performed to confirm the presence of PCR and restriction digest products. DNA was separated on a 1.6% agarose gel which was prepared by dissolving 0.8 g of agarose in 50 ml of 1x TAE. This was made molten by heating up in a microwave until boiling. Once cooled, 5  $\mu$ l of SYBR safe DNA gel stain (Invitrogen, USA) was added and the gel was poured in a 10 x 20 cm gel tank (mini-sub cell GT, BioRAD) and a 10-well comb was inserted and the gel was left to cool down at room temperature (RT). DNA sample (10  $\mu$ l) was mixed with 2  $\mu$ l gel loading dye, the size of the DNA fragment was determined by comparison with a commercial size marker. SeeBlue prestained protein marker (Invitrogen, USA) or ColorPlus Prestained Protein Marker (NEB, USA) was performed. Electrophoresis was carried out in a horizontal tank containing 1xTAE buffer and run at 80 V for 40 min. The agarose gel was imaged using a Syngene InGenius gel documentation system (SynGene Bioimaging).

#### **2.4.3 DNA sequences**

Cloned DNAs were purified and their identity confirmed by DNA sequencing (GATC-Biotech Ltd (Germany)). Sequence analysis was performed using online tools ([https://www.gatc-biotech.com/en/mygatc4/single-read-sequencing/my-watchbox/my-singlerun.html#watchboxlist\\_watchbox\\_div](https://www.gatc-biotech.com/en/mygatc4/single-read-sequencing/my-watchbox/my-singlerun.html#watchboxlist_watchbox_div)), (<http://blast.ncbi.nlm.nih.gov>), ([http://www.ebi.ac.uk/Tools/psa/emboss\\_needle/nucleotide.html](http://www.ebi.ac.uk/Tools/psa/emboss_needle/nucleotide.html)).

#### **2.4.4 Ligation of DNA fragments**

Ligation between restricted PCR products and digested vector was achieved using T4 DNA ligase (NEB). A typical reaction had a final volume

of 10 µl, and contained 400 units of T4 DNA ligase in 1× T4 DNA ligase buffer. The ligation reaction was performed in a ratio of 3:1 DNA to vector and incubated for 30 min at RT. Subsequently, the ligated products were transformed into competent cells.

#### **2.4.5 Transformation of competent bacteria**

DNA plasmids were transformed into appropriate competent bacteria (Table 1) as described by Hanahan (Hanahan, 1983). Competent cells (50 µl), stored at -80°C, were thawed on ice for 2 min and mixed gently with 2 µl of DNA. The suspension was incubated on ice before being exposed to heat shock at 42° C for 30 sec. Suspensions were incubated on ice for 2 min to allow the bacteria to recover from the heat shock. Subsequently, cells were grown by adding 200 µl LB medium with shaking at 180 rpm for 1h at 37°C. The suspension was then spread on to LB plates containing appropriate antibiotics and incubated at 37°C overnight to obtain individual colonies.

### **2.5 Purification of DNA**

#### **2.5.1 Small scale DNA purification (minipreps).**

Purification of plasmid DNA on a small scale was performed by using Sodium dodecyl sulphate (SDS)-alkaline denaturation method by the Wizard® Plus SV Minipreps DNA Purification System (Promega, UK) according to the manufacture's protocol. Single colonies of bacteria were collected from LB-agar plates and cultured in 5 ml of LB medium with an appropriate antibiotic overnight at 37°C. The bacterial suspension was spun down 5 min at 10,000 x g and the pellet resuspended with 250 µl of resuspension solution (50 mM Tris-HCl, (pH 7.5), 10 mM EDTA and 100 µg/ml RNase). An Alkaline Lysis solution was used to release the small plasmid DNA from the bacteria, whilst retaining the larger genomic DNA. This was subsequently neutralised with an acidic solution. A high concentration of potassium acetate was added to precipitate the high molecular weight of cell debris and genomic DNA and the supernatant

containing plasmid DNA was decanted to a silica gel matrix to bind the DNA. The matrix was washed two times with high salt buffer to remove remaining genomic DNA and proteins, then the plasmid DNA eluted from the Wizard® SV Mini columns by 50 µl of low salt buffer or ddH<sub>2</sub>O.

### **2.5.2 Large scale DNA purification (maxipreps)**

QIAGEN Plasmid Plus Kit (Qiagen, Germany) was performed according to the manufacture's protocol to isolate highly concentrated plasmid DNA. Single bacterial colonies were picked from a petri dish and inoculated 5 ml and incubated at 37°C for 2h to form starter culture. 200 ml LB medium/antibiotic were inoculated with starter culture and shaken over night at 37°C. The bacterial suspension was spun down 15 min at 10,000 x g and the pelleted resuspended by 15 ml of cell resuspension Solution (50 mM Tris-HCl, (pH 7.5), 10 mM EDTA and 100 µg/ml RNase). The protocol based on a modified alkaline lysis minipreps, the genomic DNA was removed by washing with low salt solution and bacterial debris were taken away by medium salt washing while plasmid DNA eluted in high salt solution. Subsequently the collected DNA was desalted by isopropanol precipitation. Determination of purified DNA concentration was obtained by using Nanodrop spectrophotometer (Thermo Fisher Scientific, USA).

## **2.6 Mammalian Cell preparation.**

### **2.6.1 Cell culture.**

The study used MCC13 cell line which is a physiologically relevant cell to study MCPyV. It has been derived from a Merkel cell carcinoma from a metastatic cervical node of an 80 year old female patient (Leonard et al., 1993). The cells were maintained in Roswell Park Memorial Institute 1640 medium (RPMI 1640, Gibco/Sigma) supplemented with 10% foetal bovine serum (FBS, Biochrom/Gibco) and 50U/ml penicillin/streptomycin (GIBCO, UK). The optimal split ratio was 1:8 (seeding density  $0.8 \times 10^4$  cells/cm<sup>2</sup>). Cells were incubated at 37°C with a relative 5% CO<sub>2</sub>. Human Embryo

Kidney 293 cells (HEK 293) was performed for studying gene silencing. All procedures were performed in a Class II cabinet.

### **2.6.2 Thawing and preparing of cells**

A vial containing 1 ml ( $1 \times 10^6$  cells) of frozen cells was taken from liquid nitrogen and rapidly defrosted in a 37°C water bath. Cells were washed once with 9 ml of media and centrifuged at 5000g for 5 min. Pelleted cells were resuspended in 9 ml of fresh media and plated in 75 cm<sup>3</sup> flask.

### **2.6.3 Counting cells and seeding out**

Determination of the cell density was determined by use of a Neubauer chamber slide. A metachromatic stain like methylene blue was used to measure the number of viable cells.

### **2.6.4 Passage of cells:**

The cells were passaged when their monolayer density reached greater than 80% confluence. The cells were routinely passaged at a constant 1:3 ratio and required splitting every 5-6 days. Media was removed from the flask and the cells were washed with sterile phosphate buffer saline (PBS, Oxoid) before 4 ml of 1x Trypsin/EDTA (Tryp E, GIBCO) was added to the cells, and the flask incubated at 37°C for 5 min. Media (8 ml) was added to the flask to inactivate the TrypE, and a single cell suspension generated by pipetting the mixture gently. Cells were subsequently added to the appropriate culture vessel at the required number.

### **2.6.5 Transfection of cell lines**

Cells were plated in 6 or 12 wells at  $2 \times 10^5$  or  $1 \times 10^5$  cells/ml respectively. Cells were incubated 24h and transfected when at ~80% confluence. The culture medium was replaced with a serum free modification of Eagle's Minimum Essential Media (Opti-MEM®, Invitrogen, USA) 30 min before transfection after washing the cells once with PBS. To prepare DNA for

transfection, polystyrene round-bottom test tube (BD Falcon) were prepared and 200  $\mu$ l of Opti-MEM was mixed with 0.5-2.5  $\mu$ g of each DNA plasmid depending upon the transfection efficiency and nature of the experiment. The mixture was incubated for 5 min at RT. Transfection reagent, a cationic liposome reagent Lipofectamine 2000 (Invitrogen, USA) or a cationic polymer transfection polyethylenimine (PEI; Polysciences Inc.) was added to the plasmids on a 3:1 ratio of transfection reagent ( $\mu$ g): total DNA ( $\mu$ g) and incubated 20 min at RT before added to each well. Transfected cells were incubated for 24-48h according to the experiment.

For immunofluorescence assay,  $1 \times 10^5$  cells were seeded on coverslip (No 1.5; Appleton Woods, UK) into 12 well and incubated for 24h at 37°C.

### **2.6.6 Harvesting cells**

Media were aspirated from the well or plate and cells washed gently with ice-cold PBS. Then 20  $\mu$ l per  $1 \times 10^6$  cells of ice-cold lysis buffer (10 mM Tris/HCl pH 7.5; 150 mM NaCl; 0.5 mM EDTA; 0.5% NP-40 and protease inhibitor cocktail (1:50; Roche) was added directly to the cells, which were then scraped into a labelled 1.5 ml Eppendorf tube. Lysed cells were incubated on ice for at least 20 min with extensive pipetting then centrifuged 10 min at  $17,000 \times g$  in 4°C to pellet the insoluble cell debris. Supernatants containing soluble material were collected into fresh Eppendorf tubes.

## **2.7 Protein preparation.**

### **2.7.1 Protein concentration estimation.**

The protein concentration of cell lysates was determined using the detergent-compatible bicinchoninic acid (BCA) protein assay kit (Thermo Fisher Scientific, USA) according to the manufacturer's protocol. Lysates were either used immediately or stored at -20°C since freeze-thaw cycles can decrease protein stability, protein lysates were stored in single use aliquots which were not re-frozen.

### **2.7.2 SDS polyacrylamide gel electrophoresis (SDS-PAGE)**

Proteins were analysed by sodium dodecyl sulphate polyacrylamide gel electrophoresis (SDS-PAGE). Proteins were run in a mini gel system (BioRAD, USA). Two gels were prepared. The resolving gel was prepared by mixing 10%, 12% or 15% v/v of Acrylamide with 375 mM Tris/Cl, pH 8.8 and 0.1% SDS, 0.1% APS and 0.01% TEMED, and stacking gel made using 6% Acrylamide, 125 mM Tris/Cl, pH 6.8; 0.1% SDS, 0.1% APS, 0.01% TEMED. The stacking gel was poured on top of the resolving gel after solidification and an appropriate comb was inserted in the stacking gel to create wells in which to load the samples. Samples were mixed 1:1 with 2x SDS loading buffer (Invitrogen, USA) which contains 10% w/v SDS, 10 mM 2-mercaptoethanol, 20% v/v Glycerol, 0.2 M Tris-HCl, pH 6.8 and 0.05% w/v Bromophenol blue and protein were denatured by heating at 80°C for 10 min. SeeBlue prestained markers (Invitrogen, USA) or ColorPlus Prestained Marker (NEB, USA) (5 µl) were analysed in parallel to experimental samples and served as protein standards. Electrophoresis was performed at 120-180 V in 1x SDS running buffer which contains 34.7 mM SDS, 250 mM Tris Base and 1.92 M Glycine until the desired protein resolution was achieved.

### **2.7.3 Western blotting**

Proteins analysed by SDS-PAGE were transferred using a Semi-Dry Cell (BioRAD) to HybondTM-C ester nitrocellulose membranes (Amersham Biosciences). A sandwich consisting of membrane stacked on the gel covered with sponges in both sides were soaked in 1x transfer buffer which contains 129 mM Glycine, 25 mM Tris Base and 20 % methanol before conducting the semidry transfer at 15 V for 60-90 min. Membranes were incubated in blocking solution, which contains 5% Marvel dried skimmed milk in TBS-T (TBS: 25 mM Tris/Cl, pH 7.5; 138 Mm NaCl and 0.1% Tween-20) for 30 min at RT on a shaking platform. The membrane was then washed twice with TBS-T and incubated with diluted primary antibody (Table 2.4) for 1h at RT with shaking or alternatively incubated overnight at 4°C on a

shaking platform. Membranes were then washed 3 times for 10 min with TBS-T at shaking platform at RT and subsequently incubated 1-3h with diluted secondary antibody (Table 2.5), conjugated to horseradish peroxidase. Antibodies were diluted in blocking solution. The membranes were washed three times again, prior to development which used equal amounts of enhanced chemiluminescent solution (ECL1, 2.5 mM Luminol, 40 nM p-coumaric acid, 100 mM Tris/Cl, pH 8.5 and ECL2 0.02% H<sub>2</sub>O, 100 mM Tris/Cl, pH 8.5) or SuperSignal West Femto Chemiluminescent Substrate (Thermo Fisher Scientific, USA), which was used only with faint protein bands. Membranes were then exposed to CL-Xposure film (Thermo Fisher Scientific, USA) or Amersham Hyperfilm ECL (GE Healthcare, UK) for an appropriate length of time (0.2-15 min). The film was automatically developed using a table-top processor (Konica SRX-101A).

*Table 2.4 Information of primary antibodies used in this study.*

antibody	manufacturer	description	Immunogen	size of target	dilution WB
$\alpha$ -GAPDH	Abcam	mouse monoclonal	rabbit muscle glyceraldehyde-3-phosphate dehydrogenase	36 kDa	1:20000
$\alpha$ -GFP	Santa Cruz Biotechnology	mouse monoclonal	full length GFP of <i>Aequorea victoria</i> origin	37 kDa	1:1000
$\alpha$ -GST	obtained from Dr S. Griffin, University of Leeds	sheep pure IgG	GST His-p7	26 kDa	1:1000
$\alpha$ -HA	Sigma	mouse monoclonal	synthetic peptide corresponding to amino acid residues 98-106 (YPYDVPDYA) of human Influenza virus	32kDa	1:5000

antibody	manufacturer	description	Immunogen	size of target	dilution WB
			hemagglutinin		
$\alpha$ -Myc	Santa Cruz Biotechnol ogy	mouse monoclonal	amino acids 408-439 within the C-terminus of human c-Myc	1.2kDa	1:1000
$\alpha$ -FLAG	Sigma	Mouse monoclonal	Synthetic peptide DYKDDDDK	1.01 kDa	1:1000
$\alpha$ -FLAG	EnoGene	Rabbit polyclonal	Synthetic peptide DYKDDDDK	1.01 kDa	1:1000
$\alpha$ -transferrin receptor (TfR)	Invitrogen	mouse monoclonal	Amino acids 3- 28 of human transferring receptor	84 kDa	1:1000
$\alpha$ Glu-Glu	Millipore	Rabbit polyclonal	Synthetic peptide Glu-Glu- (EEEEYMPME)	1.29 kDa	1:1000
$\alpha$ -PP4R1	Abcam	Rabbit, polyclonal PP4C	Synthetic peptide: APQETRGIPSK KPV	107 kDa	1:1000
$\alpha$ -PP4C	Abcam	Rabbit, polyclonal PP4R1	Synthetic peptide: FVSQDEMLTPL GRLD	35kDa	1:1000
$\alpha$ -NEMO	Abcam	Rabbit polyclonal	Anti-full length	48kDa	1:1000
$\alpha$ -IKK $\alpha$	Abcam	Rabbit, polyclonal	A synthetic peptide corresponding to residues in the N terminus of human IKK $\alpha$ .	85kDa	1:5000

antibody	manufacturer	description	Immunogen	size of target	dilution WB
$\alpha$ -IKK $\beta$	Abcam	Mouse, IgG1	This antibody was raised against the 6xHis tag full-length protein corresponding to human IKK $\beta$ .	87kDa	1:5000
$\alpha$ -Lamin B	Abcam	mouse monoclonal	Synthetic peptide conjugated to KLH derived within residues 550 to the C-terminal of Human Lamin A.	67 kDa	1:1000

*Table 2.5 Information of secondary antibodies used in this study.*

Antibody	Manufacturer	Dilution WB
$\alpha$ -mouse IgG (whole molecule) – peroxidase	Sigma, USA	1:5000
$\alpha$ -rabbit IgG (whole molecule) – peroxidase	Sigma, USA	1:5000
Alexa Fluor® 594 Goat Anti-Mouse IgG	Invitrogen, USA	1:500

#### **2.7.4 Re-probing the membrane.**

Membrane was washed twice with TBST before being incubated with the Blot Restore Membrane Rejuvenation kit (Millipore, UK). Initially membranes were incubated in Buffer A with gentle agitation for 15 min at RT to remove the secondary antibody, followed by incubation with Buffer B for 10 min to remove the primary antibody. Membranes were then incubated with blocking

buffer for 5 min to reduce the background and re-probed with an appropriate antibody.

### **2.7.5 Densitometry analysis of Western blots**

To compare protein expression levels western blot films were digitalised by scanning on an Epson Perfection V600 Photo Scanner as a 24 bit image and a resolution of 600 dpi. Protein levels were quantified using ImageJ (National Institutes of Health, USA). Clear background blot images were chosen and inverted. Target protein bands were selected by lining the bands to compare their intensities which determined by the 'measure' function. Areas of the film with no protein bands were measured and deducted as background. The resulting data was entered into OriginPro8.6 (MicroCal Inc., USA) to perform a one-way analysis of variance (ANOVA).

## **2.8 Protein interactions.**

### **2.8.1 Co-Immunoprecipitation (Co-IP)**

#### **2.8.1.1 GFP Trap precipitation**

GFP fusion proteins were precipitated using GFP-Trap magnetic beads (ChromoTek) according to their manufacturer's protocol. Cells expressing proteins of interest were lysed in GFP-Trap lysis buffer (10 mM Tris/Cl pH 7.5; 150 mM NaCl; 0.5 mM EDTA; 0.5% NP-40 and 1x protease inhibitor cocktail) as described (2.2.6). A slurry of GFP-Trap magnetic beads was washed twice with ice-cold dilution buffer (10 mM Tris/Cl pH 7.5; 150 mM NaCl; 0.5 mM EDTA) before being incubated with the cell lysate for 2h at RT or 24h at 4°C with shaking. GFP-TRAP beads were separated from the supernatant using a magnetic rack (Qiagen, Germany). The beads were then washed three times with dilution buffer before being resuspended in 50µl of 2x SDS sample buffer with 0.1% (v/v) 2-mercaptoethanol.

### **2.8.1.2 FLAG Agarose precipitation**

Precipitation of proteins containing a FLAG epitope was performed using anti-FLAG M2 Agarose Affinity Gel (Sigma). Cells expressing proteins of interest were lysed in FLAG lysis buffer (50 mM Tris HCl, pH 7.4, with 150 mM NaCl, 1 mM EDTA, 1% Triton X-100 with 1x protease inhibitor cocktail) as described (2.2.6). FLAG agarose resin was washed with 0.5 ml ice-cold TBS and cleared by centrifuged at 2000 g for 30 seconds. The supernatant was removed from the resin before incubation with cell lysate for 1h at RT. The resin was then precipitated by centrifugation and washed five times (15 min each) with TBS to decrease background. Proteins were eluted from the agarose resin with 50 µl of 2x SDS sample buffer without reducing factor to avoid contamination with heavy and light chains of the M2 antibody.

### **2.8.2 Co-immunofluorescence (Co-IF)**

#### **2.8.2.1 Cell fixation**

Cells were transfected as mentioned (2.6.5). Cells fixed using a 4% paraformaldehyde solution for 15 min at RT and permeabilised for 10 min with (1% Triton X-100) then blocked in PBS-1% bovine serum albumin (BSA) for 1 h before staining with appropriate antibodies.

#### **2.8.2.2 Staining cells with specific antibodies.**

Cells were washed three times with PBS and incubated with primary antibodies for 1h. Cells were washed three times again and incubated with the 594, Alexa Fluor-conjugated secondary antibody. Cells were washed again and coverslips mounted on glass slides with mounting medium containing the nuclear stain reagent 4', 6-diamidino-2-phenylindole) (DAPI,

UltraCruz™ Hard-set Mounting Medium, SantaCruz, UK). Coverslip edges were sealed with nail polish to prevent movement and drying out.

### **2.8.2.3 Imaging and confocal microscopy.**

Cells were viewed on a Zeiss 700 Meta laser scanning confocal microscope under a 63 oil immersion objective lens. The LSM700 with 405 nm, 488 nm, 555 nm and 639 nm laser which present four colour observations. Representative images were processed using the Zen 2012 software (Zeiss, Germany).

## **2.9 Luciferase reporter assays.**

Duplicate wells of cells were transfected with the Concanavalin A NF- $\kappa$ B reporter plasmid and an appropriate expression plasmid. Co-expression with the promoter-Renilla luciferase thymidine kinase (pRLTK) plasmid was used for transfection normalization. Cells were transfected in serum free conditions to reduce background luciferase expression. Post transfection (24h), cells were stimulated by treating with 10 ng/ml TNF- $\alpha$  and incubated for a further 6-8h. Samples were lysed in passive lysis buffer (Promega,UK), according to the manufacturer's instructions and 20  $\mu$ l of the lysate was transferred to a 96 well luminometer plates and activity measured using a dual luciferase reporter assay (Promega,UK) in MicroLumat Plus LB 96V luminometer (Berthold Technologies). First, the luminescent signal was stabilized by injection of Luciferase Assay Reagent II (LARII), then Stop & Glo reagent was injected to stop measure the levels of Renilla luciferase. Finally, the luciferase activity of each lysate was measured in triplicate, the values were averaged, and standard deviations were calculated (Griffiths et al., 2013)

## **2.10 Subcellular fractionation**

### **2.10.1 Cytoplasm and nucleus isolation.**

Cells were grown in a 10 cm dish to approximate 80% confluence prior to transfection. Untransfected cells were used as a control (Mock). Cells were scraped and lysed with 200  $\mu$ l cytoplasmic lysis buffer (20 mM Tris/Cl, pH 7.4; 100 mM NaCl; 5mM MgCl<sub>2</sub>, 0.5% NP 40; 1x Protease inhibitor cocktail). The lysate were incubated in ice for 30min with extensive pipetting. Lysates were centrifuged at 9600g for 20 min at 4°C to separate the cytoplasmic fraction which remained in the supernatant from the pellet which contained cell nuclei. To collect the nuclear fraction, pellets were washed three times with cytoplasmic lysis buffer before re-suspending in 200  $\mu$ l radio immunoprecipitation assay RIPA buffer (50mM Tris/Cl, pH7.5; 150 mM NaCl; 1% NP 40; 0.5% w/v sodium deoxycholate; 0.1% SDS; 1 x Protease inhibitor cocktail). The suspensions were cleared by centrifugation at 96000 x g for 10 min at 4°C. The supernatant accounted for the nuclear fraction. Both fractions were analysed by Western blot and immunoblotting with appropriate antibody. Anti Lamin B was used as a marker for nuclear fraction and GAPDH for the cytoplasmic (soluble) fraction, whereas Transferrin Receptor antibody (TfR) for membranous protein.

### **2.10.2 Membrane fractionation.**

Cells were scraped into 1 ml of buffer M1 (10 mM PIPES, pH 7.4; 0.5 mM MgCl<sub>2</sub>; 1 x Protease Inhibitor Cocktail (Roche) and lysed by sonication on ice. A Sonics Vibracell VC750 sonicator (Newtown, CT) was used at 30% amplitude, using 4 cycles of 1 sec pulses for 1 min followed by a 30 sec pause. Salt concentrations were adjusted by adding 250  $\mu$ l of buffer M2 (10 mM PIPES, pH 7.4; 600 mM KCl; 150 mM NaCl; 22.5 mM MgCl<sub>2</sub>). Whole cytoplasmic fractions were separated by centrifugation at 3000 g for 10 min at 4°C and removed cell nuclei and unbroken cells. The supernatants were then subjected to ultracentrifugation in a Sorvall WX Ultra 100 ultracentrifuge (Thermo Fisher Scientific, Waltham, MA), using a TH-641 swinging bucket rotor at 100000 g for 10 min at 4°C to pellet the membranous fraction

(insoluble). The pellet was extensively washed with adjusted buffer M1 and resuspended in 2 x LDS sample buffer plus 0.1% 2-mercaptoethanol. The supernatant suspension which consisted of the soluble fraction was precipitated by four volumes of acetone at -20°C followed by spinning down for 30 min at 4000 g. After washing the pelleted soluble fraction once in 70% ethanol, the samples were resuspended in 2 x LDS sample buffer plus 0.1 % (v/v) of 2-mercaptoethanol as well. Both fractions were analysed on a Western blot. An antibody against GAPDH (1:20000; Abcam) identified the soluble fraction, while an antibody against human Transferrin Receptor (1:1000; Invitrogen,USA) served as marker for the membranous fraction.

## **2.11 Protein expression in a cell free system.**

*In vitro* protein expression was conducted using the TNT® T7 Quick Coupled Transcription-Translation system (Promega, UK). The kit includes a mixture that contains both T7 polymerase for the production of mRNA from the DNA template and then translated to produce protein. T7 master mix (40 µl) was mixed in Eppendorf tube with 0.5 µg DNA template, the volume was adjust to 50 µl with ddH<sub>2</sub>O. After 90 min of incubation at 30°C, 2 µl of each proteins was detected by western blot (2.3.5) and the expressed proteins can store at -80°C at this stage.

### **2.11.1 Protein expression in bacterial cells**

Protein expression in *E. coli* was performed according to (Smith and Johnson, 1988). Recombinant GST-MCPyV sT was transformed in *E.coli* BL21 competent cell as mentioned (2.4.5). An overnight culture of transformed bacteria was grown in 100 ml LB broth with (100 µg/ml) ampicillin and incubated until the Optical Density (OD) reaches 0.6 at 600 nm. Protein expression was induced by 1 mM isopropyl-1-thio-b-D-galactosid (IPTG) per 50 ml culture and incubated again for further 2h at

37°C. The cells were pelleted and re-suspended with cold PBS containing 0.1% protease cocktail inhibitor before harvest by sonication in ice using 3 cycles of 10 sec pulses followed by a 30 sec pause. Thus soluble GST-MCPyV sT fusion proteins were released into the media and cleared by centrifugation of the suspension for 10 min at 10000 x g at 4°C. The GST-tagged sT can be kept at -80°C in this stage.

### **2.11.2 GST pulldown assays.**

Glutathione agarose gel (Thermo scientific pierce) was used to purify bacterial expressed GST fusion proteins. 40 µl of beads was washed twice with TBS and incubated with soluble GST fusion proteins for 2h at RT. Subsequently, the gel was collected by centrifugation at 2500 x g for 5 min and washed twice with PBS containing 1% TRITON X-100. The purified GST-sT in pierce glutathione agarose was incubated with TNT T7 products for 2h at RT. The agarose was washed three times with PBS to remove any non-specific interactions.

### **2.12 Evaluation of siRNA-mediated gene silencing.**

Three oligos of each siPP4C and siPP4R1 (Table 2.6), that had been shown by the previous studies to be most potent in targeted gene silencing were used (Applied Biosystems) (Chowdhury et al., 2008, Brechmann et al., 2012). Silencing of protein expression was performed in MCC13 cell line. Cells were prepared by seeding  $2 \times 10^5$  cells in 6 well plate. Cells were transfected with 1, 1.5 or 2 µM of siRNA. Scrambled control siRNA were used in all experiments. Transfections were performed as described (2.6.5). Cells incubated for 48h to allow effective knockdown. Silencing of the targeted protein was assessed by SDS-PAGE and immunoblotting with appropriate antibodies.

*Table 2.6 Sequences of siRNA of PP4C and PP4R1.*

<b>siRNA</b>	<b>Gene targeted</b>	<b>Sequence (5'→3')</b>	<b>Company</b>
siPP4C #1	PPP4C	UCAUCGAUGGCAAGAUCUUUU	Applied Biosystems
siPP4C #2	PPP4C	UCGACCGAAAGCAAGAGGUUU	
siPP4C #3	PPP4C	GGCCAGAGAGAUCUUGGUUU	
siPP4R1#1	PPP4R1	GCCCGGAGUUUGCUCGAUA	
siPP4R1#2	PPP4R1	UGUGAGAUGUGCUGCGAUU	
siPP4R1#3	PPP4R1	GGAUAGGUGUUCUUAACATT	

## Chapter 3. MCPyV sT inhibits the NF- $\kappa$ B pathway by targeting NEMO.

### 3.1 Introduction

The possible contribution of the MCPyV virus to human cancer aetiology was first hinted at by the discovery made by Feng and colleagues (2008) that around 80% of MCC contained MCPyV DNA. Further research validated that MCPyV LT and sT proteins did indeed possess oncogenic potential. For instance, sT involvement in tumour development is suggested by high sT expression in MCC cells.

Furthermore, sT also participates in cellular modifications **such as increasing DNA damage and delaying DNA repair in sT-expressing cells. In addition, MCPyV-positive MCC cells stop growing when sT is knocked down.** Identification and analysis of related cellular proteins have enhanced understanding of sT function (Shuda et al., 2011).

Evidence from a number of laboratories, including our own, suggests that sT has a cytoplasmic localisation (Shuda et al., 2011; Griffith et al., 2013). Bioinformatic analysis predicts that the C-terminus of MCPyV sT is not conserved amongst the *Polyomaviridae*, and this may account for some of the unique features of this virus.

Most viruses that cause chronic disease disrupt the host innate immune response, the first line of immune defence, to establish infection. NF- $\kappa$ B has been investigated as a potential target for several viruses as it is implicated in the regulation of more than 100 target genes, most of them participate in the host immune response (Ghosh et al., 1998).

Given the chronic nature of MCPyV infection it is highly likely that it encodes one or more immune antagonists. To address a potential role for MCPyV sT as an immune antagonist, a gene array screen was performed.

Of note, genes containing NF- $\kappa$ B consensus binding sequences in their promoters showed a substantial reduction in expression in cells containing FLAG-sT compared to control cells (Griffiths et al., 2013). These data suggested that sT might target the NF- $\kappa$ B pathway.

This chapter focuses on our initial analysis of the basic biology of MCPyV sT, including an analysis of its subcellular localisation. It also documents attempts to understand the molecular basis for inhibition of the NF- $\kappa$ B pathway. In particular, studies in our laboratory identified an interaction with the NEMO adaptor protein (Griffiths et al., 2013). NEMO is an essential element of the IKK complex, which functions to link upstream stimuli to activation of hetero-dimeric NF- $\kappa$ B transcription factors.

NEMO lacks catalytic activity and instead interacts with polyubiquitin chains, either in isolation or conjugated to upstream signalling proteins (Walczak et al., 2012, Clark et al., 2013, Vincendeau et al., 2016), to spatially organise the IKK complex in order to activate NF- $\kappa$ B signalling. The importance of the IKK complex in anti-viral immunity resulted in the evolution of a number of evasion strategies evolving in viruses. Some of these viruses such as Hepatitis B virus inhibits activation of NF- $\kappa$ B by targeting both IKK $\beta$  and IKK $\alpha$  (Liu et al., 2014). Whilst Herpes simplex virus uses ICP27 protein to inhibit IKK $\alpha$  (Hargett et al., 2006).

It has also been shown that M protein of SARS coronavirus targets IKK $\beta$  to suppress NF- $\kappa$ B activity (Fang et al., 2007). Other viruses, like human cytomegalovirus (CMV) and *Molluscum Contagiosum* virus (MCV) prevent NF- $\kappa$ B activation by targeting NEMO to disrupt the IKK complex and prevent I $\kappa$ B degradation (Randall et al., 2012, Krause et al., 2014).

This chapter describes the thorough mapping strategy employed to understand the molecular basis for the interaction between MCPyV sT and NEMO.

## 3.2 Results

### 3.2.1 Subcellular fractionation of sT in MCC13.

In order to investigate the distribution and localization of MCPyV sT within cells, subcellular fractionation of sT was performed in MCC13 cells. Two complementary experiments were performed, a biochemical analysis to determine whether sT could associate with cellular membranes, and immunofluorescence to visualize sT localisation in the cytoplasm.

#### 3.2.1.1 MCPyV sT is a soluble protein localised in the cytoplasm.

Biochemical extraction of sT was based on differential centrifugation in density gradient buffers. At the time of performing these experiments there was no access to a specific sT antibody. Accordingly, we expressed sT fused to a FLAG epitope for immune detection. The FLAG epitope is 8 amino acids with a molecular weight of 1.01 kDa, which is small and unlikely to interfere with the function of sT. MCC13 cells were transfected with a plasmid encoding FLAG-sT and then incubated for 24h before lysis. The crude cells were fractionated into nuclear and cytoplasmic fractions using a cytoplasmic lysis buffer. Cell nuclei were separated from the cytoplasm by centrifugation at 9600xg for 20 min at 4°C. The supernatant containing the cytoplasmic fraction was resolved by SDS PAGE and probed with a monoclonal antibody against the FLAG epitope. The Western blot result showed that the majority of sT was localized within the cytoplasm, with a minor fraction of the protein detectable in the nucleus (Figure 3.1A). The integrity of the fractionation was confirmed using Western blot against host proteins associated with either the cytoplasmic or nuclear fractions. In this case Lamin B was used as a marker for the nucleus and GAPDH for the cytoplasm. The cytoplasmic fraction was further fractionated into soluble cytosol and membrane bound (2.10.1). FLAG-sT was only detected in the soluble (cytosolic) fraction (Figure 3.1B). In these assays GAPDH served as a marker of the soluble fraction, whereas Transferrin **receptor** was used to identify the membranous fraction.

### **3.2.1.2 Localization of MCPyV sT in the cytoplasm of MCC13.**

Biochemical fractionation studies demonstrated that a FLAG-sT fusion associates predominantly in the soluble fraction of the cytoplasm. To investigate this further co-immunofluorescence was used to visualise sT in whole cells. MCC13 cells were transfected with plasmids encoding pEGFP or a pEGFP-sT fusion and after incubation for 24h, cells were fixed and then analysed using a confocal microscope. The pEGFP and pEGFP-tagged sT were visualised by their green fluorescent emission. The assay **showed** that EGFP-sT localized in the cytoplasm with no specific spatial localization, whereas the cells transfected with pEGFP alone established diffuse expression in both nucleus and cytoplasm (Figure 3.2).

### **3.2.2 MCPyV sT blocks NF- $\kappa$ B signalling pathway.**

Preliminary data from our laboratories indicated that in the presence of an inducible FLAG-sT, levels of NF- $\kappa$ B-dependent gene expression were lower than in control cells (Griffiths et al., 2013). These data suggested that sT might be able to antagonise this critical pathway.

To determine whether sT could regulate NF- $\kappa$ B activity, a luciferase reporter assay was performed in which luciferase expression was driven from NF- $\kappa$ B sequences from the concanavalin A promoter. MCC13 cells expressing EGFP or EGFP-sT were treated with TNF $\alpha$ , to activate the NF- $\kappa$ B pathway. After an 8 hour incubation, cells were lysed and levels of luciferase detected using a Dual-luciferase reporter system. Results from triplicate experiments showed that levels of luciferase were reduced approximately five fold in cells expressing EGFP-sT compared to EGFP (Figure 3.3A). Expression levels of each protein were confirmed by Western blot and GAPDH used as a loading control (Figure 3.3B).

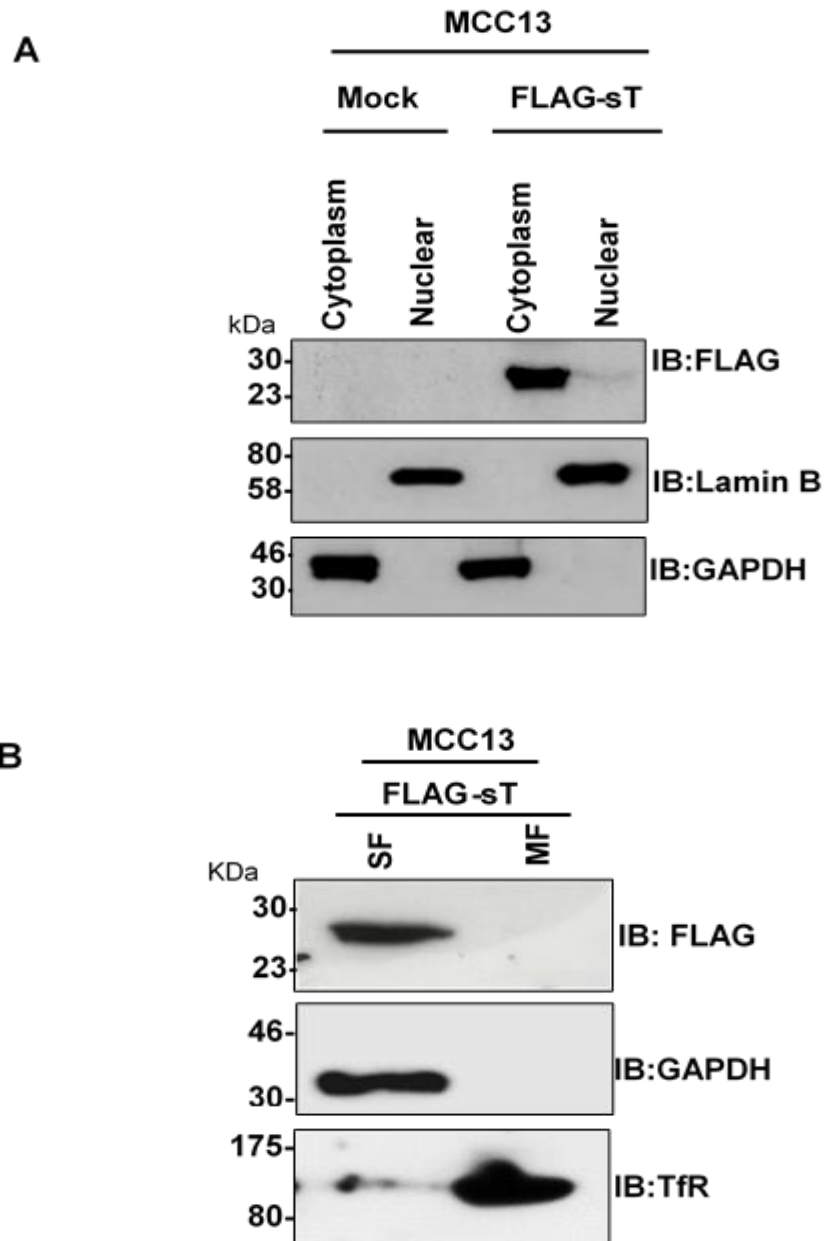


Figure 3.1: Transfected MCPyV sT enriched in the soluble fraction in a subcellular fractionation assay. MCC13 cells (A, B) were lysed by sonication and the membranous proteins separated from soluble protein by ultra-centrifugation. **A.** FLAG-sT was overexpressed in MCC13 cells and underwent subcellular fractionation 24h post transfection to isolate cytoplasmic fraction from nucleus. Untransfected cells (Mock) were used as a control. **B.** Cytoplasmic fraction of transfected MCC13 with FLAG-sT was fractionated into soluble and membranous fractions. Proteins of both fractions were separated by SDS-PAGE and the Western blot probed for FLAG-sT and a marker for nuclear protein (Lamin B) and Cytoplasmic and soluble protein (GAPDH) and for membranous protein (TfR).

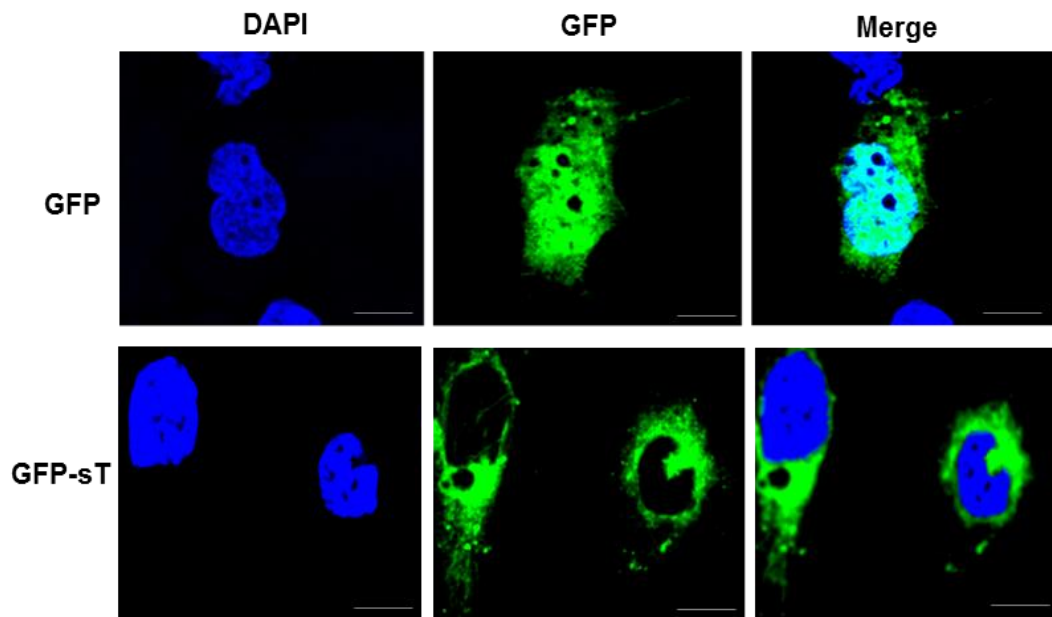


Figure 3.2 Determination of the cellular localisation of GFP-sT. MCC13 cells were transfected with GFP alone or GFP-sT. The expression of proteins was examined 24 post transfection by GFP fluorescence emission (green) and cell nuclei were labelled with DAPI (blue). Images were acquired with Zeiss LSM700 confocal microscope Representative images are shown. Scale bars = 20 $\mu$ m.

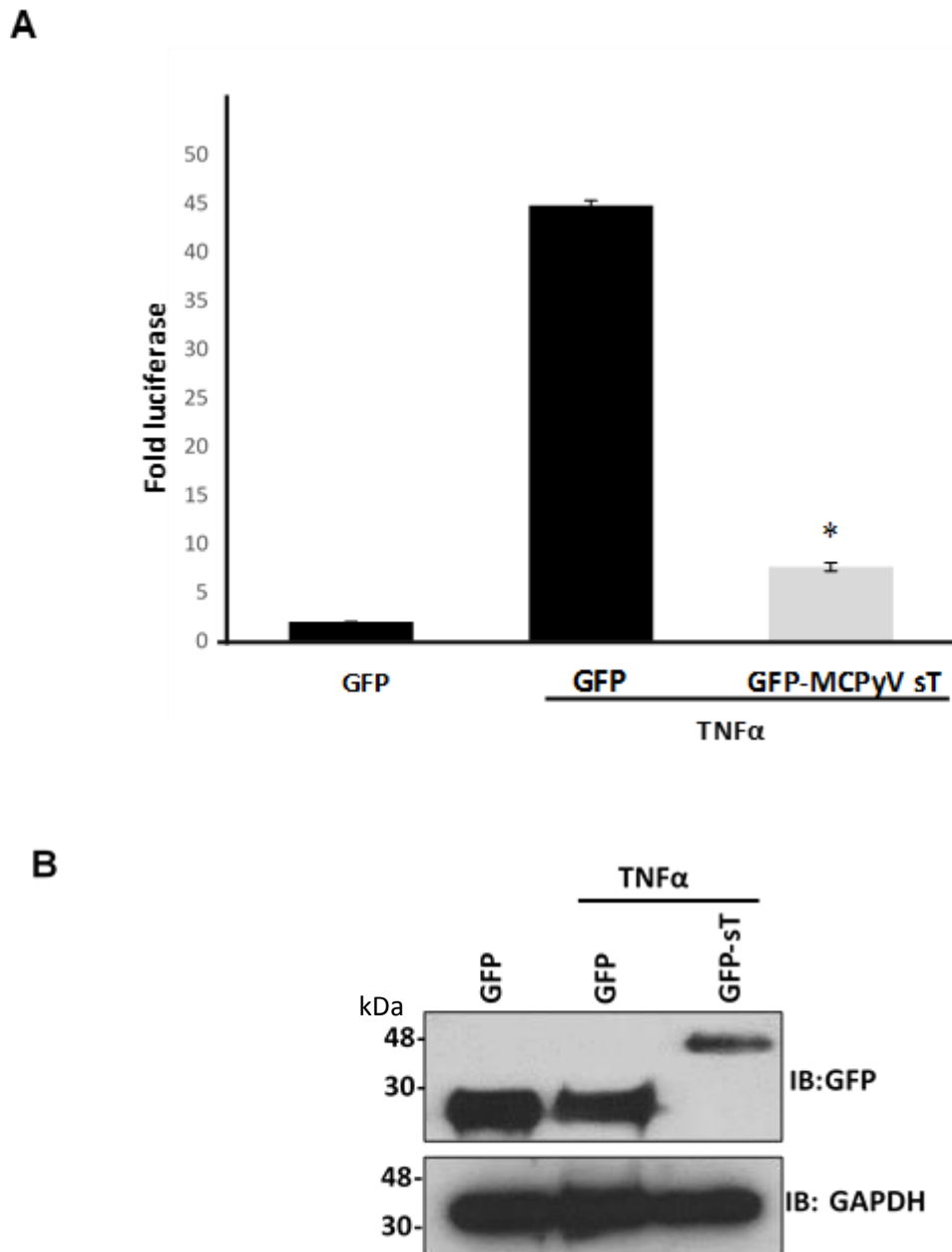


Figure 3.3: MCPyV sT mediated downregulation of NF- $\kappa$ B. **A.** Luciferase reporter assay was performed by expressing pEGFP or EGFP-sT in MCC13 cells with reporter plasmid and firefly luciferase under the control of the concanavalin A promoter. posttransfection 24 h, cells were treated with 10 ng/ml TNF- $\alpha$  for 8 h. Cells were transfected with GFP and leave without stimulated as a control. Samples were then subjected for luciferase activity. To normalize transfection efficiency, 10 ng pRLTK Renilla luciferase reporter plasmid was used, and values were normalized relative to the expression levels of the EGFP and EGFP sT vector signals. \*,  $P < 0.05$  versus GFP plus TNF- $\alpha$  ( $t$  test). **B.** Cell lysate was subjected to Western blot to detect proteins expression and GAPDH used for equal loading.

### **3.2.3 Screening for potential host binding proteins of MCPyV sT involved in NF- $\kappa$ B activation.**

A range of viruses have evolved mechanisms to inhibit the NF- $\kappa$ B pathway that result in antagonism of the innate immune response ( Ghosh et al., 1998, Valentine et al., 2010, Fiume et al., 2011). To reveal the molecular mechanism by which MCPyV sT was able to prevent NF- $\kappa$ B-mediated transcription, co-immunoprecipitation assays were performed to screen for proteins implicated in NF- $\kappa$ B signalling that might be targeted by MCPyV sT. Given the cytosolic nature of MCPyV sT, we focussed on constituents of the multi-protein complexes associated with NF- $\kappa$ B activation rather than known interacting partners of nuclear NF- $\kappa$ B. Preliminary pulldown experiments using GST fusions of host proteins and FLAG-sT identified a putative interaction with a constituent of the IKK complex (data obtained by Dr David Griffiths, University of Leeds) (Griffiths et al., 2013).

#### **3.2.3.1 MCPyV sT interacts with the NEMO.**

The trimolecular IKK complex, containing IKK $\alpha$ , IKK $\beta$  and NEMO plays a central role in the canonical NF- $\kappa$ B signalling pathway (Solt et al., 2009). Preliminary GST pulldowns indicated that MCPyV sT might target this complex by binding to the NEMO adaptor protein. To explore this possible interaction further a GFP-TRAP co-immunoprecipitation approach was adopted. For all co-immunoprecipitations data are shown from a minimum of three independent experiments. Expression of all over-expressed proteins was confirmed by Western blot.

To investigate the possible interaction between NEMO and MCPyV sT, MCC13 cells were transfected with plasmids encoding EGFP-sT and a Myc epitope NEMO fusion. Cell lysates were incubated with GFP-TRAP magnetic beads or protein G-agarose beads as a control and immune complexes were resolved by SDS PAGE and precipitates analysed by

Western blot with appropriate antibodies. Western blot of the lysates confirmed expression of all of the exogenous proteins. As shown in Figure 3.4A, immunoprecipitation with protein G-agarose beads showed no protein reactivity with either the NEMO or the GFP antibody (Figure 3.4A), suggesting that neither protein interacts non-specifically with the bead matrix. A band was observed in the EGFP-sT precipitates, corresponding to Myc-NEMO (Figure 3.4B), which was absent in the EGFP precipitate.

To exclude the possible impact of overexpression artefacts, co-immunoprecipitations of MCPyV sT with endogenous NEMO were performed in MCC13 cells. Untransfected cells (Mock) or cells transfected with pEGFP or pEGFP-sT were coimmunoprecipitated with endogenous NEMO. The pEGFP and pEGFP-sT were precipitated with the GFP-TRAP beads and NEMO was detected using a rabbit polyclonal antibody to NEMO. A band corresponding to NEMO was detected in the precipitates from cells expressing EGFP-sT but not EGFP (Figure 3.4C). Together, these data demonstrate that MCPyV sT can interact with NEMO in cells (Griffiths et al., 2013).

### **3.2.3.2 Colocalization of MCPyV sT with endogenous NEMO in MCC13**

The co-immunoprecipitation results indicated that MCPyV sT was able to interact with endogenous NEMO in a cell lysate. Whilst these data are encouraging, they do not confirm that sT is able to interact with NEMO in an intact cell. To further validate the interaction, the localisation of both proteins was assessed in cells. MCC13 cells were transfected with plasmids expressing EGFP or EGFP-sT and incubated for 24 hours prior to fixation and analysis. Endogenous NEMO was detected with a NEMO specific primary antibody and an Alex fluor 594 conjugated secondary. EGFP containing cells showed a diffuse green staining, whilst cells expressing EGFP-sT showed cytoplasmic green staining. NEMO was restricted to the cytoplasm, and co-localisation was suggested by significant yellow staining in the cytoplasm (Figure 3.5). In conjunction with the co-immunoprecipitation



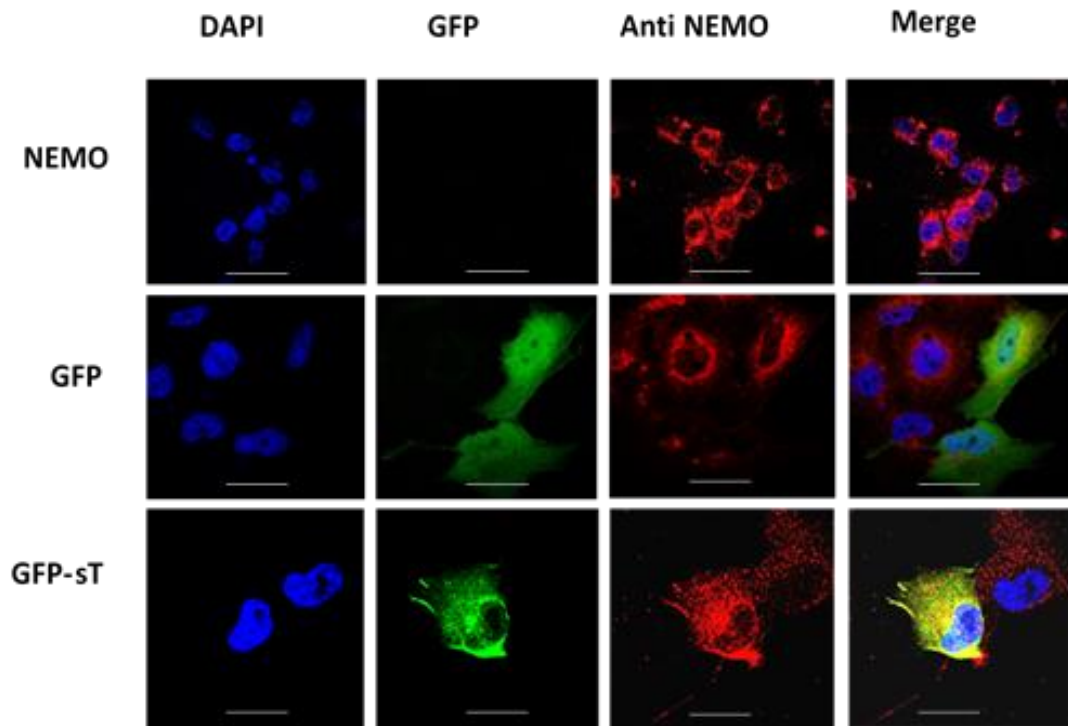


Figure 3.5: Co-immunofluorescence investigating putative colocalization of sT with NEMO in the cytoplasm of MCC13. Cells were transfected with pEGFP or pEGFP-sT. Post transfection (24h.) cells were fixed and permeabilized. The pEGFP and pEGFP-sT were detected by their green fluorescence emission and NEMO was indicated by anti NEMO (primary) and Alexa fluor 594 red fluorescent antibody (secondary). Colocalization was shown by (Yellow) puncta. Cells were stained with 4, 6-diamidino-2-phenylindole (DAPI) to stain the nuclei (blue). Images were acquired with a Zeiss LSM700 confocal microscope. Representative images were shown. Scale bars = 20 $\mu$ m.

### **3.2.4 Generating mutations in MCPyV sT to map the interaction with NEMO.**

A mutagenesis strategy was employed to broadly define the residues within MCPyV sT required for the interaction with NEMO. A series of carboxyl-terminal truncation mutants were generated terminating at the highlighted residues (1-162, 1-128, 1-95, 1-63, 1-32) as represented in the schematic (Figure 3.6A). In addition, a point mutation was engineered into full-length sT to abolish the interaction with PP2A A $\alpha$  (R7A) based on a previous publication (Shuda et al., 2012). All truncations were generated by PCR and analysed by agarose gel electrophoresis (Fig. 3.6B). Truncation and point mutant PCR products were sequenced (GATC) and cloned into the mammalian expression plasmid pEGFP-C1. Prior to co-immunoprecipitation studies, the expression levels of each mutant were confirmed in MCC13 cells, by Western blotting. As can be seen, each mutant expressed to similar levels and migrated at the expected molecular weight. Equal total protein loading was confirmed using GAPDH expression (Figure 3.6C).

#### **3.2.4.1 Residues 95-128 within MCPyV sT are required for the interaction with NEMO.**

Co-immunoprecipitation assays were performed from MCC13 cell lysates expressing Myc-NEMO and the panel of MCPyV sT truncations. Over-expressed proteins were precipitated using GFP-TRAP beads and precipitates probed by Western blot with antibodies against GFP and the Myc epitope, respectively. Co-immunoprecipitation confirmed the interaction between the wild-type sT, and NEMO (Figure 3.7). Binding was also observed for the R7A point mutant as well as truncation mutants 1-162 and 1-128. Mutants that removed amino acids beyond 95 (1-95, 1-63 and 1-32) failed to precipitate NEMO, despite expressing to similar levels as the wild-type. Thus, residues between 95-128 are likely required to bind to NEMO in cells.

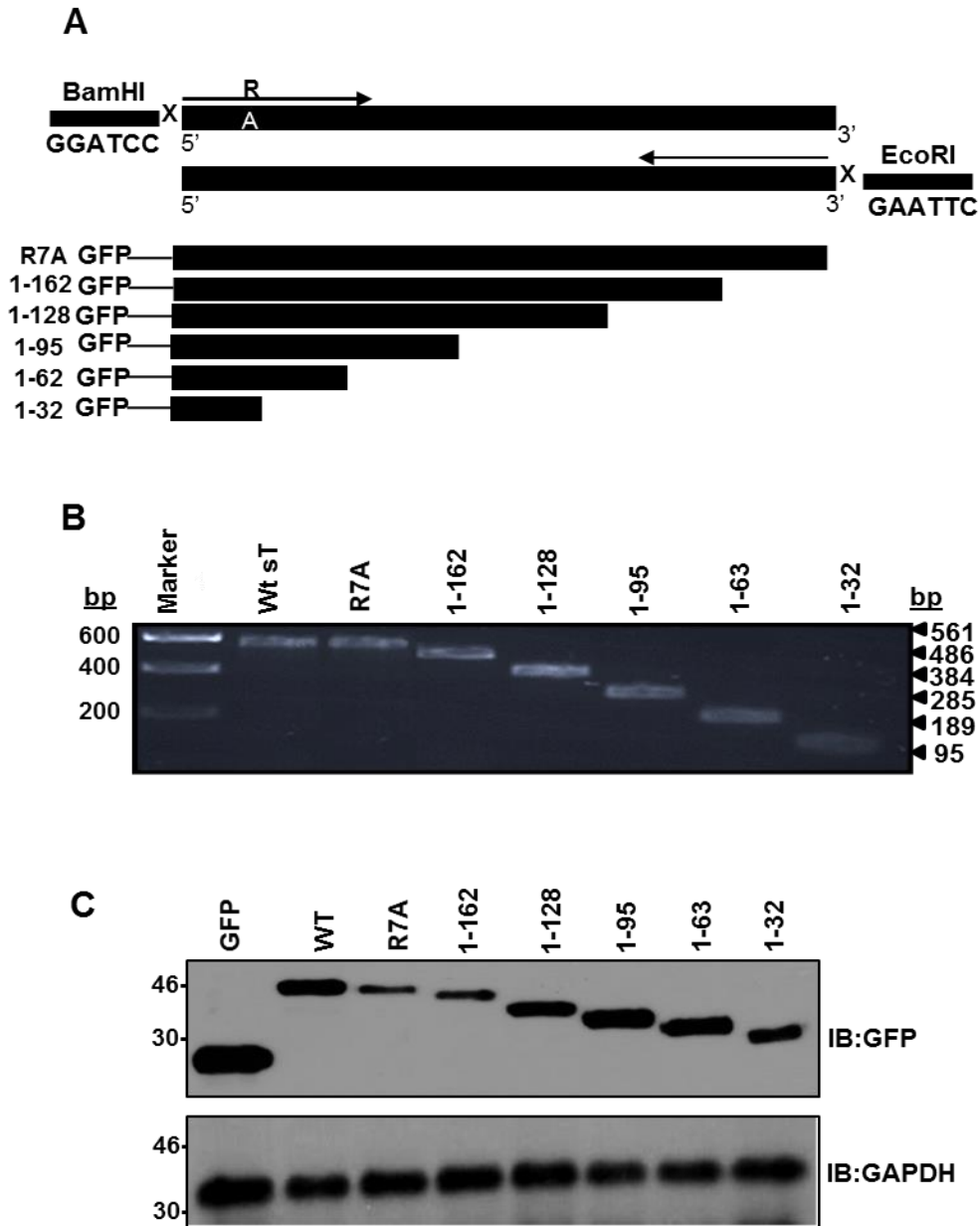
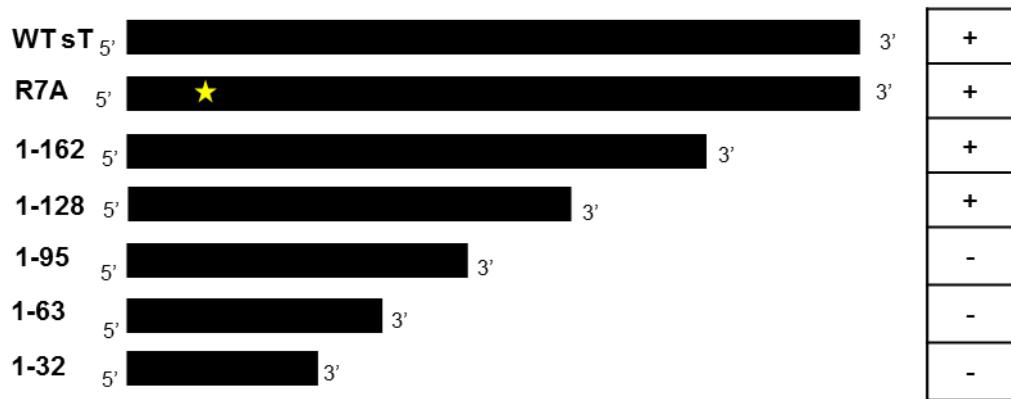


Figure 3.6: Generation of sT truncation mutants attached a C-terminal pEGFP. **(A)** Schematic representation of the sT truncation mutants. Truncation mutants named consist either of one letter changed (R7A) or a number of amino acid 1 to the number of the final amino acid before truncation. The truncation were designed in pEGFP-C1 between BamHI (forward) and EcoRI (reverse) restriction sites. **(B)** Truncation mutants were amplified by PCR and detected by gel electrophoresis which they showed right sizes compare with full length sT (Wt sT). Markers in (base pair). **(C)** Wild type GFP-sT and truncation mutants as well as R7A were expressed in MCC13 cells. Cells were lysed and proteins were isolated by SDS-PAGE and immunoblotting with GFP antibody. pEGFP alone was expressed for control and GAPDH was used as a loading control. Marker in kDa.

A



B

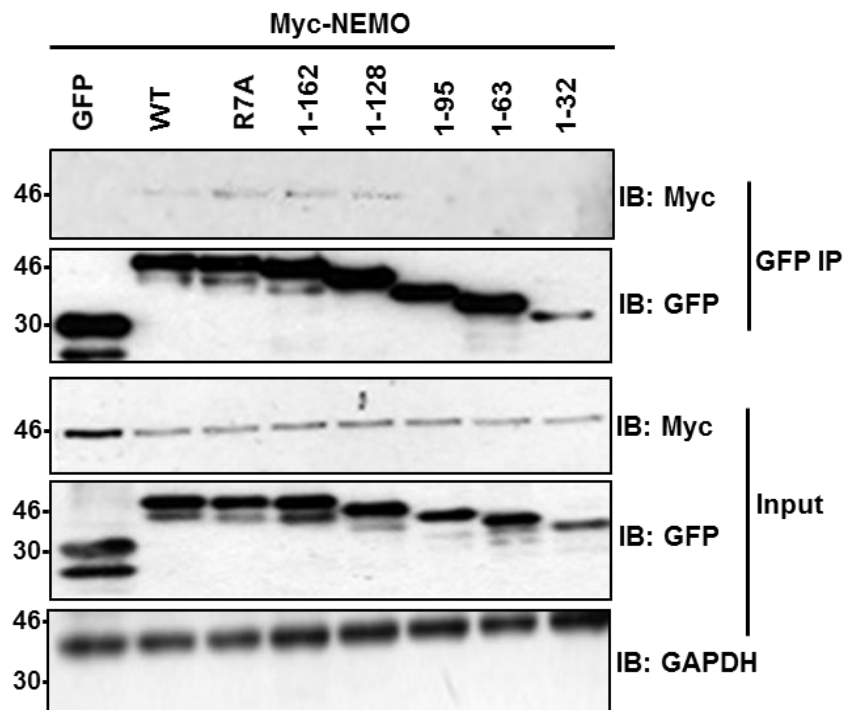


Figure 3.7: Mapping of pEGFP-sT binding site to Myc-NEMO. (A) Schematic representation of sT truncation mutant as pEGFP fusion proteins. The name of truncations were listed at the left and the star symbol refers to R7A mutant site, (+) mutation bound to NEMO and (-) mutation non-bound to NEMO (B) Co-immunoprecipitation of pEGFP-sT truncation mutants with Myc-NEMO. The pEGFP alone (control), pEGFP-sT and sT truncations were co-expressed alongside with Myc-NEMO in MCC13 cells. The Co-immunoprecipitations were performed with equal amounts of total protein using GFP-TRAP magnetic beads and probed with GFP and Myc antibodies. Representative blot is shown. Marker in kDa.

#### **3.2.4.2 NEMO binds to amino acids within 95-111 of sT.**

Two internal deletion mutants were generated to characterise the residues necessary for the MCPyV sT-NEMO interaction in cells. In this case a strategy was employed to generate internal deletion mutants that each removed half of the 32 amino acids shown to be important using the carboxy-terminal truncation studies. MCPyV sT $\Delta$ 95-111 and MCPyV sT $\Delta$ 111-128 were created by site directed mutagenesis. MCC13 cells were co-transfected either with wild type sT or with the deletion mutants in addition to Myc-NEMO. The cell lysates were coimmunoprecipitated using GFP-TRAP beads and any interaction assessed by Western blotting. Results of the co-immunoprecipitation indicated that the  $\Delta$ 95-111 mutant was not able to bind NEMO, whereas  $\Delta$ 111-128 retained the interaction (Figure 3.8).

#### **3.2.4.3 MCPyV sT residues 101-103 are required for the interaction with NEMO.**

Alanine scanning mutagenesis was next performed to probe the region of MCPyV sT between amino acids 95 and 111. Four sT mutants were generated, each containing four amino acids converted to alanine (A96-99, A100-103, A104-107 and A108-111). All mutants expressed to similar levels and were precipitated from MCC13 cell lysates using GFP-TRAP beads and interactions with co-expressed Myc-NEMO determined by Western blot. MCPyV sT A100-103 failed to interact with Myc-NEMO, whereas the other mutants retained their binding ability. This finding indicates that residues 100-103 are essential for this interaction (Figure 3.9).

Truncations and internal deletion mutants are critical for identifying regions of interaction between proteins. However, there are caveats to their use, including unexpected global changes to protein structure. Therefore, the ideal scenario would be to identify point mutations within a protein that abrogate the interaction with a binding partner under study. To determine whether such a mutant could be generated in sT to prevent the interaction

with NEMO, single amino acid mutations were introduced at residues 100-103 (N100A, A101R, R102A, and F103A) using the Q5 site directed mutagenesis kit. Mutants were sequenced and cloned into pEGFP. Co-immunoprecipitations were performed between each mutant and Myc-NEMO. The pEGFP alone and the wild type sT were used as a negative and positive controls, respectively. Western analysis revealed that N100A retained the ability to bind NEMO, whereas A101R, R102A, and F103A all lost their interaction properties (Figure 3.10), implying that the three amino acids A101, R102 and F103 are required for interaction with NEMO.

### **3.2.5 Impact of point mutations on the ability of MCPyV sT to inhibit the NF- $\kappa$ B pathway.**

Luciferase assays were employed to demonstrate whether recruitment of MCPyV sT to NEMO and the IKK complex was necessary for the inhibition of NF- $\kappa$ B signalling observed (Griffiths et al., 2013). Cells were transfected with the ConA luciferase reporter plasmid and the sT point mutants used to determine the binding requirements to NEMO. Transfected cells were subsequently treated with TNF $\alpha$  for 8 hours to activate NF- $\kappa$ B signalling. Cells were lysed in Passive Lysis Buffer (PLB) and assayed using a Dual Luciferase reporter system (Promega). The results demonstrated that N100A and A101R inhibited NF- $\kappa$ B-driven luciferase to similar levels as the wild-type sT (Figure 3.11A). The R102A and F103A mutants, which no longer interact with NEMO, were still able to inhibit NF- $\kappa$ B activity, although to less of an extent than the wild-type sT. Equal expression of each protein was demonstrated by Western blot (Figure 3.11B).

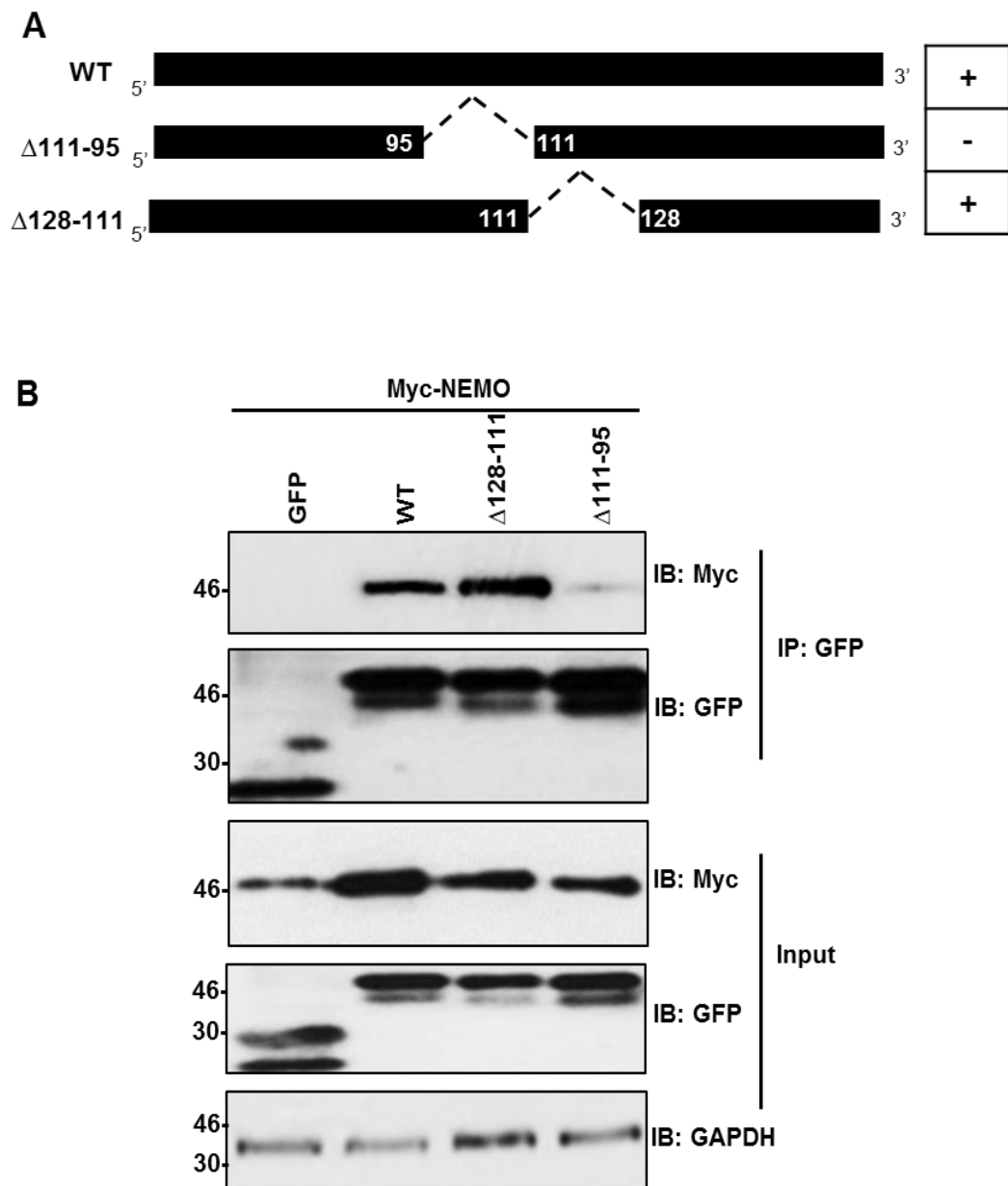


Figure 3.8: MCPyV sT required residues 95-111 to interact NEMO. **(A)** Schematic representation of sT internal deletions between residues 95-128 (dash lines), (the symbols  $\Delta$  refers to the area of deletion, (+) mutation bound to NEMO and (-) mutation non-bound to NEMO). **(B)** Co-immunoprecipitations of pEGFP alone (control), pEGFP-sT and two deletion mutants  $\Delta$ 95-111 and  $\Delta$ 111-128 with Myc-NEMO. Proteins were expressed in MCC13 cells and precipitated by GFP-TRAP magnetic beads. GFP and Myc antibodies were used to probe GFP tagged proteins and NEMO respectively. GAPDH used for loading control. Representative blot is shown. Marker in kDa.

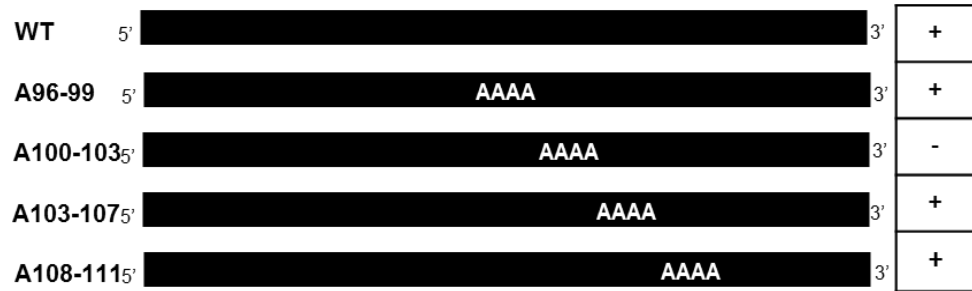
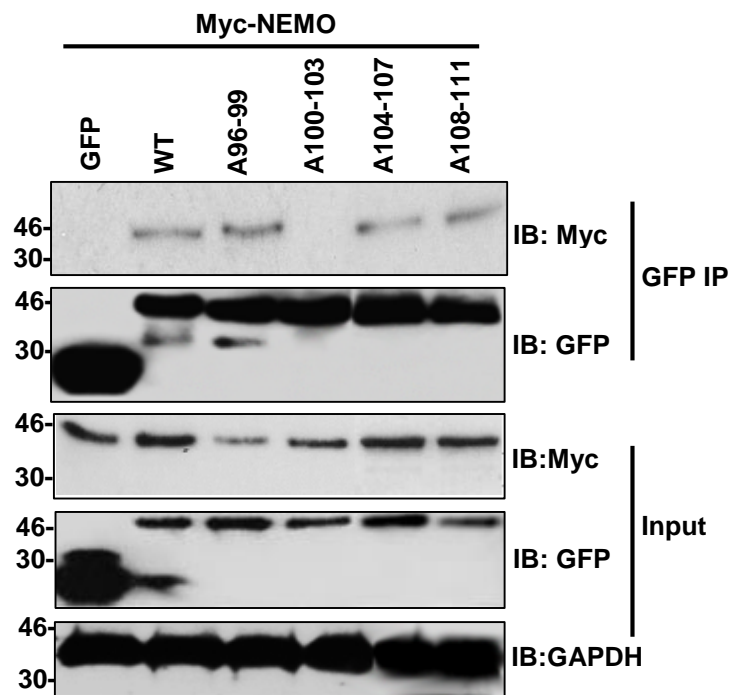
**A****B**

Figure 3.9: MCPyV sT required residues 100-103 to interact NEMO. (A) Schematic representation of sT alanine mutants within 95-111, (the letters **AAAA** refers to the amino acid replaced to alanine), (+) mutation bound to NEMO) and (-) mutation non-bound to NEMO). (B) Co-immunoprecipitations of pEGFP alone (control), pEGFP-sT and four mutants with Myc-NEMO. Proteins were expressed in MCC13 cells and precipitated by GFP-TRAP magnetic beads. GFP and Myc antibodies were used to probe GFP tagged proteins and NEMO respectively. GAPDH used for loading control. Representative blot is shown. Marker in kDa.

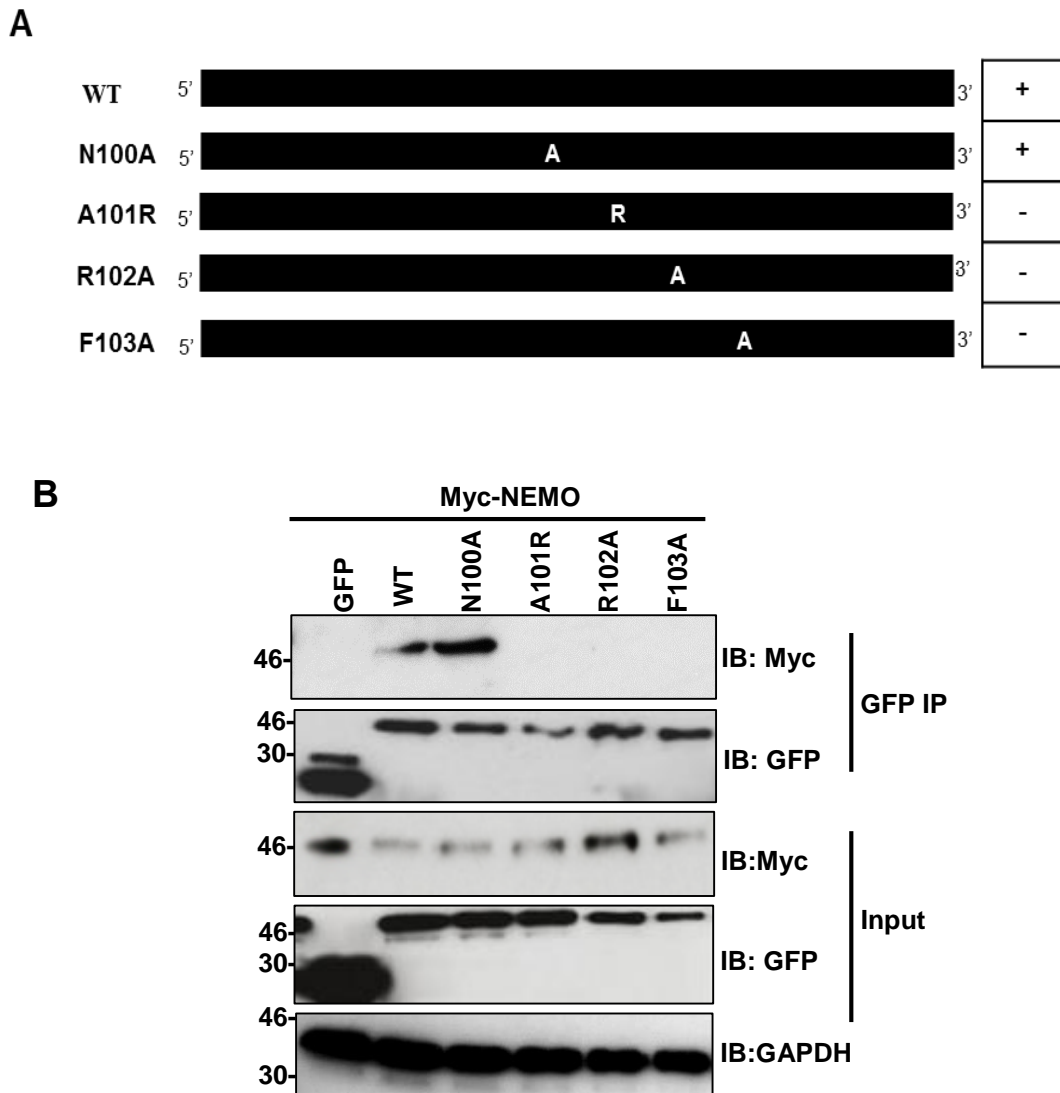


Figure 3.10: MCPyV sT required residues 101,102 and 103 to interact NEMO. (A) Schematic representation of sT point mutants within 100-103, (the letters **A** or **R** refers to the amino acid replaced). The symbol (+) refers to the mutation bound to NEMO and (-) for mutation non-bound to NEMO. (B) Co-immunoprecipitations of pEGFP alone (control), pEGFP-sT and the four point mutants with Myc-NEMO. Proteins were expressed in MCC13 cells and precipitated by GFP-TRAP magnetic beads. GFP and Myc antibodies were used to probe pEGFP tagged proteins and NEMO respectively. GAPDH used for loading control. Representative blot is shown. Marker in kDa.

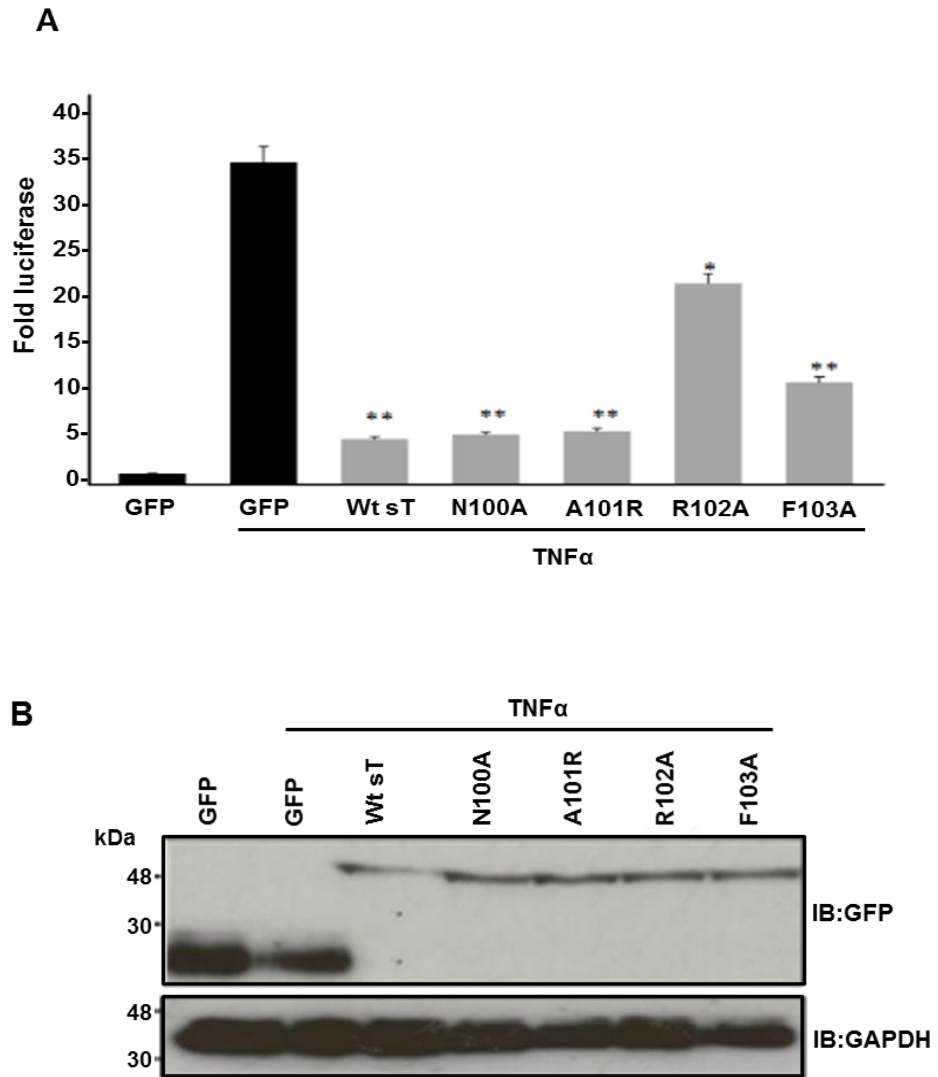


Figure 3.11: Two amino acids in MCPyV sT mediate NF- $\kappa$ B inhibition. **A**. Luciferase reporter assay was performed by expressing pEGFP, EGFP-sT or one of the point mutants in HEK 293 T cells with reporter plasmid and firefly luciferase under the control of the NF- $\kappa$ B elements from the concanavalin A promoter. Post transfection 24 h, cells were treated with 10 ng/ml TNF- $\alpha$  for 6-8 h. Unstimulated GFP was used as a control. Samples were then subjected for luciferase activity. To normalize transfection efficiency, 10 ng pRLTK Renilla luciferase reporter plasmid was used, and values were normalized relative to the densitometry expression levels of the EGFP and EGFP-ST vector signals. \*,  $P < 0.05$  versus GFP plus TNF $\alpha$  ( $t$  test)

### **3.2.6 Identifying the regions within NEMO necessary for the interaction with MCPyV sT.**

NEMO has no catalytic activity but it is required for IKK activity by mediating kinase oligomerization and interactions with upstream signalling components (Chiaravalli et al., 2011). In the absence of NEMO, the IKK complex cannot be activated and the canonical NF- $\kappa$ B signalling pathway is blocked due to the essential role of NEMO in IKK activity (Rudolph et al., 2000, Yang et al., 2011). Our studies demonstrated an interaction between MCPyV sT and endogenous NEMO (Figure 3.4). To characterise the regions in NEMO necessary for the interaction with sT a series of NEMO truncations was employed.

#### **3.2.6.1 Generation and analysis of NEMO truncation mutants.**

In order to broadly define the residues within NEMO required for interaction with MCPyV sT, a series of carboxy-terminal truncation mutants were generated terminating at the highlighted residues (1-246, 1-110, 30-246, 246-419, 246-337) as represented in the schematic (Figure 3.12A). The truncations were cloned into the mammalian expression plasmid pcDNA3.1 with an in-frame amino terminal FLAG epitope. Three of these truncations in the N terminus of NEMO (1-246, 1-110, 30-246), necessary for binding to the IKK catalytic subunits as reported by (Cote et al., 2013), and two in the C terminus (246-419, 246-337), necessary for oligomerization and ubiquitination (Emmerich et al., 2013). Co-immunoprecipitation experiments with the FLAG-NEMO truncations and GFP-sT was performed from MCC13 lysates and the protein complexes precipitated by GFP-TRAP beads. The co-immunoprecipitation illustrated that the area of interaction lies between residues 246 to 337 (Figure 3.12). This area contains the second coiled coil domain (CC2) and leucine zipper (LZ) domains that are thought to mediate NEMO oligomerization and ubiquitin binding (Grubisha et al., 2010).

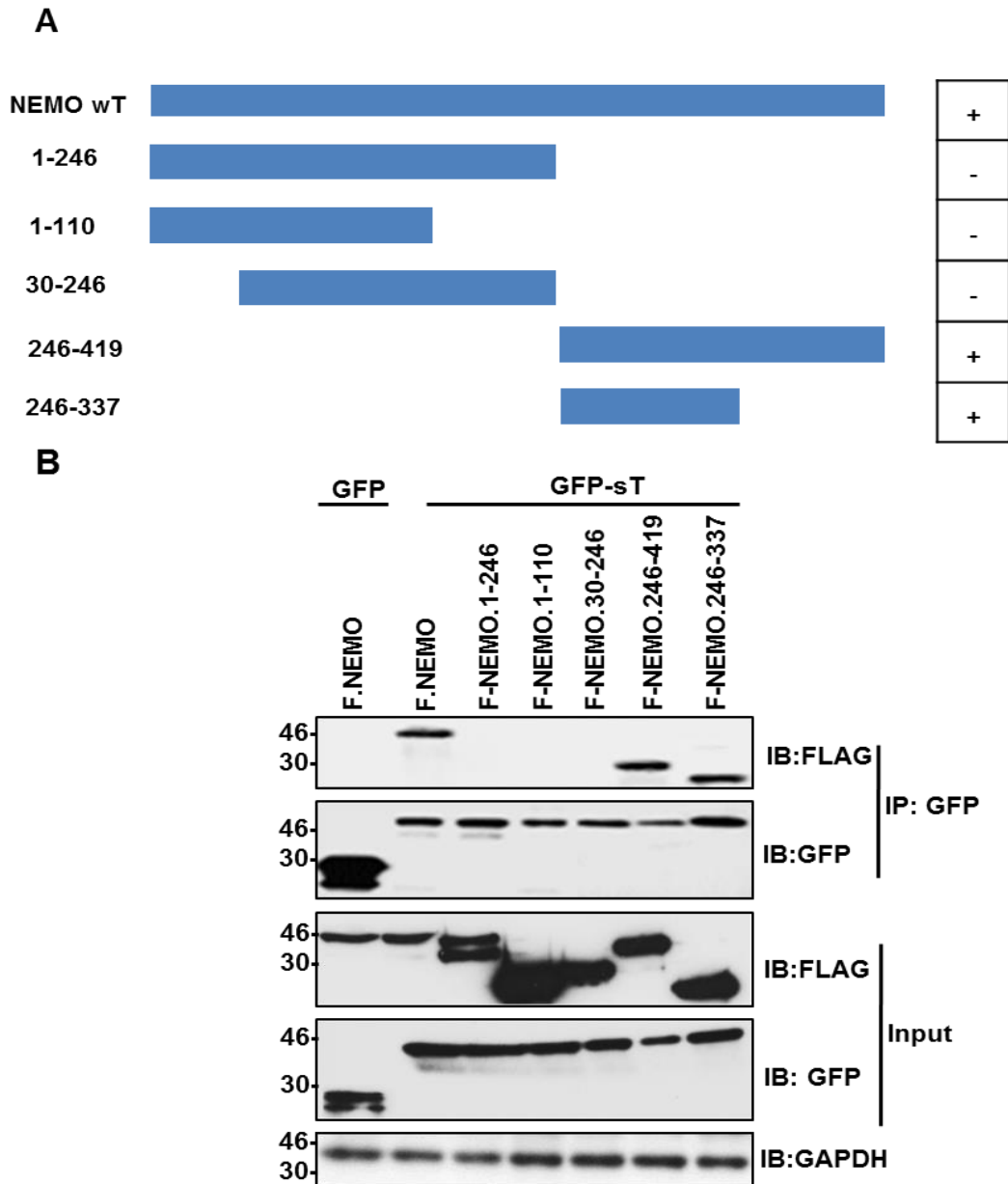


Figure 3.12: Mapping the domains within NEMO which are required for the interaction with MCPyV-sT. **(A)** Schematic representation of the full length NEMO (1-419) and five truncations were listed at the left side. The symbol (+) refers to the NEMO mutants bound to sT and (-) for mutation non-bound to sT. **(B)** Co-immunoprecipitations of full length NEMO and NEMO truncations each with GFP sT, GFP alone transfected with full length FLAG-NEMO (as a control). Cells were lysed and proteins were incubated with GFP-TRAP beads to precipitate GFP-sT. Immune complexes resolved by SDS-PAGE and immunoblotted with FLAG antibody for FLAG-NEMO and GFP antibody for GFP sT. The GAPDH performed to confirm equal loading of lysed proteins input. Representative blot is shown. Marker in kDa.

### **3.2.6.2 MCPyV-sT interacts with the NEMO ubiquitin-binding domain.**

The CC2 and LZ domains of NEMO have been shown to be essential for both the ubiquitin-binding and oligomerisation properties of NEMO, and mutations of these domains impact NF- $\kappa$ B activation (Agou et al., 2004). To reveal a minimal domain required for the interaction with sT, two internal deletion mutants of NEMO FLAG- $\Delta$ 246-302 and FLAG- $\Delta$ 302-365 were used in coimmunoprecipitation assays with GFP-sT. The results showed that the  $\Delta$ 246-302 mutant retained its ability to interact with sT, whereas loss of amino acids  $\Delta$ 302-365 abolished the interaction with sT (Figure 3.13). Thus, residues 302-365 are essential for the interaction with MCPyV sT.

### **3.2.6.3 Disease associated mutations within the ubiquitin-binding domain of NEMO prevent the interaction with MCPyV sT.**

The essential nature of the Ubiquitin-binding domain of NEMO is known from the presence of disease-associated mutations in NEMO that prevent NF- $\kappa$ B activation. Several of the identified mutations in this domain abrogate the interaction with ubiquitin molecules, and likely prevent the recruitment of the IKK complex to the correct spatial localisation to interact with the TAK1 complex. To further assign a role for this domain in the interaction with sT in cells, a small number of published mutations were engineered into NEMO. These mutants were cloned into the pEBG6P plasmid to express amino-terminal GST fusion proteins in mammalian cells. The mutants were co-transfected into MCC13 cells with GFP-sT and precipitated using GFP-TRAP beads. Precipitates were detected using antibodies against GFP and GST. Wild-type NEMO, the A288R and A317Q mutants retained an ability to interact with sT. In contrast the D311N mutation abrogated the interaction with sT and C417R significantly reduced binding (Figure 3.14).

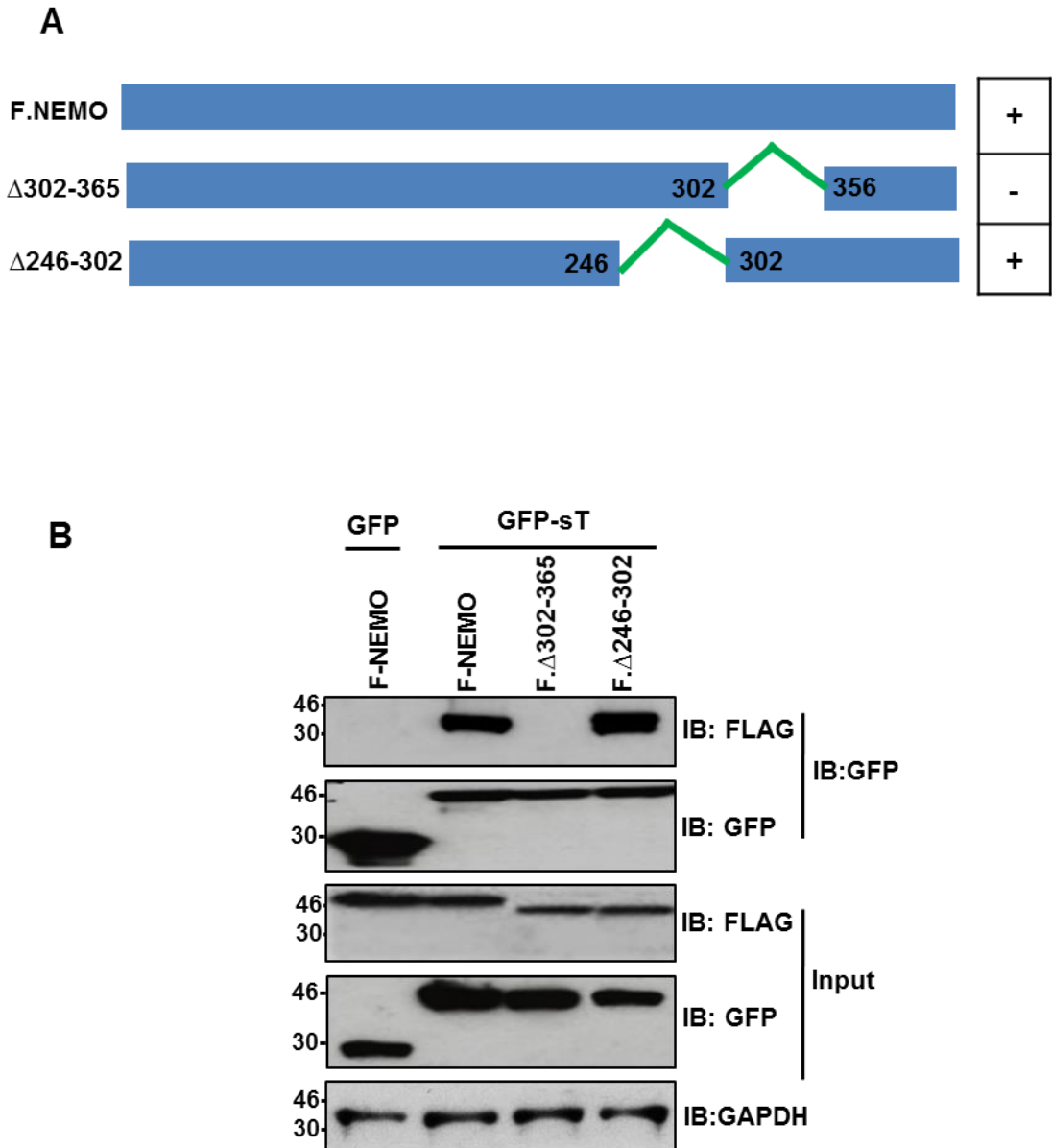


Figure 3.13: The residues 302-365 of NEMO required for the interaction with MCPyV-sT. **(A)** Schematic representation of the full length NEMO (1- 419) and two internal deletion truncations were listed at the left side. The symbol (+) refers to the NEMO mutants bound to sT and (-) for mutation non-bound to sT). **(B)** Co-immunoprecipitations of full length NEMO and Δ246-302 and Δ302-365 each with GFP sT, GFP alone transfected with full length FLAG-NEMO (as a control). Cells were lysed and protein was incubated with GFP-TRAP beads to precipitate GFP-sT. Protein complex was resolved by SDS-PAGE and immunoblotted with FLAG antibody for FLAG-NEMO and GFP antibody for GFP sT. The GAPDH performed to confirm equal loading of lysed proteins input. Representative blot is shown. Marker in kDa.

**A**

Wt NEMO	1	419	+	
A288R	----VIDKLKEEA	EQHKIVMETVPVLKAQADIYKAD	+	
D311N	----VPVLKAQADIYKAD	DFQAERAREKLAEEKELL	-	
A317Q	----VPVLKAQADIYKAD	DFQAERA	REKLAEEKELL	+
C 417R	----PPEEPPDFCCPKCQYQAPDMD	TLQIHVME	CIE	+

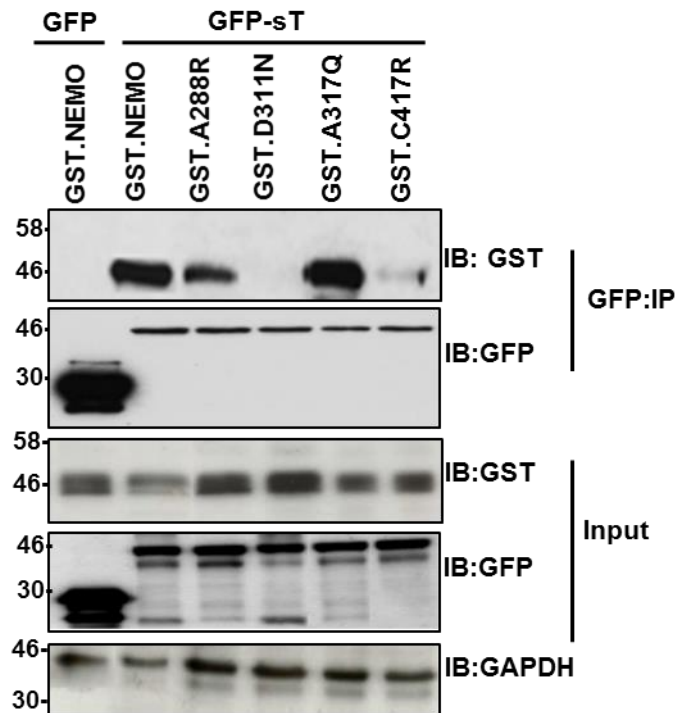
**B**

Figure 3.14: NEMO required Aspartate (D311) for interaction with MCPyV-sT. **(A)** Sequence alignment of the UBAN domain of NEMO. Full length (1- 419) and four point mutants were listed at the left side. The Red stars refers for mutant sites, symbol (+) refers to the NEMO mutants bound to sT and (-) for mutation non-bound to sT). **(B)** Co-immunoprecipitations of full length NEMO and point mutants each with GFP sT, GFP alone transfected with full length FLAG-NEMO (as a control). Cells were lysed and protein were incubated with GFP-TRAP beads to precipitate GFP-sT. Immune complexes resolved by SDS-PAGE and immunoblotted with FLAG antibody for FLAG-NEMO and GFP antibody for GFP sT. The GAPDH performed to confirm equal loaded of lysed proteins in input. Representative blot is shown. Marker in kDa.

### 3.3 Discussion:

#### 3.3.1 MCPyV sT is a soluble, cytoplasmic protein in MCC13 cells.

This study established that MCPyV sT localises in the cytosol of MCC13 cells. Further, co-immunofluorescence experiments demonstrated that sT showed a diffuse distribution **throughout the cell and** more concentrated in cytosol. These results are in agreement with other work showing an interaction between sT and the cytoplasmic actin regulatory protein Stathmin (Knight et al., 2015) and other localisation studies in the liver hepatoma cell line Huh7 (Griffiths et al., 2013). In contrast the MCPyV LT localises mainly in the nucleus, with a small percentage of the protein also found in the cytoplasm (Liu et al., 2011, Nakamura et al., 2010). Interestingly, the localisation of MCPyV sT differs from that of other *Polyomaviridae*. For example, SV40 sT localises within the nucleus, while LT can be found both in the cytoplasm and nucleus (Montano and Lane., 1984, Deppert, 2000). These data might allow speculation of MCPyV specific functions for the sT. **A time course of detection of sT within the cell may be required to determine whether the sT can change its localisation or if it is localised mainly in the cytoplasm over the time course.**

#### 3.3.2 MCPyV sT inhibits NF- $\kappa$ B activation.

Using a transcriptomics approach, our laboratory previously demonstrated that sT expression correlated with a down-regulation of NF- $\kappa$ B driven gene expression (Griffiths et al., 2013). To confirm these data, luciferase reporter assay was performed in MCC13 using a well-characterised NF- $\kappa$ B driven reporter (Mankouri et al., 2010). This assay showed an sT-dependent decrease in NF- $\kappa$ B mediated luciferase expression. **Instead of studying the role of sT in the pathway in MCPyV negative MCC cell line, it may be better to detect the action of sT in a MCPyV positive MCC cell line like MKL1 or MKL2, however these cell lines did not grow well.** Griffith and colleagues were shown an inhibition of CCL20, IL-6 and IL-8 at the transcript and protein

level in MCC13 and MKL1 (David Griffiths and Andrew Macdonald; Griffiths *et al.*, 2013). Among the polyomaviruses, only BKPyV and MCPyV have been shown to down-regulate NF- $\kappa$ B activation. A couple of mechanisms have been postulated; firstly direct targeting of the NF- $\kappa$ B pathway by MCPyV sT (Griffiths *et al.*, 2013) and alternatively down-regulation of Toll-like receptor-9 (TLR9) gene expression, which would impact on NF- $\kappa$ B activation in response to the presence of viral nucleic acids (Shahzad *et al.*, 2013). MCPyV uses both LT and sT to inhibit TLR9 expression, whereas BKPyV utilizes its LT to interact with the CCAAT/enhancer-binding protein beta (C/EBP $\beta$ ) to prevent expression of the TLR9 gene (Shahzad *et al.*, 2013). In addition to the *Polyomaviridae*, a number of viruses target the NF- $\kappa$ B pathway to evade modify the innate immune system. Epstein-Barr virus (EBV) expresses latent membrane 1 (LMP1), which leads to the activation of NF- $\kappa$ B, whereas human papillomavirus 16 (HPV16) and Hepatitis B virus (HBV) manipulate NF- $\kappa$ B pathway through inhibiting of TLR9 which induce the pathway (Fathallah, *et al.*, 2010, Martin *et al.*, 2007, Vincent *et al.*, 2011, Hasan, *et al.*, 2014, Edwards *et al.*, 2015). HPV E7 has also been shown to prevent NF- $\kappa$ B activation by reducing acetylation of the p65 protein (Richards *et al.*, 2015).

### **3.3.3 Interaction of MCPyV sT with NEMO.**

Pulldown experiments indicated that MCPyV sT was likely to interact with a protein in the NF- $\kappa$ B signalling pathway. Data presented in this chapter shows that one candidate for this protein is the adaptor NEMO. This interaction was shown using co-immunoprecipitation assays with over-expressed NEMO and confirmed with endogenous NEMO both by co-immunoprecipitation and co-immunofluorescence experiments. Moreover, NEMO could be found in discrete puncta that co-stained with sT in Huh7 (Griffiths *et al.*, 2013) and in the more physiologically relevant MCC13 cells (Figure 3.5).

NEMO is absolutely required for the canonical NF- $\kappa$ B activation pathway. The amino-terminal part of NEMO is responsible for interaction with the IKK catalytic subunits (May *et al.* 2000,

Rushe et al. 2008, Vincendeau et al., 2016). Structurally, NEMO lacks catalytic properties but its regulatory role is essential for activation NF- $\kappa$ B and mouse embryonic fibroblasts cells that lack NEMO could not activate NF- $\kappa$ B signalling (Bonizzi and Karin, 2004). This may illustrate that MCPyV sT targets NEMO to manipulate the NF- $\kappa$ B pathway. It is intriguing that NEMO was not identified in the initial SILAC-based proteomic screen of MCPyV sT binding proteins (Griffiths et al., 2013). This may indicate a transient interaction between the proteins or that this is a low affinity interaction, destabilised during the lysis and precipitation protocols. Alternatively, peptides derived from NEMO may not have contained the appropriate properties for detection during the mass spectrometry analysis. When these studies were initiated MCPyV was the only polyomavirus known to target NEMO. Despite this, a number of viruses have been shown to manipulate immune signalling by targeting NEMO. Human T-lymphotrophic virus types 1 and 2 (HTLV 1, HTLV2) encode TAX1 and TAX2, which both contain NEMO binding domains. TAX1 protein is ubiquitinated by lysine-63 polyubiquitin (K63-Ub) and subsequently interact with NEMO to activate the IKK complex and NF- $\kappa$ B pathway (Higuchi & Fujii, 2009), whilst TAX2 mediates NF- $\kappa$ B activation independent to the link with K36-Ub (Lavorigna and Harhaj, 2013 Journo et al., 2013). In addition, the viral FLICE inhibitory protein (vFLIP, K13) protein encoded by Kaposi's sarcoma-associated herpesvirus (KSHV) targets NEMO to activate the NF- $\kappa$ B pathway and prevent infected cells from undergoing apoptosis (Tolani et al., 2014, Bagneris et al., 2008). The interaction between **murine cytomegalovirus (MCMV)** protein (MC45) and NEMO has been demonstrated to inhibit TNF-induced apoptosis and suppresses the NF- $\kappa$ B pathway (Randall et al., 2012). Similarly, an HBV-encoded polymerase (pol), interacts with NEMO and isolates it from IKK kinases to disrupt the IKK complex formation (Liu et al., 2014).

### 3.3.4 Residues 101-103 in MCPyV sT are required for targeting NEMO.

A mutagenesis strategy was employed to broadly define the residues within sT required for the interaction with NEMO. Full length MCPyV sT was truncated into five truncations, three in the N-terminus 1-95, 1-63 and 1-32 and two were in the C-terminal 1-162, and 1-128 (Figure 3.6A), in addition to one point mutant R7A which has previously been reported to prevent binding to PP2A A $\alpha$  (Shuda et al., 2011). The expression abilities of these mutations was confirmed by MCPyV sT early promoter activity and the results showed they do not have a protein-folding problem (Griffith et al., 2013). The co-immunoprecipitation undertaken in this study firmly identified the region 95-128 of MCPyV sT as necessary for the interaction with NEMO. The truncation lies in the C terminal of sT, the N-terminal truncations failed to bind NEMO. In addition, the mutant R7A interacted with NEMO as well as the wild type protein. It is therefore likely that the binding area is within residues 95-128 (Figure 3.7 B). To refine the region necessary for binding to NEMO, internal deletions were employed ( $\Delta$ 95-111 and  $\Delta$ 111-128). These precipitations confirmed that residues 95-111 are needed to bind to NEMO in cells. This area is not conserved with LT, 57KT and ALTO, which are all expressed in the early region. This may suggest that neither LT nor 57KT are able to bind NEMO, however, this needs to be experimentally investigated.

Despite the promoter reporter studies, which indicated that our truncation analysis had not impacted on the global structure and function of sT (Griffiths et al., 2013), it was necessary to refine our understanding of the interaction between sT and NEMO to a minimal region. This was achieved, firstly through alanine scanning of discrete clusters of residues within the region between 95-111, and finally by use of single point mutants. These studies demonstrated that the mutants A101R, R102A and F103A abolished the interaction with NEMO in cells.

### 3.3.5 The role of the point mutants of sT in NF- $\kappa$ B pathway.

Whilst the mapping exercise identified residues in sT necessary for the interaction with NEMO in cells, it was imperative to show that preventing the interaction had an impact on the ability of sT to impair NF- $\kappa$ B signalling. Use of luciferase reporter assays provided some data potentially supporting the importance of the sT interaction with NEMO. Whilst the wild type, N100A and A101R mutants all inhibited NF- $\kappa$ B activation, the R102A and F103A mutants failed to achieve this to the same level. Firstly, none of the point mutants was able to completely prevent inhibition of NF- $\kappa$ B using the artificial promoter plasmid. Similar observations were recorded for inhibition of NF- $\kappa$ B by the E7 oncoprotein (Richards et al., 2015). In this study, mutants in the E7 protein reduced the ability of E7 to inhibit the same reporter plasmid but did not return levels of luciferase to control level. However, the same mutants were incapable of inhibiting endogenous NF- $\kappa$ B driven gene expression as shown by qRT-PCR or ELISA for the protein (Richards et al., 2015). It is possible that analysing endogenous gene expression rather than using the reporter construct would find similar results. It is also possible that another protein rather than NEMO is also required for the inhibition of NF- $\kappa$ B signalling. This might explain why the A101R mutant could still block NF- $\kappa$ B but did not bind to NEMO in co-immunoprecipitation studies. Other proteins like IKK $\alpha$ , IKK $\beta$ , TANK and RIP which form complexes with NEMO may act as a scaffold between sT and NEMO. Each of these possibilities needs to be studied in detail.

### 3.3.6 The NEMO ubiquitin-binding domain is needed for the interaction with sT in cells.

NEMO is a multi-domain adaptor protein and both the protein-protein interaction partners and the purpose of specific domains has well been characterised (Kensche et al., 2012, Emmerich et al., 2013, Vincendeau et al., 2016). We used a truncation approach to establish the region(s) of NEMO necessary for the interaction with sT in cells. This strategy identified a

stretch of residues in NEMO consisting of the so called ubiquitin binding domain (UBD), which encompasses the second coiled-coil and leucine zipper domains, as essential for the interaction with sT. Located in the C-terminal region of NEMO, this region is important both for oligomerisation and for binding to various forms of ubiquitin (Grubisha et al., 2010; Emmerich et al., 2013; Yoshikawa, et al., 2009). To back up the truncation data, we generated a small number of clinical mutants of NEMO associated with immunodeficiency disorders. Importantly, most of these mutations can be found within the UBD (containing the CC2-LZ region). One of the more successful finding was observed by interacting sT with all previous mutants except the mutant D311N (Figure 3.13). This suggests that the residue D311 in NEMO is necessary for the interaction with sT in cells. This mutant has been reported to prevent the interaction with ubiquitin chains (Rahighi et al., 2009, Hadian et al., 2011). D311 is located in NEMO-NOA domain and showed to be required for interacting the residues H68 and L8 of ubiquitin chains which are necessary for NEMO ubiquitination (Lo et al., 2009). Any mutation in this residues as well as A288 and A317 showed to completely abrogate the interaction to K63-Ub. They also been isolated from people who have sever (EDA-ID) as a result of NF- $\kappa$ B inhibition and the patient suffering with skin inflammation (Courtois and Gilmore, 2006, Sebban-Benin et al., 2007, Chiaravalli et al., 2011). Herein, we found that the mutant D311N alone can abolish the interaction with sT whilst the other A288R, A317Q and C417R retain binding to sT. It is likely that any mutant in D311 loss the ability to bind K63-linked di-Ub, whilst the A288G, A317 and C417R have not been shown to effect the interact with K63-linked di-Ub (Vinolo et al., 2006). Thus it was likely the residues D311 is necessary to sT to disrupt K63 di-Ub ubiquitin chain.

Substitution mutations in D311 also detected in cDNA from EBV-B cells and SV40-transformed fibroblasts from the patient (Hubeau et al. 2011). Recently, Vincendeau and colleague studied different point mutants within the region NOA including D311R and they identified that this mutant can prevent ubiquitination of NEMO and disrupt NF- $\kappa$ B activation (Vincendeau et al., 2016).

Data in this chapter indicate that two amino acids 102 and 103 in MCPyV sT required to mediate NF- $\kappa$ B inhibition and this is highly likely through recruitment of NEMO. The amino acid D311 in NEMO was observed to be necessary for this effect.

## **Chapter 4. MCPyV sT interacts with a number of Protein phosphatase subunits in cells**

### **4.1 Introduction**

Protein phosphatases work in contrast to kinases in cells. They hydrolyse phosphate groups from proteins that have been phosphorylated by kinases and this process is called 'dephosphorylation'. Most phosphatases hydrolyse phospho-serine (which account for 86.4%) and the others hydrolyse phospho-threonine (11.8%) as their substrate. A minority target phospho-tyrosine (1.8%) residues. It is thought that about 30 serine/threonine phosphatases can regulate thousands of dephosphorylation events in all living cells (Olsen et al., 2006). The pivotal role played by these phosphatases makes them an attractive target for viruses to develop strategies to manipulate a myriad of cellular pathways. For example, HCV utilizes its non-structural proteins (NS3/4A and NS5A) to recruit PP2A to manipulate the MAPK-ERK pathway (Duong et al., 2004). Whilst Adenovirus E4orf4 and HIV-1 Vpr proteins bind phosphatases to regulate apoptosis (Mui et al, 2015, Janoo et al., 2005) .HPV-E7 recruits PP2A to inhibit the AKT pathway (Pim et al., 2005). Polyomaviruses have also been shown to target phosphatases. For example, SV40, BKPyV and JCPyV utilize their sT proteins to manipulate different pathways by targeting PP2A (Duong et al., 2005, Shtrichman et al., 1999, Guernon et al., 2011, Griffith, et al., 2013, Kwun et al., 2015). A limited number of polyomaviruses are also able to

target other phosphatases including PP4C (Griffith, et al., 2013, Kwun et al., 2015). Two structural A subunits of the major protein phosphatase, PP2A, were identified, A $\alpha$  and A $\beta$ . Each of these isoforms is involved in different pathways (Jin et al., 2003, Calin et al., 2000). Accordingly, viruses display selectivity of binding between these isoforms according to their pathogenic mechanism. For instance, Murine polyomavirus sT interacts with PP2A A $\beta$  to negatively regulate the AKT-mTOR pathway. Whereas SV40 is unable to bind PP2A A $\beta$  (Andrabi et al., 2011, Kwun et al., 2015). On the other hand, MCPyV sT disrupts the NF- $\kappa$ B pathway via recruitment of either PP4C or/and PP2A A $\beta$  (Griffith et al., 2013).

In normal cells, NF- $\kappa$ B transcriptional activity is reduced when no longer required in part through the dephosphorylation activity of PP2A and PP4C (Brechmann et al., 2012, Zhang et al., 2014). This observation serves to reinforce the key function of phosphatases associated with NF- $\kappa$ B whilst also possibly elucidating why they are targeted not only by MCPyV but also by other viruses (e.g. SV40 and HCV) through the sT and NS5A proteins respectively (Sontag et al., 1997, Jiang et al., 2011).

Several point mutants were mapped in MCPyV sT observed to be required for interaction with phosphatase subunits. The first of these domains to be identified was R7 and L142 which they observed as essential for sT to interact with PP2A A $\alpha$  (Shuda et al., 2011). Whilst other amino acids K118 and K134 were also shown to be important for the interaction with PP2A A $\alpha$  (Kwun et al., 2015).

This chapter aims to increase our understanding of the molecular requirements for the interactions between MCPyV sT and PP4C and PP2A subunits. It identifies residues in MCPyV sT necessary for the interaction with these phosphatases. Mutant sT proteins, based on these studies, have been used to explore the functional roles of sT in MCPyV pathogenesis and immune evasion (Griffith, et al 2013, Knight et al., 2015).

## 4.2 Results

### 4.2.1 MCPyV sT targets the protein phosphatase 4 C subunit.

Screening for proteins involved in the NF- $\kappa$ B pathway has previously identified PP4C as a novel interaction partner for MCPyV sT (Griffith et al, 2013). PP4C is a serine - threonine phosphatase and plays a number of key roles in host cell physiology. A critical role for PP4C in the control of NF- $\kappa$ B activation was recently reported (Tikhonova and Aifantis, 2012; Griffith et al, 2013) through targeting the IKK complex.

To confirm a putative interaction between PP4C and MCPyV sT, MCC13 cells were transfected with pEGFP-sT and PP4C containing an in-frame amino terminal FLAG epitope fusion (FLAG-PP4C). Cell lysates were incubated with GFP-TRAP magnetic beads or control protein G-agarose beads. Protein complexes were resolved by SDS PAGE and the precipitates analysed by Western blot with antibody of GFP or FLAG. Western blotting of proteins input confirmed the expression of all of the exogenous proteins. The precipitation with protein G-agarose beads showed no protein reactivity with either the FLAG or the GFP antibody (Figure 4.1A). A clear interaction was observed between GFP-sT and FLAG-PP4C (Figure 4.1B), in contrast with GFP alone which showed no interaction.

Co-immunoprecipitations were also performed between GFP-sT and endogenous PP4C. MCC13 cells were transfected with pEGFP or pEGFP-sT and coimmunoprecipitated with endogenous PP4C using GFP-TRAP beads. PP4C was detected using a rabbit polyclonal antibody to PP4C. A band corresponding to PP4C was detected in the precipitates from cells expressing pEGFP-sT but not pEGFP (Figure 4.1C) Untransfected cells were used as a negative control (Mock). Together, these data demonstrate that MCPyV sT can interact with PP4C in MCC13 cells (Griffiths et al., 2013).

#### 4.2.2 Colocalization of MCPyV sT with endogenous PP4C in MCC13 cells.

cells.

Colocalization of MCPyV sT and endogenous PP4C was visualized in MCC13 by confocal microscopy. Cells were transfected with pEGFP or pEGFP-sT and incubated for 24 hours before fixation. Endogenous PP4C was detected by PP4C antibody and probed by an Alex fluor 594 conjugated secondary antibody, whilst GFP-sT was visualized by its Green fluorescence. EGFP-sT and PP4C showed putative colocalized in the cytoplasm (Figure 4.2). **This result would be consistent with** an interaction of sT and PP4C which was also observed by co-immunoprecipitation.

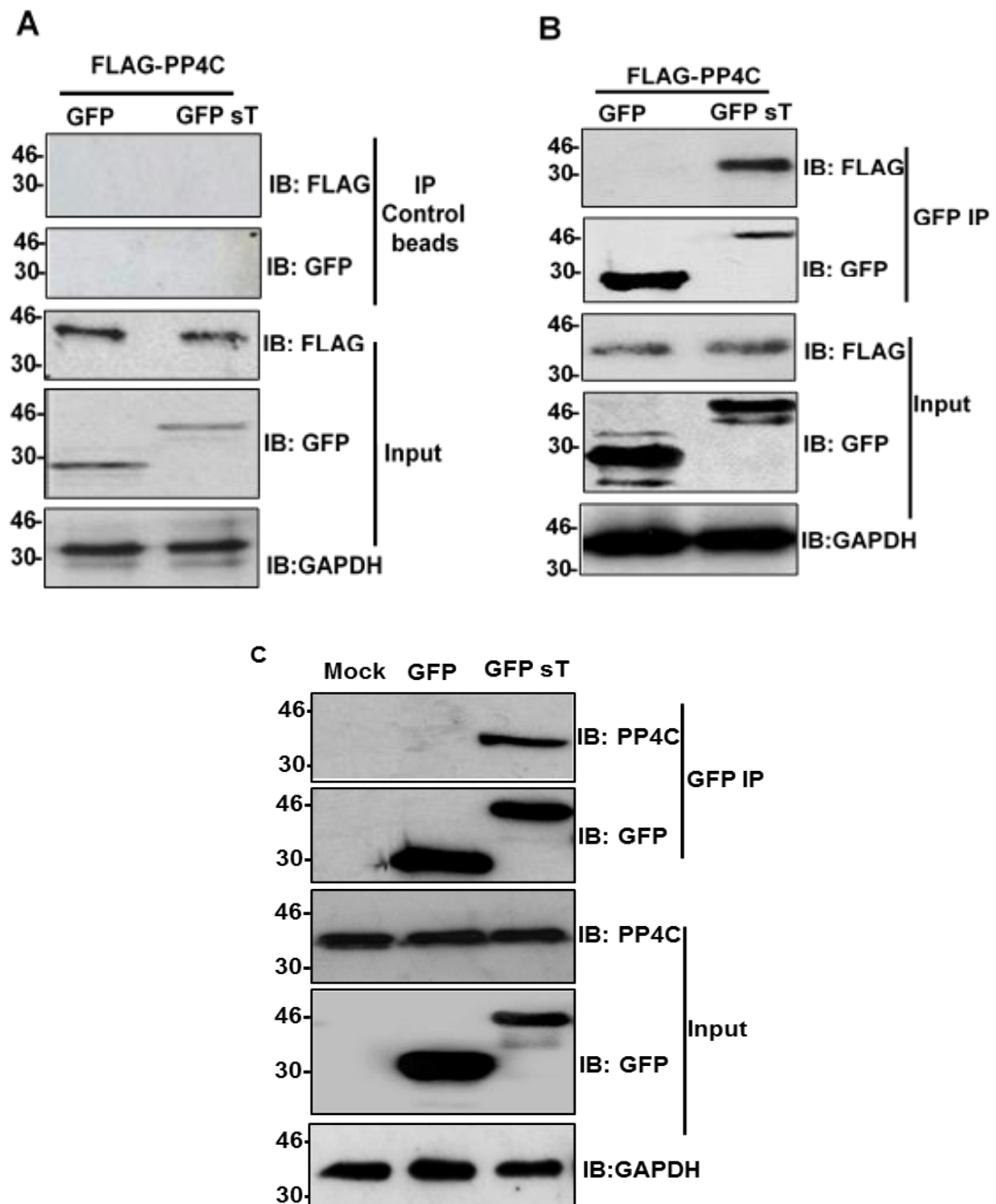


Figure 4.1: Co-immunoprecipitations confirming the interaction of MCPyV sT with the catalytic subunit of protein phosphatase 4 (PP4C). **(A, B)** MCC13 cells were cotransfected with either pEGFP or pEGFP sT and FLAG-PP4C. Post transfection 24h expression of proteins were confirmed by input the lysates. Co-immunoprecipitation were performed by incubate cellular lysate either with protein A-Sepharose beads **(A)** for the negative control or GFP-Trap magnetic beads **(B)** to precipitate pEGFP sT. expressed proteins were resolved by SDS PAGE and probed by GFP or FLAG antibodies. **(C)** Co-immunoprecipitation of endogenous PP4C with pEGFP-sT confirmed the interaction between them. Cells were transfected with pEGFP-sT and coimmunoprecipitated by GFP-TRAP beads with PP4C antibody. Untreated cells (Mock) was used as a control. GAPDH was used as a loading control. Marker in kDa.

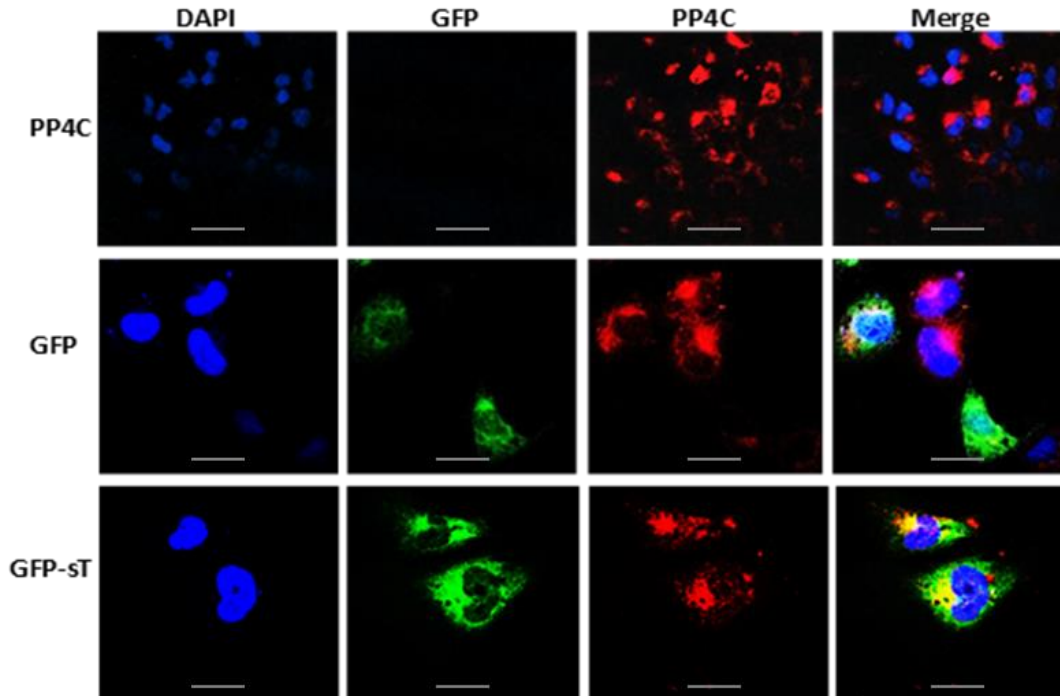


Figure 4.2: Co-immunofluorescence investigating putative colocalization of sT with PP4C in the cytoplasm of MCC13. Cells were transfected with pEGFP or pEGFP-sT. 24 h post transfection cells were fixed and permeabilized. PEGFP, pEGFP-sT was detected by their green fluorescence emission and PP4C was indicated by anti PP4C (primary) and Alexa fluor 594 red fluorescent antibody (secondary).

Colocalization was shown (Yellow) puncta. Cells were stained with 4', 6-diamidino-2-phenylindole (DAPI) to stain the nuclei (Blue). Images were acquired with Zeiss LSM700 confocal microscope. Representative images are shown. Scale bars = 20µm.

#### **4.2.3 Residues 95-128 within MCPyV sT are required for the interaction with PP4C.**

Mapping experiments were performed by co-immunoprecipitation assay to delineate the regions of sT required for binding to PP4C. MCC13 were transfected with FLAG-PP4C and the panel of sT truncations (Figure 3.6). Cells were cotransfected for 24h and then harvested. Cell lysates were precipitated using GFP-TRAP beads and protein complexes were probed by Western blot with antibodies against GFP and the FLAG epitope, respectively. The results confirmed the interaction between full length sT and PP4C (Figure 4.3). Surprisingly, co-immunoprecipitation results demonstrated that the same region that is essential for interacting with NEMO is also required for binding PP4C. The R7A point mutant as well as truncation mutants 1-162 and 1-128 were showed to interact with PP4C comparing with the mutants that removed amino acids beyond 95 (1-95, 1-63 and 1-32) which failed to precipitate PP4C. Thus, residues 95-128 are likely to be necessary for binding PP4C (Figure 4.3). Together, these data suggest that residues 95-128 are required for the interaction with both NEMO and PP4C (Griffith and et al, 2013).

#### 4.2.4 PP4C binds to residues 95-111 within sT.

Further mutagenesis studies were performed to identify a short stretch of MCPyV sT necessary for binding PP4C. The mutant sT $\Delta$ 95-111 or MCPyV sT $\Delta$ 111-128 were co-transfected with FLAG PP4C in MCC13 cells. GFP and GFP-sT were used as a negative and positive control. Cell lysates were co-immunoprecipitated using FLAG- agarose affinity beads and any interaction assessed by Western blotting. Interestingly, co-immunoprecipitation results indicated that the mutant  $\Delta$ 95-111 stopped binding PP4C, whereas  $\Delta$ 111-128 retained the interaction (Figure 4.4). Thus, residues the residues 95-111 are likely to be required to bind to PP4C in cells.

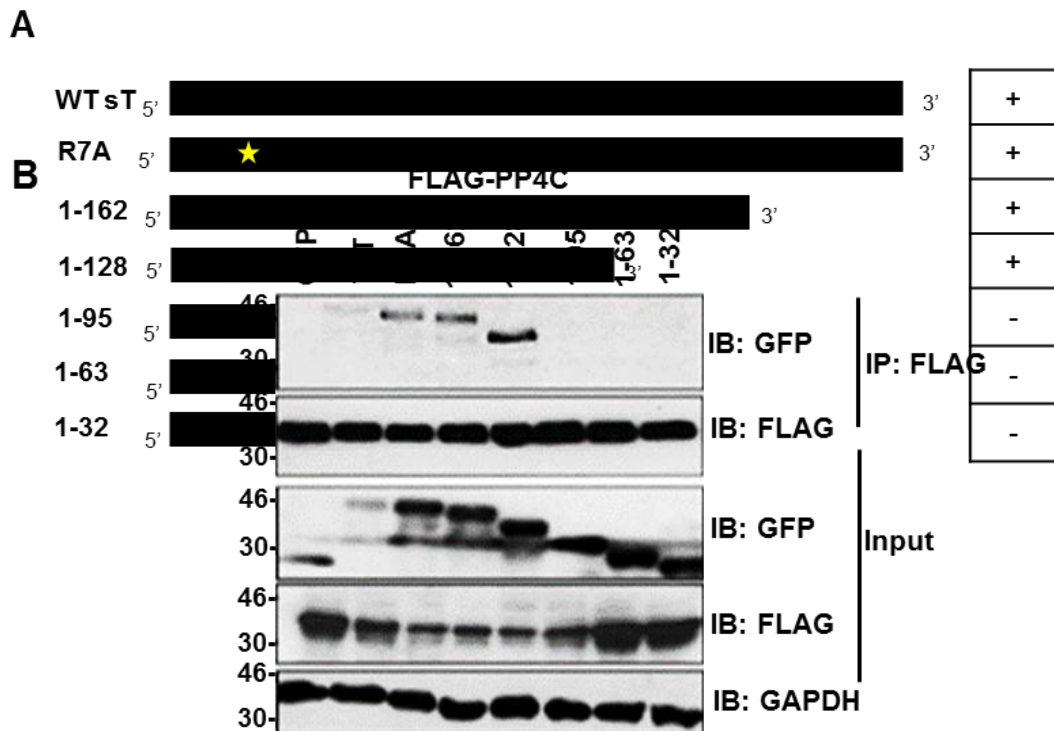


Figure 4.3: Mapping of GFP-sT binding site to FLAG-PP4C. **(A)** Schematic representation of sT truncation mutant as pEGFP fusion proteins. The name of truncations were listed at the left. The star refers to R7A mutant, **(+)** mutation bound to PP4C and **(-)** mutation non-bound to PP4C **(B)** Co-immunoprecipitation of pEGFP-sT truncation mutants with FLAG-PP4C. pEGFP alone (control), pEGFP-sT and sT truncations were co-expressed alongside with FLAG-PP4C in MCC13 cells.

The Co-immunoprecipitations were performed with equal amounts of total protein using GFP-TRAP magnetic beads and probed with GFP and FLAG antibodies. Representative blot is shown. Marker in kDa.

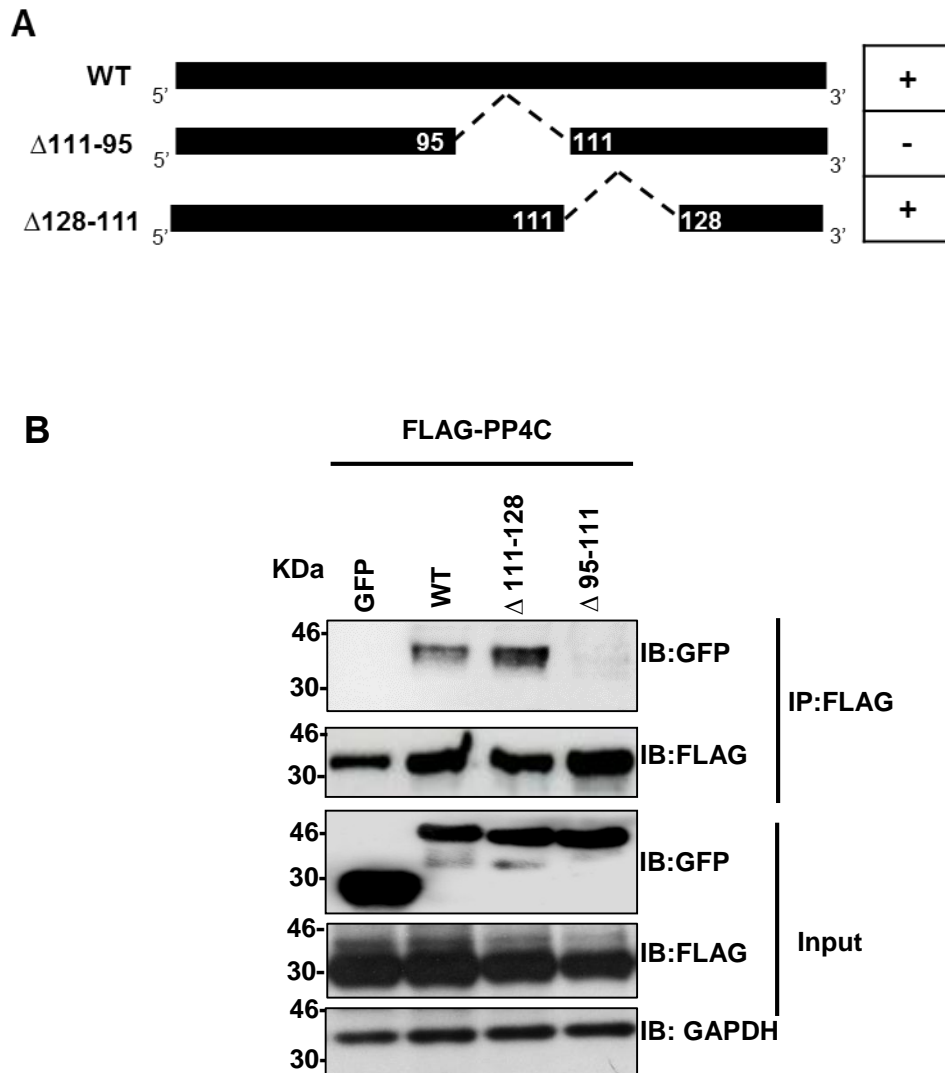


Figure 4.4: MCPyV sT required residues 95-111 to interact PP4C. **(A)** Schematic representation of sT internal deletions between residues 95-128 (dash lines), (the symbols  $\Delta$  refers to the area of deletion, (+) refers to the mutations bound to PP4C and (-) to mutation non-bound to PP4C. **(B)** Co-immunoprecipitations of pEGFP alone (control), pEGFP-sT,  $\Delta$ 95-111 and  $\Delta$ 111-128 with PP4C. Proteins were co-expressed in MCC13 cells and precipitated by PP4C agarose affinity beads. GFP and FLAG antibodies were used to probe pEGFP tagged proteins and PP4C

respectively. GAPDH used for loading control. Representative blot is shown. Marker in kDa.

#### **4.2.5 MCPyV sT residues 100-103 are required for the interaction with PP4C.**

The four sT alanine mutants (A96-99, A100-103, A104-107 and A108-111) were used to map the interaction site between MCPyV sT and NEMO. Co-immunoprecipitation between these mutants and FLAG-PP4C were performed from MCC13. Cell lysates were incubated with GFP-TRAP beads and interactions with co-expressed FLAG-PP4C determined by Western blot. The results showed that only the stretch A100-103 failed to interact with FLAG-PP4C, whereas the other mutants conserved their ability to bind PP4C. Thus, these results indicate that the residues 100-103 are essential for interaction with PP4C (Figure 4.5).

#### **4.2.6 Two amino acids (102-103) in MCPyV sT are required for the interaction with PP4C.**

To analyse the individual contribution of each residue between 100-103 to the MCPyV sT interaction with PP4C, the sT point mutant panel (N100A, A101R, R102A, and F103A) were co-immunoprecipitated with FLAG-PP4C. The pEGFP alone and the wild type sT were used as a negative and positive controls, respectively. Western analysis revealed that N100A and A101R retained the ability to bind PP4C, whereas, R102A and F103A lost their interaction properties (Figure 4.6), implying that amino acids R102 and F103 are required for the interaction with PP4C. These residues in addition to residue 101 appeared also necessary for the interaction with NEMO as previously shown (Figure 3.10).

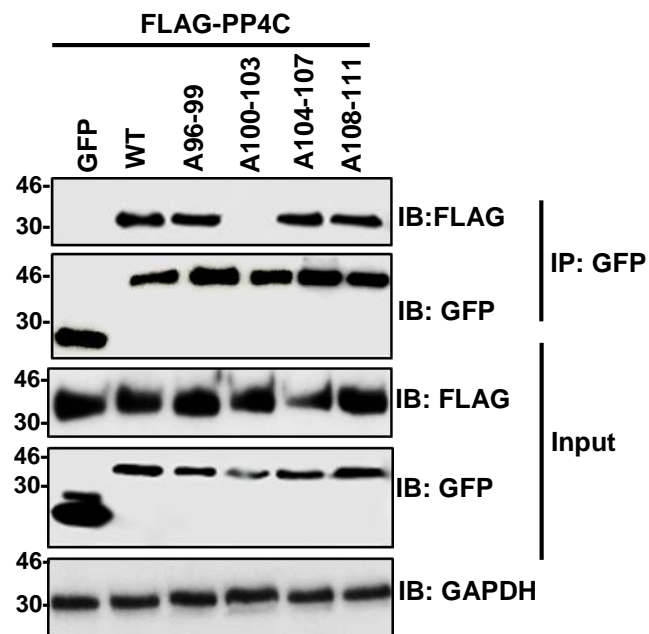
**A****B**

Figure 4.5: MCPyV sT required residues 100-103 to interact PP4C. **(A)** Schematic representation of sT alanine mutants within 95-111, the letters **AAAA** refers to the amino acid replaced to alanine, **(+)** refers to mutations bound to PP4C and **(-)** refers to mutation non-bound to PP4C. **(B)** Co-immunoprecipitations of pEGFP alone (control), pEGFP-sT and four mutants with FLAG-PP4C. Proteins were expressed in MCC13 cells and precipitated by GFP-TRAP magnetic beads. GFP and FLAG antibodies were used to probe GFP tagged proteins and PP4C respectively. GAPDH used for loading control. Representative blot is shown. Marker in kDa.

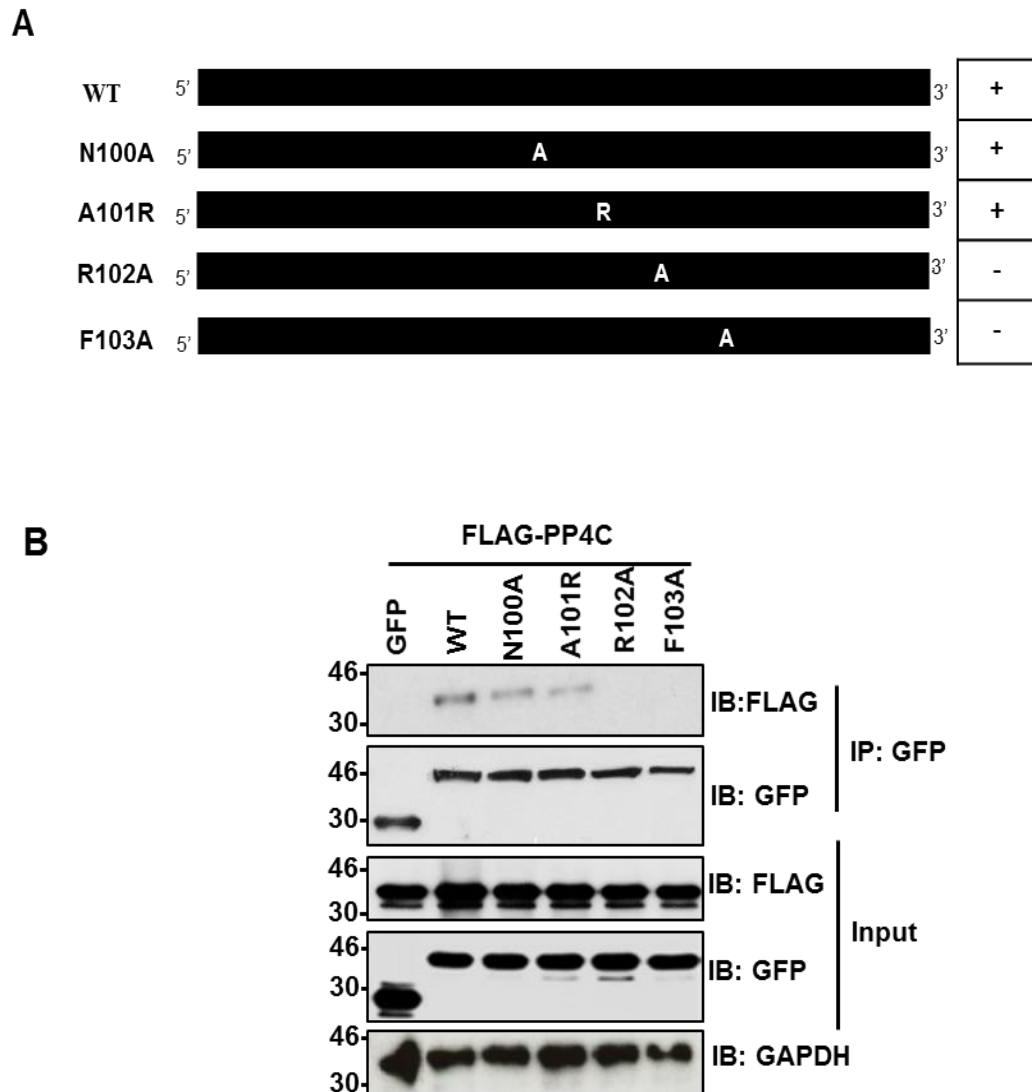


Figure 4.6: MCPyV sT required residues 102 and 103 to interact PP4C. (A) Schematic representation of sT point mutants within 100-103, (the letters **A** or **R** refers to the amino acid replaced). The symbol **(+)** refers to the mutation bound to PP4C and **(-)** for mutation non-bound to PP4C. (B) Co-immunoprecipitations of pEGFP alone (control), pEGFP-sT and the four point mutants with FLAG-PP4C. Proteins were co-expressed in MCC13 cells and precipitated by GFP-TRAP magnetic beads. GFP and FLAG antibodies were used to probe pEGFP tagged proteins and PP4C respectively. GAPDH used for loading control. Representative blot is shown. Marker in kDa.

#### **4.2.7 MCPyV sT targets other protein phosphatases in cells.**

Besides the interaction with PP4C, other phosphatases were also detected in the proteomic screen with MCPyV sT. The SILAC screen identified a potential interaction with the major Serine/threonine-protein phosphatase 2A A subunit of PP2A A $\beta$  (Griffiths et al., 2013). These data also confirm previous observations of an interaction with PP2A A $\alpha$ .

#### **4.2.8 Co-immunoprecipitation of sT with the A $\alpha$ , A $\beta$ and catalytic (C) sub-units of PP2A.**

To investigate the possible interaction between PP2A subunits and MCPyV sT, MCC13 cells were cotransfected with pEGFP-sT and EE epitope fusions of PP2A A $\alpha$ , PP2A A $\beta$  or a FLAG epitope fusion of PP2A C. Prior to co-immunoprecipitation studies, the expression levels of each protein were confirmed in MCC13 cells, by Western blotting. For co-immunoprecipitations, cell lysates were incubated with GFP-TRAP magnetic beads and immune complexes were resolved by SDS PAGE and the precipitates were analysed by Western blot with appropriate antibodies. As shown in Figure 4.7A, a band was observed in the pEGFP-sT precipitates, corresponding to EE-PP2A A $\alpha$  (Figure 4.7A). Similarly, results of the co-immunoprecipitation indicated that MCPyV sT is able to bind both PP2A A $\beta$  and PP2A C respectively (Figure 4.7B, C).

#### **3.2.9 Mapping the regions of sT necessary for interacting with PP2A A $\alpha$ and PP2A A $\beta$ .**

In order to verify MCPyV sT domains necessary for interaction MCPyV sT with PP2A A $\alpha$  and PP2A A $\beta$ , the internal deletion mutants MCPyV sT $\Delta$ 95-111 or MCPyV sT $\Delta$ 111-128 were expressed with PP2A A $\alpha$  or PP2A A $\beta$ . MCC13 cells were co-transfected either with wild type sT or with the deletion mutants in addition to PP2A A $\alpha$  or PP2A A $\beta$ .

The cellular lysates were coimmunoprecipitated using GFP-TRAP beads and any interaction assessed by Western blotting. Results of the co-immunoprecipitation indicated that the wild type sT and  $\Delta 111-128$  bind to PP2A A $\alpha$ . In addition, the point mutant R7A abolished the interaction with PP2A A $\alpha$ , and this finding is consistent with (Shuda et al., 2011). On the contrary,  $\Delta 95-111$  showed only a weak interaction (Figure 4.8A).

Intriguingly, co-immunoprecipitation assays of sT with PP2A A $\beta$  showed similar results, the full length interacts with PP2A A $\beta$ , whereas the R7A and  $\Delta 111-128$  retained their interaction ability. In addition,  $\Delta 95-111$  lost its interaction property (Figure 4.8B).

### **3.2.9.1 Mutation of amino acid 103 in MCPyV sT decreases the interaction with PP2A A $\beta$ .**

To distinguish which sT residues between 100-103 are required for the interaction with PP2A A $\beta$ , co-immunoprecipitations were performed between each sT point mutant (N100A, A101R, R102A or F103A) and EE-PP2A A $\beta$ . The pEGFP alone and the wild type sT were used as a negative and positive controls, respectively. All mutants expressed to similar levels and were precipitated from MCC13 cell lysates using GFP-TRAP beads and interactions with co-expressed EE-PP2A A $\beta$  determined by Western blot. The full length and all sT mutants, except F103A, retained their binding ability with PP2A A $\beta$ . F103A significantly decreased the interaction with PP2A A $\beta$  (Figure 4.9).

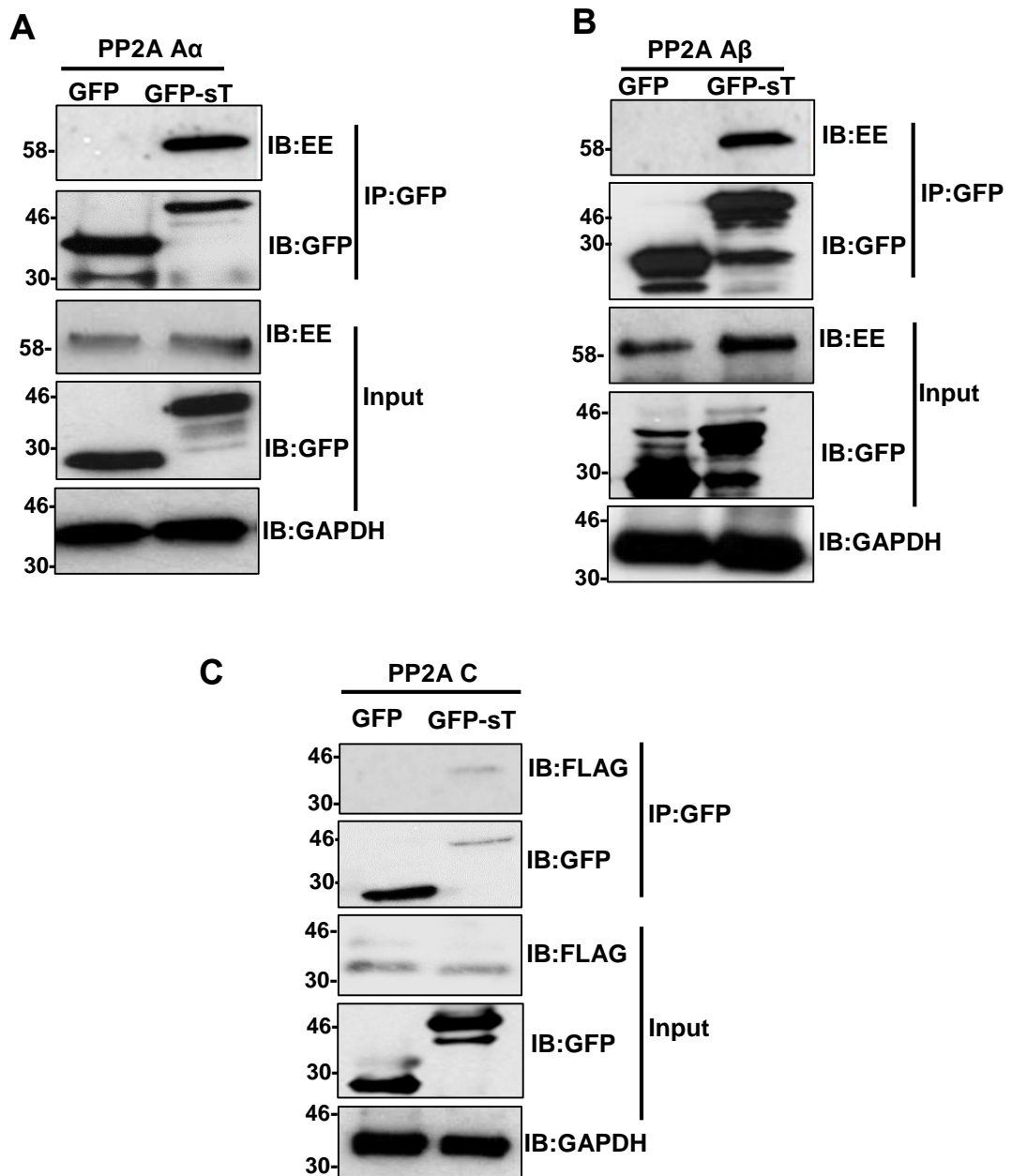


Figure 4.7: Co-immunoprecipitations confirming the interaction of MCPyV sT with PP2A A  $\alpha$ , PP2A A  $\beta$  and PP2A C (**A**, **B**, **C**) MCC13 cells were cotransfected with either pEGFP or pEGFP sT and either EE-PP2A A  $\alpha$ , EE-PP2A A  $\beta$  and FLAG-PP2A C. 24 post transfection expression of proteins were confirmed by input the lysates. Co-immunoprecipitation was performed by incubate cellular lysate with GFP-Trap magnetic beads to precipitate pEGFP sT. Precipitates were resolved by SDS PAGE and probed by GFP or EE antibody for PP2A A  $\alpha$  and PP2A A  $\beta$  or FLAG for PP2A C (**A**) Co-immunoprecipitation of pEGFP-sT with PP2A A $\alpha$  (**B**) Co-immunoprecipitation with PP2A A $\beta$  (**C**) Co-immunoprecipitation with PP2A C. Cells transfected with GFP were used as a control. GAPDH was used as a loading control. Marker in kDa.

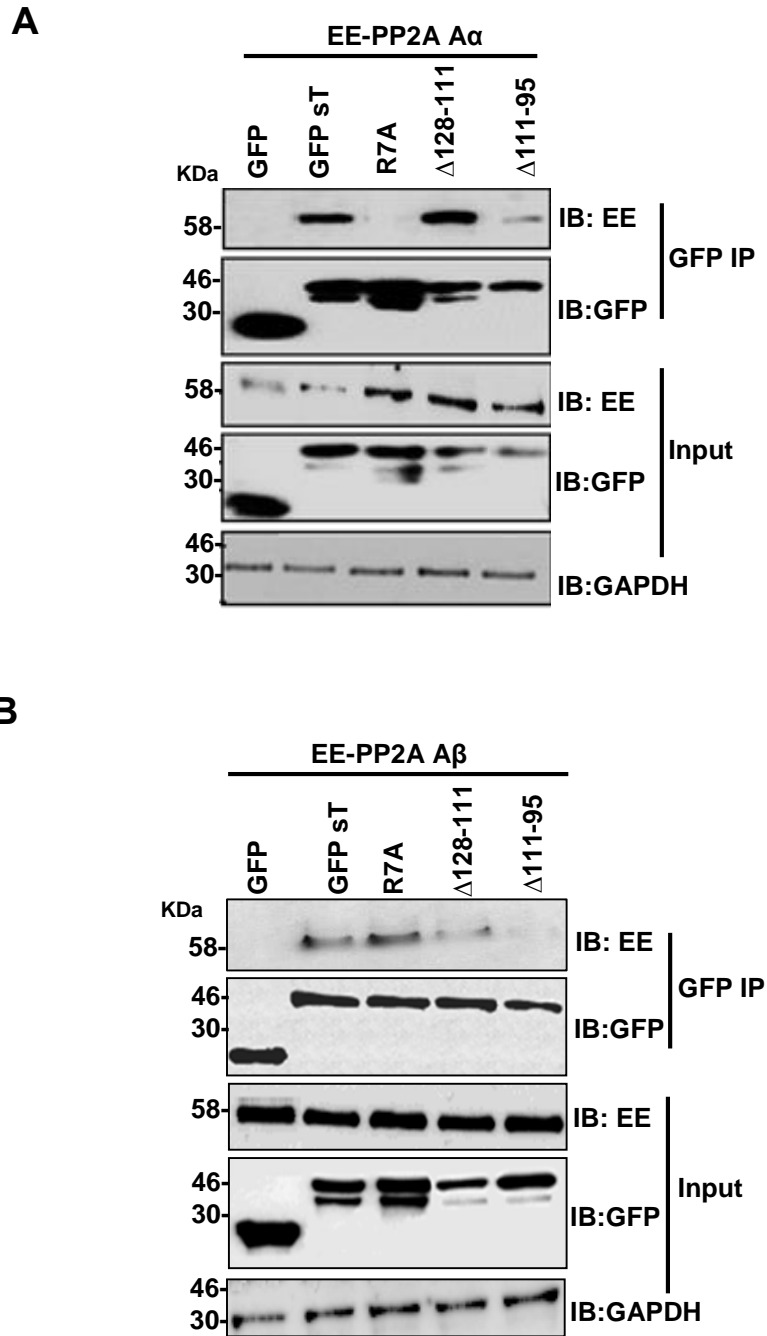


Figure 4.8: Mapping of pEGFP-sT binding site to **(A)** PP2A A $\alpha$  and **(B)** PP2A A $\beta$ . Co-immunoprecipitation of pEGFP alone (control), pEGFP-sT and sT mutants R7A,  $\Delta$ 95-111 and  $\Delta$ 111-128 with each PP2A A $\alpha$  and PP2A A $\beta$ . Proteins were expressed in MCC13 cells and precipitated by GFP-Trap magnetic beads. GFP and Glu-Glu (EE) antibodies were used to probe pEGFP, pEGFP-sT and PP2A A $\alpha$  or PP2A A $\beta$  respectively. GAPDH was used for loading control. Representative blot is shown. Marker in kDa.

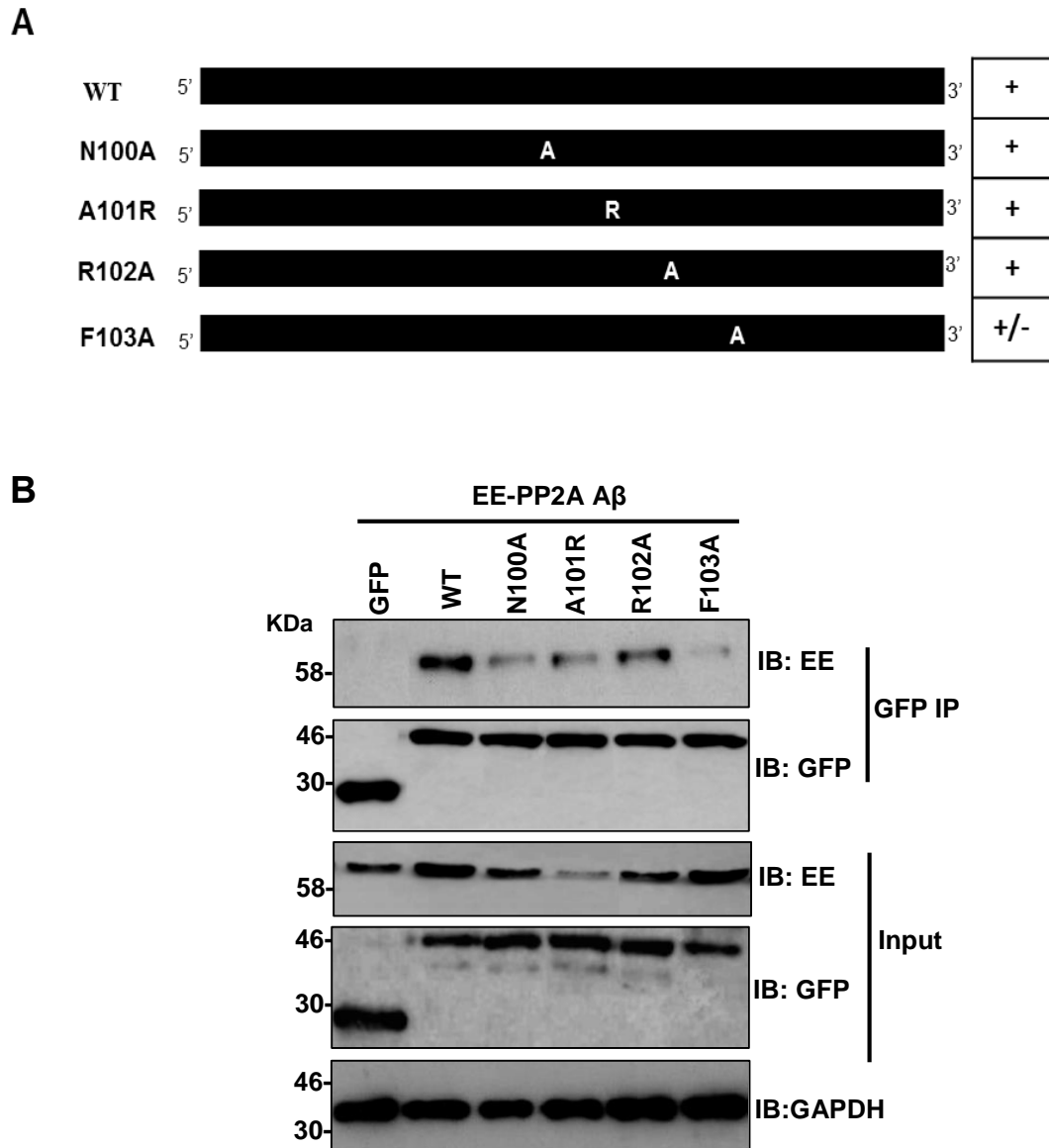


Figure 4.9: MCPyV sT required residue 103 to interact PP2A A $\beta$ . **(A)** Schematic representation of sT point mutants within 100-103, (the letters **A** or **R** refers to the amino acid replaced). The symbol **(+)** refers to the mutation bound to PP2A A $\beta$  and **(+/-)** for mutation has weak interaction. **(B)** Co-immunoprecipitation of pEGFP alone (control) or pEGFP-sT and the four point mutants with EE- PP2A A $\beta$ . Proteins were co-expressed in MCC13 cells and precipitated by GFP-TRAP beads. GFP and EE antibodies were used to probe pEGFP-sT and EE-PP2A A $\beta$  respectively. GAPDH used for loading control. Representative blot is shown. Marker in kDa.

## 4.3 Discussion

### 4.3.1 MCPyV sT targets PP4C

In this study, co-immunoprecipitations confirmed the interaction of MCPyV sT with PP4C (Figure 4.1). Similar results have recently been published by the Chang-Moore laboratory (Kwun et al., 2015). Herein the mutagenesis results showed that the same amino acid residues in sT (R102 and F103) that are needed to bind NEMO, are required to interact with PP4C. These amino acids are not conserved in LT and other MCPyV proteins as well as the other polyomavirus sT proteins. Moreover, these residues have been shown to be required for inhibiting the NF- $\kappa$ B pathway (Figure 3.11). This may suggest that MCPyV sT recruits PP4C to deregulate NF- $\kappa$ B either alone or in a complex with NEMO.

Targeting of viruses to PP4C is not well studied compared to the well-studied PP2A. The first investigation demonstrating targeting of PP4C by a virus was reported by our group in Leeds University based on co-immunoprecipitation and SILAC-based immunoprecipitation strategy (Griffith et al., 2013). Since then our group has extended these findings to demonstrate a role for PP4C in the deregulation of the microtubule-associated protein (Stathmin) in MCPyV sT-expressing cells. Subversion of Stathmin results in microtubule destabilization and cell motility. These findings suggest a possible molecular mechanism for the highly metastatic phenotype associated with MCC with the action of PP4C (Knight et al., 2015).

The results from co-immunofluorescence assay confirmed the localization between MCPyV sT and PP4C in the cytoplasm of MCC13 cells (Figure 4.2). One study highlighted shuttling of PP4C to the nucleus, where it co-localised with nuclear nuclear distribution element-like 1 (NDEL1) during microtubule regulation (Toyo-oka et al 2008). Our studies did not indicate a nuclear localisation, however, it is plausible that this shift in localisation can only be seen upon during specific stages of the cell cycle.

### 4.3.2 MCPyV sT interacts with the two isoforms of PP2A.

The co-immunoprecipitation results confirm the SILAC data showing an interaction with the structural subunit A for both PP2A isoform  $\alpha$  and  $\beta$  (PP2A A $\alpha$  and PP2A A $\beta$ ). Moreover, a weak interaction with the catalytic C subunit of PP2A (PP2A C) was also observed (Figure 4.7 A, B, C). Presumably the interaction with PP2A C was mediated through interactions with the A subunit. The interaction of MCPyV sT with PP2A A $\alpha$  is well-defined. Despite this, studies have failed to demonstrate a role for the MCPyV sT-PP2A A $\alpha$  interaction in MCPyV pathogenesis. On the contrary, SV40 tumorigenic activity is strictly dependent on the interaction with PP2A, since mutant versions within residues 97-103 of SV40 sT that are unable to bind PP2A failed to induce tumorigenic activity (Mateer, et al., 1998, Hahn et al., 2002).

PP2A regulates multiple signalling pathways, for example it contributes to the NF- $\kappa$ B pathway by targeting RelA (Yang, J. et al, 2001). The ability to bind PP2A is a conserved function of polyomavirus sT proteins and this association has been shown to play an important role in virus-induced cellular transformation by other polyomaviruses (Pallas et al., 1990). Evidence reported by Shuda and colleagues provided a physical interaction between MCPyV sT and PP2A A $\alpha$  subunit and showed it has no effect on the phosphorylation of 4E-BP1 (Shuda et al., 2011). So far, the MCPyV sT protein has been implicated in the process of viral DNA replication (Feng et al., 2011, Kwun et al., 2009) and cellular transformation (Shuda et al., 2011). Mutational analysis of sT indicates that association with PP2A is required for its ability to enhance LT's viral DNA replication function. The most recent studies were done on PP2A A $\alpha$ . The interaction between PP2A A $\beta$  and MCPyV sT was first identified using co-immunoprecipitation and SILAC immunoprecipitations (Griffith et al., 2013). Herein the results showed that MCPyV sT interacts with both PP2A A $\alpha$  and A $\beta$ .

Mutagenesis of MCPyV sT found that residues between 95-111 are required for the interaction with both PP2A isoforms (Figure 4.8). Further mutations were generated in an attempt to create a single point mutation unable to bind to PP2A A $\beta$ , in an effort to recapitulate the usefulness of the R7A mutant in

delineating the role of the PP2A A $\alpha$  interaction in MCPyV pathogenesis. The extensive mutagenesis performed in this chapter identified that the F103A mutant significantly reduces binding to PP2A A $\beta$ . Importantly, the R102A mutant retains an interaction with PP2A A $\beta$  whilst losing binding to both PP4C and NEMO, allowing for discrimination of the roles of cellular binding partners.

The results in this chapter showed that sT interacts with PP4C and both structural subunits of PP2A as well as the PP2A C subunit. The thorough mapping strategy identified that the residues essential for binding NEMO are also required for recruiting protein phosphatases. This may illustrate that sT targets both NEMO and the phosphatases in a complex to inhibit the NF- $\kappa$ B pathway (Griffith et al., 2013).

## Chapter 5. Characterisation of the protein complexes associated with MCPyV sT

### 5.1 Introduction

We have shown that an interaction between MCPyV sT and NEMO is necessary for the negative regulation of NF- $\kappa$ B, helping MCPyV to evade the host antiviral response (Griffith et al., 2013). Evidence for the inhibition of NF- $\kappa$ B originated from the observation that levels of phosphorylated I $\kappa$ B $\alpha$  were reduced in cells inducibly expressing sT, and this correlated with a reduction in the nuclear translocation of p50 and p65 NF- $\kappa$ B proteins (Griffith et al., 2013). Co-immunoprecipitation assays were used to determine potential host targets for sT that may mediate the observed effects. These revealed interactions in cells with NEMO, and a number of phosphatase sub-units (Chapters 3 and 4) (Griffith et al., 2013). Further mutagenesis studies revealed that a short stretch of amino acids (residues 101-103) in MCPyV sT was necessary for these interactions. These observations are perplexing, given the potential for steric hindrance between putative binding partners for binding to such a short region of the protein. Moreover, NEMO was not identified in the initial SILAC proteomic screen (unlike all of the phosphatase sub-units), suggesting either a transient low-affinity interaction, an incompatibility of NEMO peptides for mass spectrometry or the possibility that NEMO associates with sT as part of a larger protein complex, potentially consisting of one or more phosphatase sub-units.

The aim of this chapter was to determine whether the interactions of MCPyV sT with the panel of identified host-binding partners occurs in a direct manner *in vitro* to begin to understand the nature of these interactions.

## 5.2 Result

### 5.2.1 Identification of protein-protein interactions *in vitro*.

To elucidate the nature of the interaction between MCPyV sT and the proteins identified in Chapters 3 and 4, we applied an *in vitro* protein-protein interaction assay. Cell proteins were translated in a cell-free system using the T<sub>NT</sub> *in vitro* translation/transcription system (IVT) (Figure 5.1A) and MCPyV sT was expressed in bacteria as a GST fusion protein (Figure 5.1B). Direct binding assays were then performed with purified recombinant GST-sT and the IVT host protein, either alone or in combinations.

### 5.2.2 Validating the expression of bacterial GST-sT.

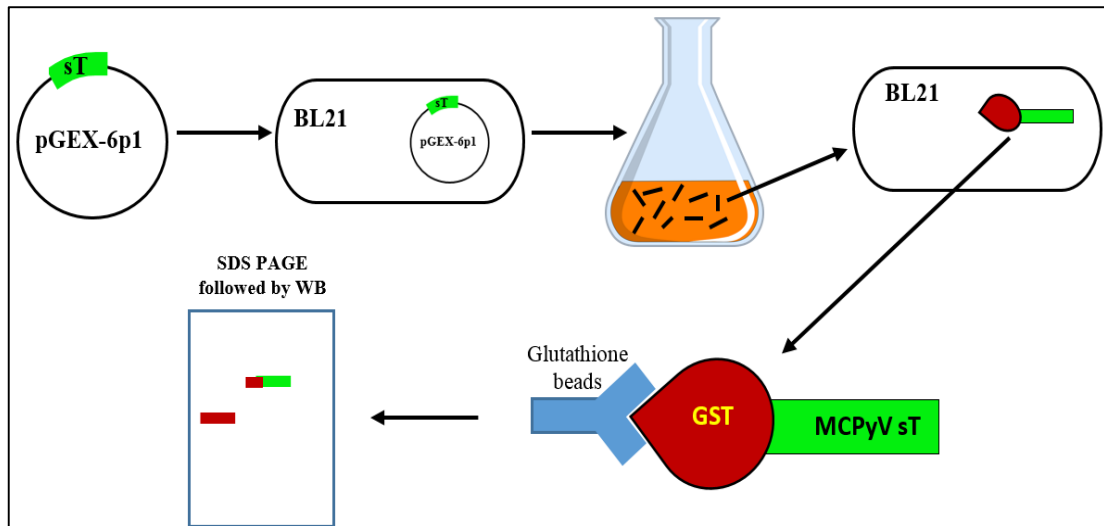
To validate the production of GST-sT from bacteria, soluble lysates were incubated with glutathione-agarose affinity matrix beads for 2h and the precipitates analysed by Western blotting with an anti-GST antibody (Figure 5.2A). Western blotting confirmed the presence of GST and GST-sT at the appropriate molecular weight, indicating that sT is expressed as a soluble protein in bacteria.

### 5.2.3 IVT production of sT binding partners.

Synthesis of cell proteins in free cell system was performed using IVT. A panel of host proteins (FLAG-NEMO, FLAG-PP4C, HA-PP4R1, EE-PP2A A $\alpha$  and EE-PP2A A $\beta$ ) were expressed by IVT and their expression confirmed by Western blotting using appropriate antibodies. **A control reaction containing no added DNA was used to allow measurement of any background incorporation of any protein in IVT.** The results revealed that each protein expressed at its expected molecular weight, and at easily detectable levels (Figure 5.2B). Together, these data indicate that the appropriate reagents

can be produced in order to study interactions with sT and its binding partners *in vitro*.

**A**



**B**

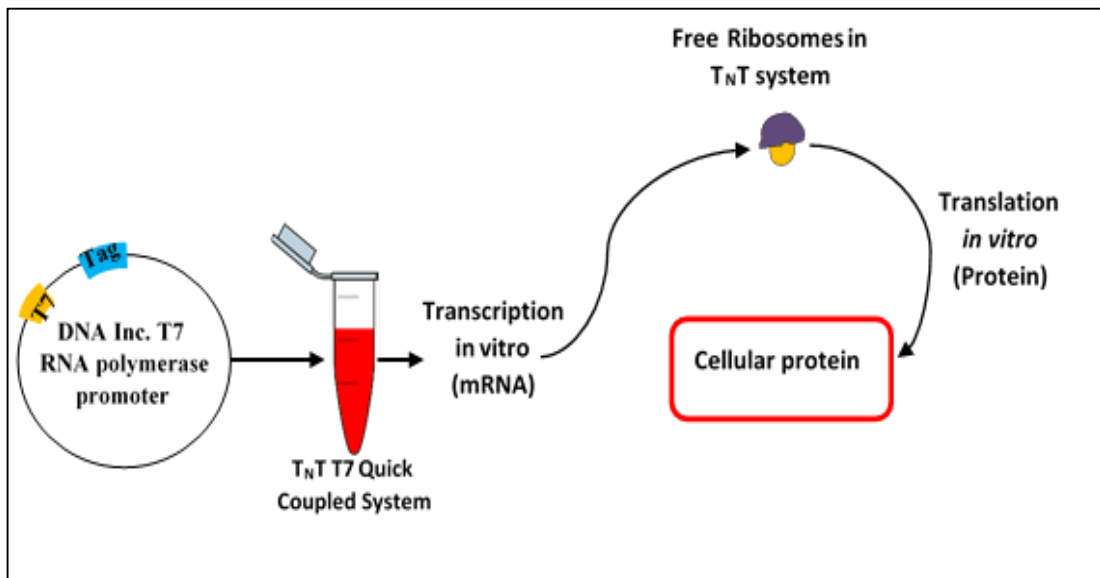


Figure 5.1: Protocols for synthesis proteins for direct binding assay. **(A)** Bacterial expression of GST and GST-sT. The plasmids were transformed in BL21 *E. coli* competent cells. GST and GST-sT proteins were extracted from bacteria by sonication and centrifugation. Protein purification was performed by Glutathione agarose beads and resolved by Western blotting. **(B)** Cell proteins were synthesized using IVT. Cellular plasmids cloned in vectors containing T7 promoter and incubated 2h with T<sub>N</sub>T master kit to produce cellular proteins which then resolved by Western blotting.

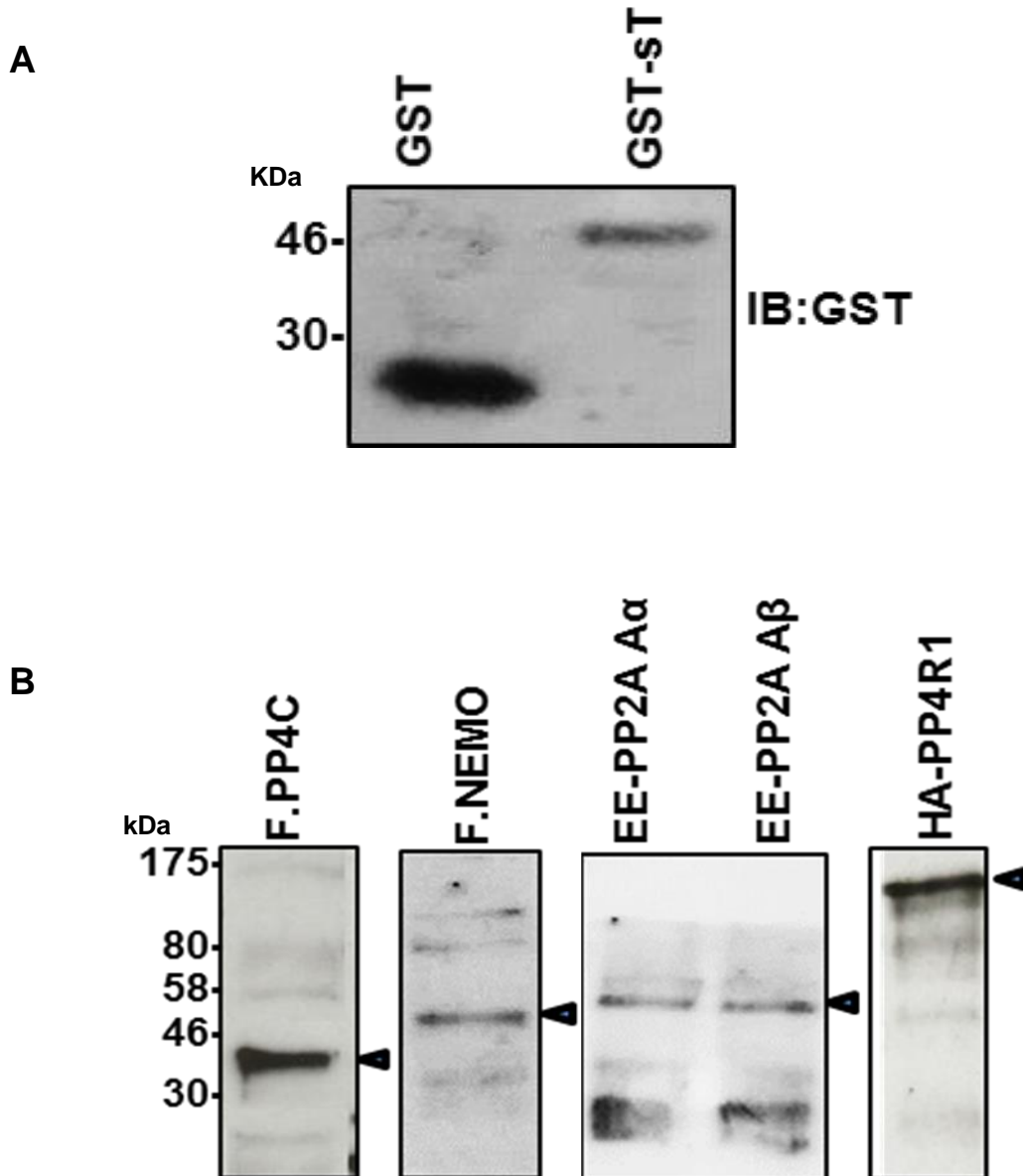


Figure 5.2 Expression of GST-sT and host proteins. **(A)** GST and GST-sT were cloned in BL21 and grown for 24h. Cells were harvested by centrifugation and sonicated to release the proteins from bacteria which were then purified by Glutathione agarose beads. **(B)** Host cell protein were produced by IVT system, names of proteins listed on the top side. The triangle symbols refer to the target proteins. Proteins were analysed by Western blotting. Representative blots are shown. Marker in kDa.

#### **5.2.4 MCPyV-sT does not bind NEMO directly.**

By co-immunoprecipitations, MCPyV sT was shown to interact with NEMO in MCC13 cells (Figure 3.4). In order to verify whether sT interacts with NEMO directly or through a complex, *in vitro* protein binding assays were performed using bacterial expressed recombinant GST-sT and IVT produced FLAG-NEMO. First, bacterial expressed GST or GST-sT was incubated with glutathione-sepharose beads for 2h at room temperature to bind the fusion proteins to the bead matrix (Frangioni and Neel, 1993), then this was used to precipitate IVT FLAG-NEMO for a further 2h. The protein complexes were resolved by SDS-PAGE and analysed by Western blot. The anti-GST Western blots confirmed equal expression of the GST fusion proteins, however, the anti-FLAG blot failed to identify a specific band relating to FLAG-NEMO. Absence of this band indicated that IVT produced NEMO is unable to interact directly with GST-sT (Figure 5.3).

#### **5.2.5 MCPyV-sT binds to PP4C directly.**

The results from the direct protein-protein interaction assay revealed that MCPyV sT did not bind NEMO directly. Thus it was likely that sT may interact with NEMO through another partner within a protein complex. One possible candidate is PP4C, which has previously been shown to be recruited to the IKK complex (Tikhonova, and Aifantis, 2012). Direct binding assays were subsequently performed using GST-sT and FLAG-PP4C. This assay showed a clear band associated with PP4C in the GST-sT sample, suggesting a direct interaction between sT and PP4C (Figure 5.4). It was possible that PP4C could act as a bridge between sT and NEMO, given that all three proteins co-localise in cells (Griffith et al., 2013). To determine if this was the case, GST-sT was mixed with a combination of IVT produced NEMO and PP4C. The results of this assay once again confirmed our previous data, that NEMO does not interact directly with sT. They also showed that the presence of PP4C was not sufficient to incur an interaction between NEMO and sT (Figure 5.4).

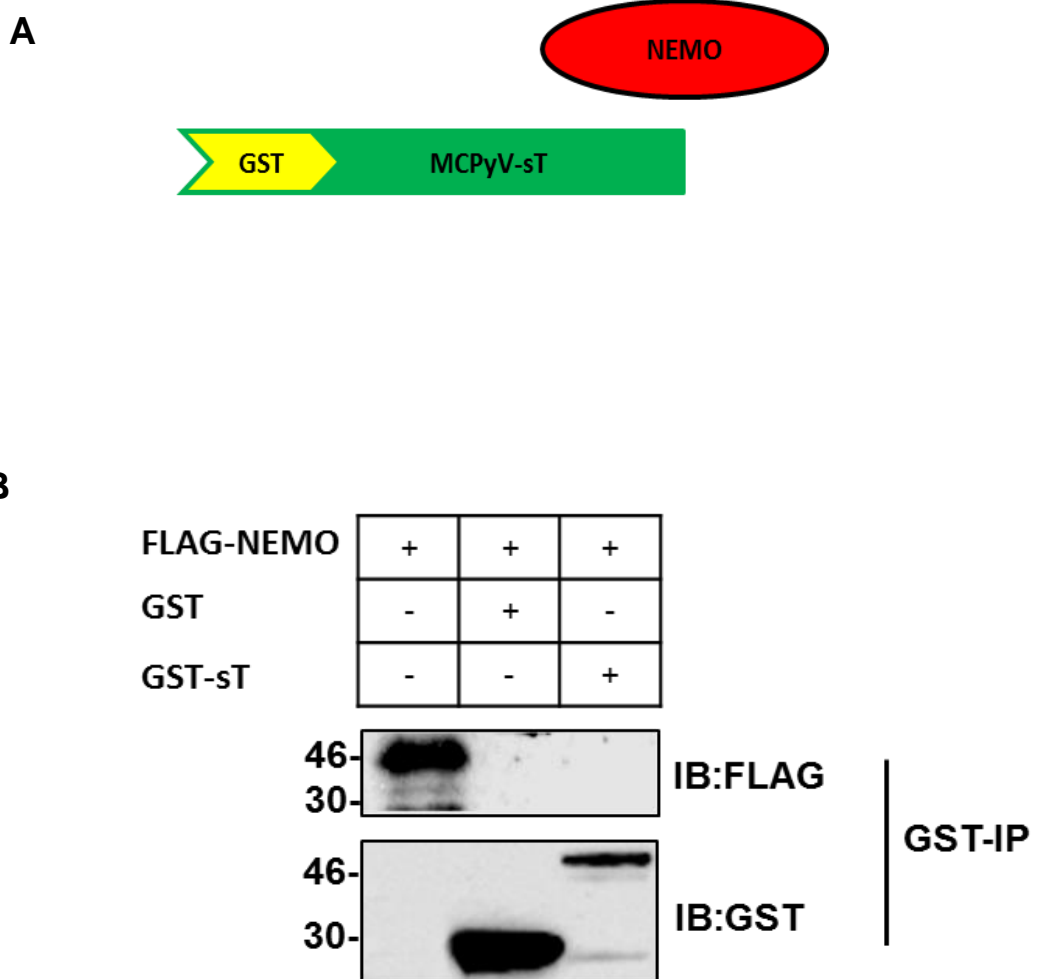


Figure 5.3: No direct interaction between MCPyV-sT and NEMO. **(A)** Schematic representation of GST-tagged sT and FLAG-NEMO. **(B)** Co-immunoprecipitation of GST (control) or GST-sT with FLAG-NEMO by using Glutathione agarose beads to precipitate GST. Input of FLAG NEMO also load to show its expression. Antibodies against GST and FLAG were used to probe GST, GST-sT and FLAG NEMO respectively. Representative blot is shown. Marker in kDa.

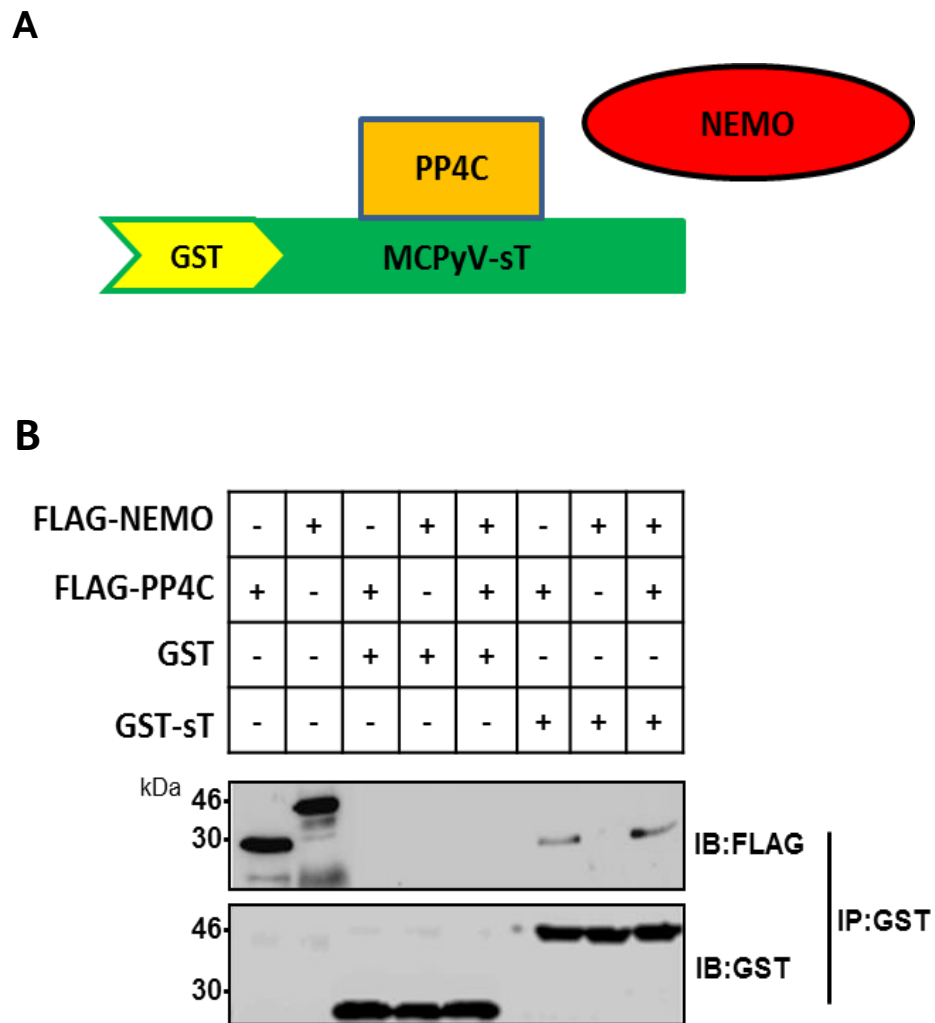


Figure 5.4: MCPyV-sT interacts directly with PP4C independent of NEMO. **(A)** Schematic representation of GST-tagged sT, FLAG-NEMO and FLAG-PP4C. **(B)** Co-immunoprecipitation of GST (control) or GST-sT with FLAG-PP4C alone, FLAG-NEMO alone or both combined. Co-immunoprecipitation was performed by using Glutathione agarose beads to precipitate GST or GST-sT. In vitro FLAG-PP4C or FLAG-NEMO or equal combination of them were incubated with GST or GST-sT in Glutathione agarose beads. Antibodies against GST and FLAG were used to probe GST, GST-sT, FLAG-PP4C and FLAG-NEMO respectively. Representative blot is shown. Marker in kDa.

## **5.2.6 PP4R1 is a PP4C binding protein and novel target of MCPyV sT.**

The dephosphorylation activity of PP4C is regulated through a range of subunits to modulate its substrate specificity. One such PP4C binding protein, PP4R1, was recently shown to be necessary to link PP4C to the IKK complex to regulate NF- $\kappa$ B activity (Brechmann et al., 2012). Given that PP4C was not sufficient to bridge sT to NEMO, attention was directed to identifying whether PP4R1 was required for this function.

### **5.2.6.1 PP4R1 interacts with NEMO in cells.**

Whilst PP4R1 has been shown to interact with the IKK complex in lymphocytes, we wished to establish whether such a complex could form in MCC13 cells. Co-immunoprecipitations were performed between endogenous PP4R1 and FLAG-NEMO using anti-FLAG M2 affinity gel. As depicted (Figure 5.5), PP4R1 was successfully precipitated by FLAG-NEMO but not with beads alone, demonstrating an interaction between PP4R1-NEMO in Merkel cells.

### **5.2.6.2 Co-immunoprecipitation assay confirmed the interaction of PP4R1 with PP4C.**

PP4R1 works together with PP4C as a central negative regulator of NF- $\kappa$ B activity (Tikhonova and Aifantis, 2012, Brechmann et al., 2012). Next, the association between PP4C and PP4R1 was confirmed by co-immunoprecipitation. MCC13 cells were transfected with FLAG-PP4C and the lysates precipitated with FLAG affinity resin. As expected, endogenous PP4R1 was precipitated by FLAG-PP4C (Figure 5.6). Together, these experiments indicate that PP4R1 is able to interact with both PP4C and NEMO in MCC13 cells.

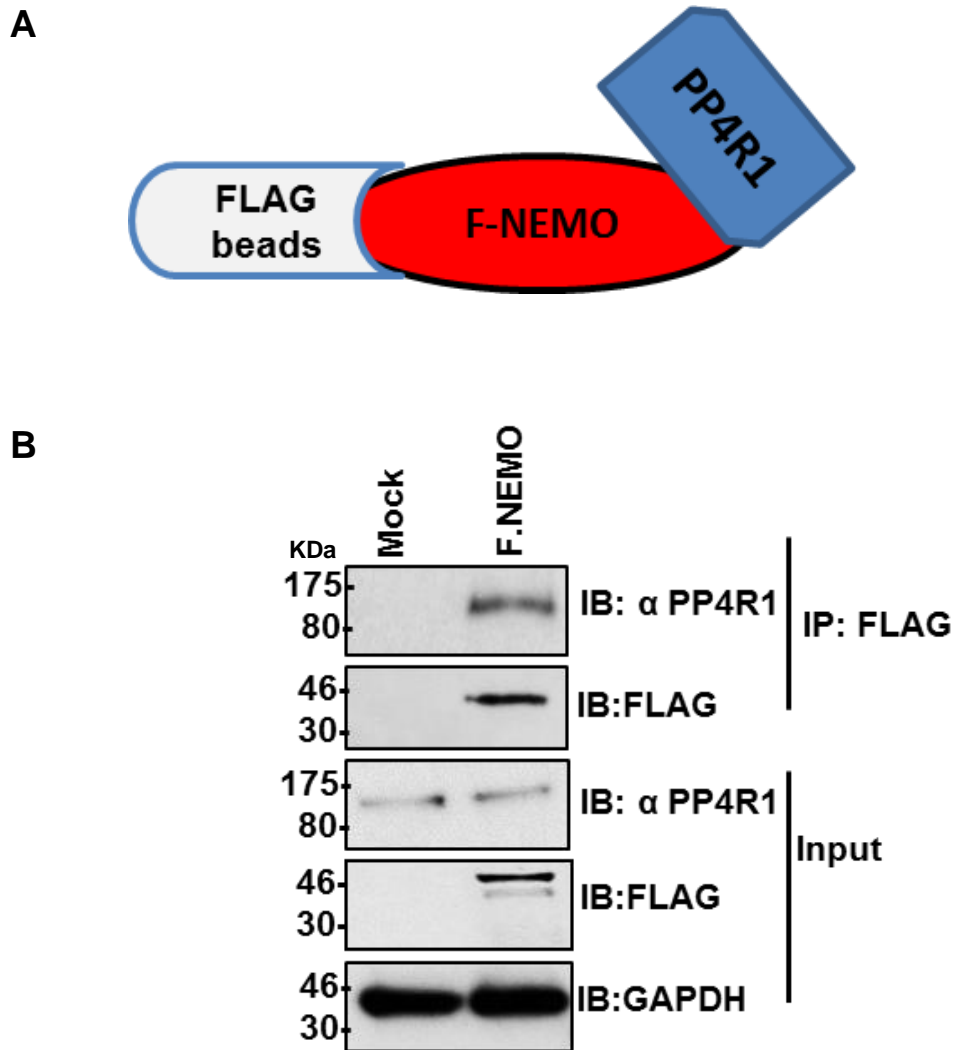
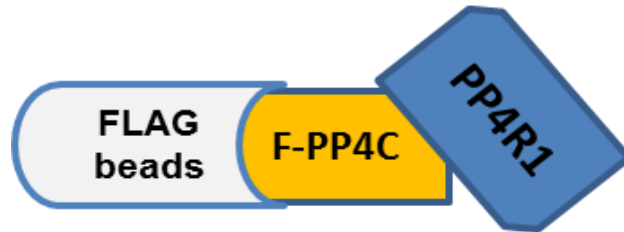


Figure 5.5: Co-immunoprecipitation confirming the interaction between FLAG-NEMO and PP4R1 in MCC13. **(A)** Schematic representation of co-immunoprecipitation of NEMO and PP4R1 by FLAG agarose beads. **(B)** Co-immunoprecipitation of FLAG-NEMO with endogenous PP4R1. Cells untransfected (Mock) or transfected with FLAG-NEMO were lysed and incubated with FLAG agarose beads to precipitate FLAG-NEMO. Protein complex resolved by SDS-PAGE and probed with FLAG or PP4R1 antibody respectively. GAPDH was used as a loading control. Representative blot is shown. Marker in kDa.

A



B

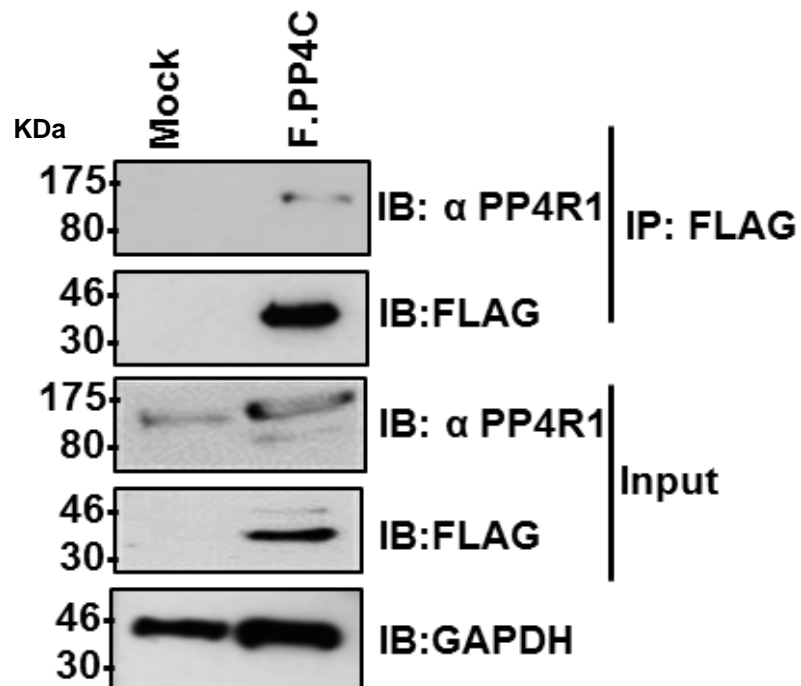


Figure 5.6 Co-immunoprecipitation confirming the interaction between FLAG-PP4C and PP4R1 in MCC13. **(A)** Schematic representation of co-immunoprecipitation of PP4C and PP4R1 by FLAG agarose beads. **(B)** Co-immunoprecipitation of FLAG-PP4C with endogenous PP4R1. Cells untransfected (Mock) or transfected with FLAG-PP4C were lysed and incubated with FLAG agarose beads to precipitate FLAG-PP4C. Immune complex resolved by SDS-PAGE and probed with FLAG or PP4R1 antibody respectively. GAPDH was used as a loading control. Representative blot is shown. Marker in kDa.

### **5.2.6.3 MCPyV-sT targets PP4R1.**

To test whether PP4R1 was a novel sT binding protein, co-immunoprecipitations were performed with EGFP-sT and endogenous PP4R1 in MCC13 cells. Western blot analysis of the GFP-TRAP precipitations clearly showed a band corresponding to PP4R1 in the EGFP-sT sample but not in the EGFP alone sample (Figure 5.7). These data indicate that PP4R1 is a novel MCPyV sT binding protein.

### **5.2.6.4 Mapping the region in sT required for the interaction with PP4R1**

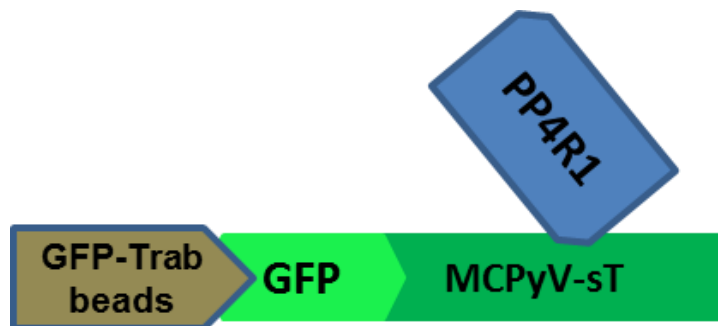
Mapping experiments were performed to delineate the regions of sT necessary for binding to PP4R1 in cells. Given that to date all identified binding partners of sT interacted with a short sequence of amino acids, we initially utilised the internal deletion mutant  $\Delta$ 95-111 and  $\Delta$ 111-128 and an overexpressed HA-epitope fused PP4R1 in MCC13 cells. As detected by SDS-PAGE and immunoblotting, wild type sT and  $\Delta$ 111-128 retained their ability to target PP4R1, whereas  $\Delta$ 95-111 abolished this interaction (Figure 5.8). Thus, PP4R1 also interacted with residues between 95-111.

### **5.2.6.5 Amino acids 101-103 in sT are required for the interaction with PP4R1**

Given the results of the co-immunoprecipitations using the internal deletion mutants of sT it is possible that the same amino acid residues in sT required for the interactions with NEMO and PP4C are also required for association with PP4R1. To answer this question, the panel of sT point mutants were used in co-immunoprecipitations with HA-PP4R1. Cell lysates were incubated with GFP-TRAP affinity beads to precipitate the GFP-sT mutants. Protein complexes were resolved by SDS-PAGE then immunoblotted with GFP and HA antibodies. The results showed that wild type and N100A retained their ability to bind to PP4R1, whereas A101R, R102A and F103A abolished this interaction (Figure 5.9). Thus, residues 101,102 and 103,

which we observed were essential for binding to NEMO are also important for PP4R1 interaction.

**A**



**B**

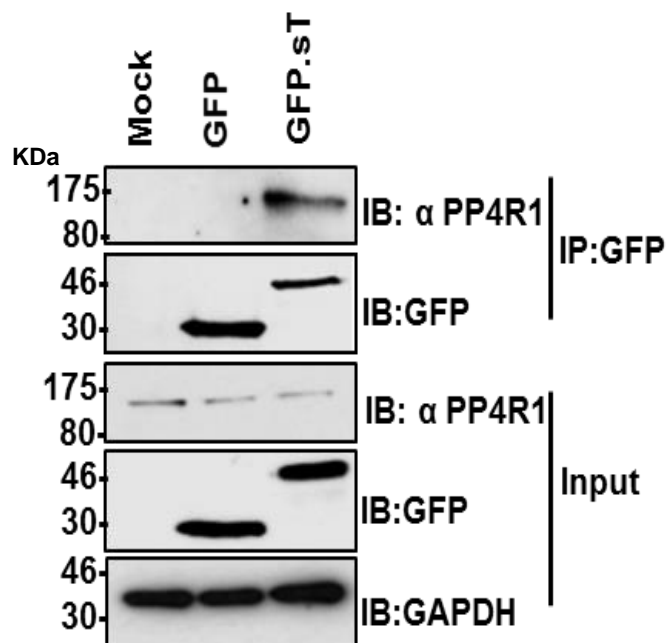


Figure 5.7: Co-immunoprecipitation confirming the interaction of MCPyV-sT with the endogenous PP4R1 in MCC13 cells. **(A)** Schematic representation of co-immunoprecipitation between GFP-sT with endogenous PP4R1 by GFP-TRAP beads. **(B)** Untransfected cells or transfected with either pEGFP or pEGFP sT. Post transfection 24h, cells were harvested and co-immunoprecipitation were performed by incubating the cellular lysates with GFP-TRAP beads. GFP antibody was used to detect GFP and GFP-sT proteins, anti PP4R1 antibody was used to probe PP4R1.

GAPDH was used as a loading control. Representative blot is shown. Marker in kDa.

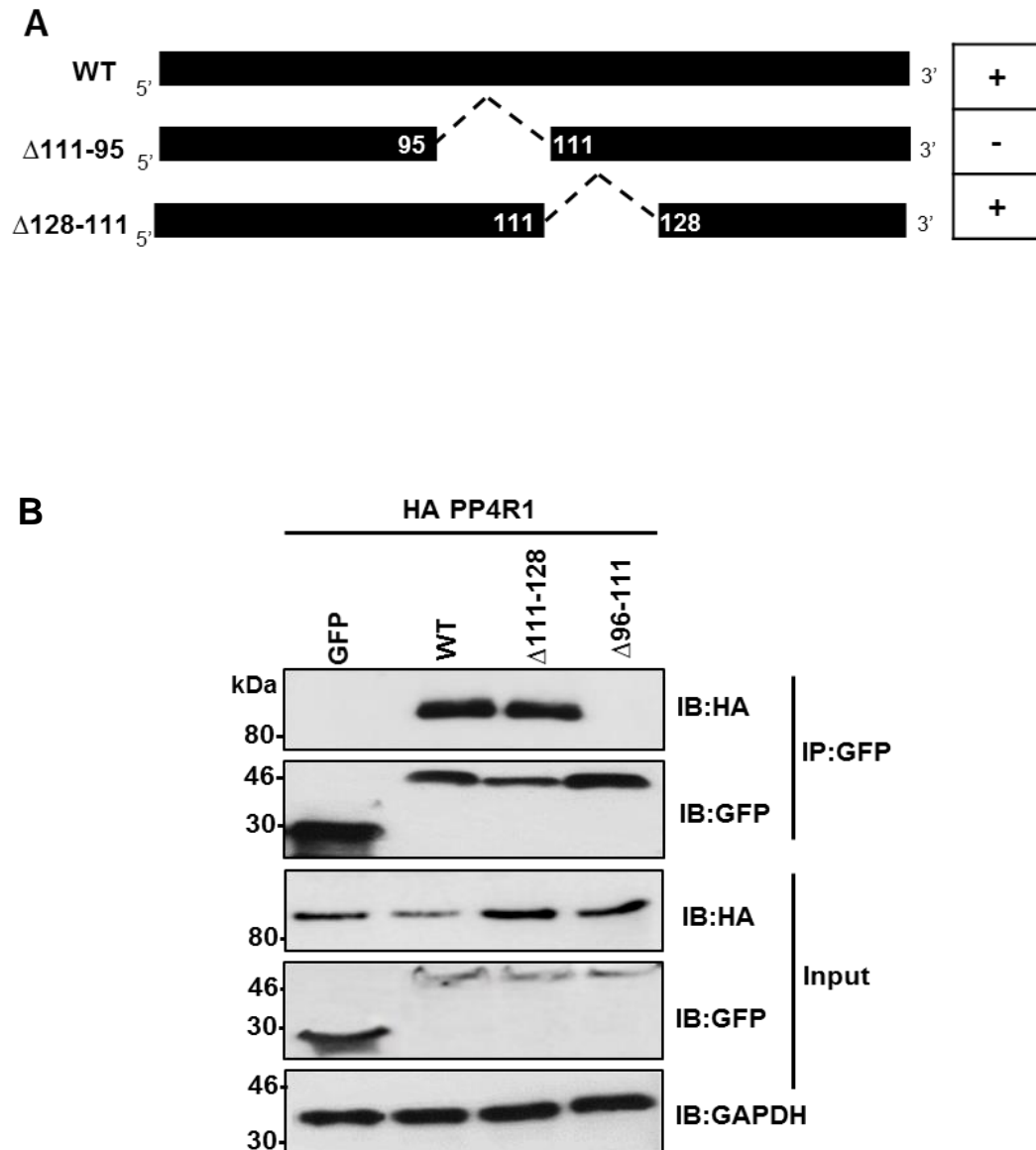


Figure 5.8: MCPyV-sT required residues 95-111 to interact PP4R1. **(A)** Co-immunoprecipitations of GFP alone (control), wild type GFP-sT and two deletion mutants  $\Delta$ 95-111 and  $\Delta$ 111-128 with HA-PP4R1. Proteins were expressed in MCC13 cells and precipitated by GFP-TRAP magnetic beads. GFP and HA antibodies were used to probe GFP-sT and HA-PP4R1 respectively. GAPDH used for loading control. Representative blot is shown. Marker in kDa.

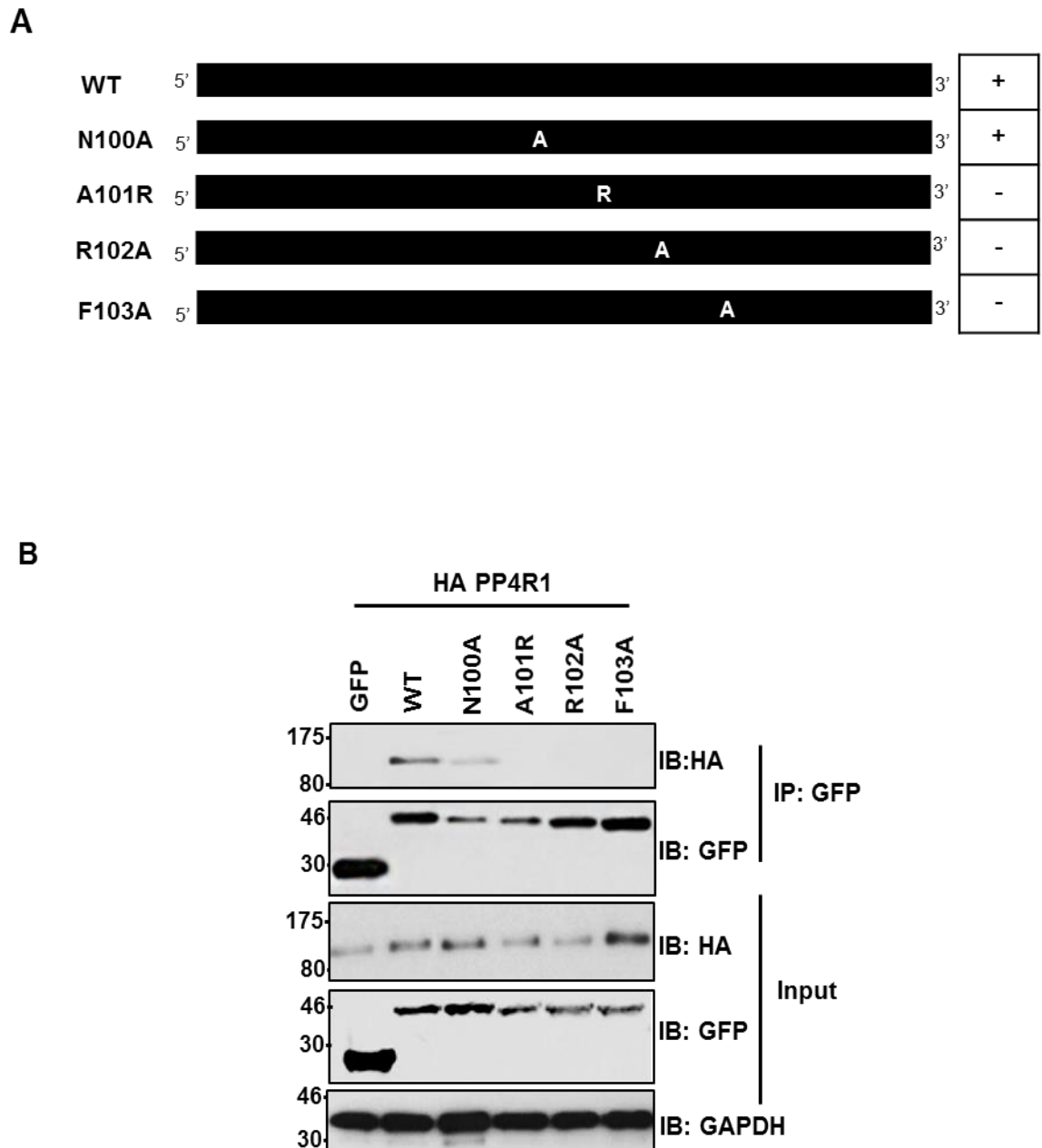


Figure 5.9: MCPyV-sT required residues 101,102 and 103 to interact PP4R1. **(A)** Schematic representation of sT point mutants within 100-103, (the letters **A** or **R** refers to the amino acid replaced). The symbol (+) refers to the mutation bound to PP4R1 and (-) for mutation non-bound to PP4R1. **(B)** Co-immunoprecipitations of pEGFP alone (control), pEGFP-sT and the four point mutants with HA-PP4R1.

Proteins were expressed in MCC13 cells and precipitated by GFP-TRAP magnetic beads. GFP and HA antibodies were used to probe GFP-sT and PP4R1 respectively. GAPDH used for loading control. Representative blot is shown. Marker in kDa.

### **5.2.7. MCPyV-sT recruits PP4R1 to interact with NEMO.**

To evaluate a potential role for PP4R1 in the NEMO-PP4C-sT complex, direct binding assays were once again performed. MCPyV sT binding proteins were generated by IVT and incubated with recombinant GST or GST-sT, as described. Western blot showed that all proteins were generated successfully. Binding assays showed that PP4R1 was able to interact directly with GST-sT but not GST alone. Interestingly, whilst NEMO could not be precipitated by GST-sT when incubated alone or in combination with either PP4C or PP4R1, a band corresponding to FLAG-NEMO was clearly observed in samples where it was co-incubated with both PP4R1 and PP4C (Figure 5.10). These data indicate that the presence of a PP4R1-PP4C complex may be required to mediate the interaction between NEMO and sT *in vitro*.

### **5.2.8 Direct interaction of PP2A A $\alpha$ or PP2A A $\beta$ with MCPyV sT.**

Whilst a number of studies have shown essential roles for PP4C in MCPyV sT mediated immune evasion (Griffiths et al., 2013) and metastasis (Knight et al., 2015), the work shown in this thesis also identifies an interaction with PP2A phosphatases (Chapter 4). We sought a better understanding of these interactions and so performed direct binding reactions with EE-PP2A A $\alpha$  or EE-PP2A A $\beta$  to ascertain whether they are able to interact directly with sT or like NEMO may constitute part of a sT binding complex. The assay clearly showed a direct interaction between GST-sT and PP2A A $\beta$ , with a weaker interaction observed for PP2A A $\alpha$  (Figure 5.11). These data mirror the SILAC proteomic results (Griffiths et al., 2013).

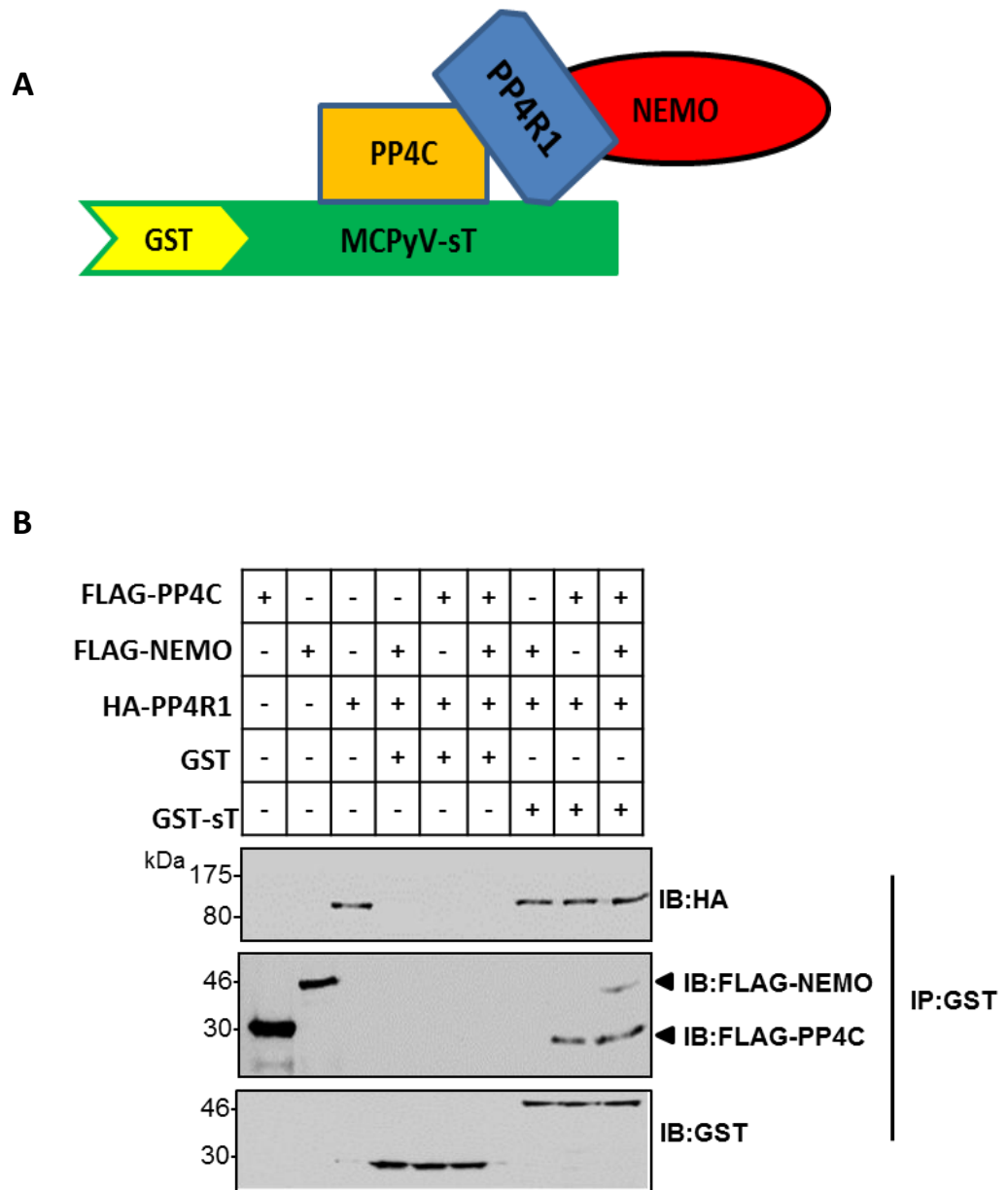


Figure 5.10: MCPyV-sT interacts NEMO through its interaction with PP4C-PP4R1 complex. **(A)** Schematic representation of GST-tagged sT, NEMO, PP4C and PP4R1. **(B)** Co-immunoprecipitations of GST (control) or GST-sT with FLAG-PP4R1 alone or with equal combinations named in the top side. Co-immunoprecipitations were performed by using Glutathione agarose beads to precipitate GST or GST-sT. Antibodies against GST, FLAG and HA were used to probe the proteins. R1 refers to PP4R1. Representative blot is shown. Marker in kDa.

### **5.2.9 MCPyV sT residues 102 and 103 necessary for the direct interaction with host proteins.**

Co-immunoprecipitation assays in cells confirmed the importance of residues 101-103 in sT for the observed interactions with a number of host proteins (Chapters 3 and 4). The interactions between sT and NEMO/PP4R1 requires three residues (amino acids 101,102 and 103), the interaction with PP4C requires amino acids 102 and 103, whereas amino acid 103 is essential for binding to PP2A A $\beta$ . To further understand the binding requirements for each protein, direct binding assays were performed with two point mutants of sT (R102A and F103A) and the panel of cellular proteins.

First, the two mutants were cloned into pGEX-6P1 to generate GST fusion proteins. GST-R102A and GST-F103A were expressed in BL21 *E. coli* strain and isolated as described (2.11.2). Direct binding assays were then performed with IVT produced NEMO, PP4C, PP2A A $\beta$ , and PP4R1. Input proteins were used as loading control and GST alone as a negative interaction control (Figure 5.12). Binding assays confirmed that wild type sT did not bind NEMO directly, as well as either of the two mutants (Figure 5.12). This confirmed the previous results that showed no interaction between sT and NEMO. In contrast, wild type sT exhibited a strong direct interaction with PP4C, PP4R1 and PP2A A $\beta$ . Both mutants completely abolished the interaction with PP4C, whereas PP4R1 showed a very low level interaction with R102A. Furthermore, PP2A A $\beta$  retained its ability to bind both R102A and F103A, although at a reduced level (Figure 5.12). Thus, these results indicate that we have successfully generated sT mutants capable of discriminating between host binding partners both in cells and in a direct binding assay.

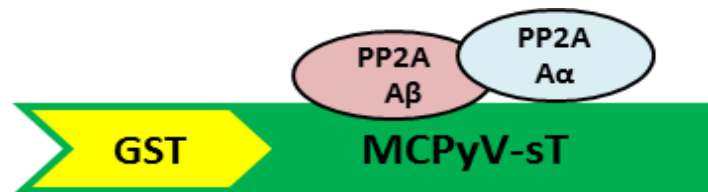
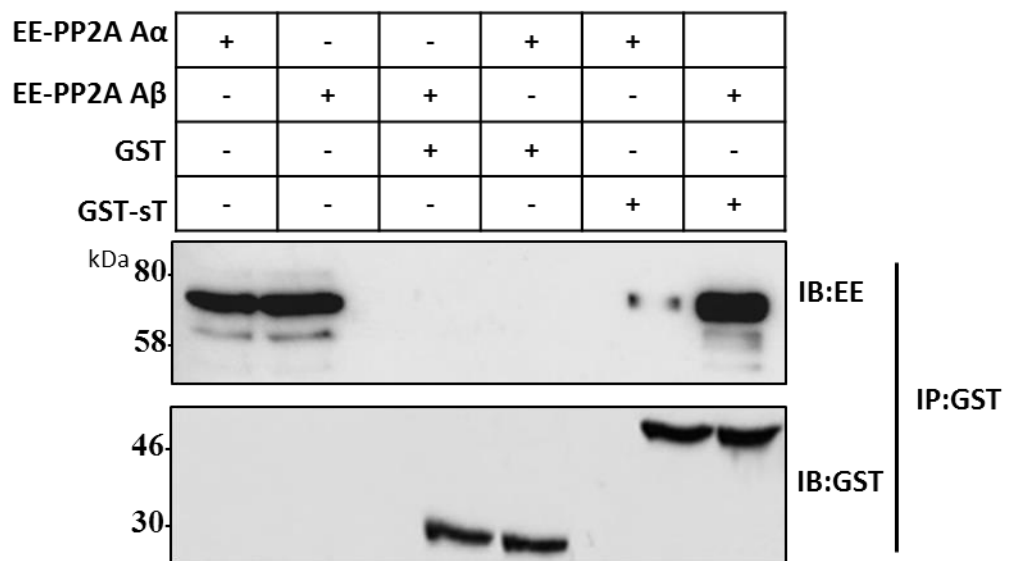
**A****B**

Figure 5.11: MCPyV-sT targets PP2A A $\beta$  directly. **(A)** Schematic representation of GST-tagged sT, PP2A A $\alpha$  and PP2A A $\beta$ . **(B)** Co-immunoprecipitations of GST (control) or GST-sT with EE-PP2A A $\alpha$  or EE-PP2A A $\beta$ . Input of in vitro PP2A proteins were loaded to confirm their expressions. Co-immunoprecipitations were performed by using Glutathione agarose beads to precipitate GST or GST-sT. Antibodies against GST and EE were used to probe the proteins. Representative blot is shown. Marker in kDa.

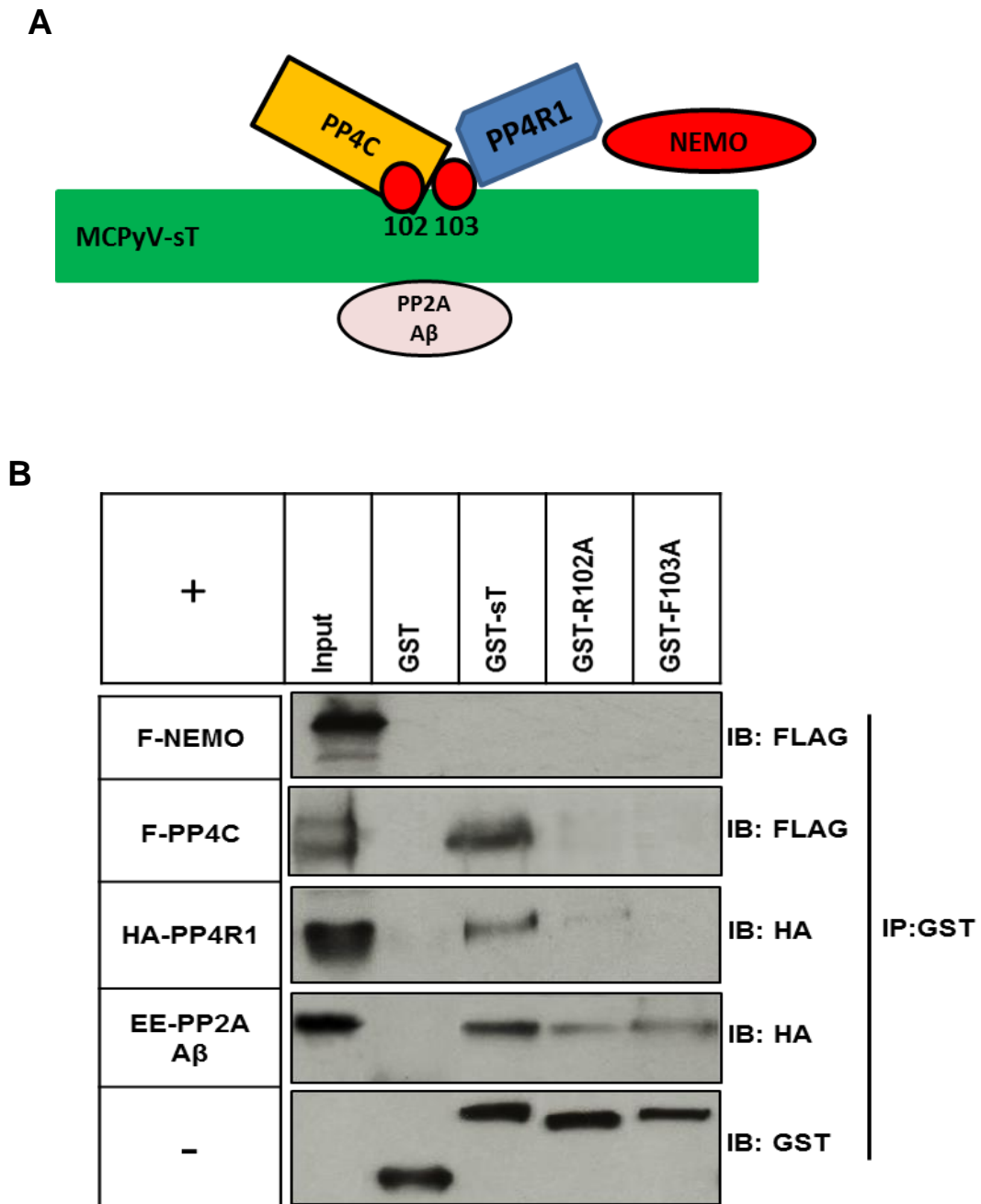


Figure 5.12: Mapping of direct interaction site of sT to the cellular protein in vitro. **(A)** Schematic representation of possible interaction between GST-sT, mutants R102A and F103A with NEMO, PP4C and PP4R1. **(B)** Co-immunoprecipitations of GST (control), GST-sT, R102A or F103A with in vitro cellular protein were performed by incubate the proteins with Glutathione agarose beads to precipitate GST-sT. Input in vitro cellular proteins detected their expression. Antibodies against GST, FLAG, EE and HA were used to probe the proteins. Representative blot is shown.

## 5.3 Discussion

### 5.3.1 MCPyV sT does not interact with NEMO directly.

Co-immunoprecipitation assays illustrated that MCPyV sT binds a number of proteins including NEMO, PP4C and PP2A. A number of avenues indicate that these interactions could lead to the disruption of NF- $\kappa$ B signalling (Griffiths *et al.*, 2013). Co-immunoprecipitation results demonstrated an interaction between MCPyV sT and NEMO. To better understand this interaction, a direct binding assay was performed between bacterial GST-sT and *in vitro* produced binding partners. Both GST-sT and the cellular proteins were produced and detected by Western blot and appeared in their approximate sizes. The direct binding assay provided the intriguing observation that MCPyV sT does not bind NEMO directly (Figure 5.3). This result is compatible with the SILAC proteomic screen performed at Leeds, which did not detect NEMO as a sT binding protein (Griffith et al., 2013). The lack of a direct interaction between sT and NEMO opens up the question about which other host cell proteins involved in NF- $\kappa$ B signalling might mediate binding with NEMO. Previous studies have shown that PP4C and PP4R1 work as partner proteins to NEMO and we showed that they are capable of interacting with MCPyV sT. Initially, the obvious candidate for acting as a bridge between NEMO and sT was PP4C, and indeed direct binding assays demonstrated a direct interaction between PP4C and sT. However, co-incubation with GST-sT and IVT produced NEMO and PP4C still failed to recapitulate the interaction with NEMO and sT. Together, these data show that whilst PP4C is a direct binding partner of sT, alone it is not enough to mediate the interaction with NEMO, indicating that **either binding with NEMO is not required or another sT-binding protein is necessary for this function. However, the IVT was observed to have minimal background of different proteins which may interfere with MCPyV sT. To avoid potential interference, purification of all required proteins in bacteria may provide a better understanding of the specificity of protein-protein interaction.**

### **5.3.2 A novel interaction between MCPyV sT and PP4R1.**

The literature demonstrates that one of the PP4C regulatory subunits, PP4R1, is necessary for PP4C-mediated IKK dephosphorylation in T cells (Tikhonova and Aifantis 2012, Brechmann et al., 2012). It was possible that in Merkel cells sT subverts PP4R1 function to target PP4C to NEMO. Our precipitation studies confirmed interactions between PP4R1 with PP4C and NEMO. They also provided the first demonstration of an interaction between PP4R1 and sT in cells. PP4R1 was first identified associated with PP4C in a 105 kDa complex by co-immunoprecipitation, microcystin-Sepharose and Mass spectrometry analysis, (Kloeker and Wadzinski, 1999). The PP4R1 N-terminus contains two heat repeats which have been observed to be required for protein- protein interaction and contains a binding domain for PP4C.(Kloeker and Wadzinski, 1999). Depletion of PP4R1 from T cells by siRNA resulted in increased secretion of NF- $\kappa$ B-dependent cytokines including IFN- $\gamma$ , IL-2 and TNF- $\alpha$ . In addition, luciferase reporter assays showed an increase in NF- $\kappa$ B-dependent transcription after PP4R1 silencing (Brechmann et al., 2012). In this study, the phenotype was explained as a defect in the dephosphorylation of the IKK complex, resulting in constitutive IKK activation and enhanced NF- $\kappa$ B signalling (Brechmann et al., 2012). However, PP4R1 has also been shown to interact with the ubiquitin ligases TRAF2 and TRAF6 to negative regulate the NF- $\kappa$ B pathway (Hadweh et al., 2014). These findings imply that PP4R1 might regulate NF- $\kappa$ B activity by a number of mechanisms.

### **5.3.3 MCPyV sT forms a complex consisting of PP4R1-PP4C-NEMO.**

Mutagenesis studies also revealed that the same residues in sT (residues 101, 102 and 103) necessary for interacting with NEMO are needed to bind to PP4R1 in cells. This could be interpreted that sT interacts with these proteins in a complex. To determine whether PP4R1 functions as a scaffold in the sT-NEMO complex, direct binding assays were performed with all three host proteins and GST-sT. Similar to PP4C, PP4R1 was shown to

directly bind to recombinant sT *in vitro*. Interestingly, as with PP4C, the presence of PP4R1 alone was not sufficient to bridge sT to NEMO, however, when PP4R1 and PP4C were combined in the reaction, sT was able to interact with NEMO, as evidenced by the appearance of a protein band of the correct molecular mass in the anti-FLAG Western blot. These data highlight that a trimeric protein complex consisting of PP4R1-PP4C-NEMO is necessary and sufficient to mediate the sT-NEMO interaction *in vitro*. Why both PP4C and PP4R1 are required to bridge NEMO to sT is currently unclear. It is conceivable that the presence of PP4C-PP4R1 results in a conformational change in either protein allowing the formation of the protein complex. Alternatively, we have not yet explored the binding requirements of NEMO using a similar direct binding assay. It is possible that only together do PP4C-PP4R1 interact directly with NEMO. Such experiments should be performed in the future to generate a clearer understanding of this protein complex.

#### **5.3.4 Direct interaction between MCPyV sT and PP2A isoforms.**

Interactions with the PP2A family of phosphatases are the hallmark of *Polyomaviridae* sT protein (Khalili et al., 2008, Cheng et al., 2009, Shuda et al., 2011, Griffiths et al., 2013, Kwun et al., 2015). The SILAC screen showed a potential interaction with both PP2A A $\alpha$  and PP2A A $\beta$ , and these interactions were confirmed by co-immunoprecipitations (Chapter 4 and Griffiths et al., 2013). Whilst the interaction with PP2A A $\alpha$  was discounted as necessary for NF- $\kappa$ B disruption due to the lack of phenotype observed with the R7A mutant (Griffiths et al., 2013), the broad scale truncation mutants used during this study were unable to distinguish between a role for PP4C and PP2A A $\beta$  in cells. However, use of dominant negative versions of PP4C gave a clear steer that this phosphatase was predominantly necessary for perturbation of NF- $\kappa$ B in our studies (Griffiths et al., 2013). Despite this, it was necessary to further understand the binding requirements for both isoforms of PP2A with sT *in vitro*. Both isoforms were able to interact directly with recombinant sT, although PP2A A $\beta$  interacted to a greater extent than

PP2A A $\alpha$ . These data mirror the SILAC proteomic results, which showed that PP2A A $\beta$  was a major binding partner of sT in cells. They also implicate PP2A A $\beta$  as a potential mediator of sT complex formation, given the *in vitro* binding.

### **5.3.6 Amino acids R102 and F103 in sT mediate the direct interactions with phosphatase sub-units *in vitro*.**

Our thorough mutagenesis approach identified residues in sT essential for interacting with a range of host binding partners including NEMO and the phosphatase sub-units in cells (Chapters 3 and 4). To further validate these results, we engineered two key mutants to allow recombinant expression in bacteria as GST fusions and compared their interactions with the panel of host proteins to wild type GST-sT. No GST-sT protein could interact with NEMO directly. Despite this, the mutants retained similar binding properties to those identified in cells and loss of R102 and F103 abrogated binding to PP4C and significantly reduced the interaction with PP4R1. Interestingly, both of these mutants retained a level of interaction with PP2A A $\beta$  that was greater than with either PP4C or PP4R1, mirroring data generated in cells. These *in vitro* data thus confirm our data generated from the cell-based co-immunoprecipitations in showing that we have generated a panel of mutants capable of discriminating between phosphatase binding partners. These mutants will be essential to allow a detailed study of which host partners are necessary for modulating cellular processes including modulation of NF- $\kappa$ B.

## Chapter 6. Contribution of PP4C-PP4R1 to the inhibition of NF- $\kappa$ B activation in MCPyV sT expressing cells

### 6.1 Introduction

Since signal transduction from activated receptors to NF- $\kappa$ B largely relies on phosphorylation events, phosphatases are expected to play a major role in the modulation and termination of NF- $\kappa$ B activity. Dephosphorylation of NF- $\kappa$ B can be accomplished by PP4C and PP4R1 in lymphocytes. These phosphatases have been shown to interact with NEMO and as a result dephosphorylate the IKK complex (Brechmann et al., 2012). Previous results demonstrated a direct interaction between MCPyV sT and PP4C-PP4R1, through which a complex is formed between sT and NEMO *in vitro*.

Studies described in this thesis have mapped the regions of each host binding partner with sT and have shown the importance of PP4C-PP4R1 for recruiting sT to NEMO *in vitro* (Chapter 5). In conjunction with the use of dominant negative forms of PP4C, we highlight the importance of PP4C for NF- $\kappa$ B signalling in sT expressing cells (Griffiths et al., 2013). Given the possible off-target impacts of dominant negative proteins, we now wished to confirm these results and also demonstrate the importance of PP4R1 for NF- $\kappa$ B regulation by depleting cells of both proteins using siRNA.

Given our observations of novel sT binding partners, we wished to extend our studies to determine whether interactions with these host proteins were unique to MCPyV or conserved amongst other human polyomavirus (e.g. BKPyV and JCPyV) and the paradigm PyV, SV40. Understanding the conservation of these interactions might give insight into conserved pathological processes.

## 6.2 Results

### 6.2.1 Validation of the efficiency of siRNA targeting PP4C.

Gene silencing of PP4C was performed using a series of previously validated oligonucleotide sequences targeting PP4C (Brechmann et al, 2012). The level of knockdown of endogenous PP4C in MCC13 cells transfected with 2  $\mu$ M of the siRNA-PP4C (#1, #2 or #3) was assessed by Western blot. Scrambled siRNA (siCtrl) was used as a negative control. Cells were harvested 48h post-transfection and the expression level of endogenous PP4C was assessed by Western blotting and densitometry. The results indicated a detectable reduction in the level of endogenous PP4C with each siPP4C compared with siCtrl. The most potent was siPP4C #3 (GGCCAGAGAGAUCUUGGUAUU), which showed a approximate 5 fold reduction in PP4C expression (Figure 6.1). GAPDH was used for protein loading control and was unaffected by the presence of the siRNA.

### 6.2.2 Validation of siRNA PP4R1 efficacy

In addition to PP4C, we also wished to understand the contribution of PP4R1 to the NF- $\kappa$ B inhibition. Accordingly, PP4R1 silencing experiments were performed in parallel using three oligo sequences of siRNA-PP4R1 (#1, #2 and #3). MCC13 were transfected with 2  $\mu$ M of the siPP4R1 for 48h to knock down the PP4R1 expression in the cells. SiCtrl was used as a negative control. Validation of the expression level of PP4R1 was detected by SDS-PAGE and Western blot of endogenous protein using a PP4R1 antibody. The result showed a reduction in PP4R1 expression level with each siPP4R1 in comparison with the negative control. PP4R1 #3 (GGAUAGGUGUUCUUAACATT) yielded the best knock down efficacy of approximately 2.5 fold (Figure 6.2). Protein loading was controlled by the detection of GAPDH.

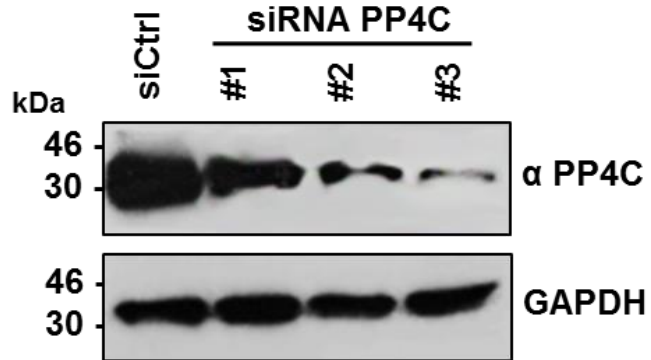
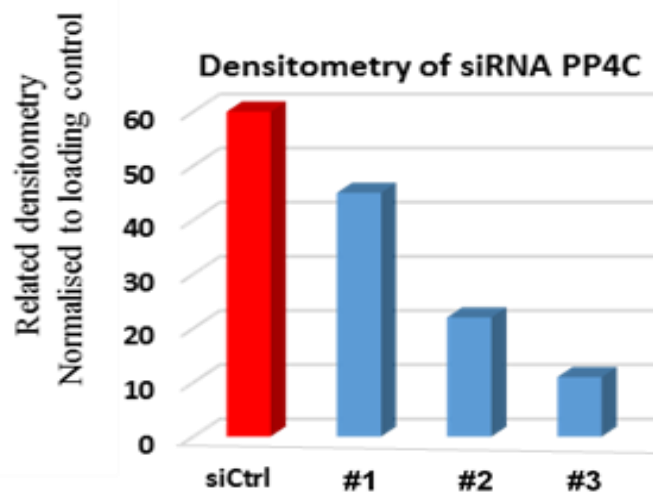
**A****B**

Figure 6.1: Alteration of cellular protein expression by using siRNA of PP4C **(A)** Western blot of cellular protein expression in MCC13. Cells were transfected with control siRNA or three different siPP4C #1, #2 or #3. After 48 h, the cellular lysates were analysed by immunoblotting using appropriate antibodies for endogenous PP4C. Marker in kDa. **(B)** Densitometry quantification of the Western blots was carried out using Image J software and is shown as a percentage of relative densitometry normalized to the loading control GAPDH (n = 3).

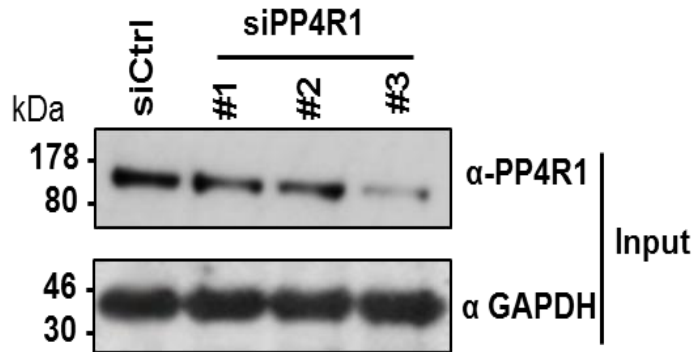
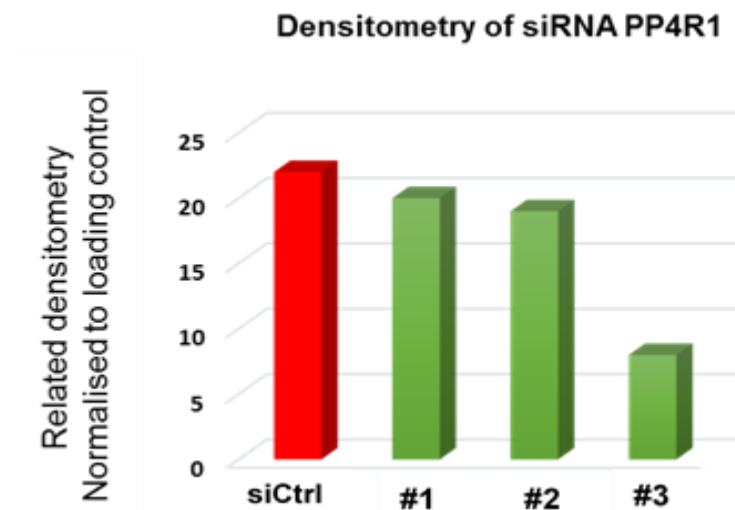
**A****B**

Figure 6.2: Alteration of cellular protein expression by using siRNA of PP4R1. **(A)** Western blot of cellular protein expression in MCC13. Cells were transfected with control siRNA or three different siPP4R1 (#1, #2 or #3). After 48 h, the cellular lysates were analysed by immunoblotting using endogenous PP4C antibody. Marker in kDa. **(B)** Densitometry quantification of the western blots was carried out using Image J software and is shown as a percentage of relative densitometry normalized to the loading control GAPDH (n = 3).

### **6.2.3 Co-immunoprecipitation of MCPyV sT with cellular proteins during PP4C silencing.**

In order to understand the role of the PP4C-PP4R1 complex in MCPyV sT targeting of the NF- $\kappa$ B complex, co-immunoprecipitation of MCPyV sT with NEMO was performed during knock down of PP4C. MCC13 cells were cotransfected with sT and 2  $\mu$ M of siPP4C #3, which was shown to be the most effective siRNA. Cells were lysed 48 h after transfection. The expression of PP4C and other target proteins were validated by Western blot prior to co-immunoprecipitation. A reduction in PP4C expression was observed (Figure 6.3A). Co-immunoprecipitations of pEGFP-sT with endogenous PP4C, PP4R1, NEMO and exogenous EE-PP2A A $\beta$  were performed using GFP-TRAP beads. Protein complexes were assessed by SDS-PAGE and Western blotting with appropriate antibodies. The assay showed that sT retained a low level interaction with PP4C during the knock down (Figure 6.3C). This is likely mediated by the residual PP4C present. PP4R1, NEMO and PP2A A $\beta$  retained their interaction with sT.

### **6.2.4 Co-immunoprecipitation of MCPyV sT with cellular proteins during silencing of PP4 R1.**

Previous co-immunoprecipitations of PP4R1-NEMO (Figure 5.5) and PP4R1-PP4C (Figure 5.6) demonstrated possible association in protein complexes. To understand the necessity for PP4R1 in this complex formation with sT, co-immunoprecipitations of sT with the target cellular proteins were performed after silencing of PP4R1. MCC13 cells were cotransfected with pEGFP-sT and 2  $\mu$ M of siPP4R1 #3 and cells were lysed 48h after transfection. The expression of PP4R1 and other target proteins was confirmed prior to co-immunoprecipitation. A reduction in PP4R1 expression was demonstrated (Figure 6.4A). Co-immunoprecipitation of pEGFP-sT with endogenous PP4R1, PP4C, NEMO and exogenous EE-PP2A A $\beta$  was performed by GFP-TRAP beads. Protein complex was assessed by SDS-PAGE and Western blotting with appropriate antibodies. The blots showed

that the interaction was lost between PP4R1 and sT in depleted cells. Interestingly, both protein phosphatases PP4C and PP2A A $\beta$  retained an interaction with sT in PP4R1 depleted cells. In contrast NEMO failed to be precipitated by EGFP-sT in PP4R1 depleted cells, suggesting that PP4R1 is essential for the sT-NEMO interaction in cells (Figure 6.4).

### **6.2.5 Specificity of host binding partners amongst PyV sT proteins.**

Studies reported in this thesis and in publications from our group (Griffiths et al., 2013; Knight et al., 2015) demonstrate the importance of interactions with NEMO and a number of host phosphatases for MCPyV pathogenesis. To address whether these interactions are unique to MCPyV or conserved amongst the *Polyomaviridae*, sT sequences were amplified from a limited number of PyV and cloned into pEGFP-C1 for expression in mammalian cells. Sequences were amplified from the two major human PyV, BKPyV and JCPyV and the paradigm PyV, SV40. Cloned sequences were verified and plasmids were co-transfected into HEK293 cells in combination with FLAG-PP4C, HA-PP4R1, EE-PP2A A $\alpha$  and EE-PP2A A $\beta$ . Prior to co-immunoprecipitation studies, the expression levels of each exogenous protein were verified by Western blotting (Figure 6.5A). Co-immunoprecipitations were performed using GFP-Trap beads and precipitates analysed by Western blotting with appropriate antibodies. The results demonstrate that MCPyV sT was able to interact with the panel of identified proteins, as previously described. Consistent with the published literature, all PyV sT bound PP2A A $\alpha$ , whereas only MCPyV sT could interact with PP2A A $\beta$ , PP4R1 and NEMO (Figure 6.5B). Surprisingly, SV40 sT was also able to interact with PP4C, although BKPyV and JCPyV could not. At the time this was the first observed interaction between SV40 sT and PP4C, although others have now confirmed this (Kwun et al., 2015). Despite the interaction with PP4C, SV40 sT was not able to interact with NEMO or PP4R1 (Figure 6.5B). In conclusion, whilst SV40 sT could also interact with PP4C, interactions with PP4R1 and NEMO are not conserved amongst the human PyV sT tested.



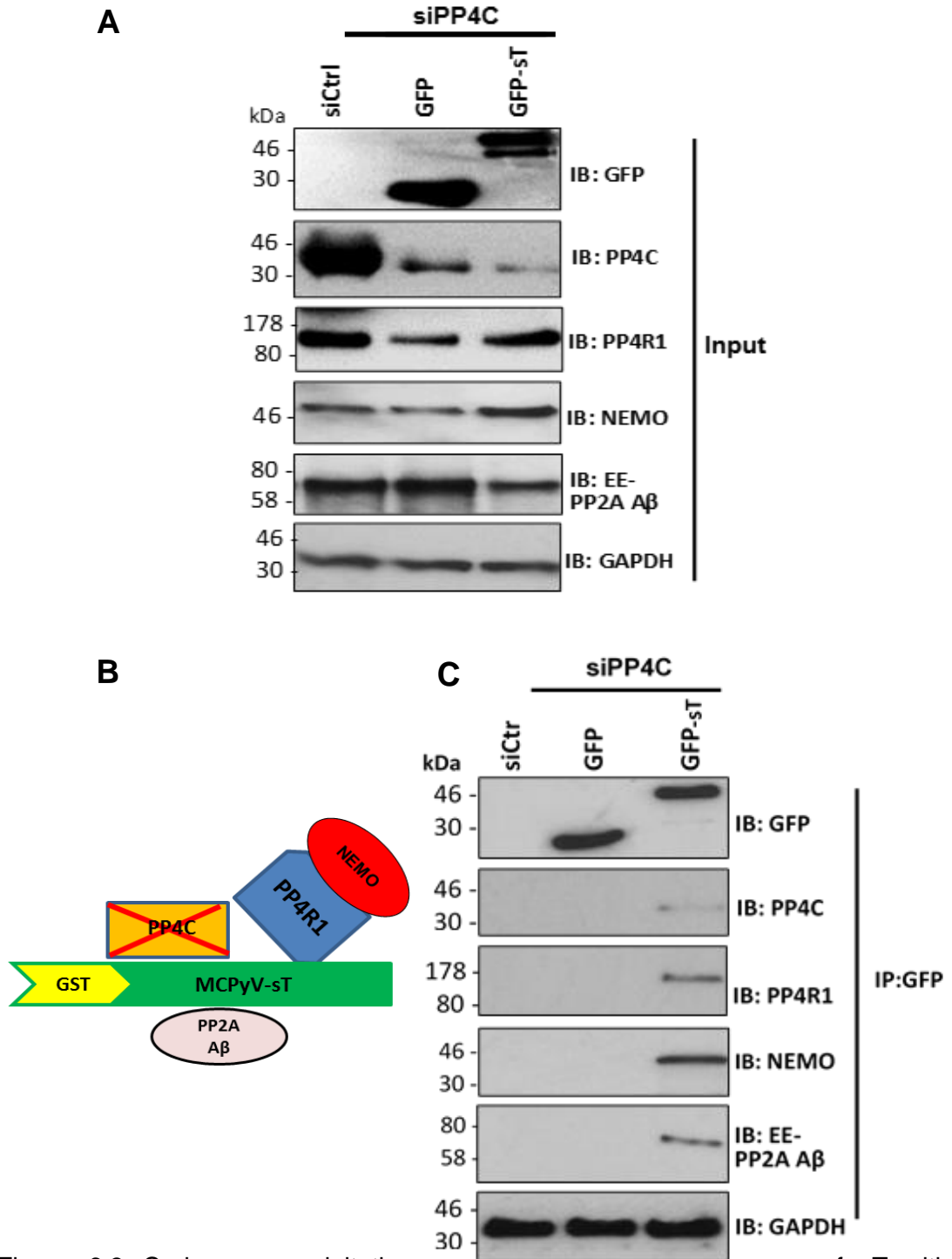


Figure 6.3 Co-immunoprecipitation of sT with target cellular proteins during PP4C silencing. Cells were cotransfected with siPP4C and pEGFP-sT then lysed after 48h. Co-immunoprecipitation was performed between sT and the endogenous proteins listed in right side. GFP-TRAP beads was used to precipitate pEGFP-sT and the immune complex was resolved by SDS-PAGE and probed with appropriate antibodies. **(A)** Alteration of cellular protein expression in knock down of PP4C. **(B)** Schematic representation of sT and PP4R1, NEMO and PP2A A $\beta$ . Knock down of PP4C. **(C)** Co-immunoprecipitation of sT with endogenous target cellular proteins. GFP was used as a control and GAPDH for protein loading control. Representative blot are shown. Marker in kDa.

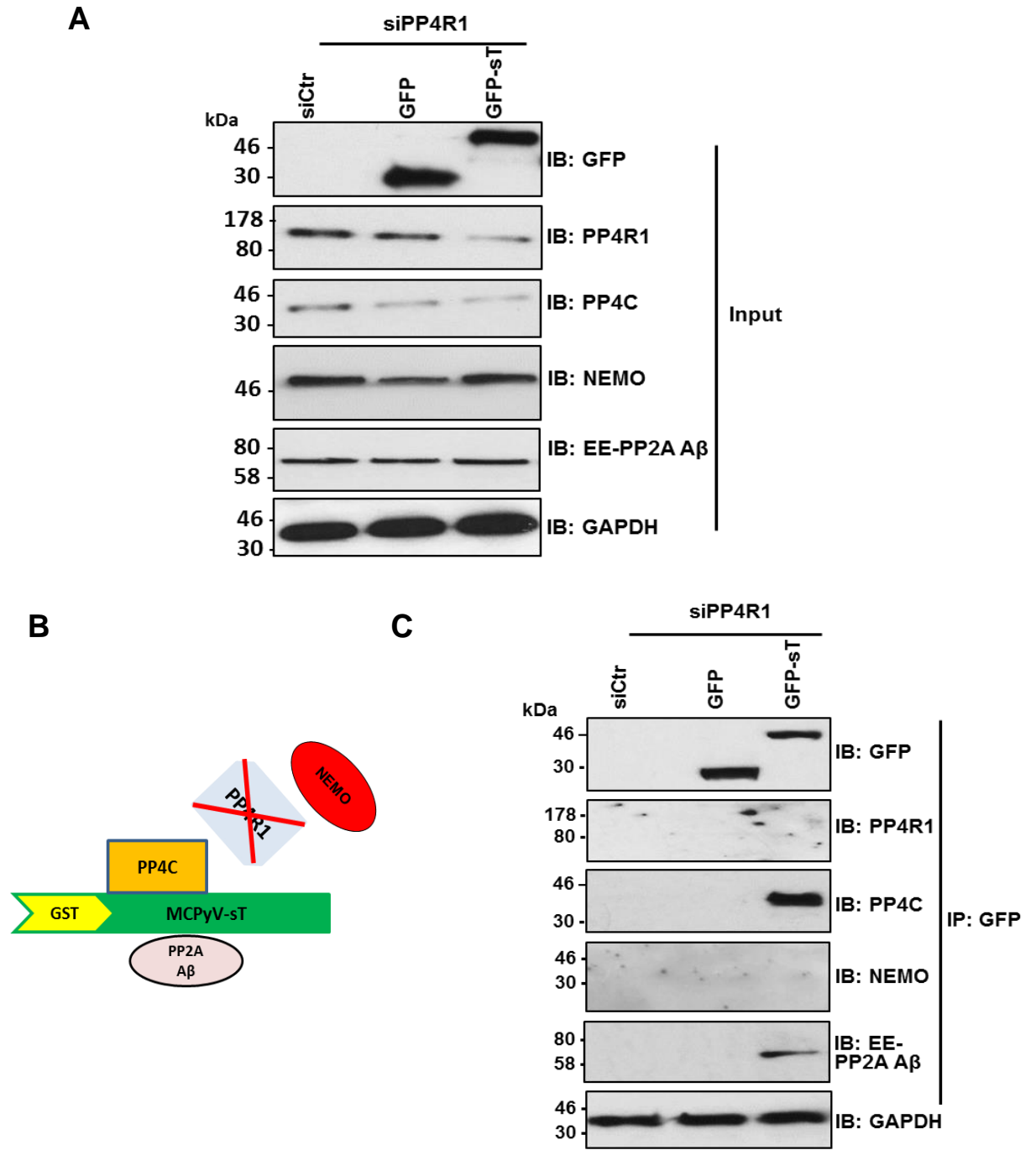


Figure 6.4 Co-immunoprecipitation of sT with target cellular proteins during knock down of PP4R1. Cells were cotransfected with siPP4C and pEGFP-sT then lysed after 48h incubation. Co-immunoprecipitation was performed between sT and the endogenous proteins that listed in right side. GFP-TRAP beads was used to precipitate pEGFP-sT. The immune complex was resolved by SDS-PAGE and probed with appropriate antibodies **(A)** Alteration of cellular protein expression in knock down of PP4R1. **(B)** Schematic representation of sT and PP4C, NEMO and PP2A A $\beta$ . Knock down of PP4R1. **(C)** Co-immunoprecipitation of sT with

endogenous target cellular proteins. GFP was used as a control and GAPDH for protein loading control. Representative blot are shown. Marker in kDa.

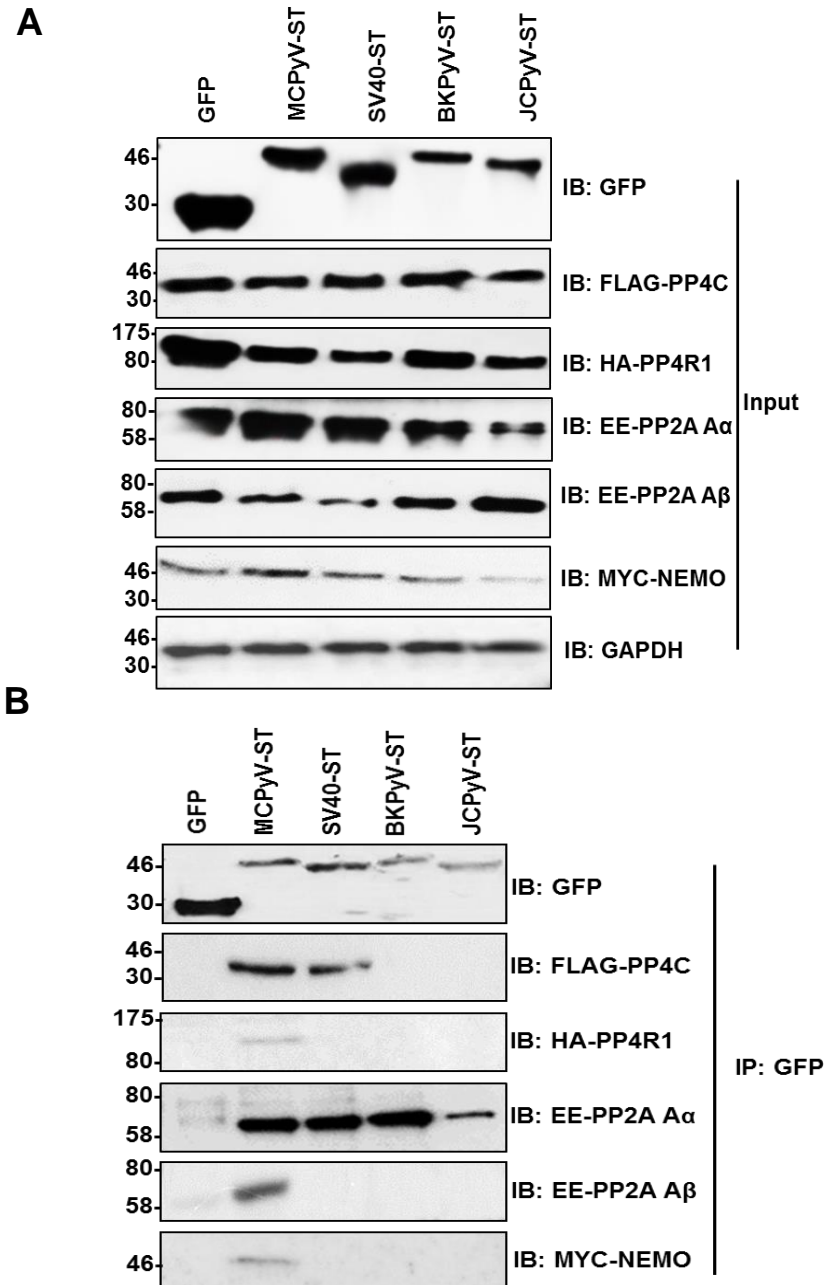


Figure 6.5 Interaction of MCPyV sT and other polyomavirus sT with target proteins. **(A)** Expression of GFP tagged MCPyV sT, SV40 sT, BKV sT and JCV sT. HEK 293 cells were co-transfected with one of polyomaviruses sT and one of cellular protein (listed in right side). Cells were harvested 24h post transfection and expressions were detected by SDS PAGE and probed by appropriate antibody. **(B)** Co-immunoprecipitation of sTs with cellular proteins. Cellular lysate was incubated 2h with GFP-Trap beads to precipitate GFP-sT. Binding proteins were detected by probing with appropriate antibodies. GFP was used as a control and GAPDH for protein loading control. Representative blot are shown.

## 6.3. Discussion

### 6.3.1 PP4R1 is essential for the interaction with NEMO in cells.

Previous studies to test the importance of protein phosphatases in modulation of NF- $\kappa$ B and Merkel cell migration had relied on the over-expression of dominant active and negative forms of each enzyme (Griffiths et al., 2013; Knight et al., 2015). Whilst this approach provides useful information, there are possible off-target effects. It was necessary to deplete cells of PP4C and PP4R1 in order to understand their contribution to the sT-NEMO complex formed in cells. A number of oligonucleotides were generated from the literature and tested for their abilities to knock-down target protein expression (Chowdhury et al., 2008, Brechmann et al, 2012). In both cases, the siRNA with the optimal level of knock-down was taken for further analysis. Co-immunoprecipitation of pEGFP-sT with endogenous host targets was performed in cells depleted of either PP4C or PP4R1. Interestingly, knockdown of PP4C did not prevent the interaction between sT and NEMO, or the interaction with PP2A A $\beta$ . This either means that in cells PP4C is not essential for the observed interaction with NEMO or that despite a significant reduction in PP4C levels, there was still sufficient protein present to function as a molecular bridge. A greater range of knock-down conditions will need to be tested to ascertain which of these is correct. In contrast, depletion of PP4R1 prevented the interaction with NEMO in cells whilst maintaining the interactions with PP4C and PP2A A $\beta$ . These results indicate that PP4R1 is critical for the interaction with NEMO in cells but is not needed for sT binding to either PP4C or PP2A A $\beta$ . **However the presence of PP4R1 alone is not enough to link MCPyV sT with NEMO as shown in the direct interaction result (Figure 5.10). It also raises a question of whether another protein complex plays a role in this interaction, like IKK catalytic subunits, especially since PP4R1 serves as a scaffold between NEMO and PP4C and links the complex with IKK $\beta$  (Brechmann et al, 2012).** Significant additional experiments would require an analysis of NF- $\kappa$ B-driven gene expression in cells transfected with sT that have been depleted of either

PP4C, PP4R1 or both, to determine whether loss of either protein impairs the inhibitory abilities of sT.

### **6.3.2 MCPyV sT binds to a unique range of host proteins associated with immune evasion.**

Virus pathogenesis can, in part, be traced to the its interactome with host proteins and the range of cellular processes that these interactions modulate. It was of great interest to determine whether the interactions observed for MCPyV sT with NEMO and the panel of phosphatase subunits was conserved amongst other human PyV, which have also been shown to be significant pathogens. Cloning issues limited this analysis to three other PyV sT. Efforts focussed on BKPyV and JCPyV as they are the best understood human PyV. We also studied SV40 since this virus is a paradigm for sT function. Our studies confirmed the promiscuous interactions between sT from all PyV studied and PP2A A $\alpha$ . In contrast PP2A A $\beta$  was only bound by MCPyV sT. Our finding fits with previous studies, which have shown that SV40 does not interact with this isoform of PP2A, whereas murine PyV sT can interact with PP2A A $\beta$  and use this interaction to deregulate the AKT pathway (Hwang et al., 2013). In addition, only MCPyV and SV40 sT were found to bind to PP4C. This finding was recently confirmed by Kwun and colleagues (2015). Despite being able to interact with PP4C, SV40 sT did not bind to either PP4R1 or NEMO in cells. Indeed, these two proteins only interacted with MCPyV sT. This observation provides further evidence that the interaction with PP4R1 is more important for bridging sT to NEMO given that SV40 sT binds to PP4C but does not interact with NEMO. These data would suggest that MCPyV might be unique in its ability to inhibit the IKK complex, **since phosphorylation activity of IKK $\alpha$  and IKK $\beta$  was decreased during sT expression and this will induce I $\kappa$ B phosphorylation leading to a block in translocation of NF- $\kappa$ B into the nucleus (Griffith et al., 2013). A similar mechanism has been detected in other viruses like CMV and MCV through targetting NEMO to disrupt IKK activation. The interaction of SV40 with PP4C also raises the question of the role of PP4C in the SV40 life cycle.**

Unlike MCPyV, there is a robust life cycle model for SV40 and an exciting project might entail an analysis of the effect of depleting PP4C from cells or expressing a dominant active mutant of the enzyme. Finally, here we just studied the interaction of sT of some other polyomaviruses with targeted proteins and we think its worth to study the contribution of other polyomaviruses with NF- $\kappa$ B in detailes which has not been previously addressed.

## Chapter 7. Summary and conclusion

The work described in this thesis contributed to a multi-group research programme aimed at increasing our understanding of the role of the small tumour (sT) antigen in MCPyV pathogenesis. It focussed on uncovering the molecular mechanisms by which sT inhibited NF- $\kappa$ B mediated signal transduction. **This study showed that specific amino acids in MCPyV sT are required for interaction with NEMO and mediated NF- $\kappa$ B inhibition. This inhibition effect was shown to be controlled by targeting of sT to phosphatase enzymes like PP4C, PP2A A $\beta$  and PP4R1.**

Modulation of NF- $\kappa$ B signalling was initially identified using a transcriptomic array protocol that measured levels of gene expression in an inducible FLAG-sT cell line. In cells inducibly expressing FLAG-sT, a significant reduction in NF- $\kappa$ B-driven gene expression was observed (Griffiths et al., 2013). These results were subsequently confirmed using a luciferase reporter assay system with GFP-sT (Chapter 3). A proteomic approach was adopted to identify possible host candidate binding partners that might be necessary for mediating the inhibition of NF- $\kappa$ B. Whilst this approach identified a number of host partners, the results were inconclusive in that they did not identify proteins within the NF- $\kappa$ B pathway. An alternative screening approach was adopted, based on over-expression of GST-fusions of proteins from the canonical NF- $\kappa$ B pathway. This method tentatively revealed an interaction with the NEMO adaptor component of the central IKK complex, which is essential for NF- $\kappa$ B activation in response to a number of stimuli, including virus infection. The goal of the work in this thesis was to understand the contribution of the interaction with NEMO for inhibition of NF- $\kappa$ B. Binding of MCPyV sT to NEMO was confirmed by co-immunoprecipitation in MCC13 cells. MCC13 cells are a MCPyV negative MCC cell line and as such are a physiologically relevant cell line of choice. This is particularly important given that primary Merkel cells are extremely difficult to source and appropriate life cycle models for the study of MCPyV are not yet available. **However, during preparation of the final version of this**

thesis, a human dermal fibroblast cell line that support the cultivation of MCPyV was described (Liu et al., 2016). This should develop our understanding of virus interference with the NF- $\kappa$ B pathway and confirm whether interaction of MCPyV sT with NEMO is required for NF- $\kappa$ B inhibition.

After the co-immunoprecipitation was confirmed the interaction between MCPyV sT and NEMO, a substantial mapping exercise was performed, using a large number of truncation and point mutants of both proteins. In particular it was necessary to identify point mutations in sT that would ablate the binding to NEMO. Such point mutants have previously been developed to prevent interaction with other cellular partners of sT (Shuda et al., 2011). These have proven effective at understanding the contribution of specific host proteins to known sT functions. My mutagenesis studies revealed that three point mutants within sT ablate (A101, R102 and F103) were necessary for the interaction with NEMO.

Reciprocal experiments were performed to identify the domains of NEMO that are necessary for the interaction with sT. NEMO contains a number of well-studied domains, each responsible for interacting with host binding partners necessary for mediating the activation, and regulation, of NF- $\kappa$ B signalling (Rushe et al., 2008, Cordier et al., 2008, Fusco et al., 2008, Grubisha et al., 2010, Emmerich et al., 2013, Zilberman-Rudenko et al., 2016). Truncations were designed to specifically target these key domains within NEMO. Interestingly, truncations studied showed that the UBAN domain was necessary and sufficient for mediating the interaction with sT in cells. Recently, this domain has been shown to be essential for interacting with ubiquitin moieties, allowing the recruitment of the IKK complex to upstream kinase complexes. The essential nature of the UBAN domain was recognised when specific mutations in this region were linked to a number of immunodeficiency disorders (Vinolo et al. 2006, Hubeau et al., 2011, Zilberman-Rudenko et al., 2016). To address whether the ubiquitin binding properties of UBAN might be necessary for the sT-NEMO interaction, a number of disease-associated point mutants were engineered into NEMO. Abrogation of ubiquitin binding resulted in a loss of sT binding in cells.

Whether this is suggestive of sT interacting with ubiquitin, or ubiquitinated proteins is not currently clear. It is possible that loss of ubiquitin binding alters the sub-cellular localisation of NEMO and prevents sT binding. To address this, future studies would need to address whether sT (or sT-associated proteins) can interact with the forms of ubiquitin bound by the UBAN (linear and K-63 linked). We found that the MCPyV sT abrogated its interaction with the mutant D311N of NEMO. This mutation has been detected in people who have severe EDA-ID as a result of NF- $\kappa$ B inhibition. Future studies will be required to determine the specificity of the amino acid D311 in its interaction with sT, along with more analysis of the NEMO domain which is involved in interaction of NEMO with sT.

Interaction studies with recombinant GST-sT and IVT produced host partners revealed the surprising observation that NEMO does not interact directly with sT, and that the interactions observed by co-immunoprecipitation assays must be as a result of a larger protein complex (Chapter 5). In spite of the fact that sT failed to bind NEMO in IVT and the SILAC assay also confirmed this result, we highly recommend the isolation of both NEMO and MCPyV sT in bacteria to exclude the interference of proteins that are present in the IVT system.

To address whether sT required other proteins for interaction with NEMO, we focussed attention on other proteins identified from our proteomic screen. In keeping with other PyV sT, we identified a number of potential host phosphatases as putative binding partners. One of these, PP2A A $\alpha$ , had previously been shown to interact with sT (Shuda et al., 2011), whilst the others were novel (PP2A A $\beta$  and PP4C). Given the importance of phosphatases for sT function in other PyV, we set out to characterise the requirements for their interaction with sT. A single point mutant (R7A) had previously been shown to abrogate the interaction between sT and PP2A A $\alpha$  (Shuda et al., 2011). This mutant thus became a control in our assays. Importantly, introduction of this amino acid change did not prevent sT binding to the other phosphatases tested. Rather, we once again demonstrated the importance of residues 102-103 for mediating binding to PP4C. These

studies allowed the development of point mutants that discriminated between the different phosphatase binding partners. This is an important development, given that previous studies from our group (Griffiths et al., 2013; Knight et al., 2015) had shown that these enzymes are important for sT function but had not been able to provide the identity of the specific host binding partners. Instead, our studies had resorted to the use of dominant active/negative forms of each phosphatase, which could potentially have off target effects. The development of these mutants will now allow an interrogation of the specific requirements of each phosphatase in sT function. Future studies could examine the interaction of sT with cellular proteins in human dermal fibroblasts using both MCPyV pseudovirus carrying a GFP reporter and MCPyV virions produced through cotransfection of sT expression plasmids (Liu et al., 2016). Then we can use coimmunoprecipitation assays to probe for sT with a mouse monoclonal antibody that is specific for MCPyV sT (CM5E1 isotype), and detect any proteins partners using specific antibodies.

Given that PP4C has been functionally linked to the NF- $\kappa$ B pathway (Tikhonova and Aifantis 2012, Brechmann et al, 2012) in its ability to dephosphorylate IKK complex and as a result stop I $\kappa$ B phosphorylation and turn off the pathway. We hypothesised that PP4C may bridge sT with NEMO. In contrast, despite demonstrating that PP4C is a direct binding partner of sT in vitro, in our hands the presence of PP4C was not enough to rescue the interaction between sT and NEMO. These data were highly suggestive of the need for an additional binding partner in this protein complex that would link sT with NEMO. Here we suggest confirming this result by using protein-protein interaction techniques other than IVT, like the yeast two hybrid screening (Y2H) or visualizing the MCPyV sT structure at the atomic level by X-ray crystallography which we think is essential for and will enhance our understanding of how sT interacts with cellular proteins.

An obvious target was the PP4 subunit, PP4R1, which had previously been shown to be required for negative regulation of NF- $\kappa$ B activation in T cells, through an interaction with the IKK complex. This study provided the first

evidence for PP4R1 as a novel sT binding partner (Chapter 5), and confirmed that in MCC13 cells PP4R1 was able to bind to both NEMO and PP4C. Moreover, mutagenesis mapping showed that the interaction was dependent on residues 102-103 in sT, which are the same as those needed to bind to NEMO. However, despite being a direct binding of sT, PP4R1 alone was not enough to rescue the interaction with NEMO *in vitro*. Instead, a trimeric complex is necessary, consisting of PP4C, PP4R1 and sT, to bridge sT to NEMO. The stoichiometry of this interaction is not clear, nor is the mechanism by which all proteins interact with such a small region of sT. It is plausible that there are distinct populations of sT, each binding either PP4C or PP4R1, and that a multi-protein complex forms to link with NEMO. Certainly, high molecular weight complexes consisting of multimers of the same proteins are common in inflammatory signalling pathways, and NF- $\kappa$ B activation. The nature of this complex also would need to be studied further. In the shorter term, a crucial experiment that would reinforce the importance of PP4C/PP4R1 in bridging NEMO to sT would involve performing co-immunoprecipitations with the NEMO mutations that abrogate sT binding with PP4C and PP4R1 to test if these prevent their recruitment. In the studies presented we did not test whether PP2A A $\beta$  was necessary for mediating the interaction with NEMO, despite also identifying it as a direct binding partner of sT. This was a conscious decision based on the results of the direct binding assay with sT point mutants. In these assays, mutants that abrogate binding to NEMO in cells retained binding to PP2A A $\beta$ , albeit at reduced levels, *in vitro*. Given that a role for PP2A A $\beta$  in MCPyV pathogenesis is not clear, future studies will need to focus on the contribution this phosphatase plays to the virus. This is particularly important given the link between this phosphatase and cancer.

Much of this thesis involved the characterisation of proteins interactions in cells or *in vitro*. Whilst this is informative, it is critical that it is linked with a functional analysis of these interactions. Towards this end, the final chapter sought to determine whether the interactions observed *in vitro* had impact on the inhibition of NF- $\kappa$ B by MCPyV sT. A dual approach was undertaken consisting of sT mutants in reporter assays and siRNA depletion of

PP4C/PP4R1 to observe the impact on protein complex formation. Interestingly, knockdown of PP4C did not prevent the interaction between sT and NEMO, or the interaction with PP2A A $\beta$ . This either means that in cells PP4C is not essential for the observed interaction with NEMO or that despite a significant reduction in PP4C levels, there was still sufficient protein present to function as a molecular bridge. A greater range of knock-down conditions **either by using different siRNAs or by utilising CRISPR/Cas system will be needed** to be tested to ascertain which of these is correct. In contrast, depletion of PP4R1 prevented the interaction with NEMO in cells whilst maintaining the interactions with PP4C and PP2A A $\beta$ . These results indicate that PP4R1 is critical for the interaction with NEMO in cells but is not needed for sT binding to either PP4C or PP2A A $\beta$ . Significant additional experiments would require an analysis of NF- $\kappa$ B-driven gene expression in cells transfected with sT that have been depleted of either PP4C or PP4R1, to determine whether loss of either protein impairs the inhibitory abilities of sT.

The luciferase data affirmed the importance of the sT-binding partners in down-regulating NF- $\kappa$ B. Point mutations in sT that abrogated the interaction with PP4R1 and NEMO were less able to impair NF- $\kappa$ B-driven transcription compared to wild-type and mutants that had no impact on binding. Whilst none of the mutants rescued luciferase levels to those of the GFP control, the differences were statistically significant. A more relevant experiment that would shed light on the true impact of these mutations would be to analyse levels of endogenous NF- $\kappa$ B-driven gene expression in response to inflammatory stimuli, for example IL-8 or CCL20. These would be less prone to potential reporter associated artefacts.

It is clear that MCPyV sT has a number of unique functions amongst the PyV encoded sT (Johnson, 2010, Shuda et al., 2011, Griffith et al., 2013, Spurgeon et al., 2015, Kwun et al., 2015). Given the number of novel binding partners identified during this work, we were interested to discover whether any were shared amongst the PyV or were unique to MCPyV. Towards this, we cloned sT from a limited number of human PyV (BPyVK and JCPyV) and

the paradigm PyV, SV40. Our results reinforce the notion that MCPyV sT performed unique functions, and utilises a novel set of host binding partners to accomplish this. JCPyV and BKPyV sT bound to PP2A A $\alpha$  but failed to interact with any of the other host proteins identified in this study. Interestingly, SV40 sT also interacted with PP4C, and this was confirmed by a study published during this work (Kwun et al, 2015). Despite this interaction, SV40 sT failed to bind NEMO or PP4R1. Given that SV40 sT does not share sequence similarity with the region of MCPyV sT required to bind to PP4C, it is possible that a distinctive region of SV40 sT is necessary for mediating the interaction. Future work could focus on mapping the regions necessary for binding and using siRNA depletion of PP4C, or expressing a dominant active mutant of the enzyme, to test its requirement during the SV40 life cycle. It would also be worth expanding the range of sT tested to include other known human PyV (e.g. KIPyV and WUPyV) to see if binding is conserved. Given the recent expansion of phylogenetic knowledge of MCPyV-related PyV, these studies could even be expanded to some non-human PyV to see if binding to these host proteins is associated with a subgroup of PyV.

In conclusion, work presented in this thesis demonstrates that MCPyV sT mediates NF- $\kappa$ B inhibition by targeting NEMO with the involvement of PP4C and PP4R, which likely form a multi-protein complex with NEMO in cells. These studies shed light on the immune evasion mechanism utilised by MCPyV, and provide novel insights into the role of PP4C-PP4R1 in the control of NF- $\kappa$ B during MCPyV expression.

## Bibliography

- ABEND, J. R., JOSEPH, A. E., DAS, D., CAMPBELL-CECEN, D. B. & IMPERIALE, M. J. 2009. A truncated T antigen expressed from an alternatively spliced BK virus early mRNA. *Journal of General Virology*, 90, 1238-1245.
- AFANASIEV, O. K., YELISTRATOVA, L., MILLER, N., NAGASE, K., PAULSON, K., IYER, J. G., IBRANI, D., KOELLE, D. M. & NGHIEM, P. 2013. Merkel polyomavirus-specific T cells fluctuate with merkel cell carcinoma burden and express therapeutically targetable PD-1 and Tim-3 exhaustion markers. *Clinical Cancer Research*, 19, 5351-5360.
- AGELLI, M. & CLEGG, L. X. 2003. Epidemiology of primary Merkel cell carcinoma in the United States. *Journal of the American Academy of Dermatology*, 49, 832-841.
- AGOU, F., COURTOIS, G., CHIARAVALLI, J., BALEUX, F., COÏC, Y. M., TRAINCARD, F., ISRAËL, A & VÉRON, M. (2004). Inhibition of NF- $\kappa$ B activation by peptides targeting NF- $\kappa$ B essential modulator (nemo) oligomerization. *Journal of Biological Chemistry*, 279(52), 54248-54257.
- ALBORES-SAAVEDRA, J., BATICH, K., CHABLE-MONTERO, F., SAGY, N., SCHWARTZ, A. M. & HENSON, D. E. 2010. Merkel cell carcinoma demographics, morphology, and survival based on 3870 cases: a population based study. *Journal of cutaneous pathology*, 37, 20-27.
- ALLANDER, T., ANDREASSON, K., GUPTA, S., BJERKNER, A., BOGDANOVIC, G., PERSSON, M. A., DALIANIS, T., RAMQVIST, T. & ANDERSSON, B. 2007. Identification of a third human polyomavirus. *Journal of virology*, 81, 4130-4136.
- ANDRABI, S., HWANG, J. H., CHOE, J. K., ROBERTS, T. M., & SCHAFFHAUSEN, B. S. (2011). Comparisons between murine polyomavirus and Simian virus 40 show significant differences in small T antigen function. *Journal of virology*, 85(20), 10649-10658.
- ANEST, V., COGSWELL, P. C. & BALDWIN, A. S. 2004. I $\kappa$ B kinase  $\alpha$  and p65/RelA contribute to optimal epidermal growth factor-induced c-fos gene expression independent of I $\kappa$ B $\alpha$  degradation. *Journal of Biological Chemistry*, 279, 31183-31189.
- ARIAS, C., WALSH, D., HARBELL, J., WILSON, A. C. & MOHR, I. 2009. Activation of host translational control pathways by a viral developmental switch. *PLoS Pathog* 2009;5:e1000334.
- ARNOLD, H. K. & SEARS, R. C. 2006. Protein phosphatase 2A regulatory subunit B56 $\alpha$  associates with c-myc and negatively regulates c-myc accumulation. *Molecular and cellular biology*, 26, 2832-2844.
- ARORA, R., SHUDA, M., GUASTAFIERRO, A., FENG, H., TOPTAN, T., TOLSTOV, Y., NORMOLLE, D., VOLLMER, L. L., VOGT, A. & DÖMLING, A. 2012. Survivin is a therapeutic target in Merkel cell carcinoma. *Science translational medicine*, 4, 133ra56-133ra56.
- AULT, G. S. & STONER, G. L. 1992. Two major types of JC virus defined in progressive multifocal leukoencephalopathy brain by early and late coding region DNA sequences. *The Journal of general virology*, 73, 2669-2678.
- AVDULOV, S., LI, S., MICHALEK, V., BURRICHTER, D., PETERSON, M., PERLMAN, D. M., MANIVEL, J. C., SONENBERG, N., YEE, D. & BITTERMAN, P. B. 2004. Activation of translation complex eIF4F is essential for the genesis and maintenance of the malignant phenotype in human mammary epithelial cells. *Cancer cell*, 5, 553-563.
- BABAKIR-MINA, M., CICCOCCHI, M., LO PRESTI, A., GRECO, F., PERNO, C. F. & CIOTTI, M. 2010. Identification of Merkel cell polyomavirus in the lower respiratory tract of Italian patients. *Journal of medical virology*, 82, 505-509.
- BACHMANN, J., KLEEFF, J., BERGMANN, F., SHRIKHANDE, S. V., HARTSCHUH, W., BÜCHLER, M. W. & FRIESS, H. 2005. Pancreatic metastasis of Merkel cell carcinoma and concomitant insulinoma: case report and literature review. *World J Surg Oncol*, 3, 58.

- BAEUERLE, P. A. & BALTIMORE, D. 1988. Activation of DNA-binding activity in an apparently cytoplasmic precursor of the NF- $\kappa$ B transcription factor. *Cell*, 53, 211-217.
- BAGNÉRIS, C., AGEICHIK, A. V., CRONIN, N., WALLACE, B., COLLINS, M., BOSHOFF, C., WAKSMAN, G. & BARRETT, T. (2008). Crystal structure of a vFlip-IKK $\gamma$  complex: insights into viral activation of the IKK signalosome. *Molecular cell*, 30(5), 620-631.
- BASITH, S., MANAVALAN, B., GOSU, V. & CHOI, S. 2013. Evolutionary, structural and functional interplay of the I $\kappa$ B family members. *PLoS One*, 8, e54178.
- BAYSAL, B. E., WILLETT-BROZICK, J. E., TASCHNER, P., DAUWERSE, J., DEVILEE, P. & DEVLIN, B. 2001. A high-resolution integrated map spanning the SDHD gene at 11q23: a 1.1-Mb BAC contig, a partial transcript map and 15 new repeat polymorphisms in a tumour-suppressor region. *European Journal of Human Genetics*, 9, 121-129.
- BECKER, J. C., HOUBEN, R., UGUREL, S., TREFZER, U., PFÖHLER, C. & SCHRAMA, D. 2009. MC polyomavirus is frequently present in Merkel cell carcinoma of European patients. *Journal of Investigative Dermatology*, 129, 248-250.
- BERETTA, L., GINGRAS, A., SVITKIN, Y., HALL, M. & SONENBERG, N. 1996. Rapamycin blocks the phosphorylation of 4E-BP1 and inhibits cap-dependent initiation of translation. *The EMBO journal*, 15, 658.
- BERNSTEIN, J., ADENIRAN, A. J., CAI, G., THEOHARIS, C. G., USTUN, B., BECKMAN, D., ASLANIAN, H. R. & HARIGOPAL, M. 2014. Endoscopic ultrasound-guided fine-needle aspiration diagnosis of merkel cell carcinoma metastatic to the pancreas. *Diagnostic cytopathology*, 42, 247-252.
- BERRIOS, C., JUNG, J., PRIMI, B., WANG, M., PEDAMALLU, C., DUKE, F., MARCELUS, C., CHENG, J., GARCEA, R. L. & MEYERSON, M. 2014. Malawi polyomavirus is a prevalent human virus that interacts with known tumor suppressors. *Journal of virology*, JVI. 02328-14.
- BHATIA, K., GOEDERT, J. J., MODALI, R., PREISS, L. & AYERS, L. W. 2010. Merkel cell carcinoma subgroups by Merkel cell polyomavirus DNA relative abundance and oncogene expression. *International Journal of Cancer*, 126, 2240-2246.
- BHATIA, S., AFANASIEV, O. & NGHIEM, P. 2011. Immunobiology of Merkel cell carcinoma: implications for immunotherapy of a polyomavirus-associated cancer. *Current oncology reports*, 13, 488-497.
- BIALASIEWICZ, S., LAMBERT, S. B., WHILEY, D. M., NISSEN, M. D. & SLOOTS, T. P. 2009. Merkel cell polyomavirus DNA in respiratory specimens from children and adults. *Emerging infectious diseases*, 15, 492.
- BICHAKJIAN, C. K., LOWE, L., LAO, C. D., SANDLER, H. M., BRADFORD, C. R., JOHNSON, T. M. & WONG, S. L. 2007. Merkel cell carcinoma: critical review with guidelines for multidisciplinary management. *Cancer*, 110, 1-12.
- BOFILL-MAS, S., RODRIGUEZ-MANZANO, J., CALGUA, B., CARRATALA, A. & GIRONES, R. 2010. Short report Newly described human polyomaviruses Merkel Cell, KI and WU are present in urban sewage and may represent potential environmental contaminants.
- BOLLAG, B., HOFSTETTER, C. A., REVIRIEGO-MENDOZA, M. M. & FRISQUE, R. J. 2010. JC virus small T antigen binds phosphatase PP2A and Rb family proteins and is required for efficient viral DNA replication activity. *PLoS One*, 5, e10606.
- BONIZZI, G. & KARIN, M. 2004. The two NF- $\kappa$ B activation pathways and their role in innate and adaptive immunity. *Trends in immunology*, 25, 280-288.
- BORCHERT, S., CZECH-SIOLI, M., NEUMANN, F., SCHMIDT, C., WIMMER, P., DOBNER, T., GRUNDHOFF, A. & FISCHER, N. 2014. High-affinity Rb binding, p53 inhibition, subcellular localization, and transformation by wild-type or tumor-derived shortened Merkel cell polyomavirus large T antigens. *Journal of virology*, 88, 3144-3160.
- BRECHMANN, M., Mock, T., Nickles, D., Kiessling, M., Weit, N., Breuer, R., ... & Booken, N. (2012). A PP4 holoenzyme balances physiological and oncogenic nuclear factor- $\kappa$ B signaling in T lymphocytes. *Immunity*, 37(4), 697-708.
- BRISSETT, A. E., OLSEN, K. D., KASPERBAUER, J. L., LEWIS, J. E., GOELLNER, J. R., SPOTTS, B. E., WEAVER, A. L. & STROME, S. E. 2002. Merkel cell carcinoma of the head and neck: a retrospective case series. *Head & neck*, 24, 982-988.

- BROEKEMA, N. M. & IMPERIALE, M. J. 2013. miRNA regulation of BK polyomavirus replication during early infection. *Proceedings of the National Academy of Sciences*, 110, 8200-8205.
- BUCHKOVICH, N. J., YU, Y., ZAMPIERI, C. A. & ALWINE, J. C. 2008. The TORrid affairs of viruses: effects of mammalian DNA viruses on the PI3K–Akt–mTOR signalling pathway. *Nature Reviews Microbiology*, 6, 266-275.
- BUCK, C. B., PHAN, G. Q., RAIJI, M. T., MURPHY, P. M., MCDERMOTT, D. H. & MCBRIDE, A. A. 2012. Complete genome sequence of a tenth human polyomavirus. *Journal of virology*, 86, 10887-10887.
- CALGUA, B., FUMIAN, T., RUSINOL, M., RODRIGUEZ-MANZANO, J., MBAYED, V. A., BOFILL-MAS, S., MIAGOSTOVICH, M. & GIRONES, R. 2013. Detection and quantification of classic and emerging viruses by skimmed-milk flocculation and PCR in river water from two geographical areas. *Water research*, 47, 2797-2810.
- CALIN, G. A., IASIO, M. G. D., CAPRINI, E., VORECHOVSKY, I., NATALI, P. G., SOZZI, G., CROCE, C. M., BARBANTI-BRODANO, G., RUSSO, G. & NEGRINI, M. 2000. Low frequency of alterations of the a (PPP2R1A) and b (PPP2R1B) isoforms of the subunit A of the serine-threonine phosphatase 2A in human neoplasms. *Oncogene*, 19, 1191-1195.
- CAMPANERO-RHODES, M. A., SMITH, A., CHAI, W., SONNINO, S., MAURI, L., CHILDS, R. A., ZHANG, Y., EWERS, H., HELENIUS, A. & IMBERTY, A. 2007. N-glycolyl GM1 ganglioside as a receptor for simian virus 40. *Journal of virology*, 81, 12846-12858.
- CARR, M. J., MCCORMACK, G. P., MUTTON, K. J. & CROWLEY, B. 2006. Unique BK virus non-coding control region (NCCR) variants in hematopoietic stem cell transplant recipients with and without hemorrhagic cystitis. *Journal of medical virology*, 78, 485-493.
- CARTER, J. J., DAUGHERTY, M. D., QI, X., BHEDA-MALGE, A., WIPF, G. C., ROBINSON, K., ROMAN, A., MALIK, H. S. & GALLOWAY, D. A. 2013. Identification of an overprinting gene in Merkel cell polyomavirus provides evolutionary insight into the birth of viral genes. *Proceedings of the National Academy of Sciences*, 110, 12744-12749.
- CARTER, J. J., PAULSON, K. G., WIPF, G. C., MIRANDA, D., MADELEINE, M. M., JOHNSON, L. G., LEMOS, B. D., LEE, S., WARCOLA, A. H. & IYER, J. G. 2009. Association of Merkel cell polyomavirus-specific antibodies with Merkel cell carcinoma. *Journal of the National Cancer Institute*.
- CARTER, R. S., GEYER, B. C., XIE, M., ACEVEDO-SUÁREZ, C. A. & BALLARD, D. W. 2001. Persistent activation of NF- $\kappa$ B by the tax transforming protein involves chronic phosphorylation of I $\kappa$ B kinase subunits IKK $\beta$  and IKK $\gamma$ . *Journal of Biological Chemistry*, 276, 24445-24448.
- CARTER, R. S., PENNINGTON, K. N., UNGURAIT, B. J., ARRATE, P. & BALLARD, D. W. 2003. Signal-induced ubiquitination of I $\kappa$ B kinase- $\beta$ . *Journal of Biological Chemistry*, 278, 48903-48906.
- CHANG, T. T., BEHSHAD, R., BRODELL, R. T. & GILLIAM, A. C. 2008. A male infant with anhidrotic ectodermal dysplasia/immunodeficiency accompanied by incontinentia pigmenti and a mutation in the NEMO pathway. *Journal of the American Academy of Dermatology*, 58, 316-320.
- CHANG, Y., CESARMAN, E., PESSIN, M. S., LEE, F., CULPEPPER, J., KNOWLES, D. M. & MOORE, P. S. 1994. Identification of herpesvirus-like DNA sequences in AIDS-associated Kaposi's sarcoma. *Science*, 266, 1865-1869.
- CHEN, G. I., TISAYAKORN, S., JORGENSEN, C., D'AMBROSIO, L. M., GOUDREAU, M. & GINGRAS, A.-C. 2008. PP4R4/KIAA1622 forms a novel stable cytosolic complex with phosphoprotein phosphatase 4. *Journal of Biological Chemistry*, 283, 29273-29284.
- CHEN, K. T. 1994. Merkel's cell (neuroendocrine) carcinoma of the vulva. *Cancer*, 73, 2186-2191.
- CHEN, I. T., Hsu, P. H., Hsu, W. C., Chen, N. J., & Tseng, P. H. (2015). Polyubiquitination of Transforming Growth Factor  $\beta$ -activated Kinase 1 (TAK1) at Lysine 562 Residue Regulates TLR4-mediated JNK and p38 MAPK Activation. *Scientific reports*, 5.
- CHEN, T., HEDMAN, L., MATTILA, P. S., JARTTI, T., RUUSKANEN, O., SÖDERLUND-VENERMO, M. & HEDMAN, K. 2011. Serological evidence of Merkel cell

- polyomavirus primary infections in childhood. *Journal of Clinical Virology*, 50, 125-129.
- CHEN, W., POSSEMATO, R., CAMPBELL, K. T., PLATTNER, C. A., PALLAS, D. C. & HAHN, W. C. 2004. Identification of specific PP2A complexes involved in human cell transformation. *Cancer cell*, 5, 127-136.
- CHEN, Y.-H., MACGREGOR, J., GOLDSTEIN, D. & HALL, M. 1979. Histone modifications in simian virus 40 and in nucleoprotein complexes containing supercoiled viral DNA. *Journal of virology*, 30, 218-224.
- CHENG, J., DECAPRIO, J. A., FLUCK, M. M., & SCHAFFHAUSEN, B. S. (2009). Cellular transformation by simian virus 40 and murine polyoma virus T antigens. In *Seminars in cancer biology* (Vol. 19, No. 4, pp. 218-228).
- CHIARAVALLI, J., FONTAN, E., FSIHI, H., COIC, Y. M., BALEUX, F., VÉRON, M., & AGOU, F. (2011). Direct inhibition of NF- $\kappa$ B activation by peptide targeting the NOA ubiquitin binding domain of NEMO. *Biochemical pharmacology*, 82(9), 1163-1174.
- CHO, U. S., MORRONE, S., SABLINA, A. A., ARROYO, J. D., HAHN, W. C. & XU, W. 2007. Structural basis of PP2A inhibition by small t antigen. *PLoS Biol*, 5, e202.
- CHO, U. S. & XU, W. 2007. Crystal structure of a protein phosphatase 2A heterotrimeric holoenzyme. *Nature*, 445, 53-57.
- CHOWDHURY, D., XU, X., ZHONG, X., AHMED, F., ZHONG, J., LIAO, J., DYKXHOORN, D. M., WEINSTOCK, D. M., PFEIFER, G. P. & LIEBERMAN, J. 2008. A PP4-phosphatase complex dephosphorylates  $\gamma$ -H2AX generated during DNA replication. *Molecular cell*, 31, 33-46.
- CLARK, K., NANDA, S. & COHEN, P. 2013. Molecular control of the NEMO family of ubiquitin-binding proteins. *Nat Rev Mol Cell Biol*, 14, 673-685.
- COHEN, P. T. 1997. Novel protein serine/threonine phosphatases: variety is the spice of life. *Trends in biochemical sciences*, 22, 245-251.
- COHEN, P. T. 2002. Protein phosphatase 1-targeted in many directions. *Journal of Cell Science*, 115, 241-256.
- COLE, C. N. 2001. Polyomaviridae: the viruses and their replication. *Fields virology*, 2141-2174.
- CORDIER, F., VINOLO, E., VÉRON, M., DELEPIERRE, M. & AGOU, F. 2008. Solution structure of NEMO zinc finger and impact of an anhidrotic ectodermal dysplasia with immunodeficiency-related point mutation. *Journal of molecular biology*, 377, 1419-1432.
- COTE, S. M., GILMORE, T. D., SHAFFER, R., WEBER, U., BOLLAM, R., GOLDEN, M. S., GLOVER, K., HERSCOVITCH, M., ENNIS, T., ALLEN, K.N. & WHITTY, A. (2013). Mutation of nonessential cysteines shows that the NF- $\kappa$ B essential modulator forms a constitutive noncovalent dimer that binds I $\kappa$ B kinase- $\beta$  with high affinity. *Biochemistry*, 52(51), 9141-9154.
- COURTOIS, G., & GILMORE, T. D. (2006). Mutations in the NF- $\kappa$ B signaling pathway: implications for human disease. *Oncogene*, 25(51), 6831-6843.
- COURTOIS, G., SMAHI, A. & ISRAËL, A. 2001. NEMO/IKK $\gamma$ : linking NF- $\kappa$ B to human disease. *Trends in molecular medicine*, 7, 427-430.
- CRAIG, P. J., CALONJE, J. E., HARRIES, M. & STEFANATO, C. M. 2009. Incidental chronic lymphocytic leukaemia in a biopsy of Merkel cell carcinoma. *Journal of cutaneous pathology*, 36, 706-710.
- CUSICK, L. & REFSUM, S. 2004. Merkel cell carcinoma of the breast: report of a case and review of the literature. *The Ulster medical journal*, 73, 137.
- DALIANIS, T. & GARCEA, R. L. Welcome to the Polyomaviridae. *Seminars in cancer biology*, 2009. Academic Press, 209-210.
- DALIANIS, T., RAMQVIST, T., ANDREASSON, K., KEAN, J. M. & GARCEA, R. L. KI, WU and Merkel cell polyomaviruses: a new era for human polyomavirus research. *Seminars in cancer biology*, 2009. Elsevier, 270-275.
- DANIELS, R., SADOWICZ, D. & HEBERT, D. N. 2007. A very late viral protein triggers the lytic release of SV40.
- DEMETRIOU, S. K., ONA-VU, K., SULLIVAN, E. M., DONG, T. K., HSU, S. W. & OH, D. H. 2012. Defective DNA repair and cell cycle arrest in cells expressing Merkel cell polyomavirus T antigen. *International Journal of Cancer*, 131, 1818-1827.
- DEPERT, W. (2000). The nuclear matrix as a target for viral and cellular oncogenes. *Critical Reviews™ in Eukaryotic Gene Expression*, 10(1).

- DIAZ, J., WANG, X., TSANG, S. H., JIAO, J. & YOU, J. 2014. Phosphorylation of large T antigen regulates Merkel cell polyomavirus replication. *Cancers*, 6, 1464-1486.
- DIDONATO, J. A., HAYAKAWA, M., ROTHWART, D. M., ZANDI, E. & KARIN, M. 1997. A cytokine-responsive I $\kappa$ B kinase that activates the transcription factor NF- $\kappa$ B. *Nature*, 388, 548-554.
- DOBRZANSKI, P., RYSECK, R.-P. & BRAVO, R. 1994. Differential interactions of Rel-NF- $\kappa$ B complexes with I $\kappa$ B $\alpha$  determine pools of constitutive and inducible NF- $\kappa$ B activity. *The EMBO journal*, 13, 4608.
- DUNCAVAGE, E. J. & PFEIFER, J. D. 2011. Human polyomaviruses 6 and 7 are not detectable in Merkel cell polyomavirus-negative Merkel cell carcinoma. *Journal of cutaneous pathology*, 38, 790-796.
- DUONG, F. H., FILIPOWICZ, M., TRIPODI, M., LA MONICA, N., & HEIM, M. H. (2004). Hepatitis C virus inhibits interferon signaling through up-regulation of protein phosphatase 2A. *Gastroenterology*, 126(1), 263-277.
- DUPUIS-GIROD, S., CANCRINI, C., LE DEIST, F., PALMA, P., BODEMER, C., PUEL, A., LIVADIOTTI, S., PICARD, C., BOSSUYT, X. & ROSSI, P. 2006. Successful allogeneic hemopoietic stem cell transplantation in a child who had anhidrotic ectodermal dysplasia with immunodeficiency. *Pediatrics*, 118, e205-e211.
- DWORKIN, A. M., TSENG, S. Y., ALLAIN, D. C., IWENOFU, O. H., PETERS, S. B. & TOLAND, A. E. 2009. Merkel cell polyomavirus in cutaneous squamous cell carcinoma of immunocompetent individuals. *Journal of Investigative Dermatology*, 129, 2868-2874.
- DYNEK, J. N., GONCHAROV, T., DUEBER, E. C., FEDOROVA, A. V., IZRAEL-TOMASEVIC, A., PHU, L., HELGASON, E., FAIRBROTHER, W.J., DESHAYES, K., KIRKPATRICK, D.S. & Vucic, D. (2010). c-IAP1 and UbcH5 promote K11-linked polyubiquitination of RIP1 in TNF signalling. *The EMBO journal*, 29(24), 4198-4209.
- EA, C.-K., DENG, L., XIA, Z.-P., PINEDA, G. & CHEN, Z. J. 2006. Activation of IKK by TNF $\alpha$  requires site-specific ubiquitination of RIP1 and polyubiquitin binding by NEMO. *Molecular cell*, 22, 245-257.
- EDDY, B. E., BORMAN, G. S., GRUBBS, G. E. & YOUNG, R. D. 1962. Identification of the oncogenic substance in rhesus monkey kidney cell cultures as simian virus 40. *Virology*, 17, 65-75.
- EDWARDS, R. H., MARQUITZ, A. R., & RAAB-TRAUB, N. (2015). Changes in Expression Induced by Epstein-Barr Virus LMP1-CTAR1: Potential Role of bcl3. *MBio*, 6(2), e00441-15.
- EMMERICH, C. H., ORDUREAU, A., STRICKSON, S., ARTHUR, J. S. C., PEDRIOLI, P. G., KOMANDER, D., & COHEN, P. (2013). Activation of the canonical IKK complex by K63/M1-linked hybrid ubiquitin chains. *Proceedings of the National Academy of Sciences*, 110(38), 15247-15252.
- ENG, T. Y., BOERSMA, M. G., FULLER, C. D., GOYTIA, V., JONES III, W. E., JOYNER, M. & NGUYEN, D. D. 2007. A comprehensive review of the treatment of Merkel cell carcinoma. *American Journal of Clinical Oncology*, 30, 624-636.
- ENGELS, E. A., BIGGAR, R. J., HALL, H. I., CROSS, H., CRUTCHFIELD, A., FINCH, J. L., GRIGG, R., HYLTON, T., PAWLISH, K. S. & MCNEEL, T. S. 2008. Cancer risk in people infected with human immunodeficiency virus in the United States. *International Journal of Cancer*, 123, 187-194.
- ENGELS, E. A., FRISCH, M., GOEDERT, J. J., BIGGAR, R. J. & MILLER, R. W. 2002. Merkel cell carcinoma and HIV infection. *The Lancet*, 359, 497-498.
- ERICKSON, K. D., GARCEA, R. L. & TSAI, B. 2009. Ganglioside GT1b is a putative host cell receptor for the Merkel cell polyomavirus. *Journal of virology*, 83, 10275-10279.
- EVANS, D. R., MYLES, T., HOFSTEENGE, J. & HEMMINGS, B. A. 1999. Functional expression of human PP2Ac in yeast permits the identification of novel C-terminal and dominant-negative mutant forms. *Journal of Biological Chemistry*, 274, 24038-24046.
- FANG, X., Gao, J., Zheng, H., Li, B., Kong, L., Zhang, Y., Wang, W., Zeng, Y. and Ye, L. (2007). The membrane protein of SARS-CoV suppresses NF- $\kappa$ B activation. *Journal of medical virology*, 79(10), 1431-1439.
- FATHALLAH, I., PARROCHE, P., GRUFFAT, H., ZANNETTI, C., JOHANSSON, H., YUE, J., MANET, E., TOMMASINO, M., SYLLA, B. S. & HASAN, U. A. 2010. EBV latent

- membrane protein 1 is a negative regulator of TLR9. *The Journal of Immunology*, 185, 6439-6447.
- FAUST, H. & DILLNER, J. 2014. Merkel Cell Polyomavirus: Epidemiology and Clinical Features of Related Cancer. *Viruses and Human Cancer*. Springer.
- FENG, H., KWUN, H. J., LIU, X., GJOERUP, O., STOLZ, D. B., CHANG, Y., & MOORE, P. S. (2011). Cellular and viral factors regulating Merkel cell polyomavirus replication. *PLoS One*, 6(7), e22468.
- FENG, H., SHUDA, M., CHANG, Y. & MOORE, P. S. 2008. Clonal integration of a polyomavirus in human Merkel cell carcinoma. *Science*, 319, 1096-1100.
- FENG, H., TAYLOR, J. L., BENOS, P. V., NEWTON, R., WADDELL, K., LUCAS, S. B., CHANG, Y. & MOORE, P. S. 2007. Human transcriptome subtraction by using short sequence tags to search for tumor viruses in conjunctival carcinoma. *Journal of virology*, 81, 11332-11340.
- FIERS, W., CONTRERAS, R., HAEGEMAN, G., ROGIERS, R., VAN DE VOORDE, A., VAN HEUVERSWYN, H., VAN HERREWEGHE, J., VOLCKAERT, G. & YSEBAERT, M. 1978. Complete nucleotide sequence of SV40 DNA. *Nature*, 273, 113-120.
- FILIPPE-SANTOS, O., BUSTAMANTE, J., HAVERKAMP, M. H., VINOLO, E., KU, C.-L., PUEL, A., FRUCHT, D. M., CHRISTEL, K., VON BERNUTH, H. & JOUANGUY, E. 2006. X-linked susceptibility to mycobacteria is caused by mutations in NEMO impairing CD40-dependent IL-12 production. *The Journal of experimental medicine*, 203, 1745-1759.
- FIUME, G., VECCHIO, E., DE LAURENTIIS, A., TRIMBOLI, F., PALMIERI, C., PISANO, A., FALCONE, C., PONTORIERO, M., ROSSI, A., SCIALDONE, A & MASCI, F. F. (2011). Human immunodeficiency virus-1 Tat activates NF- $\kappa$ B via physical interaction with I $\kappa$ B- $\alpha$  and p65. *Nucleic acids research*, gkr1224.
- FLUCK, M. M. & SCHAFFHAUSEN, B. S. 2009. Lessons in signaling and tumorigenesis from polyomavirus middle T antigen. *Microbiology and Molecular Biology Reviews*, 73, 542-563.
- FORESTER, C. M., MADDOX, J., LOUIS, J. V., GORIS, J. & VIRSHUP, D. M. 2007. Control of mitotic exit by PP2A regulation of Cdc25C and Cdk1. *Proceedings of the National Academy of Sciences*, 104, 19867-19872.
- FOULONGNE, V., COURGNAUD, V., CHAMPEAU, W. & SEGONDY, M. 2011. Detection of Merkel cell polyomavirus on environmental surfaces. *Journal of medical virology*, 83, 1435-1439.
- FOULONGNE, V., DEREURE, O., KLUGER, N., MOLES, J., GUILLOT, B. & SEGONDY, M. 2010. Merkel cell polyomavirus DNA detection in lesional and nonlesional skin from patients with Merkel cell carcinoma or other skin diseases. *British Journal of Dermatology*, 162, 59-63.
- FOX, H., LANE, E. B. & WHITEAR, M. 1980. Sensory nerve endings and receptors in fish and amphibians. *The Skin of Vertebrates*, 271-281.
- FRANGIONI, J. V., & NEEL, B. G. (1993). Solubilization and purification of enzymatically active glutathione S-transferase (pGEX) fusion proteins. *Analytical biochemistry*, 210(1), 179-187.
- FRIGERIO, B., CAPELLA, C., EUSEB, V., TENTI, P. & AZZOPARDI, J. 1983. Merkel cell carcinoma of the skin: the structure and origin of normal Merkel cells. *Histopathology*, 7, 229-249.
- FUKUGLTA, M., HOGAN, C., PEEBLES, P., KOLB, E., TURNER, M., MADORE, F., FREEDMAN, W., JACOBY, G., SANDAGE, A. & TAMMANN, G. 1994. Insulin-independent stimulation of protein synthesis by phosphorylation of a regulator of 5'-cap function. *Nature*, 371, 762-767.
- FUSCO, F., PESCATORE, A., BAL, E., GHOUL, A., PACIOLLA, M., LIOI, M. B., D'URSO, M., RABIA, S. H., BODEMER, C. & BONNEFONT, J. P. 2008. Alterations of the IKBKG locus and diseases: an update and a report of 13 novel mutations. *Human mutation*, 29, 595-604.
- GARDNER, S., FIELD, A., COLEMAN, D. & HULME, B. 1971. New human papovavirus (BK) isolated from urine after renal transplantation. *The Lancet*, 297, 1253-1257.
- GARNESKI, K. M., WARCOLA, A. H., FENG, Q., KIVIAT, N., LEONARD, J. H. & NGHIEM, P. 2009. Merkel cell polyomavirus is more frequently present in North American than Australian Merkel cell carcinoma tumors. *The Journal of investigative dermatology*, 129, 246.

- GAYNOR, A. M., NISSEN, M. D., WHILEY, D. M., MACKAY, I. M., LAMBERT, S. B., WU, G., BRENNAN, D. C., STORCH, G. A., SLOOTS, T. P. & WANG, D. 2007. Identification of a novel polyomavirus from patients with acute respiratory tract infections. *PLoS Pathog*, 3, e64.
- GEORGOPOULOU, U., TSITOURA, P., KALAMVOKI, M. & MAVROMARA, P. 2006. The protein phosphatase 2A represents a novel cellular target for hepatitis C virus NS5A protein. *Biochimie*, 88, 651-662.
- GHOSH, G., DUYNE, G. V., GHOSH, S. & SIGLER, P. B. 1995. Structure of NF- $\kappa$ B p50 homodimer bound to a kB site. *Nature*, 373, 303-310.
- GHOSH, S., & KARIN, M. (2002). Missing pieces in the NF- $\kappa$ B puzzle. *Cell*, 109(2), S81-S96.
- GHOSH, S., MAY, M. J. & KOPP, E. B. 1998. NF- $\kappa$ B and Rel proteins: evolutionarily conserved mediators of immune responses. *Annual review of immunology*, 16, 225-260.
- GILLENWATER, A. M., HESSEL, A. C., MORRISON, W. H., BURGESS, M. A., SILVA, E. G., ROBERTS, D. & GOEPFERT, H. 2001. Merkel cell carcinoma of the head and neck: effect of surgical excision and radiation on recurrence and survival. *Archives of Otolaryngology-Head & Neck Surgery*, 127, 149-154.
- GILMORE T. D (2006) Introduction to NF- $\kappa$ B: players, pathways, perspectives. *Oncogene* 25:6680-6684
- GILMORE, T. D. & TEMIN, H. M. 1986. Different localization of the product of the v-rel oncogene in chicken fibroblasts and spleen cells correlates with transformation by REV-T. *Cell*, 44, 791-800.
- GINGRAS, A.-C., CABALLERO, M., ZARSKE, M., SANCHEZ, A., HAZBUN, T. R., FIELDS, S., SONENBERG, N., HAFEN, E., RAUGHT, B. & AEBERSOLD, R. 2005. A novel, evolutionarily conserved protein phosphatase complex involved in cisplatin sensitivity. *Molecular & cellular proteomics*, 4, 1725-1740.
- GINGRAS, A.-C., SVITKIN, Y., BELSHAM, G. J., PAUSE, A. & SONENBERG, N. 1996. Activation of the translational suppressor 4E-BP1 following infection with encephalomyocarditis virus and poliovirus. *Proceedings of the National Academy of Sciences*, 93, 5578-5583.
- GOEPFERT, H., REMMLER, D., SILVA, E. & WHEELER, B. 1984. Merkel cell carcinoma (endocrine carcinoma of the skin) of the head and neck. *Archives of otolaryngology*, 110, 707-712.
- GOULD, V., MOLL, R., MOLL, I., LEE, I. & FRANKE, W. 1985. Neuroendocrine (Merkel) cells of the skin: hyperplasias, dysplasias, and neoplasms. *Laboratory investigation; a journal of technical methods and pathology*, 52, 334-353.
- GRIFFITHS, D. A., ABDUL-SADA, H., KNIGHT, L. M., JACKSON, B. R., RICHARDS, K., PRESCOTT, E. L., PEACH, A. H. S., BLAIR, G. E., MACDONALD, A. & WHITEHOUSE, A. 2013. Merkel cell polyomavirus small T antigen targets the NEMO adaptor protein to disrupt inflammatory signaling. *Journal of virology*, 87, 13853-13867.
- GROSS, L. 1953. A filterable agent, recovered from Ak leukemic extracts, causing salivary gland carcinomas in C3H mice. *Experimental Biology and Medicine*, 83, 414-421.
- GRUBISHA, O., KAMINSKA, M., DUQUERROY, S., FONTAN, E., CORDIER, F., HAOUZ, A., RAYNAL, B., CHIARAVALLI, J., DELEPIERRE, M., ISRAËL, A & Véron, M. (2010). DARPIn-assisted crystallography of the CC2-LZ domain of NEMO reveals a coupling between dimerization and ubiquitin binding. *Journal of molecular biology*, 395(1), 89-104.
- GUERGNON, J., GODET, A. N., GALIOOT, A., FALANGA, P. B., COLLE, J.-H., CAYLA, X. & GARCIA, A. 2011. PP2A targeting by viral proteins: a widespread biological strategy from DNA/RNA tumor viruses to HIV-1. *Biochimica et Biophysica Acta (BBA)-Molecular Basis of Disease*, 1812, 1498-1507.
- GUSTAFSSON, B., PRIFTAKIS, P., RUBIN, J., GIRAUD, G., RAMQVIST, T. & DALIANIS, T. 2013. Human polyomaviruses were not detected in cerebrospinal fluid of patients with neurological complications after hematopoietic stem cell transplantation. *Future Virology*, 8, 809-814.
- HADIAN, K., GRIESBACH, R. A., DORNAUER, S., WANGER, T. M., NAGEL, D., METLITZKY, M., BEISKER, W., SCHMIDT-SUPPRIAN, M. & KRAPPMANN, D. (2011). NF- $\kappa$ B essential modulator (NEMO) interaction with linear and lys-63

- ubiquitin chains contributes to NF- $\kappa$ B activation. *Journal of Biological Chemistry*, 286(29), 26107-26117.
- HADWEH, P., Habelhah, H., Kieff, E., Mosialos, G., & Hatzivassiliou, E. (2014). The PP4R1 subunit of protein phosphatase PP4 targets TRAF2 and TRAF6 to mediate inhibition of NF- $\kappa$ B activation. *Cellular signalling*, 26(12), 2730-2737.
- HAHN, W. C., DESSAIN, S. K., BROOKS, M. W., KING, J. E., ELENBAAS, B., SABATINI, D. M., DECAPRIO, J. A. & WEINBERG, R. A. 2002. Enumeration of the simian virus 40 early region elements necessary for human cell transformation. *Molecular and cellular biology*, 22, 2111-2123.
- HANAHAH, D. 1983. Studies on transformation of Escherichia coli with plasmids. *Journal of molecular biology*, 166(4), 557-580.
- HALATA, Z., COOPER, B. Y., BAUMANN, K. I., SCHWEGMANN, C. & FRIEDMAN, R. M. 1999. Sensory nerve endings in the hard palate and papilla incisiva of the goat. *Experimental brain research*, 129, 218-228.
- HALATA, Z., GRIM, M. & BAUMAN, K. I. 2003. Friedrich Sigmund Merkel and his "Merkel cell", morphology, development, and physiology: review and new results. *The Anatomical Record Part A: Discoveries in Molecular, Cellular, and Evolutionary Biology*, 271, 225-239.
- HARGETT, D., RICE, S., & BACHENHEIMER, S. L. (2006). Herpes simplex virus type 1 ICP27-dependent activation of NF- $\kappa$ B. *Journal of virology*, 80(21), 10565-10578.
- HARRISON, C. J., MEINKE, G., KWUN, H. J., ROGALIN, H., PHELAN, P. J., BULLOCK, P. A., CHANG, Y., MOORE, P. S. & BOHM, A. 2011. Asymmetric assembly of Merkel cell polyomavirus large T-antigen origin binding domains at the viral origin. *Journal of molecular biology*, 409, 529-542.
- HASAN, U. 2014. Human papillomavirus (HPV) deregulation of Toll-like receptor 9. *Oncoimmunology*, 3, e27257.
- HEIMBERG, H., HEREMANS, Y., JOBIN, C., LEEMANS, R., CARDOZO, A. K., DARVILLE, M., & EIZIRIK, D. L. (2001). Inhibition of cytokine-induced NF- $\kappa$ B activation by adenovirus-mediated expression of a NF- $\kappa$ B super-repressor prevents  $\beta$ -cell apoptosis. *Diabetes*, 50(10), 2219-2224.
- HELPS, N. R., BREWIS, N. D., LINERUTH, K., DAVIS, T., KAISER, K. & COHEN, P. 1998. Protein phosphatase 4 is an essential enzyme required for organisation of microtubules at centrosomes in Drosophila embryos. *Journal of Cell Science*, 111, 1331-1340.
- HENDRIX, P., MAYER-JACKEL, R., CRON, P., GORIS, J., HOFSTEENGE, J., MERLEVEDE, W. & HEMMINGS, B. 1993. Structure and expression of a 72-kDa regulatory subunit of protein phosphatase 2A. Evidence for different size forms produced by alternative splicing. *Journal of Biological Chemistry*, 268, 15267-15276.
- HIGUCHI, M., & FUJII, M. (2009). Distinct functions of HTLV-1 Tax1 from HTLV-2 Tax2 contribute key roles to viral pathogenesis. *Retrovirology*, 6(1), 1-11.
- HIRSCH, H. H. 2002. Polyomavirus BK Nephropathy: A (Re-) emerging Complication in Renal Transplantation. *American journal of transplantation*, 2, 25-30.
- HODGSON, N. C. 2005. Merkel cell carcinoma: changing incidence trends. *Journal of surgical oncology*, 89, 1-4.
- HOFFMANN, A., NATOLI, G. & GHOSH, G. 2006. Transcriptional regulation via the NF- $\kappa$ B signaling module. *Oncogene*, 25, 6706-6716.
- HOUBEN, R., SHUDA, M., WEINKAM, R., SCHRAMA, D., FENG, H., CHANG, Y., MOORE, P. S. & BECKER, J. C. 2010. Merkel cell polyomavirus-infected Merkel cell carcinoma cells require expression of viral T antigens. *Journal of virology*, 84, 7064-7072.
- HOWARD, R. A., DORES, G. M., CURTIS, R. E., ANDERSON, W. F. & TRAVIS, L. B. 2006. Merkel cell carcinoma and multiple primary cancers. *Cancer Epidemiology Biomarkers & Prevention*, 15, 1545-1549.
- HUANG, T. T., KUDO, N., YOSHIDA, M. & MIYAMOTO, S. 2000. A nuclear export signal in the N-terminal regulatory domain of I $\kappa$ B $\alpha$  controls cytoplasmic localization of inactive NF- $\kappa$ B/I $\kappa$ B $\alpha$  complexes. *Proceedings of the National Academy of Sciences*, 97, 1014-1019.
- HUBEAU, M., NGADJEUA, F., PUEL, A., ISRAEL, L., FEINBERG, J., CHRABIEH, M., BELANI, K., BODEMER, C., FABRE, I., PLEBANI, A. & BOISSON-DUPUIS, S. (2011). New mechanism of X-linked anhidrotic ectodermal dysplasia with

- immunodeficiency: impairment of ubiquitin binding despite normal folding of NEMO protein. *Blood*, 118(4), 926-935.
- HUSSEINY, M. I., ANASTASI, B., SINGER, J. & LACEY, S. F. 2010. A comparative study of Merkel cell, BK and JC polyomavirus infections in renal transplant recipients and healthy subjects. *Journal of Clinical Virology*, 49, 137-140.
- HWANG, J. H., JIANG, T., KULKARNI, S., FAURE, N. & SCHAFFHAUSEN, B. S. 2013. Protein Phosphatase 2A Isoforms Utilizing A $\beta$  Scaffolds Regulate Differentiation through Control of Akt Protein. *Journal of Biological Chemistry*, 288, 32064-32073.
- IWAI, K., FUJITA, H. & SASAKI, Y. 2014. Linear ubiquitin chains: NF- $\kappa$ B signalling, cell death and beyond. *Nature Reviews Molecular Cell Biology*, 15, 503-508.
- IWAI, K., & TOKUNAGA, F. (2009). Linear polyubiquitination: a new regulator of NF- $\kappa$ B activation. *EMBO reports*, 10(7), 706-713.
- IYER, J. G., AFANASIEV, O. K., MCCLURKAN, C., PAULSON, K., NAGASE, K., JING, L., MARSHAK, J. O., DONG, L., CARTER, J. & LAI, I. 2011. Merkel cell polyomavirus-specific CD8+ and CD4+ T-cell responses identified in Merkel cell carcinomas and blood. *Clinical Cancer Research*, 17, 6671-6680.
- IYER, J. G., STORER, B. E., PAULSON, K. G., LEMOS, B., PHILLIPS, J. L., BICHAKJIAN, C. K., ZEITOUNI, N., GERSHENWALD, J. E., SONDAK, V. & OTLEY, C. C. 2014. Relationships among primary tumor size, number of involved nodes, and survival for 8044 cases of Merkel cell carcinoma. *Journal of the American Academy of Dermatology*, 70, 637-643.
- JANOO, A., MORROW, P. W., & TUNG, H. Y. (2005). Activation of protein phosphatase-2A1 by HIV-1 Vpr Cell death causing peptide in intact CD4+ T cells and in vitro. *Journal of cellular biochemistry*, 94(4), 816-825.
- JANSSEN, R., VAN WENGEN, A., HOEVE, M. A., TEN DAM, M., VAN DER BURG, M., VAN DONGEN, J., VAN DE VOSSE, E., VAN TOL, M., BREDIUS, R. & OTTENHOFF, T. H. 2004. The same I $\kappa$ B $\alpha$  mutation in two related individuals leads to completely different clinical syndromes. *The Journal of experimental medicine*, 200, 559-568.
- JENSEN, K., KOHLER, S. & ROUSE, R. V. 2000. Cytokeratin staining in Merkel cell carcinoma: an immunohistochemical study of cytokeratins 5/6, 7, 17, and 20. *Applied Immunohistochemistry & Molecular Morphology*, 8, 310-315.
- JIANG, Y. F., HE, B., LI, N. P., MA, J., GONG, G. Z., & ZHANG, M. (2011). The oncogenic role of NS5A of hepatitis C virus is mediated by up-regulation of survivin gene expression in the hepatocellular cell through p53 and NF- $\kappa$ B pathways. *Cell biology international*, 35(12), 1225-1232.
- JIN, Z. H. O. U., RUEDIGER, R., & WALTER, G. (2003). Characterization of the A $\alpha$  and A $\beta$  subunit isoforms of protein phosphatase 2A: differences in expression, subunit interaction, and evolution. *Biochemical Journal*, 369(2), 387-398.
- JOHNE, R., BUCK, C. B., ALLANDER, T., ATWOOD, W. J., GARCEA, R. L., IMPERIALE, M. J., MAJOR, E. O., RAMQVIST, T. & NORKIN, L. C. 2011. Taxonomical developments in the family Polyomaviridae. *Archives of virology*, 156, 1627-1634.
- JOHNSON, E. M. 2010. Structural evaluation of new human polyomaviruses provides clues to pathobiology. *Trends in microbiology*, 18, 215-223.
- JOHNSON, K. O., YOSHIOKA, T. & VEGA-BERMUDEZ, F. 2000. Tactile functions of mechanoreceptive afferents innervating the hand. *Journal of Clinical Neurophysiology*, 17, 539-558.
- JOHNSON, P. F. 2005. Molecular stop signs: regulation of cell-cycle arrest by C/EBP transcription factors. *Journal of cell science*, 118, 2545-2555.
- JOURNO, C., BONNET, A., FAVRE-BONVIN, A., TURPIN, J., VINERA, J., CÔTÉ, E., Chevalier, S.A., Kfoury, Y., Bazarbachi, A., Pique, C. & MAHIEUX, R. (2013). Human T cell leukemia virus type 2 tax-mediated NF- $\kappa$ B activation involves a mechanism independent of Tax conjugation to ubiquitin and SUMO. *Journal of virology*, 87(2), 1123-1136.
- KAPFHAMER, D., BERGER, K. H., HOPF, F. W., SEIF, T., KHARAZIA, V., BONCI, A. & HEBERLEIN, U. 2010. Protein Phosphatase 2a and glycogen synthase kinase 3 signaling modulate prepulse inhibition of the acoustic startle response by altering cortical M-Type potassium channel activity. *The Journal of Neuroscience*, 30, 8830-8840.

- KASSEM, A., SCHÖPFLIN, A., DIAZ, C., WEYERS, W., STICKELER, E., WERNER, M. & ZUR HAUSEN, A. 2008. Frequent detection of Merkel cell polyomavirus in human Merkel cell carcinomas and identification of a unique deletion in the VP1 gene. *Cancer research*, 68, 5009-5013.
- KAWAI, T. & AKIRA, S. 2007. Antiviral signaling through pattern recognition receptors. *Journal of biochemistry*, 141, 137-145.
- KEAN, J. M., RAO, S., WANG, M. & GARCEA, R. L. 2009. Seroepidemiology of human polyomaviruses. *PLoS Pathog*, 5, e1000363.
- KENSCHKE, T., TOKUNAGA, F., IKEDA, F., GOTO, E., IWAI, K., & DIKIC, I. (2012). Analysis of nuclear factor- $\kappa$ B (NF- $\kappa$ B) essential modulator (NEMO) binding to linear and lysine-linked ubiquitin chains and its role in the activation of NF- $\kappa$ B. *Journal of Biological Chemistry*, 287(28), 23626-23634.
- KHALILI, K., Sariyer, I. K., & Safak, M. (2008). Small tumor antigen of polyomaviruses: role in viral life cycle and cell transformation. *Journal of cellular physiology*, 215(2), 309-319.
- KHEW-GOODALL, Y. & HEMMINGS, B. A. 1988. Tissue-specific expression of mRNAs encoding  $\alpha$ - and  $\beta$ -catalytic subunits of protein phosphatase 2A. *FEBS letters*, 238, 265-268.
- KILHAM, L. & MURPHY, H. W. 1953. A pneumotropic virus isolated from C3H mice carrying the Bittner milk agent. *Experimental Biology and Medicine*, 82, 133-137.
- KIRSCHNER, M. & MITCHISON, T. 1986. Beyond self-assembly: from microtubules to morphogenesis. *Cell*, 45, 329-342.
- KLEINBERGER, T. & SHENK, T. 1993. Adenovirus E4orf4 protein binds to protein phosphatase 2A, and the complex down regulates E1A-enhanced junB transcription. *Journal of virology*, 67, 7556-7560.
- KLOEKER, S. & WADZINSKI, B. E. 1999. Purification and identification of a novel subunit of protein serine/threonine phosphatase 4. *Journal of Biological Chemistry*, 274, 5339-5347.
- KNIGHT, L. M., STAKAITYTE, G., JENNIFER, J. W., ABDUL-SADA, H., GRIFFITHS, D. A., HOWELL, G. J., WHEAT, R., BLAIR, G. E., STEVEN, N. M. & MACDONALD, A. 2015. Merkel cell polyomavirus small T antigen mediates microtubule destabilization to promote cell motility and migration. *Journal of virology*, 89, 35-47.
- KONTOCHRISTOPOULOS, G., STAVROPOULOS, P., KRASAGAKIS, K., GOERDT, S. & ZOUBOULIS, C. C. 2000. Differentiation between Merkel cell carcinoma and malignant melanoma: an immunohistochemical study. *Dermatology*, 201, 123-126.
- KORALNIK, I. J., DU PASQUIER, R. A. & LETVIN, N. L. 2001. JC virus-specific cytotoxic T lymphocytes in individuals with progressive multifocal leukoencephalopathy. *Journal of virology*, 75, 3483-3487.
- KORUP, S., RIETSCHER, J., CALVIGNAC-SPENCER, S., TRUSCH, F., HOFMANN, J., MOENS, U., SAUER, I., VOIGT, S., SCHMUCK, R. & EHLERS, B. 2013. Identification of a novel human polyomavirus in organs of the gastrointestinal tract. *PLoS One*, 8, e58021.
- KRAUSE, E., DE GRAAF, M., FLISS, P. M., DÖLKEN, L., & BRUNE, W. (2014). Murine cytomegalovirus virion-associated protein M45 mediates rapid NF- $\kappa$ B activation after infection. *Journal of virology*, 88(17), 9963-9975.
- KREMMER, E., OHST, K., KIEFER, J., BREWIS, N. & WALTER, G. 1997. Separation of PP2A core enzyme and holoenzyme with monoclonal antibodies against the regulatory A subunit: abundant expression of both forms in cells. *Molecular and cellular biology*, 17, 1692-1701.
- KRESSIN, M. K. & KIM, A. S. 2012. Metastatic Merkel cell carcinoma in the bone marrow of a patient with plasma cell myeloma and therapy-related myelodysplastic syndrome. *International journal of clinical and experimental pathology*, 5, 1007.
- KUWAMOTO, S., HIGAKI, H., KANAI, K., IWASAKI, T., SANO, H., NAGATA, K., KATO, K., KATO, M., MURAKAMI, I., HORIE, Y. & YAMAMOTO, O. (2011). Association of Merkel cell polyomavirus infection with morphologic differences in Merkel cell carcinoma. *Human pathology*, 42(5), 632-640.
- KUMAR, S. H. & RANGARAJAN, A. 2009. Simian virus 40 small T antigen activates AMPK and triggers autophagy to protect cancer cells from nutrient deprivation. *Journal of virology*, 83, 8565-8574.

- KWAK, Y. T., GUO, J., SHEN, J. & GAYNOR, R. B. 2000. Analysis of domains in the IKK $\alpha$  and IKK $\beta$  proteins that regulate their kinase activity. *Journal of Biological Chemistry*, 275, 14752-14759.
- KWUN, H. J., GUASTAFIERRO, A., SHUDA, M., MEINKE, G., BOHM, A., MOORE, P. S. & CHANG, Y. 2009. The minimum replication origin of merkel cell polyomavirus has a unique large T-antigen loading architecture and requires small T-antigen expression for optimal replication. *Journal of virology*, 83, 12118-12128.
- KWUN, H. J., SHUDA, M., CAMACHO, C. J., GAMPER, A. M., THANT, M., CHANG, Y. & MOORE, P. S. 2015. Restricted protein phosphatase 2A targeting by Merkel cell polyomavirus small T antigen. *Journal of virology*, 89, 4191-4200.
- KWUN, H. J., SHUDA, M., FENG, H., CAMACHO, C. J., MOORE, P. S. & CHANG, Y. 2013. Merkel Cell Polyomavirus Small T Antigen Controls Viral Replication and Oncoprotein Expression by Targeting the Cellular Ubiquitin Ligase SCF Fbw7. *Cell host & microbe*, 14, 125-135.
- L CUBITT, X. C., HANSJÜRGEN T AGOSTINI, VIVEK R NERURKAR, IRIS SCHEIRICH, RICHARD YANAGIHARA, CAROLINE F RYSCHKEWITSCH, GERALD L STONER, CHRISTOPHER 2001. Predicted amino acid sequences for 100 JCV strains. *Journal of neurovirology*, 7, 339-344.
- LANE, E. B. & WHITEAR, M. 1977. On the occurrence of Merkel cells in the epidermis of teleost fishes. *Cell and tissue research*, 182, 235-246.
- LANOY, E., COSTAGLIOLA, D. & ENGELS, E. A. 2010. Skin cancers associated with HIV infection and solid-organ transplantation among elderly adults. *International journal of cancer*, 126, 1724-1731.
- LAPLANTINE, E., FONTAN, E., CHIARAVALLI, J., LOPEZ, T., LAKISIC, G., VERON, M., AGOU, F. & ISRAËL, A. (2009). NEMO specifically recognizes K63-linked poly-ubiquitin chains through a new bipartite ubiquitin-binding domain. *The EMBO journal*, 28(19), 2885-2895.
- LAU, L., GRAY, E. E., BRUNETTE, R. L., & STETSON, D. B. (2015). DNA tumor virus oncogenes antagonize the cGAS-STING DNA-sensing pathway. *Science*, 350(6260), 568-571.
- LAUDE, H. C., JONCHÈRE, B., MAUBEC, E., CARLOTTI, A., MARINHO, E., COUTURAUD, B., PETER, M., SASTRE-GARAU, X., AVRIL, M.-F. & DUPIN, N. 2010. Distinct merkel cell polyomavirus molecular features in tumour and non tumour specimens from patients with merkel cell carcinoma.
- LAUTTIA, S., SIHTO, H., KAVOLA, H., KOLJONEN, V., BÖHLING, T. & JOENSUU, H. 2014. Prokineticins and Merkel cell polyomavirus infection in Merkel cell carcinoma. *British journal of cancer*, 110, 1446-1455.
- LAVORGNA, A., & HARHAJ, E. W. (2013). Is there a role for ubiquitin or SUMO in human T-cell leukemia virus type 2 Tax-induced NF- $\kappa$ B activation?. *Future virology*, 8(3), 223-227.
- LEE, S., PAULSON, K. G., MURCHISON, E. P., AFANASIEV, O. K., ALKAN, C., LEONARD, J. H., BYRD, D. R., HANNON, G. J. & NGHIEM, P. 2011. Identification and validation of a novel mature microRNA encoded by the Merkel cell polyomavirus in human Merkel cell carcinomas. *Journal of Clinical Virology*, 52, 272-275.
- LEECH, S., KOLAR, A., BARRETT, P., SINCLAIR, S. & LEONARD, N. 2001. Merkel cell carcinoma can be distinguished from metastatic small cell carcinoma using antibodies to cytokeratin 20 and thyroid transcription factor 1. *Journal of clinical pathology*, 54, 727-729.
- LEITGES M, SANZ L, MARTIN P, DURAN A, BRAUN U, GARCÍA JF, CAMACHO F, DIAZ-MECO MT, RENNERT PD, MOSCAT J. 2001. Targeted disruption of the zetaPKC gene results in the impairment of the NF-kappaB pathway. *Mol. Cell.*;8:771-780.
- LEMONS, B. D., STORER, B. E., IYER, J. G., PHILLIPS, J. L., BICHAKJIAN, C. K., FANG, L. C., JOHNSON, T. M., LIEGEOIS-KWON, N. J., OTLEY, C. C. & PAULSON, K. G. 2010. Pathologic nodal evaluation improves prognostic accuracy in Merkel cell carcinoma: analysis of 5823 cases as the basis of the first consensus staging system. *Journal of the American Academy of Dermatology*, 63, 751-761.
- LEONARD, J.H., DASH, P., HOLLAND, P., KEARSLEY, J.H. AND BELL, J.R. Characterization of Merkel cell carcinoma adherent cell lines. *Int. J Cancer*, 60: 100-107, 1995.

- LEWIS, M. J., Vyse, S., Shields, A. M., Boeltz, S., Gordon, P. A., Spector, T. D., Vyse, T. J. (2015). UBE2L3 polymorphism amplifies NF- $\kappa$ B activation and promotes plasma cell development, linking linear ubiquitination to multiple autoimmune diseases. *The American Journal of Human Genetics*, 96(2), 221-234.
- LI, H., GADE, P., XIAO, W. & KALVAKOLANU, D. V. 2007a. The interferon signaling network and transcription factor C/EBP- $\beta$ . *Cellular & molecular immunology*, 4, 407.
- LI, H. H., CAI, X., SHOUSE, G. P., PILUSO, L. G. & LIU, X. 2007b. A specific PP2A regulatory subunit, B56 $\gamma$ , mediates DNA damage-induced dephosphorylation of p53 at Thr55. *The EMBO journal*, 26, 402-411.
- LI, T.-C., IWASAKI, K., KATANO, H., KATAOKA, M., NAGATA, N., KOBAYASHI, K., MIZUTANI, T., TAKEDA, N., WAKITA, T. & SUZUKI, T. 2015a. Characterization of self-assembled virus-like particles of Merkel cell polyomavirus. *PLoS One*, 10.
- LI, X., LIANG, L., HUANG, L., MA, X., LI, D. & CAI, S. 2015b. High expression of protein phosphatase 4 is associated with the aggressive malignant behavior of colorectal carcinoma. *Molecular cancer*, 14, 95.
- LIM, E. S., REYES, A., ANTONIO, M., SAHA, D., IKUMAPAYI, U. N., ADEYEMI, M., STINE, O. C., SKELTON, R., BRENNAN, D. C. & MKAKOSYA, R. S. 2013. Discovery of STL polyomavirus, a polyomavirus of ancestral recombinant origin that encodes a unique T antigen by alternative splicing. *Virology*, 436, 295-303.
- LISITSYN, N. & WIGLER, M. 1993. Cloning the differences between two complex genomes. *Science*, 259, 946-951.
- LIU, D., CUI, L., HAO, R., WANG, Y., HE, J. & GUO, D. 2014. Hepatitis B virus polymerase suppresses NF- $\kappa$ B signaling by inhibiting the activity of IKKs via interaction with Hsp90 $\beta$ . *PLoS One*, 9, e91658.
- LIU, W., YANG, R., PAYNE, A. S., SCHOWALTER, R. M., SPURGEON, M. E., LAMBERT, P. F., XU, X., BUCK, C.B. & YOU, J. (2016). Identifying the Target Cells and Mechanisms of Merkel Cell Polyomavirus Infection. *Cell Host & Microbe*.
- LIU, X., HEIN, J., RICHARDSON, S. C., BASSE, P. H., TOPTAN, T., MOORE, P. S., GJOERUP, O. V. & CHANG, Y. 2011. Merkel cell polyomavirus large T antigen disrupts lysosome clustering by translocating human Vam6p from the cytoplasm to the nucleus. *Journal of Biological Chemistry*, 286, 17079-17090.
- LOW, J. A., MAGNUSON, B., TSAI, B. & IMPERIALE, M. J. 2006. Identification of gangliosides GD1b and GT1b as receptors for BK virus. *Journal of virology*, 80, 1361-1366.
- LO, Y. C., Lin, S. C., Rospigliosi, C. C., Conze, D. B., Wu, C. J., Ashwell, J. D., ... & Wu, H. (2009). Structural basis for recognition of diubiquitins by NEMO. *Molecular cell*, 33(5), 602-615.
- LOYO, M., GUERRERO-PRESTON, R., BRAIT, M., HOQUE, M. O., CHUANG, A., KIM, M. S., SHARMA, R., LIÉGEOIS, N. J., KOCH, W. M. & CALIFANO, J. A. 2010. Quantitative detection of Merkel cell virus in human tissues and possible mode of transmission. *International journal of cancer*, 126, 2991-2996.
- LUNDBERG, R., BRYTTING, M., DAHLGREN, L., KANTER-LEWENSOHN, L., SCHLOSS, L., DALIANIS, T. & RAGNARSSON-OLDING, B. 2006. Human herpes virus DNA is rarely detected in non-UV light-associated primary malignant melanomas of mucous membranes. *Anticancer research*, 26, 3627-3631.
- LYNCH, K. J. & FRISQUE, R. J. 1990. Identification of critical elements within the JC virus DNA replication origin. *Journal of virology*, 64, 5812-5822.
- MAGINNIS, M. S., NELSON, C. D. & ATWOOD, W. J. 2014. JC polyomavirus attachment, entry, and trafficking: unlocking the keys to a fatal infection. *Journal of neurovirology*, 1-13.
- MAJUMDAR, S. & AGGARWAL, B. B. 2001. Methotrexate suppresses NF- $\kappa$ B activation through inhibition of I $\kappa$ B $\alpha$  phosphorylation and degradation. *The Journal of Immunology*, 167, 2911-2920.
- MAKRIS, C., GODFREY, V. L., KRÄHN-SENFTLEBEN, G., TAKAHASHI, T., ROBERTS, J. L., SCHWARZ, T., FENG, L., JOHNSON, R. S. & KARIN, M. 2000. Female mice heterozygous for IKK $\gamma$ /NEMO deficiencies develop a dermatopathy similar to the human X-linked disorder incontinentia pigmenti. *Molecular cell*, 5, 969-979.
- MANCINI, A. J., LAWLEY, L. P. & UZEL, G. 2008. X-linked ectodermal dysplasia with immunodeficiency caused by NEMO mutation: early recognition and diagnosis. *Archives of dermatology*, 144, 342-346.

- MANKOURI, J., FRAGKLOUDIS, R., RICHARDS, K. H., WETHERILL, L. F., HARRIS, M., KOHL, A., ELLIOTT, R. M. & MACDONALD, A. 2010. Optineurin negatively regulates the induction of IFN $\beta$  in response to RNA virus infection. *PLoS Pathog*, 6, e1000778.
- MANNOVÁ, P. & FORSTOVÁ, J. 2003. Mouse polyomavirus utilizes recycling endosomes for a traffic pathway independent of COPI vesicle transport. *Journal of virology*, 77, 1672-1681.
- MARIENFELD, R. B., PALKOWITSCH, L., & GHOSH, S. (2006). Dimerization of the I $\kappa$ B kinase-binding domain of NEMO is required for tumor necrosis factor alpha-induced NF- $\kappa$ B activity. *Molecular and cellular biology*, 26(24), 9209-9219.
- MARTEL-JANTIN, C., FILIPPONE, C., TORTEVOYE, P., AFONSO, P. V., BETSEM, E., DESCORPS-DECLERE, S., NICOL, J. T., TOUZÉ, A., COURSAGET, P. & CROUZAT, M. 2014. Molecular epidemiology of Merkel cell polyomavirus: Evidence for geographically related variant genotypes. *Journal of clinical microbiology*, 52, 1687-1690.
- MARTEL-JANTIN, C., PEDERGNANA, V., NICOL, J. T., LEBLOND, V., TRÉGOUËT, D.-A., TORTEVOYE, P., PLANCOULAIN, S., COURSAGET, P., TOUZÉ, A. & ABEL, L. 2013. Merkel cell polyomavirus infection occurs during early childhood and is transmitted between siblings. *Journal of Clinical Virology*, 58, 288-291.
- MARTIN, H. J., LEE, J. M., WALLS, D., & HAYWARD, S. D. (2007). Manipulation of the toll-like receptor 7 signaling pathway by Epstein-Barr virus. *Journal of virology*, 81(18), 9748-9758.
- MATEER, S. C., FEDOROV, S. A., & MUMBY, M. C. (1998). Identification of structural elements involved in the interaction of simian virus 40 small tumor antigen with protein phosphatase 2A. *Journal of Biological Chemistry*, 273(52), 35339-35346.
- MAURO, C., PACIFICO, F., LAVORGNA, A., MELLONE, S., IANNETTI, A., ACQUAVIVA, R., FORMISANO, S., VITO, P. & LEONARDI, A. 2006. ABIN-1 binds to NEMO/I $\kappa$ B $\beta$  and co-operates with A20 in inhibiting NF- $\kappa$ B. *Journal of Biological Chemistry*, 281, 18482-18488.
- MAY, M. J., D'ACQUISTO, F., MADGE, L. A., GLÖCKNER, J., POBER, J. S. & GHOSH, S. 2000. Selective inhibition of NF- $\kappa$ B activation by a peptide that blocks the interaction of NEMO with the I $\kappa$ B kinase complex. *Science*, 289, 1550-1554.
- MAY, M. J., LARSEN, S. E., SHIM, J. H., MADGE, L. A. & GHOSH, S. 2004. A novel ubiquitin-like domain in I $\kappa$ B kinase  $\beta$  is required for functional activity of the kinase. *Journal of Biological Chemistry*, 279, 45528-45539.
- MAYER-JAEKEL, R. E. & HEMMING, B. A. 1994. Protein phosphatase 2A—a 'menage a trois'. *Trends in cell biology*, 4, 287-291.
- MCDONALD, D. R., MOOSTER, J. L., REDDY, M., BAWLE, E., SECORD, E. & GEHA, R. S. 2007. Heterozygous N-terminal deletion of I $\kappa$ B $\alpha$  results in functional nuclear factor  $\kappa$ B haploinsufficiency, ectodermal dysplasia, and immune deficiency. *Journal of Allergy and Clinical Immunology*, 120, 900-907.
- MEHRANY, K., OTLEY, C. C., WEENIG, R. H., PHILLIPS, P. K., ROENIGK, R. K. & NGUYEN, T. H. 2002. A meta-analysis of the prognostic significance of sentinel lymph node status in Merkel cell carcinoma. *Dermatologic Surgery*, 28, 113-117.
- MELNICK, J., ALLISON, A., BUTEL, J., ECKHART, W., EDDY, B., KIT, S., LEVINE, A., MILES, J., PAGANO, J. & SACHS, L. 1974. Papovaviridae. *Intervirology*, 3, 106-120.
- MERCURIO, F., ZHU, H., MURRAY, B. W., SHEVCHENKO, A., BENNETT, B. L., WU LI, J., YOUNG, D. B., BARBOSA, M., MANN, M. & MANNING, A. 1997. IKK-1 and IKK-2: cytokine-activated I $\kappa$ B kinases essential for NF- $\kappa$ B activation. *Science*, 278, 860-866.
- MERKEL, F. 1875. Tastzellen und Tastkörperchen bei den Haustieren und beim Menschen. *Archiv für mikroskopische Anatomie*, 11, 636-652.
- MEROT, Y., CARRAUX, P. & SAURAT, J. 1987. Merkel cell mitoses in vibrissae: an ultrastructural study. *Journal of anatomy*, 153, 241.
- MILLER, R. W. & RABKIN, C. S. 1999. Merkel cell carcinoma and melanoma: aetiological similarities and differences. *Cancer Epidemiology Biomarkers & Prevention*, 8, 153-158.
- MISHRA, N., PEREIRA, M., RHODES, R. H., AN, P., PIPAS, J. M., JAIN, K., KAPOOR, A., BRIESE, T., FAUST, P.L. & LIPKIN, W. I. (2014). Identification of a novel

- polyomavirus in a pancreatic transplant recipient with retinal blindness and vasculitic myopathy. *Journal of Infectious Diseases*, jiu250.
- MOGHA, A., FAUTREL, A., MOUCHET, N., GUO, N., CORRE, S., ADAMSKI, H., WATIER, E., MISERY, L. & GALIBERT, M.-D. 2010. Merkel cell polyomavirus small T antigen mRNA level is increased following in vivo UV-radiation. *PLoS One*, 5.
- MOLL, R., MOLL, I. & FRANKE, W. W. 1984. Identification of Merkel cells in human skin by specific cytokeratin antibodies:: Changes of cell density and distribution in fetal and adult plantar epidermis. *Differentiation*, 28, 136-154.
- MONTANO, X. I., & LANE, D. P. (1984). Monoclonal antibody to simian virus 40 small t. *Journal of virology*, 51(3), 760-767.
- MOORHEAD, G., DE WEVER, V., TEMPLETON, G. & KERK, D. 2009. Evolution of protein phosphatases in plants and animals. *Biochem. J*, 417, 401-409.
- MORENO, C. S., RAMACHANDRAN, S., ASHBY, D. G., LAYCOCK, N., PLATTNER, C. A., CHEN, W., HAHN, W. C. & PALLAS, D. C. 2004. Signaling and transcriptional changes critical for transformation of human cells by simian virus 40 small tumor antigen or protein phosphatase 2A B56 $\gamma$  knockdown. *Cancer research*, 64, 6978-6988.
- MOURTADA-MAARABOUNI, M. & WILLIAMS, G. T. 2008. Protein phosphatase 4 regulates apoptosis, proliferation and mutation rate of human cells. *Biochimica et Biophysica Acta (BBA)-Molecular Cell Research*, 1783, 1490-1502.
- MUI, M. Z., ZHOU, Y., BLANCHETTE, P., CHUGHTAI, N., KNIGHT, J. F., GRUOSSO, T., PAPADAKIS, A.I., HUANG, S., PARK, M., GINGRAS, A.C. and BRANTON, P.E (2015). The human adenovirus type 5 E4orf4 protein targets two phosphatase regulators of the Hippo signaling pathway. *Journal of virology*, 89(17), 8855-8870.
- MÜLLER, C. W., REY, F. A. & SODEOKA, M. 1995. Structure of the NF- $\kappa$ B p50 homodimer bound to DNA. *Nature*, 373, 311.
- MUMBY, M. C. & WALTER, G. 1993. Protein serine/threonine phosphatases: structure, regulation, and functions in cell growth. *Physiological reviews*, 73, 673-673.
- MUSA, F. & SCHNEIDER, R. 2015. Targeting the PI3K/AKT/mTOR pathway in ovarian cancer. *Translational Cancer Research*, 4, 97-106.
- NAGY, J., FEHÉR, L. Z., SONKODI, I., LESZNYÁK, J., IVÁNYI, B. & PUSKÁS, L. G. 2005. A second field metachronous Merkel cell carcinoma of the lip and the palatine tonsil confirmed by microarray-based comparative genomic hybridisation. *Virchows Archiv*, 446, 278-286.
- NAKADA, S., CHEN, G. I., GINGRAS, A. C. & DUROCHER, D. 2008. PP4 is a  $\gamma$ H2AX phosphatase required for recovery from the DNA damage checkpoint. *EMBO reports*, 9, 1019-1026.
- NAKAMURA, T., SATO, Y., WATANABE, D., ITO, H., SHIMONOHARA, N., TSUJI, T., NAKAJIMA, N., SUZUKI, Y., MATSUO, K., NAKAGAWA, H., & SATA, T. (2010). Nuclear localization of Merkel cell polyomavirus large T antigen in Merkel cell carcinoma. *Virology*, 398(2), 273-279.
- NATHAN, J. A., KIM, H. T., TING, L., GYGI, S. P. & GOLDBERG, A. L. 2013. Why do cellular proteins linked to K63-polyubiquitin chains not associate with proteasomes? *The EMBO journal*, 32, 552-565.
- NEU, U., ALLEN, S.-A. A., BLAUM, B. S., LIU, Y., FRANK, M., PALMA, A. S., STROH, L., FEIZI, T., PETERS, T. & ATWOOD, W. J. 2013. A structure-guided mutation in the major capsid protein retargets BK polyomavirus. *PLoS Pathog*, 9, e1003688.
- NEU, U., HENGEL, H., BLAUM, B. S., SCHOWALTER, R. M., MACEJAK, D., GILBERT, M., WAKARCHUK, W. W., IMAMURA, A., ANDO, H. & KISO, M. 2012. Structures of Merkel cell polyomavirus VP1 complexes define a sialic acid binding site required for infection.
- NICHOLS, D. B. & SHISLER, J. L. 2006. The MC160 protein expressed by the dermatotropic poxvirus molluscum contagiosum virus prevents tumor necrosis factor alpha-induced NF- $\kappa$ B activation via inhibition of I kappa kinase complex formation. *Journal of virology*, 80, 578-586.
- NICOL, J. T., ROBINOT, R., CARPENTIER, A., CARANDINA, G., MAZZONI, E., TOGNON, M., TOUZÉ, A. & COURSAGET, P. 2013. Age-specific seroprevalences of merkel cell polyomavirus, human polyomaviruses 6, 7, and 9, and trichodysplasia spinulosa-associated polyomavirus. *Clinical and Vaccine Immunology*, 20, 363-368.

- NISHIKAWA, M., OMAI, S. B., TOYODA, H., TAWARA, I., SHIMA, H., NAGAO, M., HEMMINGS, B. A., MUMBY, M. C. & DEGUCHI, K. 1994. Expression of the catalytic and regulatory subunits of protein phosphatase type 2A may be differentially modulated during retinoic acid-induced granulocytic differentiation of HL-60 cells. *Cancer research*, 54, 4879-4884.
- OHSHIMA, D. & ICHIKAWA, K. 2014. Regulation of nuclear NF- $\kappa$ B oscillation by a diffusion coefficient and its biological implications. *PLoS One*, 9, e109895.
- OLSEN, J. V., BLAGOEV, B., GNAD, F., MACEK, B., KUMAR, C., MORTENSEN, P., & MANN, M. (2006). Global, in vivo, and site-specific phosphorylation dynamics in signaling networks. *Cell*, 127(3), 635-648.
- PADGETT, B., ZURHEIN, G., WALKER, D., ECKROADE, R. & DESSEL, B. 1971. Cultivation of papova-like virus from human brain with progressive multifocal leucoencephalopathy. *The Lancet*, 297, 1257-1260.
- PALELLA JR, F. J., DELANEY, K. M., MOORMAN, A. C., LOVELESS, M. O., FUHRER, J., SATTEN, G. A., ASCHMAN, D. J. & HOLMBERG, S. D. 1998. Declining morbidity and mortality among patients with advanced human immunodeficiency virus infection. *New England Journal of Medicine*, 338, 853-860.
- PALLAS, D. C., SHAHRIK, L. K., MARTIN, B. L., JASPERS, S., MILLER, T. B., BRAUTIGAN, D. L. & ROBERTS, T. M. 1990. Polyoma small and middle T antigens and SV40 small t antigen form stable complexes with protein phosphatase 2A. *Cell*, 60, 167-176.
- PASTRANA, D. V., TOLSTOV, Y. L., BECKER, J. C., MOORE, P. S., CHANG, Y. & BUCK, C. B. 2009. Quantitation of human seroresponsiveness to Merkel cell polyomavirus. *PLoS Pathog*, 5, e1000578.
- PAULSON, K. G., LEMOS, B. D., FENG, B., JAIMES, N., PEÑAS, P. F., BI, X., MAHER, E., COHEN, L., LEONARD, J. H. & GRANTER, S. R. 2009. Array-CGH reveals recurrent genomic changes in Merkel cell carcinoma including amplification of L-Myc. *Journal of Investigative Dermatology*, 129, 1547-1555.
- PEARSE, A. 1980. The neuroendocrine (APUD) cells of the skin. *The American Journal of Dermatopathology*, 2, 121-123.
- PEARSE, A. 1986. The diffuse neuroendocrine system: peptides, amines, placodes and the APUD theory. *Progress in brain research*, 68, 25.
- PÉREZ-GIL, G., LANDA-CARDEÑA, A., COUTIÑO, R., GARCÍA-ROMÁN, R., SAMPIERI, C., MORA, S. & MONTERO, H. 2015. 4EBP1 Is Dephosphorylated by Respiratory Syncytial Virus Infection. *Intervirology*, 58, 205-208.
- PILLONI, L., MANIELI, C., SENES, G., RIBUFFO, D. & FAA, G. 2009. Merkel cell carcinoma with an unusual immunohistochemical profile. *European journal of histochemistry: EJH*, 53.
- PIM, D., MASSIMI, P., DILWORTH, S. M. & BANKS, L. 2005. Activation of the protein kinase B pathway by the HPV-16 E7 oncoprotein occurs through a mechanism involving interaction with PP2A. *Oncogene*, 24, 7830-7838.
- PISKOROWSKI, R., HAEBERLE, H., PANDITRAO, M. V. & LUMPKIN, E. A. 2008. Voltage-activated ion channels and Ca<sup>2+</sup>-induced Ca<sup>2+</sup> release shape Ca<sup>2+</sup> signaling in Merkel cells. *Pflügers Archiv-European Journal of Physiology*, 457, 197-209.
- POLIVKA, J. & JANKU, F. 2014. Molecular targets for cancer therapy in the PI3K/AKT/mTOR pathway. *Pharmacology & therapeutics*, 142, 164-175.
- POULIN, D. L. & DECAPRIO, J. A. 2006. Is there a role for SV40 in human cancer? *Journal of clinical oncology*, 24, 4356-4365.
- PRICE, N. E. & MUMBY, M. C. 2000. Effects of regulatory subunits on the kinetics of protein phosphatase 2A. *Biochemistry*, 39, 11312-11318.
- PUNTENER, D., & GREBER, U. F. 2009. DNA-tumor virus entry—From plasma membrane to the nucleus. In *Seminars in cell & developmental biology* (Vol. 20, No. 5, pp. 631-642). Academic Press.
- PURDIE, K. J., PENNINGTON, J., PROBY, C. M., KHALAF, S., DE VILLIERS, E. M., LEIGH, I. M. & STOREY, A. 1999. The promoter of a novel human papillomavirus (HPV77) associated with skin cancer displays UV responsiveness, which is mediated through a consensus p53 binding sequence. *The EMBO journal*, 18, 5359-5369.
- RAHIGHI, S., IKEDA, F., KAWASAKI, M., AKUTSU, M., SUZUKI, N., KATO, R., KENSCHKE, T., UEJIMA, T., BLOOR, S., KOMANDER, D. & RANDOW, F. (2009). Specific

- recognition of linear ubiquitin chains by NEMO is important for NF- $\kappa$ B activation. *Cell*, 136(6), 1098-1109.
- RANDALL, C. M., JOKELA, J. A. & SHISLER, J. L. 2012. The MC159 protein from the molluscum contagiosum poxvirus inhibits NF- $\kappa$ B activation by interacting with the I $\kappa$ B kinase complex. *The Journal of Immunology*, 188, 2371-2379.
- RAO, P., HAYDEN, M. S., LONG, M., SCOTT, M. L., WEST, A. P., ZHANG, D., OECKINGHAUS, A., LYNCH, C., HOFFMANN, A. & BALTIMORE, D. 2010. I [kgr] B [bgr] acts to inhibit and activate gene expression during the inflammatory response. *Nature*, 466, 1115-1119.
- RICHARDS, K. H., Wasson, C. W., Watherston, O., Doble, R., Blair, G. E., Wittmann, M., & Macdonald, A. (2015). The human papillomavirus (HPV) E7 protein antagonises an Imiquimod-induced inflammatory pathway in primary human keratinocytes. *Scientific reports*, 5.
- RIDD, K., YU, S. & BASTIAN, B. C. 2009. The presence of polyomavirus in non-melanoma skin cancer in organ transplant recipients is rare. *The Journal of investigative dermatology*, 129, 250.
- RIGHI, A., BETTS, C. M., MARCHETTI, C., MARUCCI, G., MONTEBUGNOLI, L., PRATI, C., EUSEBI, L. H., MUZZI, L., RAGAZZINI, T. & FOSCHINI, M. P. 2006. Merkel cells in the oral mucosa. *International journal of surgical pathology*, 14, 206-211.
- RILEY, M. I., YOO, W., MDA, N. Y. & FOLK, W. R. 1997. Tiny T antigen: an autonomous polyomavirus T antigen amino-terminal domain. *Journal of virology*, 71, 6068-6074.
- RINALDO, C. H., TRAAVIK, T. & HEY, A. 1998. The agnogene of the human polyomavirus BK is expressed. *Journal of virology*, 72, 6233-6236.
- ROCAK, S. & LINDER, P. 2004. DEAD-box proteins: the driving forces behind RNA metabolism. *Nature Reviews Molecular Cell Biology*, 5, 232-241.
- RODIG, S. J., CHENG, J., WARDZALA, J., DOROSARIO, A., SCANLON, J. J., LAGA, A. C., MARTINEZ-FERNANDEZ, A., BARLETTA, J. A., BELLIZZI, A. M. & SADASIVAM, S. 2012. Improved detection suggests all Merkel cell carcinomas harbor Merkel polyomavirus. *The Journal of clinical investigation*, 122, 4645.
- RODRIGUEZ-VICIANA, P., COLLINS, C. & FRIED, M. 2006. Polyoma and SV40 proteins differentially regulate PP2A to activate distinct cellular signaling pathways involved in growth control. *Proceedings of the National Academy of Sciences*, 103, 19290-19295.
- RONAI, Z. & WEINSTEIN, I. 1988. Identification of a UV-induced trans-acting protein that stimulates polyomavirus DNA replication. *Journal of virology*, 62, 1057-1060.
- RONAI, Z. A. & WEINSTEIN, I. B. 1990. Identification of ultraviolet-inducible proteins that bind to a TGACAACA sequence in the polyoma virus regulatory region. *Cancer research*, 50, 5374-5381.
- ROOHVAND, F., MAILLARD, P., LAVERGNE, J.-P., BOULANT, S., WALIC, M., ANDRÉO, U., GOUESLAIN, L., HELLE, F., MALLET, A. & MCLAUCHLAN, J. 2009. Initiation of Hepatitis C Virus Infection Requires the Dynamic Microtubule Network ROLE OF THE VIRAL NUCLEOCAPSID PROTEIN. *Journal of Biological Chemistry*, 284, 13778-13791.
- ROSEN, S., HARMON, W., KRENSKY, A. M., EDELSON, P. J., PADGETT, B. L., GRINNELL, B. W., RUBINO, M. J. & WALKER, D. L. 1983. Tubulo-interstitial nephritis associated with polyomavirus (BK type) infection. *New England Journal of Medicine*, 308, 1192-1196.
- RUDOLPH, D., YE, W.-C., WAKEHAM, A., RUDOLPH, B., NALLAINATHAN, D., POTTER, J., ELIA, A. J. & MAK, T. W. 2000. Severe liver degeneration and lack of NF- $\kappa$ B activation in NEMO/IKK $\gamma$ -deficient mice. *Genes & development*, 14, 854-862.
- RUEDIGER, R., PHAM, H. T. & WALTER, G. 2001. Disruption of protein phosphatase 2A subunit interaction in human cancers with mutations in the A $\alpha$  subunit gene. *Oncogene*, 20, 10-15.
- RUEDIGER, R., RUIZ, J. & WALTER, G. 2011. Human cancer-associated mutations in the A $\alpha$  subunit of protein phosphatase 2A increase lung cancer incidence in A $\alpha$  knock-in and knockout mice. *Molecular and cellular biology*, 31, 3832-3844.
- RUSHE, M., SILVIAN, L., BIXLER, S., CHEN, L. L., CHEUNG, A., BOWES, S., Cuervo, H., Berkowitz, S., Zheng, T., Guckian, K. & PELLEGRINI, M. (2008). Structure of a NEMO/IKK-associating domain reveals architecture of the interaction site. *Structure*, 16(5), 798-808.

- RUTBERG, S. E., YANG, Y. M. & RONAI, Z. 1992. Functional role of the ultraviolet light responsive element (URE; TGACAACA) in the transcription and replication of polyoma DNA. *Nucleic acids research*, 20, 4305-4310.
- RYSECK, R.-P., BULL, P., TAKAMIYA, M., BOURS, V., SIEBENLIST, U., DOBRZANSKI, P. & BRAVO, R. 1992. RelB, a new Rel family transcription activator that can interact with p50-NF-kappa B. *Molecular and cellular biology*, 12, 674-684.
- SABLINA, A. A. & HAHN, W. C. 2007. The role of PP2A A subunits in tumor suppression. *Cell adhesion & migration*, 1, 140-141.
- SACHDEV, S., HOFFMANN, A. & HANNINK, M. 1998. Nuclear localization of I $\kappa$ B $\alpha$  is mediated by the second ankyrin repeat: the I $\kappa$ B $\alpha$  ankyrin repeats define a novel class of cis-acting nuclear import sequences. *Molecular and cellular biology*, 18, 2524-2534.
- SADEGHI, M., RIIPINEN, A., VAISANEN, E., CHEN, T., KANTOLA, K., SURCEL, H.-M., KARIKOSKI, R., TASKINEN, H., SODERLUND-VENERMO, M. & HEDMAN, K. 2010. Newly discovered KI, WU, and Merkel cell polyomaviruses: no evidence of mother-to-fetus transmission. *Virology*, 407, 251.
- SADOWSKA, B., BARRUCCO, R., KHALILI, K. & SAFAK, M. 2003. Regulation of human polyomavirus JC virus gene transcription by AP-1 in glial cells. *Journal of virology*, 77, 665-672.
- SAENZ-ROBLES, M. T., SULLIVAN, C. S. & PIPAS, J. M. 2001. Transforming functions of simian virus 40. *Oncogene*, 20, 7899-7907.
- SALÁKOVÁ, M., KOŠLABOVÁ, E., VOJTĚCHOVÁ, Z., TACHEZY, R. & ŠROLLER, V. 2015. The detection of human polyomaviruses MCPyV, HPyV6, and HPyV7 in malignant and non-malignant tonsillar tissues. *Journal of medical virology*.
- SAPP, M. & DAY, P. M. 2009. Structure, attachment and entry of polyoma- and papillomaviruses. *Virology*, 384, 400-409.
- SAURAT, J.-H., DIDIERJEAN, L., SKALLI, O., SIEGENTHALER, G. & GABBIANI, G. 1984. The intermediate filament proteins of rabbit normal epidermal Merkel cells are cytokeratins. *Journal of investigative dermatology*, 83, 431-435.
- SAUVAGE, V., FOULONGNE, V., CHEVAL, J., AR GOUILH, M., PARIENTE, K., DEREURE, O., MANUGUERRA, J. C., RICHARDSON, J., LECUIT, M. & BURGUIÈRE, A. 2011. Human polyomavirus related to African green monkey lymphotropic polyomavirus. *Emerg Infect Dis*, 17, 1364-70.
- SAXOD, R. 1978. Development of Cutaneous Sensory Receptors Birds. *Development of sensory systems*. Springer.
- SCARIA, V. & JADHAV, V. 2007. microRNAs in viral oncogenesis. *Retrovirology*, 4, 82.
- SCHEIDEREIT, C. (2006). I $\kappa$ B kinase complexes: gateways to NF-kappaB activation and transcription. *Oncogene* 25, 6685–6705.
- SCHNEIDER, S., THURNHER, D. & EROVIC, B. M. 2013. Merkel cell carcinoma: interdisciplinary management of a rare disease. *Journal of skin cancer*, 2013.
- SCHOWALTER, R. M. & BUCK, C. B. 2013. The Merkel cell polyomavirus minor capsid protein.
- SCHOWALTER, R. M., PASTRANA, D. V., PUMPHREY, K. A., MOYER, A. L. & BUCK, C. B. 2010. Merkel cell polyomavirus and two previously unknown polyomaviruses are chronically shed from human skin. *Cell host & microbe*, 7, 509-515.
- SCHOWALTER, R. M., REINHOLD, W. C. & BUCK, C. B. 2012. Entry tropism of BK and Merkel cell polyomaviruses in cell culture. *PLoS One*, 7, e42181.
- SCHWARZ, T. & SCHWARZ, A. 2011. Molecular mechanisms of ultraviolet radiation-induced immunosuppression. *European journal of cell biology*, 90, 560-564.
- SEBBAN-BENIN, H., PESCATORE, A., FUSCO, F., PASCUALE, V., GAUTHERON, J., YAMAOKA, S., MONCLA A, URSINI MV, & COURTOIS, G. (2007). Identification of TRAF6-dependent NEMO polyubiquitination sites through analysis of a new NEMO mutation causing incontinentia pigmenti. *Human molecular genetics*, 16(23), 2805-2815.
- SENDA, T., MATSUMINE, A., YANAI, H. & AKIYAMA, T. 1999. Localization of MCC (mutated in colorectal cancer) in various tissues of mice and its involvement in cell differentiation. *Journal of Histochemistry & Cytochemistry*, 47, 1149-1157.

- SENFLEBEN, U., CAO, Y., XIAO, G., GRETEN, F. R., KRÄHN, G., BONIZZI, G., CHEN, Y., HU, Y., FONG, A. & SUN, S.-C. 2001. Activation by IKK $\alpha$  of a second, evolutionary conserved, NF- $\kappa$ B signaling pathway. *Science*, 293, 1495-1499.
- SEO, G., FINK, L., O'HARA, B., ATWOOD, W. & SULLIVAN, C. 2008. Evolutionarily conserved function of a viral microRNA. *Journal of virology*, 82, 9823-9828.
- SEO, G. J., CHEN, C. J. & SULLIVAN, C. S. 2009. Merkel cell polyomavirus encodes a microRNA with the ability to autoregulate viral gene expression. *Virology*, 383, 183-187.
- SHAHZAD, N., SHUDA, M., GHEIT, T., KWUN, H. J., CORNET, I., SAIDJ, D., ZANNETTI, C., HASAN, U., CHANG, Y. & MOORE, P. S. 2013. The T antigen locus of Merkel cell polyomavirus downregulates human Toll-like receptor 9 expression. *Journal of virology*, 87, 13009-13019.
- SHEMBADE, N., MA, A. & HARHAJ, E. W. 2010. Inhibition of NF- $\kappa$ B signaling by A20 through disruption of ubiquitin enzyme complexes. *Science*, 327, 1135-1139.
- SHIH, V. F., DAVIS-TURAK, J., MACAL, M., HUANG, J. Q., PONOMARENKO, J., KEARNS, J. D., & HOFFMANN, A. (2012). Control of RelB during dendritic cell activation integrates canonical and noncanonical NF- $\kappa$ B pathways. *Nature immunology*, 13(12), 1162-1170.
- SHIM, J.-H., XIAO, C., PASCHAL, A. E., BAILEY, S. T., RAO, P., HAYDEN, M. S., LEE, K.-Y., BUSSEY, C., STECKEL, M. & TANAKA, N. 2005. TAK1, but not TAB1 or TAB2, plays an essential role in multiple signaling pathways in vivo. *Genes & development*, 19, 2668-2681.
- SHTRICHMAN, R., SHARF, R., BARR, H., DOBNER, T., & KLEINBERGER, T. (1999). Induction of apoptosis by adenovirus E4orf4 protein is specific to transformed cells and requires an interaction with protein phosphatase 2A. *Proceedings of the National Academy of Sciences*, 96(18), 10080-10085.
- SHUDA, M., FENG, H., KWUN, H. J., ROSEN, S. T., GJOERUP, O., MOORE, P. S. & CHANG, Y. 2008. T antigen mutations are a human tumor-specific signature for Merkel cell polyomavirus. *Proceedings of the National Academy of Sciences*, 105, 16272-16277.
- SHUDA, M., KWUN, H. J., FENG, H., CHANG, Y. & MOORE, P. S. 2011. Human Merkel cell polyomavirus small T antigen is an oncoprotein targeting the 4E-BP1 translation regulator. *The Journal of clinical investigation*, 121, 3623.
- SIDIROPOULOS, M., HANNA, W., RAPHAEL, S. J. & GHORAB, Z. 2011. Expression of TdT in Merkel cell carcinoma and small cell lung carcinoma. *American journal of clinical pathology*, 135, 831-838.
- SIEBRASSE, E. A., REYES, A., LIM, E. S., ZHAO, G., MKAKOSYA, R. S., MANARY, M. J., GORDON, J. I. & WANG, D. 2012. Identification of MW polyomavirus, a novel polyomavirus in human stool. *Journal of virology*, 86, 10321-10326.
- SOLT, L. A., MADGE, L. A., & MAY, M. J. (2009). NEMO-binding domains of both IKK $\alpha$  and IKK $\beta$  regulate I $\kappa$ B kinase complex assembly and classical NF- $\kappa$ B activation. *Journal of Biological Chemistry*, 284(40), 27596-27608.
- SONTAG, E., FEDOROV, S., KAMIBAYASHI, C., ROBBINS, D., COBB, M. & MUMBY, M. 1993. The interaction of SV40 small tumor antigen with protein phosphatase 2A stimulates the map kinase pathway and induces cell proliferation. *Cell*, 75, 887-897.
- SONTAG, E., SONTAG, J. M., & GARCIA, A. (1997). Protein phosphatase 2A is a critical regulator of protein kinase C  $\zeta$  signaling targeted by SV40 small t to promote cell growth and NF- $\kappa$ B activation. *The EMBO Journal*, 16(18), 5662-5671.
- SPURGEON, M. E., CHENG, J., BRONSON, R. T., LAMBERT, P. F. & DECAPRIO, J. A. 2015. Tumorigenic activity of Merkel cell polyomavirus T antigens expressed in the stratified epithelium of mice. *Cancer research*, 75, 1068-1079.
- STEWART, S. E., EDDY, B. E. & BORGESSE, N. 1958. Neoplasms in mice inoculated with a tumor agent carried in tissue culture. *Journal of the National Cancer Institute*, 20, 1223-1243.
- SULLIVAN, C. S., GRUNDHOFF, A. T., TEVETHIA, S., PIPAS, J. M. & GANEM, D. 2005. SV40-encoded microRNAs regulate viral gene expression and reduce susceptibility to cytotoxic T cells. *Nature*, 435, 682-686.
- SWEET, B. H. & HILLEMANN, M. R. 1960. The vacuolating virus, SV 40. *Experimental Biology and Medicine*, 105, 420-427.

- SYRIGOS KN, TZANNOU I, KATIRTZOGLU N, GEORGIU E. Skin cancer in the elderly. *In Vivo* 2005; 19(3):643-52.
- TADMOR, T., AVIV, A. & POLLIACK, A. 2011. Merkel cell carcinoma, chronic lymphocytic leukemia and other lymphoproliferative disorders: an old bond with possible new viral ties. *Annals of Oncology*, 22, 250-256.
- TAIRA, K., NARISAWA, Y., NAKAFUSA, J., MISAGO, N. & TANAKA, T. 2002. Spatial relationship between Merkel cells and Langerhans cells in human hair follicles. *Journal of dermatological science*, 30, 195-204.
- TANG, C. K. & TOKER, C. 1978. Trabecular carcinoma of the skin. An ultrastructural study. *Cancer*, 42, 2311-2321.
- TEGETHOFF, S., BEHLKE, J., & SCHEIDEREIT, C. (2003). Tetrameric oligomerization of I $\kappa$ B kinase  $\gamma$  (IKK $\gamma$ ) is obligatory for IKK complex activity and NF- $\kappa$ B activation. *Molecular and cellular biology*, 23(6), 2029-2041.
- TENNVALL, J., BIÖRKLUND, A., JOHANSSON, L. & AKERMAN, M. 1989. Merkel cell carcinoma: management of primary, recurrent and metastatic disease. A clinicopathological study of 17 patients. *European journal of surgical oncology: the journal of the European Society of Surgical Oncology and the British Association of Surgical Oncology*, 15, 1-9.
- THEISS, J. M., GÜNTHER, T., ALAWI, M., NEUMANN, F., TESSMER, U., FISCHER, N., & GRUNDHOFF, A. (2015). A Comprehensive Analysis of Replicating Merkel Cell Polyomavirus Genomes Delineates the Viral Transcription Program and Suggests a Role for mcv-miR-M1 in Episomal Persistence. *PLoS Pathog*, 11(7), e1004974.
- TIKHONOVA, A. & AIFANTIS, I. 2012. The Taming of the NF- $\kappa$ B: PP4R1 navigates while PP4c dephosphorylates. *Immunity*, 37, 594-596.
- TOKER, C. 1972. Trabecular carcinoma of the skin. *Archives of dermatology*, 105, 107-110.
- TOKUNAGA, F., SAKATA, S. I., SAEKI, Y., SATOMI, Y., KIRISAKO, T., KAMEI, K., NAKAGAWA, T., KATO, M., MURATA, S., YAMAOKA, S. & YAMAMOTO, M. (2009). Involvement of linear polyubiquitylation of NEMO in NF- $\kappa$ B activation. *Nature cell biology*, 11(2), 123-132.
- TOLANI, B., MATTA, H., GOPALAKRISHNAN, R., PUNJ, V., & CHAUDHARY, P. M. (2014). NEMO is essential for Kaposi's sarcoma-associated herpesvirus-encoded vFLIP K13-induced gene expression and protection against death receptor-induced cell death, and its N-terminal 251 residues are sufficient for this process. *Journal of virology*, 88(11), 6345-6354.
- TOLSTOV, Y. L., PASTRANA, D. V., FENG, H., BECKER, J. C., JENKINS, F. J., MOSCHOS, S., CHANG, Y., BUCK, C. B. & MOORE, P. S. 2009. Human Merkel cell polyomavirus infection II. MCV is a common human infection that can be detected by conformational capsid epitope immunoassays. *International journal of cancer*, 125, 1250-1256.
- TOUZÉ, A., GAITAN, J., ARNOLD, F., CAZAL, R., FLEURY, M. J., COMBELAS, N., SIZARET, P.-Y., GUYETANT, S., MARUANI, A. & BAAY, M. 2010. Generation of Merkel cell polyomavirus (MCV)-like particles and their application to detection of MCV antibodies. *Journal of clinical microbiology*, 48, 1767-1770.
- TOYO-OKA, K., MORI, D., YANO, Y., SHIOTA, M., IWAO, H., GOTO, H., INAGAKI, M., HIRAIWA, N., MURAMATSU, M. & WYNshaw-BORIS, A. 2008. Protein phosphatase 4 catalytic subunit regulates Cdk1 activity and microtubule organization via NDEL1 dephosphorylation. *The Journal of cell biology*, 180, 1133-1147.
- TROWBRIDGE, P. W. & FRISQUE, R. J. 1995. Identification of three new JC virus proteins generated by alternative splicing of the early viral mRNA. *Journal of neurovirology*, 1, 195-206.
- TRUITT, M. L., CONN, C. S., SHI, Z., PANG, X., TOKUYASU, T., COADY, A. M., SEO, Y., BARNA, M. & RUGGERO, D. 2015. Differential requirements for eIF4E dose in normal development and cancer. *Cell*, 162, 59-71.
- TSAI, B., GILBERT, J. M., STEHLE, T., LENCER, W., BENJAMIN, T. L. & RAPOPORT, T. A. 2003. Gangliosides are receptors for murine polyoma virus and SV40. *The EMBO journal*, 22, 4346-4355.
- TSANG, S. H., WANG, X., LI, J., BUCK, C. B. & YOU, J. 2014. Host DNA damage response factors localize to Merkel cell polyomavirus DNA replication sites to support efficient viral DNA replication. *Journal of virology*, 88, 3285-3297.

- TSUCHIYA, Y., ASANO, T., NAKAYAMA, K., KATO, T., KARIN, M. & KAMATA, H. 2010. Nuclear IKK $\beta$  is an adaptor protein for I $\kappa$ B $\alpha$  ubiquitination and degradation in UV-induced NF- $\kappa$ B activation. *Molecular cell*, 39, 570-582.
- TWEEDLE, C. 1978. Ultrastructure of Merkel cell development in aneurogenic and control amphibian larvae (*Ambystoma*). *Neuroscience*, 3, 481-486.
- VALENTINE, R., DAWSON, C. W., HU, C., SHAH, K. M., OWEN, T. J., DATE, K. L., MAIA, S.P., SHAO, J., ARRAND, J.R., YOUNG, L.S. & O'NEIL, J. (2010). Epstein-Barr virus-encoded EBNA1 inhibits the canonical NF- $\kappa$ B pathway in carcinoma cells by inhibiting IKK phosphorylation. *Molecular cancer*, 9(1), 1.
- VAN DER MEIJDEN, E., JANSSENS, R., LAUBER, C., BOUWES BAVINCK, J. N., GORBALENYA, A. E. & FELTKAMP, M. 2010. Discovery of a new human polyomavirus associated with trichodysplasia spinulosa in an immunocompromized patient. *PLoS Pathog*, 6, e1001024.
- VAN GELE, M., VAN ROY, N., RONAN, S., MESSIAEN, L., VANDESOMPELE, J., GEERTS, M., NAEYAERT, J., BLENNOW, E., BAR-AM, I. & DAS GUPTA, T. 1998. Molecular analysis of 1p36 breakpoints in two Merkel cell carcinomas. *Genes, Chromosomes and Cancer*, 23, 67-71.
- VANLOOCK, M. S., ALEXANDROV, A., YU, X., COZZARELLI, N. R. & EGELMAN, E. H. 2002. SV40 large T antigen hexamer structure: domain organization and DNA-induced conformational changes. *Current biology*, 12, 472-476.
- VERMA, I. M., STEVENSON, J. K., SCHWARZ, E. M., VAN ANTWERP, D. & MIYAMOTO, S. 1995. Rel/NF-kappa B/I kappa B family: intimate tales of association and dissociation. *Genes & development*, 9, 2723-2735.
- VERNADAKIS, S., MORIS, D., BANKFALVI, A., MAKRIS, N. & SOTIROPOULOS, G. C. 2013. Metastatic Merkel cell carcinoma (MCC) of pancreas and breast: a unique case. *World J. Surg. Oncol*, 11, 261.
- VINCENT, I. E., ZANNETTI, C., LUCIFORA, J., NORDER, H., PROTZER, U., HAINAUT, P., ZOULIM, F., TOMMASINO, M., TRÉPO, C., HASAN, U. & CHEMIN, I. (2011). Hepatitis B virus impairs TLR9 expression and function in plasmacytoid dendritic cells. *PLoS One*, 6(10).
- VINOLO, E., SEBBAN, H., CHAFFOTTE, A., ISRAËL, A., COURTOIS, G., VÉRON, M., & AGOU, F. (2006). A point mutation in NEMO associated with anhidrotic ectodermal dysplasia with immunodeficiency pathology results in destabilization of the oligomer and reduces lipopolysaccharide-and tumor necrosis factor-mediated NF- $\kappa$ B activation. *Journal of Biological Chemistry*, 281(10), 6334-6348.
- VINCENDEAU, M., HADIAN, K., MESSIAS, A. C., BRENKE, J. K., HALANDER, J., GRIESBACH, R., GREZMIEL, U., BERTOSSI, A., STEHLE, R. & NAGEL, D. 2016. Inhibition of Canonical NF- $\kappa$ B Signaling by a Small Molecule Targeting NEMO-Ubiquitin Interaction. *Scientific reports*, 6, 18934.
- VISCIDI, R. P., ROLLISON, D. E., SONDAK, V. K., SILVER, B., MESSINA, J. L., GIULIANO, A. R., FULP, W., AJIDAHUN, A. & RIVANERA, D. (2011). Age-specific seroprevalence of Merkel cell polyomavirus, BK virus, and JC virus. *Clinical and Vaccine Immunology*, 18(10), 1737-1743.
- WAGNER, S., CARPENTIER, I., ROGOV, V., KREIKE, M., IKEDA, F., LÖHR, F., WU, C., ASHWELL, J., DÖTSCH, V. & DIKIC, I. 2008. Ubiquitin binding mediates the NF- $\kappa$ B inhibitory potential of ABIN proteins. *Oncogene*, 27, 3739-3745.
- WALCZAK, H., IWAI, K. & DIKIC, I. 2012. Generation and physiological roles of linear ubiquitin chains. *BMC biology*, 10, 23.
- WANG, B., ZHAO, A., SUN, L., ZHONG, X., ZHONG, J., WANG, H., CAI, M., LI, J., XU, Y. & LIAO, J. 2008. Protein phosphatase PP4 is overexpressed in human breast and lung tumors. *Cell research*, 18, 974.
- WANG, S. S., ESPLIN, E. D., LI, J. L., HUANG, L., GAZDAR, A., MINNA, J. & EVANS, G. A. 1998. Alterations of the PPP2R1B gene in human lung and colon cancer. *Science*, 282, 284-287.
- WANG, X., LI, J., SCHOWALTER, R. M., JIAO, J., BUCK, C. B., & YOU, J. (2012). Bromodomain protein Brd4 plays a key role in Merkel cell polyomavirus DNA replication. *PLoS Pathog*, 8(11), e1003021.
- WATANABE, S. & YOSHIIKE, K. 1986. Evolutionary changes of transcriptional control region in a minute-plaque viable deletion mutant of BK virus. *Journal of virology*, 59, 260-266.

- WENG, S., WANG, H., CHEN, W., KATZ, M. H., CHATTERJEE, D., LEE, J. E., PISTERS, P. W., GOMEZ, H. F., ABBRUZZESE, J. L. & FLEMING, J. B. 2012. Overexpression of protein phosphatase 4 correlates with poor prognosis in patients with stage II pancreatic ductal adenocarcinoma. *Cancer Epidemiology Biomarkers & Prevention*, 21, 1336-1343.
- WESSEL, R., SCHWEIZER, J. & STAHL, H. 1992. Simian virus 40 T-antigen DNA helicase is a hexamer which forms a binary complex during bidirectional unwinding from the viral origin of DNA replication. *Journal of Virology*, 66, 804-815.
- WHALEN, K. A., DE JESUS, R., KEAN, J. A. & SCHAFFHAUSEN, B. S. 2005. Genetic analysis of the polyomavirus DnaJ domain. *Journal of virology*, 79, 9982-9990.
- WHITE, M. K., SAFAK, M. & KHALILI, K. 2009. Regulation of gene expression in primate polyomaviruses. *Journal of virology*, 83, 10846-10856.
- WHITESIDE, S. T. & ISRAËL, A. I $\kappa$ B proteins: structure, function and regulation. *Seminars in cancer biology*, 1997. Elsevier, 75-82.
- WIELAND, U., MAUCH, C., KREUTER, A., KRIEG, T. & PFISTER, H. 2009. Merkel cell polyomavirus DNA in persons without merkel cell carcinoma. *Emerging infectious diseases*, 15, 1496.
- WOLF-PEETERS, D., MARIEN, K., MEBIS, J. & DESMET, V. 1980. A cutaneous APUDoma or Merkel cell tumor? A morphologically recognizable tumor with a biological and histological malignant aspect in contrast with its clinical behavior. *Cancer*, 46, 1810-1816.
- WOOLFORD, L., RECTOR, A., VAN RANST, M., DUCKI, A., BENNETT, M. D., NICHOLLS, P. K., WARREN, K. S., SWAN, R. A., WILCOX, G. E. & O'HARA, A. J. 2007. A novel virus detected in papillomas and carcinomas of the endangered western barred bandicoot (*Perameles bougainville*) exhibits genomic features of both the Papillomaviridae and Polyomaviridae. *Journal of virology*, 81, 13280-13290.
- XIAO, G., & SUN, S. C. (2000). Negative regulation of the nuclear factor  $\kappa$ B-inducing kinase by a cis-acting domain. *Journal of Biological Chemistry*, 275(28), 21081-21085.
- XIE, H., LEE, L., CARAMUTA, S., HÖÖG, A., BROWALDH, N., BJÖRNHAGEN, V., LARSSON, C. & LUI, W.-O. 2014. MicroRNA expression patterns related to merkel cell polyomavirus infection in human merkel cell carcinoma. *Journal of Investigative Dermatology*, 134, 507-517.
- XU, G., LO, Y.-C., LI, Q., NAPOLITANO, G., WU, X., JIANG, X., DREANO, M., KARIN, M. & WU, H. 2011. Crystal structure of inhibitor of [kgr] B kinase [bgr]. *Nature*, 472, 325-330.
- YAMAOKA, S., COURTOIS, G., BESSIA, C., WHITESIDE, S. T., WEIL, R., AGOU, F., KIRK, H. E., KAY, R. J. & ISRAËL, A. 1998. Complementation cloning of NEMO, a component of the I $\kappa$ B kinase complex essential for NF- $\kappa$ B activation. *Cell*, 93, 1231-1240.
- YANG, J., FAN, G. H., WADZINSKI, B. E., SAKURAI, H., & RICHMOND, A. (2001). Protein phosphatase 2A interacts with and directly dephosphorylates RelA. *Journal of Biological Chemistry*, 276(51), 47828-47833.
- YANG, Y., XIA, F., HERMANCE, N., MABB, A., SIMONSON, S., MORRISSEY, S., GANDHI, P., MUNSON, M., MIYAMOTO, S. & KELLIHER, M. A. 2011. A cytosolic ATM/NEMO/RIP1 complex recruits TAK1 to mediate the NF- $\kappa$ B and p38 mitogen-activated protein kinase (MAPK)/MAPK-activated protein 2 responses to DNA damage. *Molecular and cellular biology*, 31, 2774-2786.
- YOGO, Y., SUGIMOTO, C., ZHENG, H. Y., IKEGAYA, H., TAKASAKA, T., & KITAMURA, T. (2004). JC virus genotyping offers a new paradigm in the study of human populations. *Reviews in medical virology*, 14(3), 179-191.
- YOSHIKAWA, A., SATO, Y., YAMASHITA, M., MIMURA, H., YAMAGATA, A., & FUKAI, S. (2009). Crystal structure of the NEMO ubiquitin-binding domain in complex with Lys 63-linked di-ubiquitin. *FEBS letters*, 583(20), 3317-3322.
- YU, G., GRENINGER, A. L., ISA, P., PHAN, T. G., MARTÍNEZ, M. A., DE LA LUZ SANCHEZ, M., CONTRERAS, J. F., SANTOS-PRECIADO, J. I., PARSONNET, J. & MILLER, S. 2012. Discovery of a novel polyomavirus in acute diarrheal samples from children.
- YU, Y., KUDCHODKAR, S. B. & ALWINE, J. C. 2005. Effects of simian virus 40 large and small tumor antigens on mammalian target of rapamycin signaling: small tumor

- antigen mediates hypophosphorylation of eIF4E-binding protein 1 late in infection. *Journal of virology*, 79, 6882-6889.
- ZANDI, E., ROTHWART, D. M., DELHASE, M., HAYAKAWA, M. & KARIN, M. 1997. The I $\kappa$ B kinase complex (IKK) contains two kinase subunits, IKK $\alpha$  and IKK $\beta$ , necessary for I $\kappa$ B phosphorylation and NF- $\kappa$ B activation. *Cell*, 91, 243-252.
- ZERRAHN, J., KNIPPSCHILD, U., WINKLER, T. & DEPERT, W. 1993. Independent expression of the transforming amino-terminal domain of SV40 large I antigen from an alternatively spliced third SV40 early mRNA. *The EMBO journal*, 12, 4739.
- ZHANG, C., LIU, F., HE, Z., DENG, Q., PAN, Y., LIU, Y., ZHANG, C., NING, T., GUO, C. & LIANG, Y. 2014. Seroprevalence of Merkel cell polyomavirus in the general rural population of Anyang, China.
- ZHANG, G., LIU, R., ZHONG, Y., PLOTNIKOV, A. N., ZHANG, W., ZENG, L., RUSINOVA, E., GERONA-NEVARRO, G., MOSHKINA, N., JOSHUA, J. & CHUANG, P. Y. (2012). Down-regulation of NF- $\kappa$ B transcriptional activity in HIV-associated kidney disease by BRD4 inhibition. *Journal of Biological Chemistry*, 287(34), 28840-28851.
- ZHANG, J., Clark, K., Lawrence, T., Pegg, M. W., & Cohen, P. (2014). An unexpected twist to the activation of IKK $\beta$ : TAK1 primes IKK $\beta$  for activation by autophosphorylation. *Biochemical Journal*, 461(3), 531-537.
- ZHANG, X., OZAWA, Y., LEE, H., WEN, Y.-D., TAN, T.-H., WADZINSKI, B. E. & SETO, E. 2005. Histone deacetylase 3 (HDAC3) activity is regulated by interaction with protein serine/threonine phosphatase 4. *Genes & development*, 19, 827-839.
- ZHOU, G., BOOMER, J. S. & TAN, T.-H. 2004. Protein phosphatase 4 is a positive regulator of hematopoietic progenitor kinase 1. *Journal of Biological Chemistry*, 279, 49551-49561.
- ZHOU, J., PHAM, H., RUEDIGER, R. & WALTER, G. 2003. Characterization of the A $\alpha$  and A $\beta$  subunit isoforms of protein phosphatase 2A: differences in expression, subunit interaction, and evolution. *Biochem. J*, 369, 387-398.
- ZILBERMAN-RUDENKO, J., SHAWVER, L. M., WESSEL, A. W., LUO, Y., PELLETIER, M., TSAI, W. L., LEE, Y., VONORTAS, S., CHENG, L. & ASHWELL, J. D. 2016. Recruitment of A20 by the C-terminal domain of NEMO suppresses NF- $\kappa$ B activation and autoinflammatory disease. *Proceedings of the National Academy of Sciences*, 201518163.